



**UNIVERSITÉ
DE GENÈVE**

Archive ouverte UNIGE

<https://archive-ouverte.unige.ch>

Thèse

2020

Open Access

This version of the publication is provided by the author(s) and made available in accordance with the copyright holder(s).

Understanding the interactions of gold nanoparticles with B lymphocytes in vitro and in vivo

Hocevar, Sandra

How to cite

HOCEVAR, Sandra. Understanding the interactions of gold nanoparticles with B lymphocytes in vitro and in vivo. Doctoral Thesis, 2020. doi: 10.13097/archive-ouverte/unige:133930

This publication URL: <https://archive-ouverte.unige.ch/unige:133930>

Publication DOI: [10.13097/archive-ouverte/unige:133930](https://doi.org/10.13097/archive-ouverte/unige:133930)

Understanding the interactions of gold nanoparticles with B lymphocytes *in vitro* and *in vivo*

THÈSE

Présentée à la Faculté des sciences de l'Université de Genève
pour obtenir le grade de Docteur ès sciences,
mention sciences pharmaceutiques

Par

Sandra HOČEVAR

De

Slovénie (Ljubljana)

Thesis N°: 5437

GENÈVE

2020



**UNIVERSITÉ
DE GENÈVE**

FACULTÉ DES SCIENCES

**DOCTORAT ÈS SCIENCES, MENTION SCIENCES
PHARMACEUTIQUES**

Thèse de Madame Sandra HOCEVAR

intitulée :

**«Understanding the Interactions of Gold
Nanoparticles with B Lymphocytes *in Vitro* and
in Vivo»**

La Faculté des sciences, sur le préavis de Madame C. BOURQUIN, professeure ordinaire et directrice de thèse (Section des sciences pharmaceutiques), Madame F. DELIE SALMON, docteure (Section des sciences pharmaceutiques), Madame C. JANDUS, professeure (Département d'oncologie, Université de Lausanne, Centre hospitalier Universitaire Vaudois, Epalinges, Suisse), Monsieur L. TANG, professeur (Laboratory of Biomaterials for Immunoengineering, Ecole Polytechnique Fédérale de Lausanne (EPFL), Suisse) et Monsieur M. J.D. CLIFT, professeur (In Vitro Toxicology Group, Swansea University, Swansea, United Kingdom), autorise l'impression de la présente thèse, sans exprimer d'opinion sur les propositions qui y sont énoncées.

Genève, le 30 janvier 2020

Thèse - 5437 -

Le Décanat

TABLE OF CONTENTS

TABLE OF CONTENTS	2
LIST OF FIGURES	5
LIST OF TABLES	5
LIST OF ABBREVIATIONS	6
RÉSUMÉ EN FRANÇAIS	8
SUMMARY IN ENGLISH	10
GENERAL INTRODUCTION	12
1. Introduction to nanotechnology	12
1.1 Nanoparticles	12
2. Nanomedicine	13
2.1 Challenges in nanomedicine	14
3. NP-cell interactions and the relevance of biological environment	16
3.1 Protein corona	16
3.2 Effect of NP properties in relation to protein corona	17
3.2.1 <i>Composition</i>	17
3.2.2 <i>Size and shape</i>	17
3.2.3 <i>Surface charge</i>	18
3.2.4 <i>Hydrophobicity</i>	19
3.2.5 <i>NP interactions with the components of the immune system</i>	19
3.3 Effect of the environment	20
3.4 Biodistribution and clearance of NPs <i>in vivo</i>	20
4. Mechanisms of nanoparticle internalization	21
4.1 Phagocytosis	22
4.2 Macropinocytosis	22
4.3 Clathrin- and caveolae-mediated endocytosis	22
4.4 B cell-mediated endocytosis	23
5. Toxicity of nanoparticles	23
5.1 The mechanisms of nanotoxicity	24
6. The immune system	25
6.1 The innate immune system	25

Table of Contents

6.1.1	<i>Macrophages and dendritic cells</i>	26
6.1.2	<i>Induction of the innate immune response</i>	26
6.2	The adaptive immune system	26
6.2.1	<i>B lymphocytes and their roles in the immune response</i>	27
7.	Immunological properties of engineered nanoparticles	28
7.1	Innate immune response towards NPs	28
7.2	Adaptive immune response towards NPs	31
7.2.1	<i>Cellular immune response</i>	31
7.2.2	<i>Humoral immune response</i>	31
8.	Nanoparticles and the modulation of the immune response	32
8.1	Nanovaccines	32
8.2	Nanoparticles and B lymphocytes in health and disease	34
9.	Gold nanoparticles	35
9.1	Synthesis	35
9.2	Properties	36
9.3	Applications	36
9.3.1	<i>In vitro and in vivo diagnostics</i>	36
9.3.2	<i>Therapy</i>	37
9.3.3	<i>GNP applications in immunology</i>	38
9.3.4	<i>Considerations and perspectives</i>	39
OBJECTIVES OF THE THESIS		40
RESULTS		43
1.	Manuscript 1: Polymer-coated gold nanospheres do not impair the innate immune function of human B lymphocytes <i>in vitro</i>	43
1.1	Supporting information for manuscript 1	70
2.	Manuscript 2: Polymer-coated gold nanoparticles inhibit adaptive B cell function in mice	81
2.1	Supporting information for manuscript 2	115
GENERAL DISCUSSION		128
1.	GNP cytotoxicity and immune cells	128
1.1	Considerations for future immunotoxicological studies of GNP	129
2.	Biodistribution of GNPs	130
3.	Effect of physico-chemical properties of GNPs on B cells	131

Table of Contents

4. GNP effect on B cells and their function	133
4.1 Effect on the B cell innate-like immune response	133
4.2 Effect on the B cell adaptive immune response	134
5. B cell experimental models and their relevance	135
5.1 Human <i>in vitro</i> model	135
5.2 Mouse <i>in vitro</i> model	135
5.3 Mouse <i>in vivo</i> model	136
5.4 Room for improvement	136
6. Cross-species comparison of B cell-GNP interactions	137
6.1 Dose prediction for translation to clinical trials	140
7. Conclusions	140
8. Outlook	141
REFERENCES	142
APPENDICES	155
1. Appendix 1: Overview of the results obtained by a master student	155
CURRICULUM VITAE	156
ACKNOWLEDGMENTS	158

LIST OF FIGURES

Figure 1: Nanomedicine development and its challenges.	15
Figure 2: PubMed May 2019: Number of publications per year, searching for the term “nanotoxicology” and “nanotechnology”.	24
Figure 3: Human peripheral blood B lymphocytes.	27
Figure 4: Examples of different formulations of NPs used as vaccine delivery systems.	33
Figure 5: PEGylated gold nanospheres and gold nanorods.	36
Figure 6: Graphical abstract of manuscript 1.	43
Figure 7: Graphical abstract of manuscript 2.	81

LIST OF TABLES

Table 1: Examples of nanomedicines currently on the market based on their formulation.	13
Table 2: List of NPs currently in clinical trials for their therapeutic properties.	14
Table 3: Examples of different nanoparticle immunological and cytotoxic properties on different innate immune cell types and with regard to NP composition, physico-chemical characteristics and exposure concentrations.	30
Table 4: Overview of the GNPs and their physico-chemical characteristics used throughout the project.	132
Table 5: Overview of the GNP impact on the mouse and human primary B cells in vitro.	139

LIST OF ABBREVIATIONS

ABC: accelerated blood clearance
AD: animal dose
AFM: atomic force microscopy
AP-1: activating protein-1
APC: antigen-presenting cell
BCR: B cell receptor
Blimp-1: B lymphocyte-induced maturation protein-1
BMDCs: bone marrow-derived dendritic cells
BSA: bovine serum albumin
C1r: complement component 1r
C3: complement component 3
CCL5: Chemokine (C-C motif) ligand 5
CD3: Cluster of Differentiation 3
CD4: Cluster of Differentiation 4
CD8: Cluster of Differentiation 8
CD19: Cluster of Differentiation 19
CD20: Cluster of Differentiation 20
CD40: Cluster of Differentiation 40
CD69: Cluster of Differentiation 69
CD80: Cluster of Differentiation 80
CD83: Cluster of Differentiation 83
CD86: Cluster of Differentiation 86
CNS: central nervous system
CpG: cytosine triphosphate and guanine triphosphate oligodeoxynucleotides
DC: dendritic cell
DMEM: Dulbecco's Modified Eagle Medium
DNA: deoxyribonucleic acid
EMA: European Medicines Agency
Fab: antigen-binding fragment
FBS: fetal bovine serum
Fc: fragment crystallizable region
FcγR: Fc-gamma receptor
FDA: Food and Drug Administration
GNP: gold nanoparticle
GNR: gold nanorod
GNS: gold nanosphere
HED: human equivalent dose
HIV: human immunodeficiency virus
IFN-γ: interferon-gamma
Ig γ-1: immunoglobulin gamma-1 heavy chain
Ig γ-3: immunoglobulin gamma-3 heavy chain
Ig κ: immunoglobulin kappa light chain

List of Abbreviations

IL-12: interleukin-12
IL-18: interleukin-18
IL-1 β : interleukin-1 beta
IL-2: interleukin-2
IL-6: interleukin-6
IL-8: interleukin-8
iRNA: interference ribonucleic acid
I κ B α : nuclear factor kappa-light-chain-enhancer of activated B cells inhibitor, alpha
LPS: lipopolysaccharide
MBP: myelin basic protein
MDDCs: monocyte-derived dendritic cells
MDMs: monocyte-derived macrophages
MHC I: major histocompatibility complex class I
MHC II: major histocompatibility complex class II
MSN: mesoporous silica nanoparticles
MWCNT: multi-walled carbon nanotubes
NADPH: nicotinamide adenine dinucleotide phosphate
NF- κ B: nuclear factor kappa-light-chain-enhancer of activated B cells
NLRP3: NOD-, leucine-rich repeat- and pyrin domain-containing protein 3
NOD: nucleotide oligomerization domain
NP: nanoparticle
Pax5: paired box protein 5
PEG: polyethylene glycol
PLA: poly(lactic acid)
PLGA: poly(lactic-co-glycolic acid)
PM₁₀: particulate matter smaller than 10 μ m
PM_{2.5}: particulate matter smaller than 2.5 μ m
PPT: plasmonic photo-thermal
PPTT: plasmonic photo-thermal therapy
PVA: polyvinyl alcohol
RA: rheumatoid arthritis
rhTNF: recombinant human tumor necrosis factor
ROS: reactive oxygen species
RPMI: Roswell Park Memorial Institute medium
SEM: scanning electron microscope
SPR: surface plasmon resonance
ssRNA: single strain ribonucleic acid
SWCNT: single-walled carbon nanotubes
TEM: transmission electron microscope
Th: T helper cell
TI: T cell-independent
TLRs: Toll-like receptors (-1,-2,-3,-4,-5,-6,-7,-8, -9)
TNF- α : tumor necrosis factor-alpha
UFP: ultrafine particle
VLP: virus-like particle

RÉSUMÉ EN FRANÇAIS

La nanomédecine est une discipline prometteuse au sein de la nanotechnologie, utilisant des nanoparticules (objets de dimensions externes comprises entre 1 et 100 nm) pour améliorer le transport de médicaments, le diagnostic et la thérapie. Les nanoparticules d'or (NPO) sont couramment utilisées dans diverses applications biomédicales en raison de leurs propriétés hautement bénéfiques. Cela inclut leur biocompatibilité généralement élevée, leur capacité à transporter des médicaments et des vaccins et leurs propriétés optiques uniques. Ces atouts optiques sont particulièrement utiles pour les diagnostics *in vitro* et *in vivo* tels que l'imagerie et la biodétection, ainsi que pour les thérapies à base de photothermie.

Néanmoins, la question demeure quant à l'éventuel impact négatif des NPO sur la fonction des cellules immunitaires. La majorité de la littérature actuelle se concentre sur les cellules immunitaires innées phagocytaires telles que les macrophages et les cellules dendritiques. Cependant, la compréhension de l'influence des NPO sur les acteurs importants de l'immunité adaptative, tels que les cellules B, est insuffisante. La fonction des cellules B n'est pas limitée à la production d'anticorps induite par le récepteur des cellules B (BCR). En fait, les cellules B possèdent certaines caractéristiques de type inné telles que la présentation de l'antigène et la production de cytokines et d'anticorps induites par les récepteurs de l'immunité innée. Toutes ces fonctions sont interdépendantes et cruciales pour une performance optimale des cellules B. Ainsi, le double rôle des cellules B dans le système immunitaire en fait une cible d'intérêt important en termes d'exposition aux NPO. Le but de cette thèse était d'étudier l'impact de différentes NPO modifiées et façonnées en surface sur la viabilité, l'internalisation et la fonction immunitaire innée et adaptative *in vitro* et *in vivo* des lymphocytes B.

Dans la première partie du projet, l'accent était mis sur l'influence des NPO sur les cellules B humaines primaires. À cette fin, nous avons exposé les cellules à des concentrations croissantes de nanosphères d'or d'environ 15 nm protégées par du polyéthylène glycol (PEG) ou d'une combinaison d'alcool polyvinylique et de PEG et de nanobâtonnets d'or PEGylé. De manière importante, aucune des NPO testées aux concentrations les plus élevées n'a provoqué une augmentation de la mort cellulaire ni une activation immunitaire des cellules B. Nous avons montré que le manque de polymère protecteur entraînait une forte instabilité des NPO dans les milieux biologiques, ce qui entraînait l'agrégation des NPO, une internalisation accrue par les cellules B et une suppression de la production de cytokines. Au contraire, les nanosphères d'or revêtues de polymères étaient mal absorbées par les cellules, sans signe de modulation de la fonction des cellules B. De manière différente, le passage de la forme sphérique à la forme de tige a considérablement diminué la réponse pro-inflammatoire. Ces résultats

Summary in French

ont mis en évidence l'importance de la forme des NPO et de l'enrobage protecteur du polymère par rapport à la réponse immunitaire de type innée précoce des cellules B humaines.

Les parties II et III de la thèse visaient à étudier la réponse des cellules B de souris *in vitro* et *in vivo* après exposition aux NPO. Le modèle de souris a servi à comprendre l'impact des NPO sur les cellules B dans des organismes complets dotés d'un système immunitaire fonctionnel. Nous avons utilisé des nanosphères d'or de ~15 nm protégées par un polymère avec un marqueur fluorescent afin d'observer leur biodistribution dans différentes cellules et différents organes immunitaires. Ces nanosphères chargées positivement ont été internalisées de manière significative par des cellules B activées par un adjuvant *in vitro*, ce qui a entraîné la suppression de la production de cytokines et de la production d'anticorps indépendante de l'activation du BCR. Cependant, la viabilité cellulaire n'a pas été affectée. *In vivo*, les NPO ont été très tôt détectées dans les cellules B de la zone marginale de la rate, mais pas dans les cellules B des ganglions lymphatiques. En outre, l'administration simultanée d'antigène et de NPO a entraîné la suppression de la production d'anticorps induite par le BCR 14 jours après les injections. De plus, nous avons observé que l'internalisation des NPO était accrue dans les cellules B exposées avec l'antigène et que les NPO s'accumulaient de préférence dans les cellules B de la zone germinale splénique. L'ensemble de ces résultats ont indiqué la capacité des NPO à interagir et à moduler la réponse immunitaire adaptative de type B innée et adaptative.

Il est important de noter que tout au long du projet, nous avons démontré que les NPO étaient hautement biocompatibles avec les cellules B. L'effet immuno-modulateur des NPO sur les cellules B fonctionnellement actives doit être étudié de manière plus approfondie en ce qui concerne les mécanismes, l'impact éventuel à long terme et l'éventuel effet indirect sur les cellules immunitaires dépendantes des cellules B. Nos résultats fournissent des informations importantes qui peuvent aider à évaluer l'adéquation des NPO pour les applications biomédicales et à mieux prévoir leur sécurité et leur succès pour leurs futures applications translationnelles en clinique.

SUMMARY IN ENGLISH

Nanomedicine is a promising discipline within nanotechnology, using nanoparticles (objects with any external dimensions between 1-100 nm) for the improvement of drug delivery, diagnostics and therapy. Gold nanoparticles (GNPs) are commonly used in a variety of biomedical applications due to their highly beneficial properties. This includes their generally high biocompatibility, their ability to deliver drugs and vaccines, and their unique optical properties. The latter is a useful tool for *in vitro* and *in vivo* diagnostics such as imaging and biosensing as well as photothermal-based therapies.

Nonetheless, the question remains regarding the possible adverse impact of GNPs on the immune cell function. The majority of the current literature is focused on phagocytic innate immune cells such as macrophages and dendritic cells. Yet, the understanding of GNP influence on the important actors of adaptive immunity, such as B cells, is insufficient. B cell function is not limited only to the B cell receptor (BCR)-induced antibody production. In fact, B cells possess certain innate-like characteristics such as antigen presentation, and cytokine and antibody production induced through the receptors of innate immunity. All these functions are interdependent and crucial for optimal performance of B cells. Thus, the dual role of B cells in the immune system makes them an important target of interest in terms of exposure to GNPs. The aim of this PhD thesis was to investigate the impact of different surface-modified and shaped GNPs on B cell viability, internalization, and innate-like and adaptive immune function *in vitro* and *in vivo*.

In the first part of the project, the focus was on GNP influence on primary human B cells. For this purpose, we exposed cells to increasing concentrations of ~15 nm gold nanospheres (GNS) protected with polyethylene glycol (PEG), or combination of polyvinyl alcohol (PVA) and PEG (PEG/PVA), and PEGylated gold nanorods (GNR). Importantly, none of the GNPs tested elicited an increase in cell death or caused B cell immune activation after short-term exposure and the highest concentration tested. We showed that the lack of protective polymer caused strong GNP instability in biological media, which resulted in GNP aggregation, increased B cell internalization and suppression in cytokine production. On the contrary, polymer-coated GNS were poorly taken up by the cells, with no signs of modulation of B cell function. Differently, the change from sphere to rod shape significantly decreased pro-inflammatory response. These results pointed out the importance of the GNP shape and protective polymer-coating in respect to the early innate-like immune response in human B cells.

Summary in English

Part II and part III of the thesis were aimed at mouse B cell response *in vitro* and *in vivo* upon GNP exposure. The purpose of the mouse model was to understand the impact of GNPs on B cells in complete organisms with a functional immune system. We used a ~15 nm and polymer-protected GNS with a fluorescent label in order to monitor their biodistribution across different immune cells and organs. These positively-charged GNS were significantly taken up in adjuvant-activated B cells *in vitro*, which resulted in suppression of cytokine and BCR-independent antibody production, however, the cell viability was not affected. *In vivo*, GNPs were detected in marginal zone B cells in the spleen at early time-points, but not in lymph node B cells. Furthermore, the simultaneous administration of antigen and GNPs caused suppression of BCR-induced antibody production 14 days after injections. Additionally, we observed that GNP internalization was increased in antigen-primed B cells and that GNPs preferentially accumulated in splenic germinal zone B cells. These results together indicated the ability of GNPs to interact and modulate the innate-like and adaptive B cell immune response.

Importantly, throughout the project, we demonstrated that GNPs are highly biocompatible with B cells. The immune-modulatory effect of GNP in functionally active B cells should be further investigated for the mechanisms, possible long term impact and potential indirect effect on the function of B cell-dependent immune cells. Our results provide important information which can help to evaluate the appropriateness of GNP for biomedical applications and better predict their safety and success for future translation of GNP applications to clinical studies.

GENERAL INTRODUCTION

1. Introduction to nanotechnology

Nanotechnology is a field of knowledge that involves applications of various nanomaterials, which are developed on a scientific basis (*i.e.*, nanoscience) in order to improve the performance of a product (*e.g.*, the stability of a drug) or serve as useful tools on their own (*e.g.*, as biosensors, carriers).¹ According to the definition by the International Organization for Standardization (ISO/TS 80004-1:2015), a nanomaterial is a material with any external dimension in the nanoscale (1-100 nm) or having any internal or external structures in the nanoscale.² The first visions of nanotechnology were presented by physicists and Nobel Prize laureate Richard Feynman in 1959 in his paper titled “There’s plenty of room at the bottom”, which encouraged scientists to begin with research on the “small scale” material.³ Along with the development of high-resolution microscopy in the 20th century, the evolution of nanotechnology has quickly progressed and the options for its use became broader.⁴ Today, nanotechnology is a constantly developing field with numerous promising applications in areas such as medicine, food products, sporting goods, electronics, environmental remediation, renewable energy and textiles.⁵⁻¹⁰

1.1 Nanoparticles

A sizeable part of nanotechnology involves nanoparticle applications. Nanoparticles (NPs) are nano-objects, with defined external boundaries where all dimensions are in the nanoscale range.¹¹ One of the main advantages of the NPs is their high surface area-to-volume ratio. This feature allows more pronounced adsorption of molecules on their surface, compared to larger particles with smaller area to volume ratio. Thus, NPs can be engineered as powerful carriers for drugs, used as biosensors as they can bind an analyte of interest or can be used as a cleaning tool by removing contaminants in the water.⁵ Furthermore, NPs can gain other new and unique physiochemical properties that are not present in their “bulk form”. For example, unlike iron in its normal form, iron oxide NPs poses superparamagnetic properties. This unique quality makes iron oxide NPs a great contrast agent for magnetic resonance imaging or for the purpose of magnetically induced thermal therapies.¹² Depending on their chemical composition, NPs can be generally classified as organic (*e.g.*, liposomes, polymer NPs, carbon-based NPs), inorganic (*e.g.*, gold nanoparticles (GNPs), titanium NPs), crystalline and amorphous NPs (*e.g.*, silica NPs).¹³

2. Nanomedicine

Nanomedicine is a discipline within nanotechnology, which uses nanomaterials for *in vitro* and *in vivo* diagnostics, as delivery systems for therapy and in novel implant technologies.⁵ Two or more of these features can be carried out by one NP formulation. NPs engineered with combined function of drug delivery, diagnostics and therapy are referred to as theranostics.¹⁴ Multifunctionality of NPs is one of the key reasons for their increased use in the pre-clinical studies. Several NP applications have already reached translation to clinical practice. In the European Union (EU) there are currently around 50 nanomedicines in phase I-III clinical trials.¹⁵ Furthermore, there is approximately 50 Food and Drug Administration (FDA) and over 30 European Medicines Agency (EMA) approved nanomedicines.^{15–17} Majority of NP-based medicines that are currently available on the market are intended to improve the performance and delivery of the already existing drugs, compounds or elements. This includes NP formulations such as liposomes, nanocrystals, polymer-based, protein-based and metal-based NPs. Examples of some the most known and recently available nanomedicines on the market are presented in Table 1.

Table 1: Examples of nanomedicines currently on the market based on their formulation.

Type of nanomedicine formulation	Name (Company)	Indication	Improved existing drug/compound/element/molecule	Advantage	Year of approval
Lipid-based	VYXEOS (Jazz Pharma.)	Acute myeloid leukaemia	cytarabine/daunorubicin	Improved efficacy	2017
	ONPATTRO/Patisiran (Alnylam Pharma.)	Transthyretin-mediated amyloidosis	iRNA	First approved iRNA delivery by NPs	2018
	Doxil® (Janssen)	Ovarian cancer	doxorubicin	Improved delivery	1995
Nanocrystals	Emed® (Merc)	Anti-emetic	aprepitant	Increased solubility and bioavailability	2003
	Rapamune® (Wyeth Pharma.)	Immuno-suppression	sirolimus	Increased bioavailability	2010
Polymer-based	Cimzia®-PEGylated drug (UCB)	Autoimmunity	Fab antibody fragment against TNF-α	Improved half-life	2008
	Copaxone® (Teva)	Multiple sclerosis	L-glutamate/L-tyrosine/L-lysine/L-alanine	Controlled clearance	1996
Protein-based	Abrexane® (Celgene)	Breast cancer	paclitaxel	Increased passive delivery and solubility	2005
	Ontak® (Eisai)	T-cell lymphoma	diphtheria toxin protein	Active targeting	1999
Metal-based	NBTR3/Hensify (Nanobiotix)	Squamous cell carcinoma	hafnium oxide	Enhancement of radiotherapy	2019
	Feraheme® (AMAG Pharma.)	Anemia	iron	Increased cell uptake	2009

iRNA: interference RNA; Fab: variable part of the antibody; Sources:^{15,16,18,19}

General Introduction

There is an increase in number of various NPs types used for drug delivery and diagnostics in clinical trials. For example, fluorescent silica NPs are used for imaging of nodal metastasis (phase II, NCT02106598) and gold nanoparticles for delivery of spherical nucleic acid to target and treat glioblastoma (early phase I, NCT03020017).²⁰ On the other hand, there is an increase in the number of clinical trials using intrinsic properties of NPs for treatment, such as photo and magnetic induction of heat (Table 2). To this day, Nanotherm is the only metal-based nanomedicine (superparamagnetic iron oxide NPs) with approval for therapy of solid tumors in the EU.²¹

Table 2: List of NPs currently in clinical trials for their therapeutic properties.¹⁹

Name (company)	NP type	Indication	Clinical Phase	Clinical trial ID
Nanotherm (Magforce)	Iron oxide	Magnetically induced thermotherapy of glioblastoma	Phase II ²²	DRKS00005476 (European CE certificate, 2011)
AuroLase (Nanospectra Biosciences)	Silica/gold nanoshell	Photothermal therapy of solid and metastatic lung tumors	N/A	NCT01679470 NCT02680535 NCT00848042
CNM-Au8 (Clene Nanomedicine)	Gold nanocrystals	Treatment of re-myelination failure in multiple sclerosis	Phase II	NCT03536559
Magnablate	Iron	Magnetic thermoablation for prostate cancer	Phase 0	NCT02033447
NANOM FIM trail	Gold/silica	Photothermal therapy to treat arteriosclerosis	Phase I ²³	NCT01270139

Sources: www.clinicaltrials.gov (last access: 19.10.2019); www.drks.de/drks_web/ (last access: 19.10.2019), www.magforce.com/en/home (last access: 19.10.2019), www.nanospectra.com (last access: 19.10.2019), www.clene.com (last access: 19.10.2019); N/A: no information.

These examples (Table 1 and 2) show that NPs have a high potential as theranostics for various medical conditions. Moreover, the same NP application can often be easily adapted for the treatment of other types of diseases and conditions or used in combination with the standard of care treatments. Thus, nanomedicines are gaining increasing popularity within clinical research.

2.1 Challenges in nanomedicine

New questions and challenges are constantly evolving with regard to nanomedicines and the likelihood of their translation towards clinical application. To increase the chances for such a translation, a high level of optimization and reproducibility is needed at the pre-clinical stage. On one side, an optimized synthesis and well-defined characterization of NPs is fundamental prior to biological testing. This includes NP physico-chemical properties, kinetic properties as well as type of methods used for NP characterization. On the other hand, biological systems used for NP testing need to be also well-optimized. This is important as the effects of NPs can differ significantly across different experimental models and in variable biological conditions. In order to minimize translation issues, the use of advanced *in vitro* and *in vivo* models are highly encouraged. This includes biological systems such as human primary cell cultures, tissue-on-a-chip approaches or humanized mouse models.^{17, 24}

General Introduction

Pharmacokinetics and biodistribution of nanomedicines are strongly conditioned by their complex physico-chemical characteristics. Therefore, the production of a highly biostable nanomedicine with no adverse effects presents a major challenge. For example, nanomedicine interactions with plasma proteins can intensify undesirable immune responses and instantly decrease biocompatibility level of a nanomedical product. Therefore, pharmacokinetic studies are of great importance as a part of nanomedicine evaluation in order to assure their safety and high performance.¹⁷

Furthermore, once a nanomedicine receives the 'green-light' for the market, the scale-up manufacturing might face a challenge in the process control. Where the synthesis on a small-scale is easy to control and optimize, one must consider how the nanomaterial will behave in the large scale production to assure high reproducibility.^{25,26} Additionally, another issue of the scale-up manufacture of nanomedicines is the cost-effectiveness. Currently, there is a very high per-units-cost in nanomedicine production or so-called diseconomies of scale, which pushes the final nanomedical product at higher price.²⁷ The stages of the long process of nanomedicine development, as well as the challenges and consideration involved, are summarized in Figure 1.

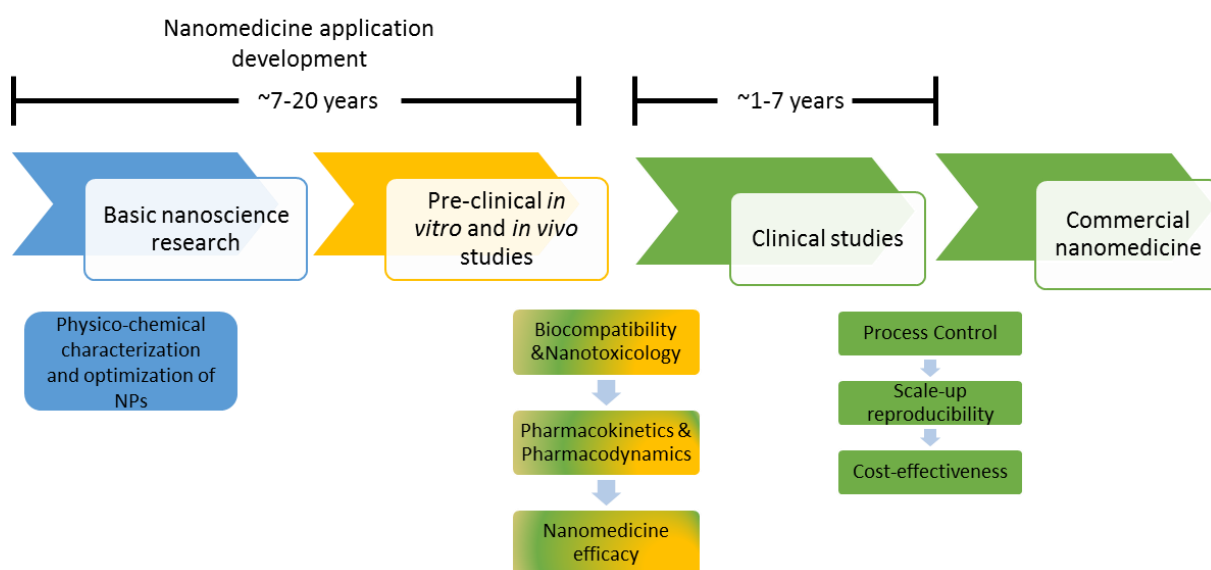


Figure 1: Nanomedicine development and its challenges. (Adapted from Soares *et al.*, *Front. Chem.*, 2018¹⁷ and Etheridge *et al.*, *Nanomedicine*, 2013²⁸)

Currently, there is a lack of specific regulations and guidelines with defined testing criteria for nanomedicines by the regulatory health agencies. Indeed, many of the regulatory agencies are pursuing some initial guidelines and reflection papers, which provide recommendations and requirements in order to better assess nanotechnology-based products and pharmaceuticals. For example, FDA in 2017 presented a draft of guidelines for the industry for drug and biological products that contain nanomaterials.¹⁵ Yet, the draft is not finalized to this day. EMA since 2013 released several reflection papers on more specific nanotechnology-related topics. This includes requirements for

General Introduction

intravenous iron-based, nano-colloidal and liposomal products, and considerations for administration of coated nanomedicine products.²⁹ However, all these documents are not legally binding and do not yet provide a specific regulation for numerous complex theranostic nanomedicines, which are increasingly entering the clinical trials.³⁰ Nevertheless, with several nanomedicines already on the market, the establishment of regulations for fast coming follow-up nanomedicines (“nanosimilars”) is vastly needed as well. A major issue is the lack of regulations and guidelines for the follow-up nanomedicines of non-biological origin or so-called non-biological complex drugs, which are in the EU currently evaluated case by case by EMA.³¹ Taken together, by establishing a more solid, defined and unified “ground rules” for the assessment of NP-based medicines, a smoother transition of nanomedicines from pre-clinical and clinical studies to the safe use in clinical practice may be achieved.

3. NP-cell interactions and the relevance of biological environment

NPs used for therapy and drug delivery purposes inevitable come in direct contact with the complex biological environment (cells, serum proteins, lipids, nucleic acids, extracellular fluid, shear stress, *etc.*).^{32,33} The NP-biomolecule interactions can significantly influence upon further NP-cell contact *in vitro* as well as upon *in vivo* biodistribution of the nanomaterial. Therefore, it is essential to understand potential changes of the NP characteristics once NPs are introduced to the biological system, and consequently, how these may impact upon the system’s (patho-)physiology (*e.g.*, change in the cell interaction/entry, metabolism, cell signaling, immune response, cytotoxicity).

3.1 Protein corona

NPs exposed to a protein-rich environment (*e.g.*, blood or serum-rich culture media) are prone to the formation of a protein coat, known as protein corona. The protein corona has been theorized to consist of two kinetically distinct forms – (i) the “hard corona”, with high protein affinity towards NP surface and (ii) the “soft corona”, with weak affinity.³⁴ The affinity is based on the attractive or repulsive forces (*e.g.*, van der Waals, electrostatic, covalent) between the NP surface and the proteins as well as between the proteins themselves.³² NP physico-chemical properties and the conditions in the surrounding environment are crucial factors that dictate the composition of the protein corona.³² The formation of protein corona is accompanied by the Vroman effect.³⁵ Vroman effect is a phenomenon responsible for displacement and abundance of proteins, which hypothetically causes changes in protein corona composition over time. Based on the concentration/composition of the surrounding proteins and nature of the NP surface, proteins can bind in a competitive manner, undergo structural conformations and can cause NP dissolution.³² Importantly, malformed proteins can be potentially further involved in cell pathology due to disruption of their primary function, for instance inhibition of enzymatic activity.³⁶

General Introduction

A comprehensive study found the protein corona to be consisted of nearly 300 proteins.³⁷ The authors studied the kinetics of the protein corona and showed that the composition of NP-specific corona is defined as early as in the first 30 seconds after incubation in a protein-rich environment. They further demonstrated that the ratio of the bound proteins is dramatically changing in a time-dependent manner, whereas no significant change in protein corona composition was identified over time. Most importantly, the proteins bind in the early time points were responsible for lesser cell death in comparison to later time points.³⁷ This is most likely the result of the increase of NP aggregates at later time points followed by higher NP uptake, which presents higher risk for toxicity. Therefore, NP-protein interactions in relation to specific exposure times should be well-considered when assessing the safety of the NPs. Nonetheless, the protein corona of human plasma proteins, in general, consists of the most abundant proteins, independent of the NP type and physico-chemical characteristics – albumin, immunoglobulins, lipoproteins, coagulation proteins and complement proteins.³⁸

3.2 Effect of NP properties in relation to protein corona

3.2.1 Composition

The NP composition has been shown to be linked with distinct protein binding profiles. For example, similar human plasma protein patterns were detected on titanium and silica NPs, whereas zinc NPs revealed distinct protein binding profile despite the comparable negative surface charge.³⁹ The NP-specific protein pattern might be correlated with specific biological responses such as the cellular interaction, toxicity and biodistribution. Walkey *et al.* developed a model that could better predict these biological outcomes based on the protein corona fingerprints in an extensive library of gold and silver NPs.⁴⁰ In theory, this type of *in silico* tools would help to achieve a rapid evaluation of the most appropriate NP candidate for future nanomedicines.

3.2.2 Size and shape

The size of a NP is one of the parameters which is associated with the presence and the amount of a certain protein on NP surface. More specifically, protein fingerprint is dependent on the surface-to-volume ratio of the NP and the curvature.⁴¹ For instance, it has been shown that the presence of a common blood protein apolipoprotein A-I decreased with the increasing size of silica NPs (between 9 nm - 76 nm) incubated in human serum.⁴² Proteins like lipoproteins are involved in the transportation of biomolecules (*eg.*, lipids and cholesterol) to ensure their sufficient supply for the cell and its function. Once bound to the NPs, these transport proteins similarly participate in the trafficking of NPs into the cell *via* ligand-receptor interactions.^{38,43} Further, bigger polystyrene NPs (~200 nm) provided a suitable surface for the formation of coagulation activation complexes, whereas smaller NPs (~30 nm) inhibited the initiation of coagulation cascades. This is suggesting the importance of the size-

General Introduction

dependent change in curvature of sphere-shaped NPs in the manipulation of the blood coagulation pathway.⁴⁴

Different curvatures of titanium nanorods and nanospheres have also resulted in distinct protein corona fingerprints that can affect the level of the internalization into the cell.^{39,45} A study, involving several distinct shapes of PEG-protected GNPs, reported increasingly internalized NPs by the cells in the following order: nanostars > nanorods > nanotriangles.⁴⁶ It was also suggested that the type of entry mechanism might play an important role across these different NP shapes. However, despite increased cellular association/entry of NPs of a certain shape does not necessarily mean the most efficient therapeutic response in the case of nanomedical applications. For example, it has been shown that higher uptake of antigen-coated gold nanorod vaccine had a less efficient antibody response compared to 40 nm gold nanospheres with a lower level of internalization. Additionally, the potential influence of a surface charge, surface area and efficacy of antigen coating on sphere vs. rod was tested. All these factors were excluded as the possible reasons for the differences in the cell response, which suggested that shape indeed plays a role in NP-cell interactions.⁴⁷ Nevertheless, the exact involvement of NP shape with the cell uptake mechanisms and cell function is still not well understood.

3.2.3 Surface charge

It has been commonly suggested that a negatively charged cell membrane may be more efficient in attracting positively charged NPs, resulting in a higher internalization compared to negatively charged surfaces.^{48,49} However, in the protein-rich environment, irrespectively to their surface charge, NPs bind a larger amount of negatively charged proteins (*e.g.*, highly abundant serum albumin with ζ -potential of -19 mV). This masks the NP's original surface charge and balances their overall charge towards negative values.^{37,50} Thus, there are other factors that can explain the increased internalization of positively charged NPs in protein-rich environments. One reason is a decreased level of colloidal stability of positively charged NPs in biological media, which as a result, leads to the formation of larger aggregates/agglomerates.⁵¹ Agglomeration can significantly increase the cell uptake *in vitro* due to faster sedimentation and change in dosimetry compared to well-dispersed NPs.⁵² Moreover, a higher level of protein conformational changes was found on a surface of positively charged NPs, which caused higher cell uptake and toxicity as opposed to negatively charged ones.⁵³ Further, the localization of cationic NPs in an acidic environment of lysosomes may cause lysosomal swelling that leads to the burst of the membrane and spillage of the content in the cytosol.³² The latter may induce cytotoxic effect by the production of reactive oxygen species (ROS), mitochondrial damage and acute inflammation.³⁶

3.2.4 Hydrophobicity

Increasing hydrophobicity of NP surfaces leads to increased intensity in protein adsorption, which is driven by hydrophobic forces in the aqueous environment. Elevation of opsonized NPs results in their shorter half-life because they are recognized more effectively by the cells, internalized and consequently removed faster from the system.⁵⁴ NPs can be functionalized with hydrophilic polymers such as polyethylene glycol (PEG) and polyethylene alcohol (PVA) to reduce their hydrophobic surface and are commonly used in nanomedical applications. In contrast to hydrophobic surfaces, the steric repulsion forces on hydrophilic surfaces prevent excessive protein corona formation, which reduces NP recognition by the phagocytic cells and consequently improves NP half-life in the circulation.^{55,56}

In normal conditions, cellular hydrophobic molecules are hidden and well preserved from the aqueous environment. In the case of distress (*e.g.*, cell necrosis), hydrophobic molecules become exposed to external environment, forming disordered structures and aggregates. These hydrophobic anomalies are recognized by the cells as damage-associated molecular patterns, which results in innate immune response.⁵⁷ Moyano *et al.*, proposed that the hydrophobic NP surface can be recognized in a similar way. They showed that the increased hydrophobicity of PEGylated NPs is correlated with an elevation in the expression of pro-inflammatory cytokines (IL-2, IL-6, TNF- α , IFN- γ) in mouse splenocytes.⁵⁸ However, whether higher hydrophobicity was also connected to increase in NP internalization, was not reported in the study.

3.2.5 NP interactions with the components of the immune system

Antibodies and complement proteins are an important fraction of serum plasma proteins, which are part of the immune system and are important in fighting against pathogens. Together, they can form immune complexes by opsonization of antigens, microbes or foreign material and induce an immune response through interactions with immune cells and complement system activation.⁵⁹ Immunoglobulins such as constant regions of Ig κ , Ig γ -1 and Ig γ -3 chains, and complement C3 and C1r subcomponent were among 20 most abundant proteins found in the protein corona across 11 physico-chemically different NPs.³⁷ Furthermore, it has been shown that natural antibodies (exist in the absence of the exogenous antigen), present in the protein corona, bind and increase opsonization of NPs with complement proteins, especially C3.⁶⁰ Based on this data, it is clear that composition of protein corona is as well dependent on the native protein-protein interactions. Moreover, due to these specific antibody-complement interactions within protein corona, one cannot exclude the possibility that they might be able to induce complement-mediated immune responses. Therefore, consideration of the primary roles of proteins in the context of protein corona might help to predict possible biological responses to NP-protein formations.

3.3 Effect of the environment

Conditions in the biological environment indeed affect how NPs interact with the cells. Firstly, the type of culture medium used in the *in vitro* experiments can be an important factor. Roswell Park Memorial Institute (RPMI) medium and Dulbecco's Modified Eagle Medium (DMEM) are commonly used cell culture media, which differ in the composition of amino acids, salts and glucose.⁶¹ It has been shown that NPs incubated in DMEM (+10% FBS) have a higher abundance of proteins, yet more stable protein corona, compared to NPs exposed to RPMI (+10% FBS). Lower stability of protein corona in RPMI exposed NPs caused higher NP aggregation, cell uptake and toxicity, compared to NPs in DMEM environment.⁶¹ Secondly, chemical and physical conditions of the environment significantly affect the NP-protein interactions. For example, pH and temperature are factors that influence the stability of NP-bound proteins and their adsorption dynamics. As these conditions can quickly vary in biological set-ups, they can cause changes in protein composition and cause protein denaturation. Together with the level of reactivity of the NP surface, this can trigger cellular internalization and possibly further adverse effects, such as inflammation and apoptosis.^{62,63} There are several other factors that may change the course of the NP-bio interface, including protein concentration, cell type and its level of metabolic activity, exposure time, micro-environment and *in vivo* shear stress effect.^{64,65}

3.4 Biodistribution and clearance of NPs *in vivo*

Physico-chemical properties of NPs, such as size, shape, surface charge and composition drive to differences in route of clearance and accumulation in the body. In general, after intravenous injection, NPs can be, to a certain extent, detected throughout the body, including blood, lung, heart, brain, kidneys, liver, spleen, thymus *etc.*⁶⁶ However, the level of the biodistribution is dependent on several factors such as size and shape. For instance, the distribution of smaller GNPs (15 and 50 nm) was higher, moderately detected in blood and all main organs, compared to larger NPs (100 and 200 nm), which were dominantly detected in liver, spleen and lungs, but not detected in blood 24 h after intravenous injection.⁶⁷ Moreover, in a biodistribution study of polymeric NPs, it was shown that NP size, as well as geometry, played an important role in their accumulation in the tumor. While small spherical NPs (~20 nm) were found in higher amounts in the tumor, rods and worm-shaped NPs, dominantly accumulated in liver and spleen.⁶⁸ Furthermore, NP-lymph node trafficking after subcutaneous administration strongly rely on NP size. This is mainly important in the case of vaccine-based NPs as it has been reported that subcutaneously injected NPs between 5-100 nm are able to passively reach draining lymph nodes, whereas larger particles (>1000 nm) are transported to the lymph node by the resident dendritic cells or are retained at the site of injection.⁶⁹ Taken together, information about the NP biodistribution is especially relevant in designing of nanomedicines in order

General Introduction

to choose NPs with appropriate physical and chemical characteristics to assure their high therapeutic/prophylactic efficacy.

One of the advantages of NP size is their ability to cross brain-blood barrier in order to deliver drugs, which alone cannot reach the central nervous system (CNS).⁷⁰ NPs can reach the brain either by passive delivery through disruption of tight junctions (up to 80 nm) or active delivery through receptor-mediated endocytosis (up to 200 nm).⁷¹ NP-based drugs for targeting glioblastoma has already been developed, some already on the market, many in the clinical trials.¹⁹ Despite this type of promising medical studies, the off-target effects of NPs on the CNS need to be considered as this could potentially have some major consequences, such as interruptions in neurotransmission, disruption of BBB, neuroinflammation and apoptosis of CNS cells.⁷⁰

Size and surface charge of the NPs greatly control the NPs clearance. A study on the renal clearance of quantum dots (used for *in vivo* imaging in diagnostics) set a reference for the size-dependent renal clearance of NPs. The authors showed that only NPs with hydrodynamic diameter below 6 nm were detected in the urine, with 50% of total body clearance after 4h. Differently, NPs larger than 8 nm had a very low signal in the bladder, but were substantially accumulated in liver, spleen and lungs. Importantly, they showed that surface charge increased protein adsorption and increased hydrodynamic diameter for ~15 nm. Protecting NPs with PEG helped to significantly reduce the protein binding and improved their half-life. However, the total diameter could not be reached below 10 nm, therefore, PEGylated NPs could not clear via renal system.⁷²

NPs that are not cleared by the renal system are commonly removed by the liver. Tsoi *et al.*, based on their results, proposed a mechanism for clearance of “hard” NPs in the liver. They showed that the slow blood flow in the liver (1000 fold slower compared to the systemic circulation) assures high removal of quantum dots by liver-resident cells, mainly accumulating in macrophages (Kupffer cells), also in hepatic B cells and endothelial cells, but not in T cells and hepatocytes, 12 h post intravenous injection.⁷³ Differently, positively charged silica NPs were detected in the hepatocytes 2h post-injection, suggesting the hepatobiliary clearance of these NPs from the system.⁷⁴ Taken together, the mechanism and time of clearance of NPs are most likely dependent on physico-chemical characteristics, which can consequently result in differences in NP toxicity.

4. Mechanisms of nanoparticle internalization

The route of cellular uptake of the NPs depends on NP characteristics, bioenvironmental conditions and cell type that is being exposed. Lipid-based NPs are capable of energy-independent internalization by fusion with the cell membrane (lipid rafts), fine NPs (~5 nm) can potentially enter the cell passively

General Introduction

by membrane translocation.^{75,76} In contrast, NPs can undergo the uptake through several actin-dependent ways, which are described below.⁷⁷

4.1 Phagocytosis

Phagocytosis is an important active process of phagocytes (*e.g.*, macrophages, monocytes, neutrophils, dendritic cells) with the main purpose to protect the system by engulfing and destroying foreign material. Phagocytosis is initiated through interactions with the cell scavenger, Fc or complement receptors. For example, phagocytic cells can recognize fragment crystallizable region (Fc) on IgG-opsonized NPs by Fc γ receptor (Fc γ R).⁷⁸ This mechanism of endocytosis is normally route of uptake for larger particles such as 2-3 μ m polymeric microspheres.⁷⁹ However, it was shown that phagocytosis can be also size-independent as cells can take up NPs such are lipid NPs between 20 and 100 nm equally through the complement receptor-mediated phagocytosis.⁸⁰ While FcR and complement-mediated phagocytosis is commonly followed by (pro-) inflammatory responses, certain type of scavenger receptors, involved in removal of endogenous apoptotic and dead cells, do not cause inflammation upon endocytosis.⁸¹ Therefore, it is commonly suggested that NPs internalized *via* scavenger receptors (*e.g.*, GNP <100 nm) are less likely to induce (pro-)inflammatory mediators.⁸²

4.2 Macropinocytosis

Macropinocytosis involves “swallowing” of extracellular fluid through the formation of membrane ruffles. This type of endocytosis results in the formation of macropinosomes, within a size range from 0.2 to 0.5 μ m. Therefore, random and nonspecific internalization of NPs is possible through this pathway.⁷⁷

4.3 Clathrin- and caveolae-mediated endocytosis

Clathrin-mediated endocytosis is responsible for the delivery of nutrients and constituents of the cell membrane by ligand-receptor mediated process, localized in the membrane areas consisting of clathrin pits. In the process of endocytosis, vesicles of approximately 150 nm in size are formed.⁷⁷ Thus, NPs with a diameter in the biological matrix of <200 nm are preferentially taken up by the cell through this type of receptor-dependent route. Moreover, transferrin is a protein that transports iron into the cell by binding to transferrin receptors in the clathrin pits. Therefore, conjugation of NPs with transferrin can be useful to promote clathrin-mediated endocytosis, which can also lead to uptake of larger NPs (>500 nm).⁸³ However, receptor-independent endocytosis is possible by accidental adhesion of NP to clathrin pits through electrostatic forces.⁷⁷

Caveolae-mediated endocytosis is responsible for lipid homeostasis and is involved in cell signaling. Caveolin is a membrane protein in control of the formation of lipid rafts that cause endocytosis in a

General Introduction

receptor-dependent manner. Cells such as epithelial cells, fibroblasts and adipocytes preferably take up NP (up to 500 nm) through this route of entry. Caveolae-dependent endocytosis is also predominantly responsible for albumin-coated NP uptake in endothelial cells due to the increased presence of albumin receptors in the caveolae.⁷⁷

4.4 B cell-mediated endocytosis

It is known that the recognition of antigens by B cell receptor causes their internalization, which is crucial for B cells to process and present antigen to T cells. B cell receptor-dependent phagocytosis was shown to be involved in the uptake of antigen-covered particles (*e.g.*, 1-3 μm microbeads and virus-like particles), which consequently induced activation and proliferation of T helper cells.^{84,85} On the other hand, virus-like particles taken up by marginal zone B cells, did not induce T helper cell proliferation. Instead, complement receptor-dependent uptake of NPs was suggested for this T cell-independent B cell subtype.⁸⁴ Nonetheless, the knowledge about the mechanisms of the NP uptake by B lymphocytes is very limited and requires further investigation.

5. Toxicity of nanoparticles

Nanotechnology, with its promising beneficial applications, has turned into a fast-rising and trending field. Nevertheless, a quick progression of this relatively new branch of technology has increased doubts concerning its safety due to the inevitable exposure of engineered NPs to humans and the environment. Such anxiety is raised based upon strong evidence of adverse human health effects following exposure to airborne particulate matter (PM) such as PM_{10} (<10 μm), $\text{PM}_{2.5}$ (<2.5 μm) and ultrafine particles (UFP) (<100 nm). Such variant sizes of PM have shown strong links with pulmonary inflammation, cardiovascular diseases and evidence to affect central nervous system.⁸⁶

Reports about the hostile effects of occupational exposures (*e.g.*, coal mining) to metal fumes and silica quartz on the respiratory system are available since the beginning of the 20th century.⁸⁷ However, the connection between the nanoscale properties of the particles and the specific biological adverse outcomes was not been acknowledged until the '80s.⁸⁸ The inhalation-based toxicity studies were first to report that smaller UFP (20 nm) had a greater ability to cross the alveolar membrane, which caused increased pro-inflammatory outcome, compared to larger particles (250 nm).⁸⁹ Soon after, the importance of the high surface-to-volume ratio of smaller particles and correlation to increased respiratory-related toxicity was reported.⁹⁰

A sub-discipline – known as “nanotoxicology” – emerged based on this fundamental knowledge available in the field of particle toxicology in order to evaluate possible adverse effects of otherwise considerably highly advantageous properties of engineered NPs.⁹¹ Furthermore, in the 2000's the

General Introduction

question about the role of the protein corona in NP toxicity has raised.⁹² The reported change of NP stability, conformational changes of proteins and increased uptake of protein-coated NP are some of the observation, which led to additional considerations regarding the mechanisms of nanotoxicity. This aspect of nanotoxicology became especially important in the field of nanomedicine, where NPs are intentionally administrated systematically and therefore strongly exposed to a complex biomolecular environment. As a result, this can potentially further alter the therapeutic outcome of the nanomedicine and potentially induce unexpected side effects. Thus, over the past two decades, the field of “nanotoxicology” has continuously grown, evolving alongside nanotech-related studies (Figure 5).

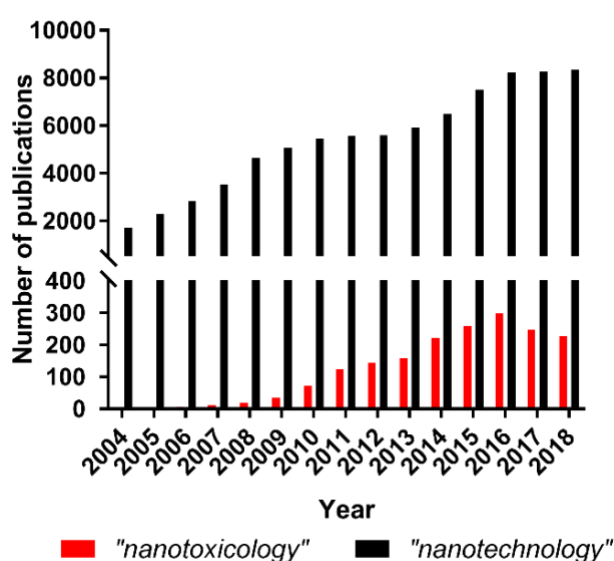


Figure 2: PubMed May 2019: Number of publications per year, searching for the term “nanotoxicology” and “nanotechnology”.

5.1 The mechanisms of nanotoxicity

Production of reactive oxygen species (ROS) and thus, induction of oxidative stress upon exposure to NPs is a well-evidenced mechanism and the most commonly reported cause of nanotoxicity.⁹³ There are two main sources of ROS generation in relation to NP exposure. Firstly, NP-specific physico-chemical properties can dictate the level of chemical reactivity. NPs surface can offer an optimal site for chemical reactions, which can result in ROS production. Secondly, the NPs can physically interact with cellular components and machinery that is involved in biological redox reactions and in this way elevate the intrinsic ROS production.⁹⁴ Depending on the route of internalization, the fate of the NPs can be within different intracellular compartments (*e.g.*, lysosomes, endoplasmic reticulum, mitochondria, cytosol). Mitochondria and cytosol are crucial NPs’ targets for the endogenous ROS generation, which is result of disruption of the respiratory chain, physical damage of the mitochondrial membrane and activation NADPH oxidases. Oxidative stress, as a result of elevated ROS production, is

General Introduction

responsible for severe damage of biomolecules and interference with important signaling pathways, leading to inflammation, apoptosis and genotoxicity.⁹⁴ Additionally, it has been suggested that NP-induced toxicity can also be ROS-independent, initiated through interaction with membrane receptors such as epidermal growth factor receptors, which are associated with activation pro-apoptotic signaling pathway.⁹⁵ However, these types of mechanisms are still not well understood and require further investigation.

Immune cells have been strongly linked to adverse responses upon NP exposure.⁹⁶ The toxic impact of NPs on professional phagocytic, innate immune cells (*e.g.*, macrophages) is based on their natural ability of internalization of foreign material and initiation of innate immune responses.⁵⁹ For instance, it has been shown that NPs are able to induce ROS-mediated activation of signaling pathways (*e.g.*, NF- κ B) and production of pro-inflammatory mediators such as TNF- α , IL-8, IL-6 and IL-1 β .⁹⁷ The ability of NPs to create inflammatory conditions could potentially have severe consequences, *e.g.* forming development allergic reactions to autoimmune diseases.⁹⁸ Some studies have suggested the potential involvement of NPs allergic responses, showing elevated levels of allergy-related antibody production (IgE), 14 days after exposure to multi-walled carbon nanotubes (MWCNTs).⁹⁹ Moreover, the surface reactivity of NPs has been shown to be responsible for structural changes in the proteins resulting in exposure of "cryptic epitopes".¹⁰⁰ In theory, these exposed epitopes could act as self-antigens and contribute to development of autoimmune conditions. Thus, identification of direct and indirect mechanisms of NP toxicity is crucial especially in the complex system of cells and modulators such is immune system to further understand potential adverse effects of diverse characteristics of engineered NPs.

6. The immune system

The immune system is the fundamental defense mechanism against pathogens. It consists of a complex network of specialized cell types, tissues, and molecules that fight and eliminate microorganisms, as well as protect against the repetition of infection due to the development of immunological memory. Cells of the immune system originate from common hematopoietic progenitor cells and differentiate into the lymphoid or myeloid lineage, together referred to as white blood cells, or leukocytes. Based on the specificity and rapidity of the immune response, the immune system divides on innate and adaptive immunity.⁵⁹

6.1 The innate immune system

Innate immunity provides first, fast and non-specific responses against pathogens and foreign molecules. The innate immune system is represented by monocytes and macrophages, dendritic cells (DCs), natural killer cells and granulocytes.⁵⁹

General Introduction

6.1.1 Macrophages and dendritic cells

Monocytes are immune cell type that surveillance vasculature and tissues and upon encounter with pathogen-associated molecular patterns differentiate into tissue-resident macrophages. The primary role of macrophages is to eliminate microbes, dead cells and foreign material from the body through the process of phagocytosis. Activated macrophages produce inflammatory modulators (cytokines, chemokines) and mediate innate immune response. Macrophages are able to degrade and display antigens on major histocompatibility complex class II (MHC II) molecules in the process called antigen presentation, which results in the activation of helper CD4 T lymphocytes.¹⁰¹ DCs, on the other hand, are a type of professional antigen-presenting cells (APCs) that are able to process and present antigens to T cells not only on MHC II but as well on MHC I. The ability of exposing antigens on MHC I is known as cross-presentation and it is important for activation of cytotoxic CD8 T cells, responsible for killing virus-infected and tumor cells. DCs are therefore an important bridge between innate and adaptive immunity as they can process a broader variety of antigens in the periphery and deliver them to secondary lymphoid organs (*e.g.*, lymph nodes) where they activate CD4 and CD8 T cell-mediated adaptive immune responses.¹⁰²

6.1.2 Induction of the innate immune response

Several immune cell types are able to recognize pathogen-associated molecular patterns through pattern recognition receptors such as Toll-like receptors (TLRs) and nucleotide oligomerization domain (NOD)-like receptors. TLRs are localized on the plasma membrane and in the endosomal compartments. Cell surface TLRs recognize pathogen-associated molecular patterns like lipopolysaccharide (LPS) (TLR 4), components of the bacterial wall (TLR 1, 2, 6) or flagellin (TLR 5). Intracellularly localized TLRs recognize sRNA (TLR 3), dsRNA (TLR 7 and 8) and CpG DNA (TLR 9). Activation of TLRs triggers the activation of inflammatory pathways (*e.g.*, NF- κ B) which leads to the secretion of pro-inflammatory cytokines, such as IL-6, IL-12, IL-18, TNF- α , IFN- γ amongst others. NOD-like receptors such as NLRP3 are involved in the complex of proteins called inflammasome that, upon activation, results in the expression of pro-inflammatory genes (*e.g.*, pro-IL-1 β). Depending on the site of infection and type of the pathogen, the innate immune cells regulate T helper cell-mediated immune responses.⁵⁹

6.2 The adaptive immune system

The adaptive immune system involves specialized immune cell types that are highly antigen-specific. The important property of adaptive immunity is the ability to develop immunological memory, which provides specific life-long protection against pathogens. Adaptive immunity includes T lymphocytes (cellular immunity) and B lymphocytes (humoral immunity).⁵⁹

General Introduction

6.2.1 B lymphocytes and their roles in the immune response

B lymphocytes, also known as B cells, are a type of adaptive immune cells with their principle effector role as antibody-producing cells. B cells develop in the bone marrow from pro-B cells to pre-B cells and then into immature B cells. Following the maturation process, B cells enter the blood circulation as transitional or mature naïve B cells (Figure 3). The main feature of B cell is B cell receptor (BCR), which serves as a binding site for epitopes on protein antigens as well as for less specific polyvalent antigens such as polysaccharides, nucleic acids, lipids, *etc.* BCR consists of heavy and light chains, which belong to immunoglobulin protein family. Both chains hold constant (Fc) and variable (Fab) region. In early developmental stages, B cells go through the rearrangement of heavy and light chain gens. The role of these combinative rearrangements is to produce highly diverse and antigen-specific B cells. After the encounter with an antigen, B cells differentiate into their terminal form as plasma cells.¹⁰³

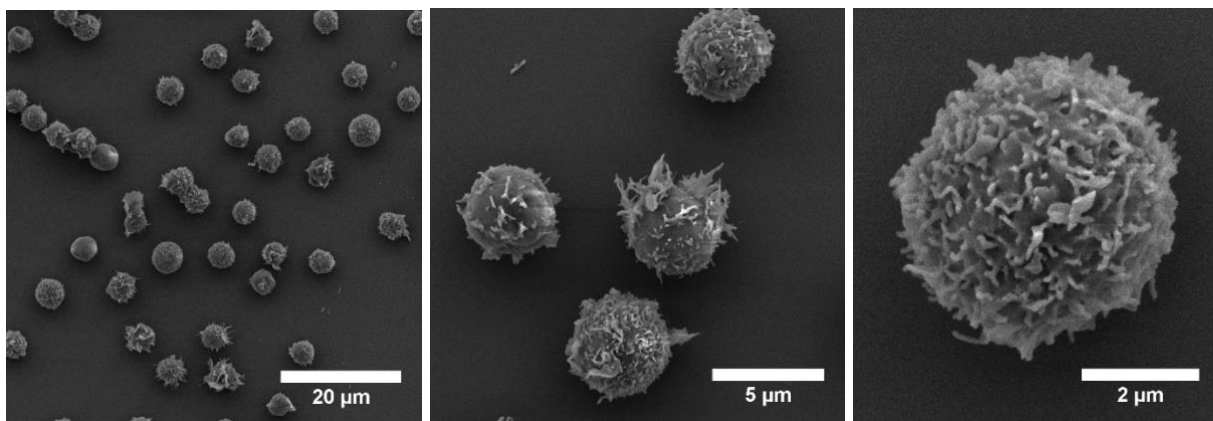


Figure 3: Human peripheral blood B lymphocytes. Images were taken with a scanning electron microscope (SEM) at magnifications 4000 x, 15000 x and 34000 x (left to right). CD19⁺ B cells were isolated from human buffy coats of healthy donors with magnetic-activated cell sorting. SEM B cell samples were prepared with alternative drying protocol previously described.¹⁰⁴ SEM B cell samples were spin-coated with 4 nm gold layer prior SEM analysis.

A majority of the mature B cells are residents of secondary lymphoid organs (*e.g.*, spleen, lymph nodes) where they diverge into distinct subsets, based on their function and anatomical localization: transitional, follicular, marginal zone, B1, regulatory B10 and memory B cells. The key B cell lineage markers are CD20 (B220 in mice) and CD19.¹⁰⁵

Antigen-activated follicular B cells, with the help of T helper cells, form germinal centers inside B cell follicles, where they undergo clonal expansion, class switch recombination (constant region) and somatic hypermutations (variable region). Isotype switching provides a great B cell plasticity, which is important for fighting numerous types of infections at different sites of the body. On the other hand, supermutations of the variable region assure great specificity and high affinity of BCR with the antigens.⁵⁹ These processes lastly drive B cell differentiation into antibody-producing, long-lived plasma cells and memory B cells. The immunological memory of B cells is responsible for generation of fast and efficient B cell immune responses after secondary activation with cognate antigen.¹⁰⁶

General Introduction

Subsets of B cells, such as marginal zone cells and B1 cells, can participate in T cell-independent immune responses. These innate-like responses are initiated with T cell-independent antigens. This includes polyvalent antigens that can cause the engagement of both, TLRs and BCRs. T cell-independent B cell activation results in differentiation into short-lived plasma cells, with faster but low affinity antibody response.¹⁰⁷ B cells are as well characterized as professional APCs, which in comparison to other APCs recognize and internalize specific antigens through BCR. Processed antigens are then loaded on MHC II and presented to T cells. It has been shown that B cells are able to prime naive T cells alone, without help other APC types. However, engagement of co-stimulatory receptors on B cell with surface ligands on T cell is crucial for B cell maturation into fully functional APCs.¹⁰⁸

7. Immunological properties of engineered nanoparticles

One of the first nanotoxicological studies implemented mainly occupational inhalation based exposures with NPs (*e.g.*, ultrafine titanium and aluminum particles).⁹⁴ It became clear that innate immune cells such as alveolar macrophages play an important role in inflammatory responses against inhaled ultrafine particles. Therefore, the questions about the appropriateness of engineered NPs for the use in the field of nanomedicine raised with regard to their immuno-toxic potential. To this day, there are numerous studies defining the immunological potential of NPs of various types.¹⁰⁹

7.1 Innate immune response towards NPs

ROS production triggered by NPs can cause interference with inflammatory signaling pathways. For example, redox-sensitive pro-inflammatory transcription factors such as NF- κ B and activating protein-1 (AP-1) are readily manipulated by ROS. Consequently, this can result in increased production of (pro-)inflammatory cytokines (*e.g.*, TNF- α , IL-6, IL-8).¹¹⁰ Certain NPs (*e.g.*, titanium and silica NPs) were shown to initiate ROS-related activation of NLRP3 inflammasome and production of IL-1 β in human and mouse macrophages.¹¹¹ Production of immune mediators is not necessarily conditioned by the NP uptake and can be potentially triggered directly through electrostatic binding of NPs to cell membrane receptors. For instance, single-walled carbon nanotubes (SWCNT) caused the production of CCL5 chemokine *via* TLR2 and TLR4 activation in human monocyte-derived macrophages (MDMs) in protein-free conditions.¹¹²

On the other hand, certain types of NPs can elicit immunosuppressive action in macrophages and dendritic cells. GNPs are known for their anti-inflammatory properties by interaction and inhibition of NF- κ B constituents.¹¹³ Likewise, C₆₀ fullerenes at lower concentrations have shown antioxidant properties by directly depleting nitric oxide.¹¹⁴

General Introduction

Indeed, the immunogenicity of NPs strongly depends on the combination of factors described in chapter 3 (NP characteristics, bioenvironment, biological model, *etc.*). Therefore, some contradictory results can be found among otherwise seemingly similar NP characteristics, which is most probably the result of differently optimized experimental conditions. Innate immune cells, such as macrophages and dendritic cells, have been extensively studied in nanotoxicology due to their role as the first responders in the defense against foreign material. Therefore, current literature is dominated by studies focused on innate immunity. To emphasize this, Table 3 summarises only some of the studies that cover numerous types of different NPs and their immunological impact based on NP physico-chemical characteristics and type of innate immune cell used.

General Introduction

Table 3: Examples of different nanoparticle immunological and cytotoxic properties on different innate immune cell types and with regard to NP composition, physico-chemical characteristics and exposure concentrations.*

Type of NP	Size	Concentration	Surface Chemistry	Surface charge	Biological model	Immunomodulatory/toxic effects
GNPs ¹¹⁵	Spheres: 4,11,19,35 and 45 nm	10-50 ug/ml	PEG	n/a	Mouse macrophages (RAW 264.7)	No toxicity, inhibition of NF- κ B and JNK pathway and TLR9 function predominantly by 4 nm NPs (40 ug/ml)
GNPs ¹¹⁶	Rods with high AR	0.5-50 ug/ml	/	49.1 mV	Human dendritic cells (MDDCs)	No toxicity or activation of immune activation markers (CD40, CD80, CD83, CD86)
GNPs ¹¹⁷	Spheres: 2-40 nm	1 and 10 ug/ml	/	-60 mV	J774 A1	Size- and concentration- dependent cytotoxicity and decrease in proliferation. Upregulation of IL-1, IL-6 TNF- α genes with smaller NPs (1-10 nm)
GNPs ¹¹⁸	Spheres: 15 nm	20 and 100 ug/ml	PEG, PEG-COOH, PEG+PVA-COOH, PEG+PVA-NH ₂ , PVA-COOH or PVA-NH ₂	Negative (-30 mV) or positive (7 mV)	Human dendritic cells (MDDCs)	Concentration-dependent toxicity (PVA-NH ₂); increased TNF- α (PEG-COOH) and increased IL-1 β (PVA-NH ₂ and PEG+PVA-NH ₂)
GNPs ¹¹⁹	Spheres: 13 nm	0.17, 0.85 and 4.26 mg/kg, i.v.	PEG	n/a	BALBc mice	Acute inflammation in the liver (an increase of IL-1 β , IL-6, IL-10, IL-12 β and TNF- α)
Fe ₂ O ₃ ¹²⁰	Spheres : 22 and 280 nm	0.8-20 mg/kg (inhaled)	/	n/a	Rat	Dose dependent and size independent increase of ROS production, inflammation in lungs
Ag NPs ¹²¹	Spheres: 5, 25 and 100 nm	0.5-6.25 ug/ml	/	-9 mV (5 and 25 nm) 2 mV (100 nm)	Human monocytes	Size dependent inflammasome activation and IL-1 β production (5 and 25 nm)
Ag NPs ¹²²	Spheres: < 100 nm	1-100 ug/ml	/	n/a	Human macrophages (THP-1)	Dose dependent IL-8 release; different NP reactivity of BSA vs human serum
ZnO ¹²³	Spheres: 20 or 100 nm	<i>In vitro</i> : 2.5-80 ug/ml <i>In vivo</i> : 750 mg/kg/day (oral)	/	-40-80 mV	Mouse macrophages (RAW 264.7) and C57BL/6 mice	<i>In vitro</i> and <i>in vivo</i> size and surface charge-dependent toxicity and immunosuppression of IL-1 β , TNF- α , IL-10, IFN- γ , IL-12p70
TiO ₂ ¹²⁴	Spheres: 20 nm	2.5-80 ug/ml	BSA	negative	Mouse macrophages (RAW 264.7)	Apoptosis and increased TLR4/9/12/13 activation through ROS production
MWCNTs ¹²⁵	Length: 0.5-2 um Width: 8 - 50 nm	100 ug/ml	/	n/a	Mouse macrophages (RAW 264.7)	Size-dependent cytotoxicity apoptosis and ROS production
MSNs ¹²⁶	50,100 and 250 nm	25-1000 ug/ml	/	Positive (50, 100 and 250 nm) and negative (100 nm)	Human macrophages (THP-1)	Charge and size dependent cytotoxicity activation, ROS production and inflammatory genes activation through NF- κ B and AP-1 (positive charge, >100 nm NPs)
SiO ₃ NPs ¹²⁷	150, 250, 500 and 850 nm	1000 particles /cell	COOH	-60 mV	Mouse macrophages (RAW 264.7)	Size-dependent cytotoxicity, inflammation and ROS production (850 nm)
PLA NPs ¹²⁸	900 nm	50-500 ug/ml	Chitosan, chitosan hydrochloride or polyethyleneimine	-20-30 mV	Mouse macrophages (RAW 264.7)	No cytotoxicity
PLGA NPs ¹²⁹	100-200 nm	1-400 ug/ml	PVA, chitosan, PF68	-20, -5 and 30 mV	Human (MDDCs) and mouse (BMDCs) dendritic cells	No cytotoxicity; surface functionalization-dependent MAPK pathway activation, cytokine release. Higher activation in human cells

*MWCNTs: multi-walled carbon nanotubes; MSN: mesoporous silica nanoparticles; PLA NPs: poly(lactic acid) NPs; PLGA: poly(lactic-co-glycolic acid) NPs; PEG: polyethylene glycol; PVA: polyvinyl alcohol; BSA: bovine serum albumin; PF68: stabilizer; RAW 264.7 and J774A.1: mouse macrophage cell lines; MDDCs: monocyte-derived dendritic cells, THP-1: human monocyte cell line; BMDCs: bone marrow-derived dendritic cells

7.2 Adaptive immune response towards NPs

7.2.1 Cellular immune response

NPs efficiently help to activate adaptive immune response by delivery of antigens and adjuvants as therapeutic and prophylactic vaccines.¹³⁰ Although, very little is known about how the cells of adaptive immune response are affected by NPs alone, in non-therapeutic or off-target circumstances. T cells have been shown to be mainly affected by NPs indirectly because their phagocytic abilities are poor and their immune activation strongly relies on the help of APCs. Thus, the inflammatory signals from DCs caused by NPs showed to be most likely responsible for the activation of naïve T cells and the initiation of their proliferation. Moreover, depending on the APC reaction to NPs, this can then change the ratio between Th1/Th2/Th17 responses.¹³¹

7.2.2 Humoral immune response

Immunogenicity is the ability of a substance to elicit a humoral or cellular immune response. Antigenicity, on the other hand, is ability of a substance or antigen to specifically bind to the products of the immune response – antibodies. Haptens are small molecules, which unless they are bind to a carrier (*e.g.*, protein), cannot initiate immune response on their own. Hence, they are not immunogenic. However, haptens are antigenic as they are able to specifically bind to antibodies.⁵⁹ Similarly, NPs are not considered highly immunogenic due to their small sizes. However, studies suggested that some smaller NPs (C₆₀ fullerene derivatives and dendrimers) are able to elicit production of NP-specific antibodies only when conjugated to a protein carrier. This property of NPs resembles one of the haptens.^{132,133} On the contrary, NPs can act as a carrier for haptens or antigens in order to induce or enhance their immunogenicity and are in this sense considered as adjuvants.¹³⁴

In recent years, the production of anti-PEG specific antibodies has been reported as the result of repeated exposure to PEGylated medicines. Drugs such as PEGylated liposomes (Doxil), asparaginase (Oncaspar) and uricase (Krystexxa) showed to be involved in the production anti-PEG.¹³⁵ PEG-specific antibodies are responsible for the rapid clearance of PEG-coated products through a phenomenon called accelerated blood clearance (ABC).¹³⁵ Therefore, more research is being conducted to understand the mechanism behind anti-PEG antibody production in treatments with PEGylated NPs. For instance Shimizu *et al.*, reported that marginal zone B cells are most likely the facilitators for the production of anti-PEG IgM after second administration of PEGylated liposomes in rats. The authors showed that binding of anti-PEG to liposomes triggered complement activation. This resulted in formation of immune complexes of liposomes-anti-PEG-complement, which were recognized by marginal B cell complement receptors but not by BCR or IgM Fc receptors.¹³⁶ This emphasizes the probability of complement system involvement in the anti-PEG production and consequently the ABC.

General Introduction

B cells are crucial players in the humoral immune response. Therefore, it is important to evaluate possible off-target effects of nanomedicines on B cells as well as to better understand B cell involvement in the NP-cell interactions and their impact on the immune response. It has been reported that polymer-free GNPs were internalized and caused antibody secretion through activation of the NF- κ B pathway in a B cell line.¹³⁷ Another study also reported increased IgG production in myeloma-splenic cell hybrids after exposure with PEGylated GNPs.¹³⁸ This increased antibody secretion was shown to be a result of GNP interference on expression of transcriptional regulators (B lymphocyte-induced maturation protein (blimp)-1 and paired box protein (pax)-5), responsible for antibody production and B cell lineage development. However, the authors did not investigate whether these exact mechanisms are as well affected in primary B cells or *in vivo* as the “artificial” B cell models used in these studies do not efficiently reflect the natural B cell immune response. Differently, Dutt *et al.*, focused on toxic effect of SWCNT on B cells *in vivo*. The authors showed that SWCNT were significantly internalized by LPS-activated B cells, which resulted in their increased cell death. Nevertheless, this study did not look into the B cell immune response that might accompany decrease in B cell viability.¹³⁹

These limited reports indicate a lack of information about how NPs interact with B cells and how they interfere with their important immune function. Therefore, further studies are needed to fill the knowledge gap to fully evaluate the safety of NPs not only for the innate immune system but as well for the adaptive immunity. Understanding the potential adverse effects of NPs on B cells and their function is important from two major perspectives. Firstly, in the development of NPs for the purposes of immunotherapy and vaccination, where B cells are often a key target and secondly in other NP applications where B cells can suffer from potential off-target impact by NPs.

8. Nanoparticles and the modulation of the immune response

Due to the size range resemblance between NPs and viruses and their ability to enter the host cell, the idea for using NP-based vaccines emerged. Thus, NPs turn out to be beneficial as part of formulations for vaccines, achieving improved delivery of antigens and adjuvants to the immune cells. Moreover, easy manipulation of the NP surface with specific antibodies can turn them into active drug carriers for the treatment of different autoimmune conditions and malignancies.

8.1 Nanovaccines

Nanovaccines are a type of nanomedicines, where NPs are conjugated or loaded with specific antigens, adjuvants, DNA or RNA molecules in order to target and stimulate cells of the immune system and consequently protect our body against pathogens or treat cancer.^{140,141}

General Introduction

One of the first approaches of nanovaccine development was studied in the 1970's, where Birrenbach and Speiser prepared and tested approximately 80 nm polymerized micelles encapsulating an antigen such as tetanus toxoid.¹⁴² Shortly after, natural and self-assembling virus-like particles (VLPs) gain an interest in vaccinology. VLPs, 20-800 nm in size, are able to mimic the structure of a virus. They are formed from capsid proteins of a virus and carrying specific antigens, but do not include viral RNA or DNA and are, therefore, not infectious.¹⁴³ There are several VLP-based vaccines on the market, with the first VLP vaccine for hepatitis B commercialized in 1986. Currently, novel *in silico* approaches are arising in order to engineer well-optimized VLP vaccines and predict their efficacy.^{144,145}

With the success of VLPs, numerous NP types are now being applied for vaccine delivery purposes such as polymer-based NPs, GNPs, carbon-based NPs, silica NPs, liposomes, *etc.* (Figure 3).¹³⁴ Thus, engineered NPs offer novel possibilities to achieve the most efficient vaccine delivery by tuning NP characteristics and using their unique properties.

NP-based vaccines have been claimed to have several advantages over traditional vaccines:^{146–148}

- NPs provide better stability for poorly soluble peptide antigens
- NP improve low immunogenicity of certain antigens such as haptens
- Controlled antigen loading on/in the particle
- Targeted delivery of vaccine (*e.g.*, NPs coated with cell-specific ligands)
- Co-delivery of several immunostimulants (*e.g.*, multiple adjuvants and antigens)
- Conditional release of vaccine components (*e.g.*, pH-dependent)
- Reduced systemic side effects of adjuvants

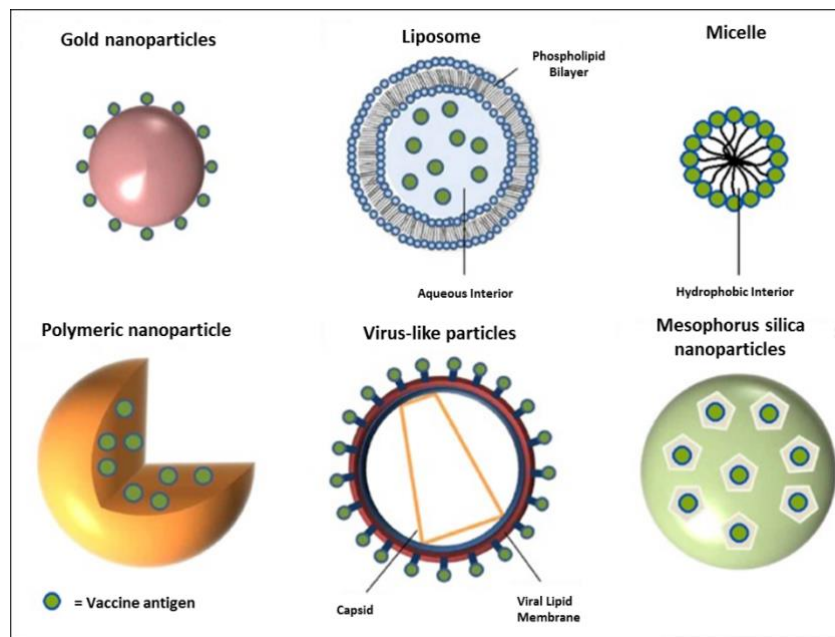


Figure 4: Examples of different formulations of NPs used as vaccine delivery systems. (Adapted from Smith et al., *Curr. Opin. Biotechnol*, 2015¹⁴⁹)

8.2 Nanoparticles and B lymphocytes in health and disease

In vaccine development, an enhanced antigen presentation capacity to the T cells and induction of a strong B cell effector function is crucial and heavily relies on the immunogenicity of the specific antigen. The latter also depends on the antigen form that B cells come across with. It has been shown that antigen-specific B cells became dominant APCs when antigens were displayed on NPs, in contrast to free antigens, where dendritic cells took over the role in antigen-presentation.⁸⁴ Exposing antigens on the surface of the NPs serves as an advantage, as NP-bound antigens cause a cross-linking of BCRs (gathering of several BCRs on the cell surface). This results in a stronger BCR-dependent signaling and a more potent interaction with T helper cells (Figure 4). Furthermore, addition of TLR agonists (*e.g.*, CpG) to the nanovaccine formulation caused activation of B cells through TLRs, which led to faster, both T cell-independent and -dependent antigen-specific antibody responses.¹⁵⁰ Thus, several antigen/adjuvant carrying NPs such as lipid NPs, poly(lactic-co-glycolic acid) (PLGA) NPs, calcium NPs, VLPs and GNPs were shown to improve specific antibody production against pathogens such as influenza viruses, Simian immunodeficiency virus (SIV), West Nile Virus (WNV), human immunodeficiency virus (HIV) and others.^{47,140,151}

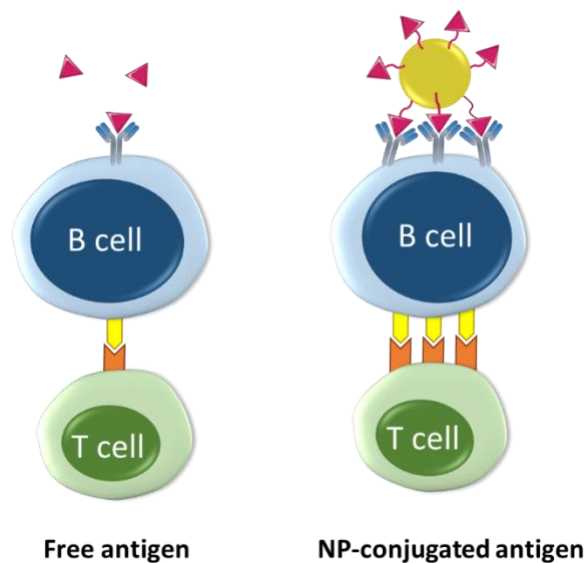


Figure 4: The principle of B lymphocyte activation by NP-antigen conjugate, compared to the free antigen. After B cell binds a free antigen to its receptor, moderate activation of T cells is induced (left). On the other hand, antigens conjugated with a NP cause cross-linking of BCRs, which results in enhanced B cell activation and consequently leads to a strong T cell activation (right). (Inspired by Rappuoli & Serruto, *Cell*, 2019¹⁵²)

Because B lymphocytes play an important role in humoral immunity, a failure in their function can contribute to the development and progression of several autoimmune conditions. As NPs showed to be a successful B cell-delivery tool for prophylactic vaccines, the same approach has been applied for therapeutic purposes involving pathological B cells. B cell-targeting therapy with NPs, therefore, improves the potency of the treatment. For example, B lymphocytes contribute to an autoimmune

General Introduction

reaction against myelin basic protein (MBP) in the development of multiple sclerosis.¹⁵³ It has been shown that targeted delivery of MBP fragments encapsulated in liposomes decreased the production of auto-antibodies as the defective B cells developed MBP tolerance. Consequently, the progression of the disease was significantly suppressed.¹⁵³ Following a similar principle, PLGA NPs were used as peptide carriers to target autoreactive B cells in rheumatoid arthritis (RA).¹⁵⁴

There are several B cell-targeting drugs used in clinical practice, anti-CD20 being one of the most pronounced ones. For instance, rituximab is a monoclonal antibody drug that causes CD20⁺ B cell depletion and is used for the treatment of non-Hodgkin's syndrome, chronic lymphocytic leukemia and RA.¹⁵⁵ Mesoporous silica NPs have been loaded with a cytostatic drug (doxorubicin) and equipped with rituximab. This anti-tumor delivery system helped to avoid systemic toxicity of chemotherapeutic by direct targeting of malignant B cells.¹⁵⁶ Furthermore, NP can be used for diagnostics and monitoring of the efficacy of the treatment. For example, NPs conjugated with fluorescent ligands and B cell-specific antibodies were used to improve *in vivo* visualization of B cell malignancies.¹⁵⁷ Taken together, B cells as important immunological protectors are target of interest in health and disease. NP applications are, therefore, a convenient tool for more efficacious modulation of B cells and their function.

9. Gold nanoparticles

GNPs become an attractive nanomaterial in nanomedicine due to their easy and non-expensive preparation, unique and therapeutically-beneficial physico-chemical properties, and high biocompatibility. Their high usefulness in both, diagnostic and therapy, has advantages over some other nanomaterials, so they present a strong candidate as a theranostic tool. Moreover, their immunosuppressive properties are also appreciated in the treatment of autoimmune diseases. The comprehensive pre-clinical studies of GNPs are showing, in general, absence of toxicity and are now slowly breaking into the clinical research.¹⁵⁸

9.1 Synthesis

The beginning of the synthetic colloidal gold particles began in 1951 when Turkevich *et al.* developed the method for GNP synthesis, which involves a reduction of hydrogen tetrachloroaurate (HAuCl₄) with sodium citrate (Na₃-citrate) in boiling water.¹⁵⁹ Fren later improved the method, with optimization of the particle sizing. This was achieved by defining the chloroauric acid/citrate ratio. Sizes between 1-100 nm can be reached using this method. GNP solutions give their typical color depending on the particle size range. For smaller particles orange (~15 nm), then red for 20-40 nm, dark red for ~70 nm and violet for ~100 nm GNPs.¹⁶⁰ Besides gold nanospheres (GNS), the variety of GNP shapes can be

General Introduction

produced, using different synthetic protocols (nanorod, nanocage, nanoshell, nanostar, nanoplate, nanocube, *etc.*) (Figure 5).

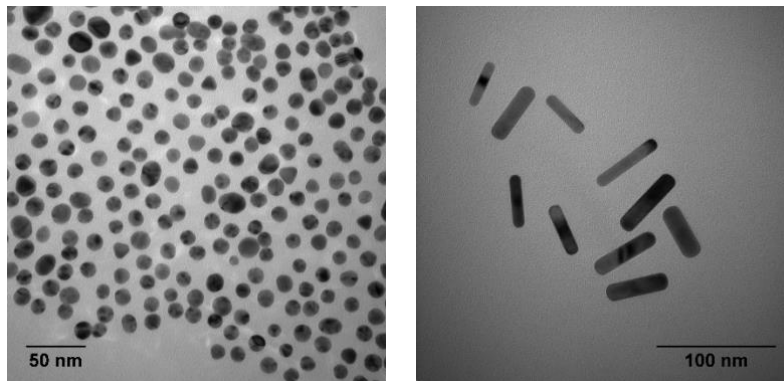


Figure 5: PEGylated gold nanospheres and gold nanorods. Gold nanospheres were synthesized by following Turkevich *et al.* protocol and gold nanorods by seed-mediated growth method, followed by coating with PEG.^{159,161} Transmission electron microscope (TEM) samples were prepared as described by Hocevar *et al.*¹⁶¹

9.2 Properties

GNPs have a high atomic number (79) and high electron density (19.32 g/cm^3) that give them strong capabilities as a contrast agent.⁵ GNPs are well-known for their unique and tunable optical properties. Thus, colloidal GNPs are able to absorb light at approximately 520 nm wavelength, depending on their size. This absorbance is based on the ability of surface plasmon resonance (SPR). SPR is a phenomenon that occurs due to the light-induced oscillation of conductive electrons across GNPs. SPR absorbance bands can be shifted not only due to the increase in size but also because of a different shape. Gold nanorods, for example, have their distinct double bands, indicating transversal ($\sim 520 \text{ nm}$) and longitudinal (600-1800 nm) SPR. Further, GNPs possess plasmonic photo-thermal (PPT) properties as the absorbed light by GNPs is converted into heat due to electron-electron and electron-photon relaxation.¹⁶²

9.3 Applications

9.3.1 *In vitro* and *in vivo* diagnostics

Colloidal gold has been already used for immunochemistry purposes in the '70s. By attaching specific antibodies on the gold surface, they serve an immunochemical marker, visualized with electron microscopy (*e.g.*, TEM). Today GNPs are used as bioimaging agents in other state-of-the-art technologies such as confocal microscopy, two-photon microscopy, photoacoustic imaging, and surface-enhanced Raman spectroscopy imaging. GNPs, therefore, serve as a sensitive detector and provide a strong signal, which is an advantage over the quenching side effect of fluorescent labels.¹⁵⁸

General Introduction

GNP can serve as a convenient and simple biosensor for analytical diagnostic methods. Specific biomolecules such as proteins or DNA can be detected with antigen-coated or oligonucleotide-conjugated GNPs, respectively. The detection of the analyte is most commonly based on the change of the GNP agglomeration status (red-shift in the spectrum) or change in the absorption spectrum after analyte attachment. This is measured by the spectrometric method or simply visualized by the change of color.¹⁵⁸ Unmodified GNPs can be a sensor on its own. They have been presented as a tool for fast and simple *in vitro* diagnostic tests for cancer. This was achieved through distinct GNP-cancerous DNA interactions, which can be detected spectrophotometrically.¹⁶³ Furthermore, the great surface properties and simplicity of GNPs allowed their breakthrough in clinical practice as an *in vitro* diagnostic tool for Alzheimer's disease, hepatitis B, HIV, diabetes, and others.¹⁵⁸

Due to distinctive optical properties and high electron density, GNPs are used as a sensitive contrast agent in CT and X-ray imaging *in vivo*. Their contrast property can be combined with a cell-specific targeting. For example, conjugation with a ligand such as folic acid orientate GNPs towards the tumors, locate, visualize and treat them.¹⁶⁴

9.3.2 Therapy

The ability of GNPs to excite heat gain high interest for their use in plasmon photothermal therapy (PPTT). The most common PPTT application with GNPs is for the treatment of solid tumors. The principal of the therapy is based on the systemic administration of GNPs, which either passively or actively (*e.g.*, coated with tumor-specific antibodies) reach the tumor site. Followed by irradiation of tumors with laser pulses, GNP-associated cancer cells undergo hyperthermia and consequently cell death. Gold nanorods are especially desirable in these types of therapy as they absorb light in the near-infrared spectrum and allow the light to reach deeper in the tissue. Besides cancer treatment, PPTT with GNPs can be also used for the treatment of other pathological conditions such as atherosclerosis. The latter was achieved by placing a bioengineered patch with GNPs on the site of affected artery. Artery plaques were disrupted with intra-vessel near-infrared laser, resulting in reduction of total atheroma volume.²³ Another application of GNPs in therapy was presented by Saha *et al.*, where GNPs showed the ability to activate endoplasmic reticulum stress. This resulted in decreased secretion of growth factors and cytokines in tumor cells, which caused inhibition of tumor cell proliferation and blocked cross-talk with stromal cells.¹⁶⁵

Besides therapeutic properties in cancer treatment, GNPs are proved to be useful as a drug delivery system and are widely applied for the delivery of anti-cancer drugs. For example, GNP-rhTNF conjugate was used for more efficient treatment and reduction of toxicity of the free drug, which successfully passed phase I clinical trial.¹⁶⁶ Furthermore, another GNP-based drug was recently approved by the

General Introduction

FDA as an investigational new drug. The drug is based on 13 nm PEGylated GNS conjugated with interference RNA to target and eliminate glioblastoma and is currently in phase I clinical trial.¹⁶⁷ Taken together, GNPs are a well-appreciated theranostic tool in the biomedical field because of the combination of diagnostic ability, drug delivery and therapeutic potential.

9.3.3 GNP applications in immunology

Antibodies are an ideal tool for the use in diagnostics, biological research and treatment.¹⁶⁸ However, the preparation of antibodies against low-molecular-weight antigens is facing challenges. Antigens like haptens are not able to elicit antibody production on their own. Therefore, preparation of antibodies *in vivo* against weak antigens is solved by attaching them to a compound of higher molecular weight (*e.g.*, protein). This provides better immunogenicity of the antigen, therefore better antibody production by the animal model. Nevertheless, protein carriers can be immunogenic, causing secretion of unwanted antibodies against the carrier itself. This leads to low antigen-specific antibody yield and needs further purification steps. As GNPs lack the immunogenic potential they can provide high and pure antibody titer, compared to the use of traditional adjuvants and protein-based antigen carriers.⁸¹

For prophylactic purposes GNPs have been to this day widely used in nanovaccine applications and serve as an efficient delivery system for adjuvants or immunostimulators (*e.g.*, CpG, R848) and antigens to the immune cells.^{169–171} Besides protein antigens, they have been successfully used as a carrier in DNA immunization. For example, gold nanorods were acting as an adjuvant, when delivering HIV DNA to DCs. Consequently, T cell and B cell responses were activated more efficiently than HIV-1 Env plasmid alone.¹⁷²

The antioxidative property of GNPs was observed already in the early years of 20th century. Gold salts were used as a standard practice to treat RA by direct injection into the affected joints.¹⁷³ In the '90s the treatment with gold was slowly dropped due to adverse effects and more prominent novel drugs.¹⁶ Nevertheless, the progress in nanotechnology with controlled GNP physico-chemical manipulation and improved surface biocompatibility pushed GNPs further into research for the benefits in arthritis treatment.¹⁷⁴ Today, colloidal gold solutions (~3.2 nm) or tablets (< 20 nm) are commercially available as a food supplement in order to help with the swollen joints and are presented as safe and non-toxic (*e.g.*, Aurasol, Mesogold).^{175,176} Nevertheless, the treatment of other autoimmune diseases with GNPs is currently under investigation. Gold nanocrystals are in phase II clinical trial for the treatment of multiple sclerosis based on the ability of GNPs to promote differentiation of oligodendrocytes and an increase in axon myelination.¹⁷⁷

9.3.4 Considerations and perspectives

GNP potential cytotoxicity has been studied for over 20 years *in vitro* and *in vivo*, which strongly suggests that they are not causing any severe adverse effects.¹⁷⁸ Therefore, GNPs are considered highly inert and biocompatible compared to some other types of NPs. This is reflected in their increased use as biomedical applications in clinical trials. Nevertheless, there is still some controversy about GNP toxicity, where some studies showing adverse outcomes, such as inflammation and apoptosis.¹⁷⁹ Some of these negative effects can be a consequence of poor characterization and GNP optimization, lack of surface stabilization, high doses, *etc.* Additionally, as an inorganic material, GNPs have more difficulties reaching human trails, compared to biodegradable NPs. Their lack of biodegradability and longer accumulation in the system is indeed considered as their weak point. However, the continuous research of the beneficial properties of GNPs and their potential as theranostic tools prove that they are still strong candidates for future therapies. In order to assure their better translation to the clinic, further studies are needed in order to understand every aspect of GNP properties and how they affect specific biological systems, their mechanisms and function.

OBJECTIVES OF THE THESIS

GNPs have been extensively studied for various diagnostic and therapeutic purposes because they possess some unique and beneficial properties. The assurance of their safety is crucial for their future use in nanomedicine. Indeed, there is an awareness of the importance to understand the potential interferences of NP applications with biological systems, the immune system being one of the most important ones. Whereas the knowledge about the biocompatibility of GNPs with the innate immune cells has been generally well established, there is a lack of information about their impact on the cells of the adaptive immune system such as B lymphocytes. Therefore, the aim of this thesis was to investigate if a set of GNPs with different shape and surface functionalization (i) have a potentially lethal effect on B cells, (ii) if GNPs are taken up by the B cells, and (iii) if GNPs cause any modulations of the immunological function of B cells. It was hypothesized that the GNPs will elicit different activation and immune responses in B cells, based on their specific physico-chemical GNP properties, such as polymer coating and shape, *in vitro* and *in vivo*.

The specific objectives of the project are divided into three parts, based on the biological model:

Part I - Human B cells *in vitro*: The aim of the first part of the thesis was to investigate interactions (*e.g.*, internalization and localization) of the set of GNPs with primary human B cells and evaluate their potential adverse effects (*e.g.*, cytotoxicity) as well as their potential manipulation with B cell innate-like immune response *in vitro* (*e.g.*, pro-inflammatory response).

In order to obtain this information, citrate-stabilized gold nanospheres (GNS) were synthesized with ~15 nm gold core, followed by coating with polyethylene glycol (PEG) or combination of polyvinyl alcohol (PEG/PVA) to ensure their colloidal stability. PEGylated gold nanorods (GNRs) were also synthesized to include the NP shape variety. GNPs were extensively characterized for their physico-chemical properties (*e.g.*, size, aspect ratio, surface charge) as well as their stability in a protein-rich environment. The latter was important in order to evaluate the potential contribution of GNP-biological environment interactions on GNP stability.

A pure B cell culture was obtained from human buffy coats of healthy donors. Cells were exposed to GNPs at increasing concentrations for a short period of time (24 h), to determine an early impact of GNPs on B cells. Additionally, cells were simultaneously treated with or without a known adjuvant. This allowed the comparison of the effect of the GNPs on the activated vs unstimulated B cells. Importantly, the effect of the absence (citrate-stabilized GNS) or presence of different protective polymers (PEG and PEG/PVA) as well as the shape (sphere vs rod) was compared with regard to GNP

Objectives of the Thesis

internalization and localization, (pro-)inflammatory cytokine production and expression of immune activation markers.

From this first part of the thesis, it was explained as to how the panel of physically and chemically different GNPs affect primary human B cell activation, internalization and if they potentially interfere with the innate immune response in the presence of a known adjuvant.

Part II - Mouse B cells *in vitro*: The aim of part II was to investigate if GNPs impact B cells isolated from mouse lymphoid organs (*e.g.*, spleen, lymph nodes). Similarly to part I, the aim was to evaluate the interactions of GNP with B cells, GNP cytotoxic potential and how they influence mouse B cell innate immune response.

A set of differently formulated PEGylated GNS (~15 nm) with a fluorescent tag was introduced in order to follow the GNP biodistribution across different B cell subtypes. The purified mouse B cells were exposed to GNPs and analyzed for potential GNP effects at different time points (up to 24 h). Again, this was performed in a presence or absence of a known adjuvant in order to compare GNP impact on activated vs nonactivated B cells.

From the results obtained within part II, it was evaluated as to how GNPs specifically interact with mouse B cells and potentially affect mouse B cell innate-like immune response (*e.g.*, cytokine production and antigen-independent antibody production). Moreover, this information also served as a pre-evaluation of the appropriateness of the GNP formulation in order to proceed with *in vivo* experimentation.

Part III- Mouse *in vivo*: The aim of the third part was to investigate whether GNPs influence B cell innate and adaptive immune response *in vivo*. Additionally, the aim was to evaluate the GNPs biodistribution within different organs (spleen, lymph nodes, liver) and blood to determine which B cell subsets are the most prone to physically interact with GNPs *in vivo* and how this is related to potential changes in B cell function.

A fluorescently labeled and PEGylated GNPs (~15 nm) were used in order to track their biodistribution. Different administration routes (intravenous and subcutaneous injection) and different incubation times were performed in order to follow B cells across different lymphoid organs (spleen, lymph nodes) over time. To determine GNP impact on innate-immune response and activation of B cells, GNPs were administered together with a known adjuvant. Whereas a known antigen and GNP were simultaneously administered in order to investigate the possible influence on B cell antigen-specific antibody production.

Objectives of the Thesis

By using a complete organism with the functional immune system it was evaluated whether (i) GNPs alone have the ability to activate B cells and whether (ii) GNPs have the ability to interfere with/modulate the innate and adaptive immune function in the presence of a known adjuvant and antigen, respectively.

Together, the results are expected to provide new information about the appropriateness of GNP-based applications for use in the clinic. It is important to identify possible adverse effects of GNPs on B cells as well as potentially beneficial GNP-B cell interactions. This will help with further consideration of the use of this type of nanomaterial in therapy and diagnostics.

RESULTS

1. Manuscript 1: Polymer-coated gold nanospheres do not impair the innate immune function of human B lymphocytes *in vitro*

The first part of my PhD project was focused on GNPs and how they interact with primary human B cells. A set of GNPs with distinct physico-chemical characteristics was tested for potential impairment of B cell viability, activation and early immune response *in vitro*.

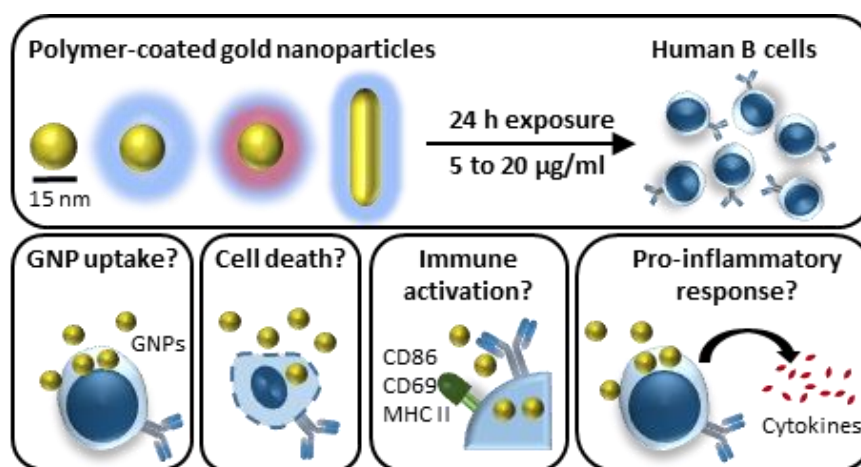


Figure 6: Graphical abstract of manuscript 1. We established a set of well-characterized GNPs of different shapes (sphere and rod) and distinct protective polymer coatings (polyethylene glycol (PEG) and combination of PEG and polyvinyl alcohol (PEG/PVA)). Human B cells were isolated from buffy coats of healthy donors and exposed to increasing concentrations of GNPs (5-20 $\mu\text{g}/\text{ml}$) for 24h *in vitro*. GNP effect on B cell uptake, viability, immune activation and pro-inflammatory immune response was investigated. (Hočevár et al., *ACS Nano*, 2019)

This study entitled “Polymer-coated gold nanospheres do not impair the innate immune function of human B lymphocytes *in vitro*” was published in 2019 in *ACS Nano* (doi: 10.1021/acsnano.9b01492). The accepted version of the manuscript is presented below, followed by supplementary information.

Polymer-Coated Gold Nanospheres Do Not Impair the Innate Immune Function of Human B Lymphocytes *In Vitro*

Sandra Hočevár^{1,2}, Ana Milošević^{1,†}, Laura Rodriguez-Lorenzo^{1,§}, Liliane Ackermann-Hirschi¹, Ines Mottas^{2,3}, Alke Petri-Fink¹, Barbara Rothen-Rutishauser¹, Carole Bourquin^{2,3,4,*}, Martin James David Clift^{1,5,*}

¹BioNanomaterials, Adolphe Merkle Institute, University of Fribourg, 1700 Fribourg, Switzerland.

²School of Pharmaceutical Sciences, University of Geneva, University of Lausanne, 1211 Geneva, Switzerland

³Chair of Pharmacology, Faculty of Science and Medicine, University of Fribourg, 1700 Fribourg, Switzerland

⁴Faculty of Medicine, University of Geneva, Rue Michel-Servet 1, 1211 Geneva, Switzerland

⁵In Vitro Toxicology Group, Swansea University Medical School, Wales, SA2 8PP, UK

ABSTRACT

Gold nanoparticles (GNPs) are intended for use within a variety of biomedical applications due to their physicochemical properties. Although, in general, biocompatibility of GNPs with immune cells such as macrophages and dendritic cells is well established, the impact of GNPs on B lymphocyte immune function remains to be determined. Since B lymphocytes play an important role in health and disease, the suitability of GNPs as a B cell-targeting tool is of high relevance. Thus, we provide information on the interactions of GNPs with B lymphocytes. Herein, we exposed freshly isolated human B lymphocytes to a set of well-characterized and biomedically relevant GNPs with distinct surface (polyethylene glycol (PEG), PEG/polyvinyl alcohol (PEG/PVA)) and shape (spheres, rods) characteristics. Polymer-coated GNPs poorly interacted with B lymphocytes, in contrast to uncoated GNPs. Importantly, none of the GNPs significantly affected cell viability, even at the highest concentration of 20 µg/ml over a 24 h suspension exposure period. Furthermore, none of the nanosphere formulations affected the expression of activation markers (CD69, CD86, MHC II) of the naïve B lymphocytes, nor did they cause an increase in the secretion of pro-inflammatory cytokines (i.e., IL-6, IL-1β). However, the absence of polymer coating on the sphere GNPs and the rod shape caused a decrease in IL-6 cytokine production by activated B lymphocytes, suggesting a functional impairment. With these findings, the present study contributes imperative knowledge towards the safe-by-design approaches being conducted to benefit the development of nanomaterials, specifically those as theranostic tools.

KEYWORDS: gold nanoparticles, B lymphocytes, nanotoxicology, innate immunity, antigen- presenting cells

INTRODUCTION

B lymphocytes, often referred to as B cells, are an important sub-population of immune cells that are found throughout the body in the blood and lymphoid organs. As the sole producers of antibodies, they are essential effectors of protective immunity against infections. B cells also regulate the function of other immune cells, such as T lymphocytes, by presenting processed antigens via the major histocompatibility complex (MHC) and by secreting various cytokines that act as immune mediators. In pathological conditions, B cell dysfunction can lead to diseases such as allergy, autoimmunity or cancer.¹ Because of their critical role in health and disease, B cells have generated increased interest in recent years as a target for drug delivery. Indeed, B cells have been successfully targeted by 80 nm lipid nanoparticles (NPs) carrying vaccines against influenza, HIV or Zika virus, or immunotherapies against allergic diseases.²⁻⁴ Despite these recent advances, the direct impact of NPs on B lymphocytes is still poorly understood. Importantly, B cells can respond in an innate, antigen-independent manner to different stimuli following activation via conserved pattern-recognition receptors, *i.e.* Toll-like receptors (TLRs). This initial innate stimulation critically modulates subsequent activation and differentiation of B cells.⁵ Thus, in consideration of the human health impact of exposure to NPs it is imperative to understand how NPs may affect B cells, including their possible cytotoxic profile, as well as their ability to modulate their innate immune function.

The immunotoxicity of NPs has, to date, been studied essentially upon myeloid immune cells such as macrophages and dendritic cells. The phagocytic nature of these cells leads to engulfment of the NPs, which in turn can promote interference with immune functions.⁶ Thus, some types of NPs (*e.g.*, carbon nanotubes, zinc oxide and silica NPs) can cause dysfunctions in cell-intrinsic mechanisms such as autophagy and increases in secretion of pro-inflammatory cytokines, which consequentially may trigger oxidative stress and potentially genotoxicity.⁷⁻⁹ To minimize the potential toxicity of NPs and to improve their half-life in the body, NP surface functionalization integrated with protective polymer surface coatings are used. Polyethylene glycol (PEG) and polyvinyl alcohol (PVA) as well as their copolymer formulation are commonly used as protectors in cosmetic products, food supplements and pharmaceuticals.^{10,11} However, use of these polymer coatings for NPs designed for therapeutic applications also has undesired effects: it may lead to the production of anti-polymer antibodies, which cause NP opsonization. This then increases clearance of the NPs and therefore affects the efficacy of treatment.¹² To better evaluate the safety of the NPs for the immune system as a whole therefore, it is important to understand distinct effects that NPs may have on different immune subsets. Moreover, direct impact of NPs on B lymphocytes is currently a significant knowledge gap in the field, evidenced by the limited literature on the topic.

Results: Manuscript 1

Among the variety of nanomaterials available, gold core-based nanoparticles (GNPs) are frequently used as nanomedical tools in therapy, diagnostics and drug delivery. The optical properties of GNPs and their high biocompatibility make them highly useful imaging tools, biosensors, and nanocarriers.¹³ Furthermore, GNPs efficiently deliver vaccines and immunotherapies to immune cells, achieving effective immune responses with low amounts of cargo.^{14,15} In view of the emerging strategies to target B lymphocytes with nanocarriers, and the lack of information about NP immunotoxicity on B cells, we have investigated here the impact of a set of well-characterized GNPs on the phenotype and function of freshly isolated CD20⁺ human B lymphocytes from peripheral blood.

RESULTS

GNPs with different polymer coatings and shapes were observed to be stable in a biological environment. To examine the impact of GNPs on B lymphocytes, we selected a panel of GNPs with different functionalizations and shapes that have previously been well characterized. Specifically, these were citrate-stabilized gold nanospheres (Citrate-GNS) and polymer-functionalized gold nanospheres coated either with PEG (PEG-GNS) or a combination of PEG and PVA (PEG/PVA-GNS), as well as PEGylated gold nanorods (PEG-GNR).^{16,17} Gold core diameters were measured by transmission electron microscopy (TEM) as 13.4±2.3, 15.7±1.9 and 14.6±1.8 nm for citrate-GNS, PEG-GNS and PEG/PVA-GNS, respectively. Dimensions of the PEG-GNR were measured at 57±12 nm x 15±3 nm, giving the aspect ratio of 3±0.8 (**Figure 1A** and **Table 1**).

UV-Vis measurements confirmed the stability in H₂O of all GNPs, as previously described (**Figure 1B**).¹⁸ Since biological media can affect NP colloidal stability,^{19,20} GNPs were incubated for 24 h at 37° C, 5% CO₂ in complete cell culture media supplemented with 10% human plasma (Roswell Park Memorial Institute 1640 medium + human plasma (RPMI+HP)) or in PBS. A loss in stability was observed for Citrate-GNS due to aggregation in culture media, as previously described.²¹ Complete aggregation of citrate-GNS was present in PBS (**Figure 1B**). In contrast, no signs of increased colloidal instability were detected for either type of polymer-coated GNS or the PEG-GNR.

To further examine their colloidal stability, the hydrodynamic diameter of GNPs in biological media was characterized (**Table 1**). Negatively charged, non-polymer coated, citrate-stabilized NPs are known to interact strongly with a protein-rich environment, leading to a change in hydrodynamic diameter due to the formation of a protein corona.^{22–24} Indeed, dynamic depolarized light scattering (DLS) results showed a strong increase in Citrate-GNS diameter in RPMI+HP compared to H₂O. For polymer-coated GNPs, the radius did not change in cell culture media, suggesting that a high-density PEG or PEG/PVA coating of the GNPs prevented surface protein adsorption.²⁵ In addition, PEG-GNR were tested for the efficiency of PEG coverage in relation to cetyltrimethylammonium bromide (CTAB)

Results: Manuscript 1

residues that might be still present from the synthesis. The results shown in **Table 1** reveal that PEGylated GNRs presented higher hydrodynamic radii than the as-synthesized GNRs: 34.8 ± 0.2 nm vs. 20.7 ± 0.3 nm. The surface grafted PEG chains can acquire either a “brush” or “mushroom” conformation. The latter mainly occurs when the attachment distance of PEG to the surface (D) is larger than the Flory radius (R_F), while the brush conformation is observed when D is smaller than R_F .²⁶ PEGylated GNRs presented a grafting coverage of 0.22 PEG molecules per nm^2 and D of 2.26 nm, as obtained by a method previously described.²⁷ This indicated that the PEG layers deposited on the GNRs possessed a brush-like conformation because the R_F for 5,000 Da PEG is 4.9 nm. This allowed us to conclude that no potential interference of otherwise toxic CTAB²⁸ remained on the surface of the GNRs.²⁹

The significance of the NP surface charge and the role that it plays in the NP-cell interface is frequently stressed.^{30, 31} We assessed the effect of the biological environment on the surface charge of GNPs and found that the charge of citrate-GNS considerably changed in RPMI+HP compared to H_2O , most likely due to the surface adsorption of the plasma protein.^{32, 33} In contrast, polymer-coated GNPs presented a slightly negative charge in both H_2O and RPMI+HP with no major change (**Table 1**). This confirms that surface charge can vary significantly depending on the GNP surface chemistry, therefore, well-designed polymer functionalization is needed in order to avoid unwanted interactions of GNPs with biological media.

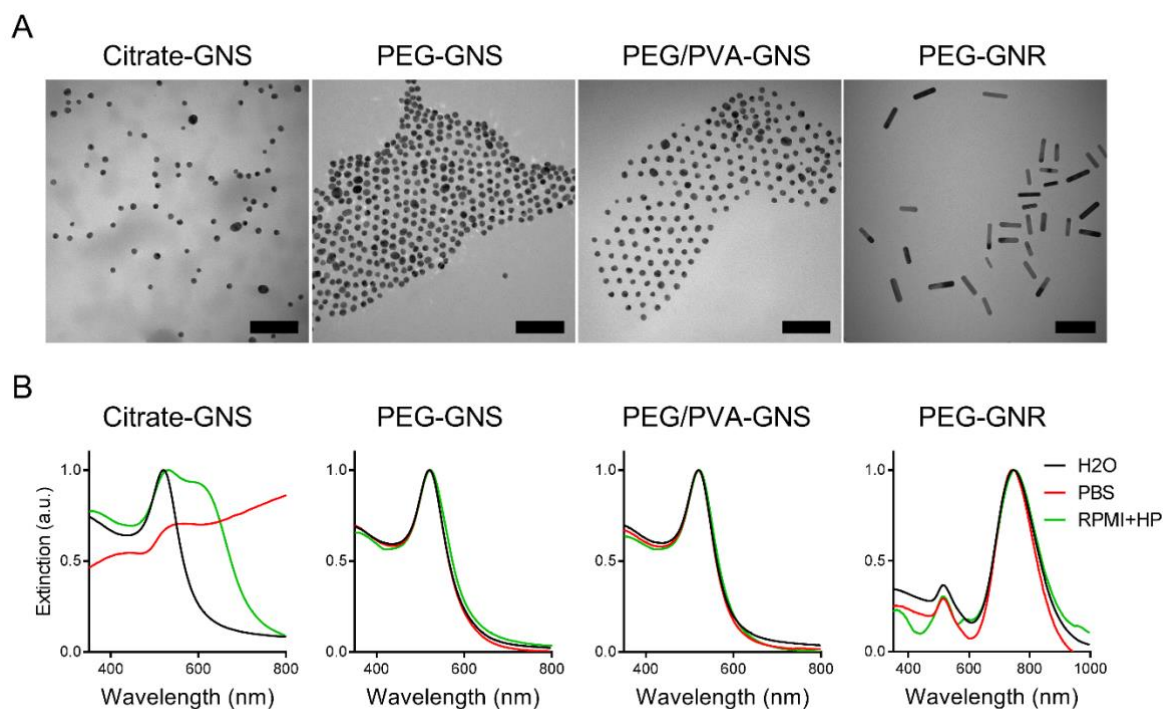


Figure 1. Characterization of gold nanoparticles (GNPs). **(A)** Representative TEM images of citrate-stabilized gold nanospheres (Citrate-GNS), gold nanospheres with a polyethylene glycol polymer coating (PEG-GNS), gold nanospheres with a combination of PEG and PVA polymer coating (PEG/PVA-GNS), and gold nanorods with PEG coating (PEG-GNR) in H₂O. Scale bars: 100 nm. **(B)** UV-Vis spectra of GNPs in different biological media. Each spectrum was normalized relative to their maximum wavelength. RPMI+HP: complete culture medium consisting of Roswell Park Memorial Institute 1640 with 1% Penicillin/Streptomycin, 1% L-Glutamine and 10% human plasma.

Table 1. Characterization of gold nanoparticle size and surface charge in complete culture medium, phosphate buffered saline (PBS) and water (H₂O).

	Size (nm)			ζ -potential (mV)		
	TEM (d_c)	DDLS (d_h)		H ₂ O	PBS	RPMI+HP
		H ₂ O	RPMI+HP			
Citrate-GNS	13.4±2.3	16.8±0.1	48.0±0.5	-34.7±1.0	Aggregated	-9.7±2.1
PEG-GNS	15.7±1.9	26.8±0.3	27.1±0.2	-5.8±1.3	-6.8±0.8	-7.4±1.4
PEG/PVA-GNS	14.6±1.8	23.7±0.8	25.5±1.6	-6.5±0.9	-13.7±0.9	-8.9±1.6
PEG-GNR	Length: 57±12 Width: 15±3	34.8±0.2	33.9±0.3	-13.6±1.5	-3.4±1.7	-9.9±2.9
GNR	n/a	20.7±0.3	n/a	n/a	n/a	n/a

d_c : core diameter, d_h : hydrodynamic diameter, RPMI+HP: complete culture medium consisting of Roswell Park Memorial Institute 1640 with 1% Penicillin/Streptomycin, 1% L-Glutamine and 10% human plasma.

GNPs do not affect B lymphocyte viability. The biological impact of GNPs on immune cells varies according to their physicochemical properties. Several groups have shown that characteristics such as size, shape and polymer coating affect the toxicity of GNPs on macrophages and dendritic cells.^{34–36} To assess whether the GNPs described above impact B lymphocyte viability, total CD20⁺ human B lymphocytes were freshly isolated from the blood of healthy donors and exposed to increasing concentrations of GNPs. This cell population consists mainly of naïve B cells (65-75%), with 20-25% memory B cells.³⁷ A 24 h exposure time was selected in order to detect early B-cell responses toward GNPs. Then, cells were stained with amine-reactive fluorescent viability dye (Zombie NIR) and analyzed by flow cytometry. The polymer-functionalized GNS (PEG and PEG/PVA) as well as citrate-GNS caused no significant cell death at concentrations up to 20 µg/ml (**Figure 2A**). PEG-GNR, studied at the highest concentration of 20 µg/ml only, also did not impact B cell viability. This latter finding demonstrating that neither the type of polymer coating nor geometry impacts upon B cell viability following GNP exposure (**Figure 2B**). In addition, phase contrast images did not show decrease in B cell density nor a change in cell morphology upon 24 h GNP exposure (**Figure S1A**).

The small molecule R848 has been reported as an antigen-independent immune activator and stimulator of B lymphocyte proliferation by signaling via the receptor TLR7.^{38, 39} Importantly, B cell viability was not compromised following exposure to GNPs together with the stimulant, irrespective of their shape or functionalization (**Figure 2**).

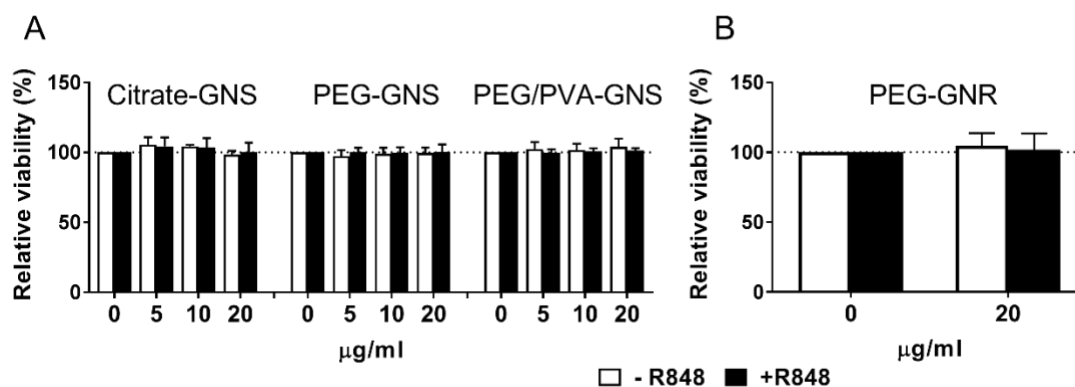


Figure 2. GNPs do not impact upon B lymphocyte viability. Viability of human B lymphocytes was determined by staining cells with Zombie NIR viability dye (1:1000) and measured by flow cytometry after 24 h exposure to GNS (5-20 µg/ml) with different surface functionalizations (**A**) or to PEG-GNR (20 µg/ml) (**B**). Cells were incubated with and without the immunostimulant R848 (2 µg/ml). Data are presented relative to control cells without GNP exposure (=100%). Data represent mean \pm SD of three separate experiments on different donors (n=3). Data were assessed by a two-way ANOVA, followed by Tukey's multiple comparison post-hoc test. The alpha value was set at 0.05.

Citrate-GNPs are taken up by B lymphocytes, but not polymer-coated GNPs. B lymphocytes are professional antigen-presenting cells and as such they have the ability to take up pathogens, in particular via B cell receptor-mediated endocytosis.⁴⁰ To examine whether B lymphocytes could take up GNPs, freshly isolated human B cells were exposed to GNPs for 24 h. The highest GNP concentration tested (20 µg/ml) was considered to be in the sub-lethal range as it did not cause significant B cell death. Therefore, it was further used in NP-cell association experiments. Macrophages and dendritic cells are professional phagocytic cells and known to easily take up NPs.⁴¹ Therefore, human monocytes-derived macrophages (MDMs) and monocyte-derived dendritic cells (MDDCs) were also exposed to the previously described GNPs under the same conditions as the B cell experiments. MDMs and MDDCs served as a control for GNP-B cell interaction as well as for comparison of GNP-B cell association across different antigen-presenting cell (APC) types.

The cells and the GNP uptake were first visualized by dark field hyperspectral imaging (DF-HSI) coupled with fluorescent detection. For citrate-GNS, which were noted to readily aggregate in biological media, clusters of NPs were clearly visible on the surface of B cells (**Figure 3A**). The particles were also detectable within the B cells themselves (**insert Figure 3A**). Citrate-GNS were further observed to be internalized by MDMs and MDDCs, as expected for these highly phagocytotic cell types (**Figure 3A** and **Figure S1B** and **S1C**). In contrast to citrate-stabilized GNS, no interaction (either internalization or cell surface association) of polymer-coated GNS with B lymphocytes was detected by DF-HSI. Similarly, PEG-GNR did not show any association with B cells (**Figure S3**). In MDMs, only a few intracellular aggregates of PEG-GNS and PEG/PVA-GNS were detected by DF-HSI (**Figure 3A**).

A subsequent approach to determine NP internalization by mammalian cells is through changes in light scattering detected by flow cytometry. This was previously reported by Zucker *et al.*,⁴² who demonstrated that the internalization of TiO₂ NPs increased side scatter (SSC) and decreased forward scatter (FSC) by epithelial cells. An increase in SSC was observed for B cells exposed to citrate-GNS, but not to polymer-coated GNS (**Figure S4**). In contrast, in MDMs and MDDCs, an increase in side scatter was observed for polymer-coated GNS. Overall, these results supported the observations collected from the DF-HSI images.

To quantify the uptake of GNPs with human B cells and to compare this to the association by other APCs, we measured the gold content within B cells and MDMs after exposure to 20 µg/ml of GNPs by using inductively coupled plasma mass spectroscopy (ICP-MS). This technique allows precise quantification of the gold ion content in biological samples.⁴³ The uptake of citrate-GNS by B cells was confirmed, with approximately 10 µg gold measured per 10⁶ cells (calculated by dividing measured GNP mass per total cell count and multiplying by 10⁶) (**Figure 3B**). This corresponds to approximately

Results: Manuscript 1

1% GNP-B cell association, as a function of measured GNP mass per total exposed GNP mass. In contrast, polymer-coated GNPs were detected at very low levels in B lymphocytes, confirming the findings obtained by DF-HSI. In comparison to B cells, MDMs internalized polymer-coated GNPs approximately 10 times more efficiently. Similar to B cells, citrate-GNS associated with MDMs with high efficiency compared to the polymer-coated GNS (**Figure 3B**).

Here we demonstrate using DF-HSI that primary human B lymphocytes can internalize aggregated citrate-GNPs. This is in accordance with a previous report in a mouse B cell line of the uptake of citrate GNPs aggregates, visualized in the endosomal compartments.⁴⁴ Clearly, as shown in the present study, PEG-containing polymer coating prevents the uptake of the GNP both in B cells and in myeloid cells such as macrophages and dendritic cells. This agrees with previous results in dendritic cells, where GNPs coated with the combination of PEG/PVA had a significantly lower uptake than with PVA coating alone, presumably due to the shielding role of PEG.¹⁶ Our current results suggest that shape does not have a significant effect upon the uptake by either B cells or macrophages and dendritic cells. Nevertheless, the exact mechanisms and possible surface receptors involved in the GNP uptake by B lymphocytes across different physiochemical properties of GNPs remain unknown.

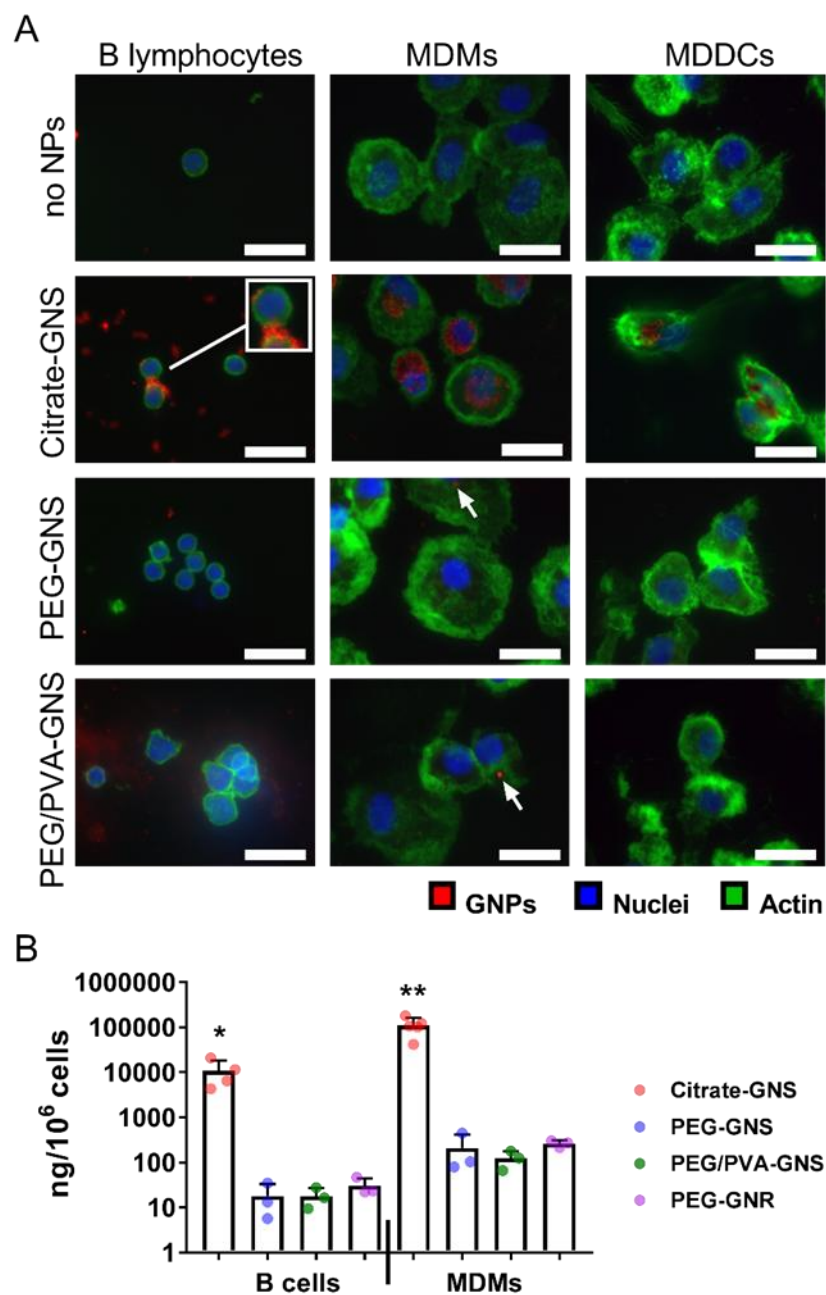


Figure 3. Polymer-coated GNPs cause limited B lymphocyte uptake. **(A)** Dark field hyperspectral images of B cells and other antigen-presenting cells exposed to GNS at 20 $\mu\text{g}/\text{ml}$ for 24 h. Scale bars: 5 μm . The white arrows indicate intracellular GNS. **(B)** Quantification by ICP-MS of gold ion content in B lymphocytes and MDMs exposed to GNPs at 20 $\mu\text{g}/\text{ml}$ for 24 h. Each dot represents one biological sample. Bars represent the mean \pm SD of 3-4 biological replicates; * $p < 0.05$, ** $p < 0.01$. Data were evaluated by a one-way ANOVA, followed by Tukey's multiple comparison post-hoc test.

GNPs do not impair B lymphocyte activation. Since gold-based nanoparticles have been shown in some instances to stimulate B cell lines,⁴⁵ we investigated whether the GNPs used in this study could lead to antigen-independent activation of primary human B cells. The immune cell activation markers CD69, CD86 and MHC II were assessed on B cells by flow cytometry after exposure of the cells to GNPs. The TLR7 ligand R848 was used as positive control for antigen-independent B-cell activation.⁴⁶ In the absence of R848, expression of activation markers was not increased after exposure to any of the tested GNS at concentrations up to 20 µg/ml for 24 h (**Figure 4A**). Upon R848 stimulation, B cells showed upregulation of all three activation markers, as expected. Importantly, exposure to GNS did not impair the pharmacological activation of B cells by R848. Similar results were obtained for PEG-GNR at 20 µg/ml, which neither activated B cells nor inhibited their stimulation by R848 (**Figure 4B**). The activation status of MDMs and MDCCs exposed to GNS was also assessed: the nanospheres did not activate these cells nor did they impair their stimulation by R848 (**Figure S6**). Thus, the GNPs used in this study did not stimulate human B cells, and they did not interfere with their drug-induced activation.

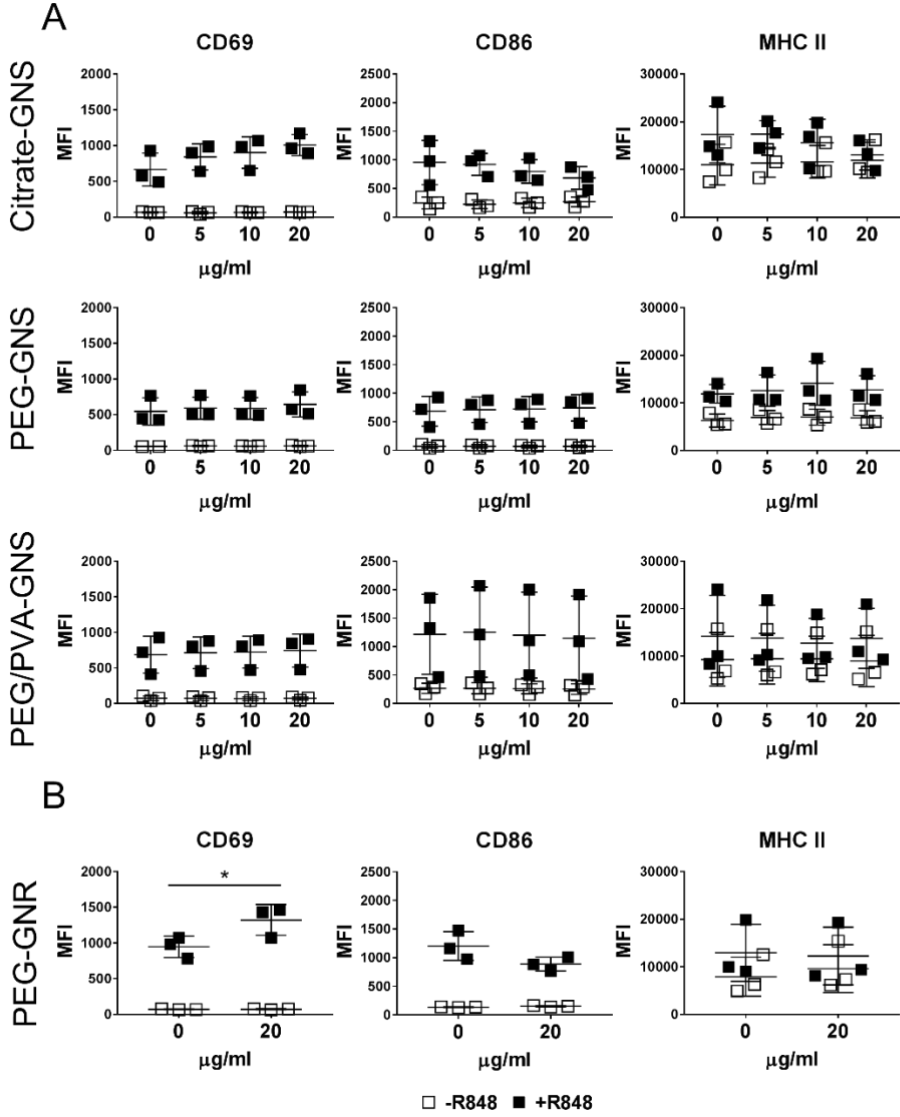


Figure 4. B lymphocyte activation. Surface activation markers on B lymphocytes (CD69, CD86 and MHC-II) measured by flow cytometry after 24 h exposure of B cells to GNS (5-20 µg/ml) with different surface functionalization **(A)** or to PEG-GNR (20 µg/ml) **(B)**. B cells were incubated with or without the immunostimulant R848 (2 µg/ml). Each point represents one donor (n=3). Error bars: mean ± SD; *p<0.05. Data were evaluated by a two-way ANOVA, followed by Tukey’s multiple comparison post-hoc test. The alpha value was set at 0.05.

Pro-inflammatory responses are not enhanced by GNPs. Nanoparticles have been shown to induce the production of pro-inflammatory mediators in immune cells.⁴⁷ In particular, nanoparticles have been noted as able to trigger activation of the inflammasome complex, which causes to the secretion of pro-inflammatory cytokines such as IL-1 β .⁴⁸ Since inflammation can result in severe side effects in patients, it is essential to test the pro-inflammatory potential of NPs destined for biomedical applications early in their development process. To assess whether GNPs induced the production of pro-inflammatory mediators in B cells, we measured the secretion of the pro-inflammatory cytokines IL-6 and IL-1 β by B cells after a 24 h incubation with GNPs, with or without R848. The levels of cytokines were determined by ELISA in the cell culture supernatant. IL-6 and IL-1 β secretion was not induced by GNS at concentrations up to 20 μ g/ml, regardless of their functionalization, nor by PEG-GNR (**Figure 5A**). R848 stimulation induced production of both IL-6 and IL-1 β by B cells, as expected for a TLR7 agonist, but this cytokine production was not affected by polymer-coated GNS. Interestingly, PEG-GNR at 20 μ g/ml caused a significant drop in IL-6 concentration from otherwise increased IL-6 levels of B cells induced by R848 (**Figure 5B**). Similarly, citrate-GNS caused suppression of IL-6 production in R848-activated cells in a concentration-dependent fashion, although the decrease was not statistically significant due to high variation between the cells from the different donors.

In order to further compare the effect of GNPs across APCs, pro-inflammatory cytokines of MDMs and MDDCs were measured after exposure to all types of GNS at the highest concentration only (20 μ g/ml). Similarly to B cells, GNS did not induce cytokine release in the absence of R848. Interestingly, citrate-GNS did not interfere with efficiency of the R848-induced cytokine release by MDMs and MDDCs, in contrast to the observations for activated B lymphocytes (**Figure S7**).

The potential interference of GNPs, which possess light-absorbing properties, with optical-based assays such as ELISA must be considered. To exclude such an interference, we carefully assessed potential background caused by GNPs alone in the optical signal of the plate reader and found that all GNPs, even at the highest concentration of 20 μ g/ml, were below the detection level of the ELISA (data not shown). Further, we controlled for the possible absorbance of cytokines onto the surface of the GNPs, which could impact upon the reliable reading of cytokine concentrations via this method. We detected no effect of the GNPs on cytokine concentrations in this cell-free assay (**Figure S8**).

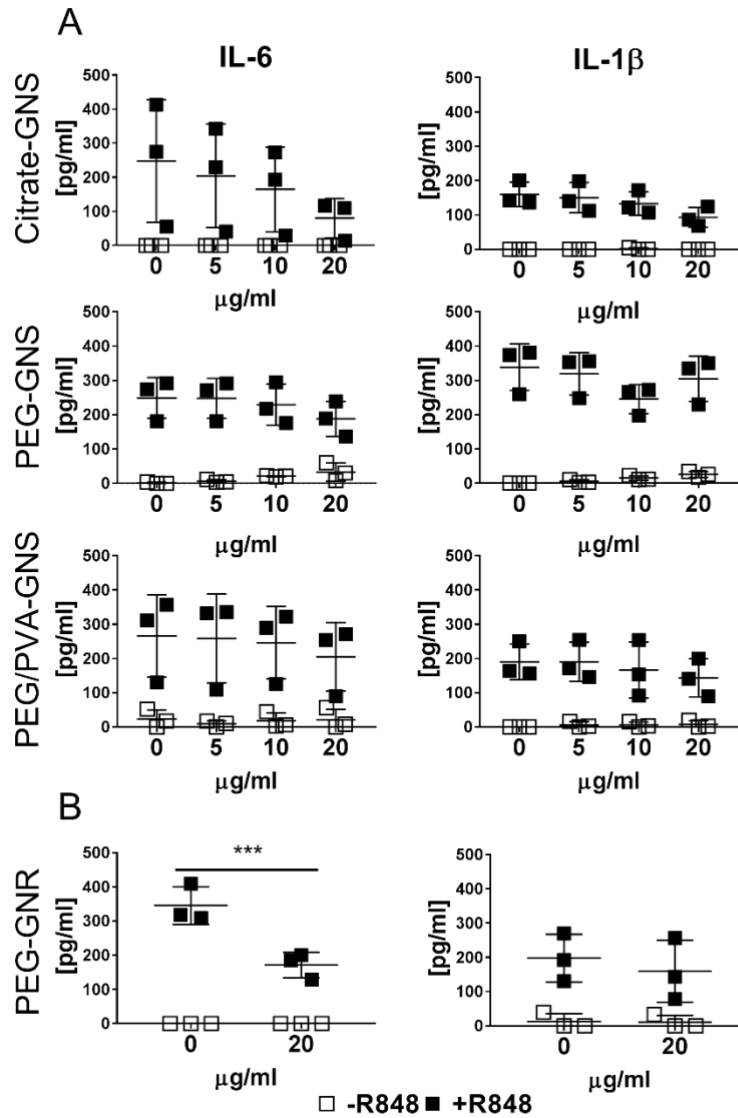


Figure 5. B lymphocyte pro-inflammatory response. Release of pro-inflammatory cytokines after 24 h exposure of B cells to GNS (5-20 $\mu\text{g/ml}$) with different surface functionalization **(A)** or to PEG-GNR (20 $\mu\text{g/ml}$) **(B)**. B cells were incubated with or without the immunostimulant R848 (2 $\mu\text{g/ml}$). Each point represents one donor ($n=3$). Error bars: mean \pm SD; *** $p<0.001$. Data were evaluated by a two-way ANOVA, followed by Tukey's multiple comparison post-hoc test. The alpha value was set at 0.05.

DISCUSSION

The interactions of GNPs with B lymphocytes are important for biomedical applications, especially in view of the selective targeting of B lymphocytes by NPs. Although B lymphocytes are generally not considered professional phagocytic cells, they are capable of, in theory, actively taking up large particulate material through B-cell and complement receptors.⁴⁹ Our results confirmed that GNPs which have a polymer-protected surface trigger very low uptake by primary human B lymphocytes. In contrast, uncoated GNPs, which were opsonized by plasma proteins, were highly taken up even by naïve B cells. This heightened interaction may be due, in part, to the formation of NP aggregates in the cell culture medium, which could trigger stronger internalization by the B cells compared to well-dispersed polymer-coated NPs.⁵⁰ It has recently been shown that NP-bound antigens can be efficiently taken up by antigen-specific B lymphocytes, which then act as APCs to stimulate CD4 T cell responses.⁵¹ Taken together, polymer-coated GNPs loaded with antigen may selectively target only those B lymphocytes recognizing their cognate antigen, thus enhancing selectivity of novel vaccine strategies.

Cytotoxicity of GNPs, which depends on size, shape, dose, coating and surface characteristics, is a major concern. Our results show that the formulations of GNPs used in this study, including uncoated GNS and rod-shape GNPs, do not cause significant B cell cytotoxicity after 24 h exposure *in vitro*. These results give us valuable information for the further biomedical development of safe GNPs, particularly those that are foreseen to come in direct contact with the immune system. In addition, gold nanomaterials have immunomodulatory properties and are able to induce activation in immune cells.⁵² One of the reasons is the insufficient GNP polymer surface coverage, which initiates binding and deformation of proteins that can then act as immunostimulants.^{53, 54} Our data provide evidence that GNPs that are well-protected by polymers do not activate B lymphocytes, nor do they interfere with the action of an immunostimulatory drug (R848).

Interestingly, we show that uncoated GNS, which aggregate in biological media, and rod-shaped GNPs impaired IL-6 cytokine production in TLR7 stimulated B lymphocytes. This suggests that the particle shape controls interference with early, antigen-independent activation events in B lymphocytes. However, further studies are needed to clarify possible mechanisms behind this impairment.

CONCLUSION

The safety of NPs and their consequences on the immune system are of crucial importance. Indeed, as stressed by FDA draft guidelines on nanomaterials for the industry, characterization of the nanomaterial should be carefully assessed.⁵⁵ The defined physicochemical characteristics of the NPs should be taken into consideration to cross-relate them for their stability in a biological environment and to determine the exact mechanisms of cell type-specific biological responses. Therefore, to

Results: Manuscript 1

evaluate the adequacy of GNP use in clinical studies, the impact of GNPs on the immune system (*e.g.*, immunogenicity and immunotoxicity) is an important aspect that needs to be further investigated and specified. With our study, we have gained insight as to the impact of GNPs on B lymphocytes and showed that the absence of polymer coating and GNP shape are important factors that lead to different outcomes in GNP-B cell association and B cell efficiency of the cytokine release, which should be considered for future development of GNP for biomedical use.

METHODS

Chemicals and Reagents. All the chemicals were used without further purification. All chemicals and reagents purchased from Sigma-Aldrich (Switzerland) were used as received, unless otherwise stated.

GNP synthesis. Methoxy polyethylene glycol thiol (mPEG SH; 5 kDa) was purchased from Creative PEGWorks. Polyvinyl alcohol (PVA, Mowiol 3 85, 14 kDa) was purchased from Omy AG. All glassware was cleaned with aqua regia and extensively rinsed with water prior to use. Milli-Q grade water was used in all preparations.

Citrate-stabilized gold nanoparticles (GNPs) 15 nm in diameter, were synthesized as previously described by Turkevich *et al.*⁵⁶ Briefly, the aqueous solution of tetrachloroauric acid ($\text{HAuCl}_4 \times 3\text{H}_2\text{O}$; 500 mL, 0.5 mM) was heated to 100 °C and left to boil for 10 min, which was followed by rapid addition of 25 mL of 34 mM sodium citrate previously heated to 60 °C. Within 20 min the color of the solution changed to red, indicating the formation of GNPs. After cooling down to the room temperature, NPs were kept in the glass container, in the dark, and at a temperature of 4 °C.

Preparation of PEG-GNS. Aqueous solution of mPEG-SH (3.4 mg/mL, 2.5 mL), equivalent to 10 PEG nm⁻², were sonicated for 30 min and was subsequently mixed with 50 mL of citrate-coated GNS suspension. The mixture was left to react at room temperature for 24 h. To remove any excess polymer, the PEGylated GNS were centrifuged at 10000 × g for 1 h and redispersed in water.

Preparation of PEG/PVA-GNS. Separately, an aqueous solution containing 6 mg of polyvinyl alcohol (PVA) and 6 mg of mPEG-SH was prepared and sonicated for 20 min. Then, the polymer solution was added dropwise at room temperature under shaking to GNS suspension (20 mL). The mixture was left overnight under dark conditions. The final GNS-PEG/PVA suspension was then centrifuged (10000 × g, 1 h) to remove excess polymer and re-dispersed in water.

Synthesis of GNRs. GNRs were prepared by the seed-mediated growth method.⁵⁷ The Au seeds were synthesized by mixing a hexadecyltrimethylammonium bromide (CTAB) solution (0.1 M, 4.7 mL) with $\text{HAuCl}_4 \times 3\text{H}_2\text{O}$ (50 mM, 0.025 mL) at 28 °C for 5 min. To this solution, fresh sodium borohydride (NaBH_4) aqueous solution (10 mM, 0.3 mL) was added under vigorous stirring for 2 min. The mixture

Results: Manuscript 1

immediately turned light brown indicating the formation of seed particles. The seed dispersion was aged for 1 h at 28 °C before using it. Separately, a gold growth solution was prepared by adding $\text{HAuCl}_4 \times 3\text{H}_2\text{O}$ solution (50 mM, 2.23 mL) to CTAB (0.1 M, 200 mL) and mixed by inversion. Silver nitrate (AgNO_3) was then added (10 mM, 2.6 mL), followed by HCl (1 M, 3.84 mL) and mixed again by inversion. Next, L-ascorbic acid was added (0.1 M, 1.6 mL) and the solution was mixed vigorously until the solution turned colorless. Finally, the Au seeds (960 μL) were added to the growth solution and followed by brief inversion mixing. The resulting suspension was left overnight at 28 °C for the GNR formation. GNRs then underwent further manipulation in order to have a polymer coating.

Preparation of PEG-GNR by two steps method. PEGylated GNRs were prepared as previously described by Kinnear *et al.*²⁹ Briefly, the GNRs (10 mL, $[\text{Au}] = 0.15 \text{ mM}$) were purified twice by centrifugation ($8000 \times g$ for 50 min) leading to a residual $[\text{CTAB}] = 0.1 \text{ mM}$. Under shaking, a solution of mPEG-SH was added (10 mg/mL, 50.5 μL), equivalent to 10 PEG nm^{-2} , and mixed over 24 hours. The partially PEGylated GNRs were then centrifuged at $8000 \times g$ for 50 min and redispersed in ethanol (90% v/v ethanol, 9.5 mL). To this, an ethanolic solution of mPEG-SH (1 mg/mL in 90% v/v ethanol, 505 μL) was added under shaking and gently mixed over 24 hours. Finally, completely PEGylated GNRs were centrifuged three times at $8000 \times g$ for 50 min to remove unreacted PEG and displaced CTAB with redispersion in water.

GNP characterization. *Transmission electron microscopy (TEM).* GNP diameter was assessed through TEM, operating at 120 kV (FEI Technai Spirit microscope, USA) and equipped with Veleta CDD camera (Olympus, Japan). In order to avoid drying-related artifacts of drop-casting, Citrate-GNS and PEG-GNR TEM samples were prepared as previously described.⁵⁸ Briefly, samples were suspended to 1:1 ratio in the corresponding concentration of bovine serum albumin (BSA, Sigma-Aldrich, USA) solution and left at 4 °C overnight. Polymer-coated GNS samples were prepared without BSA incubation, in order to obtain more dense images of these type of NPs. A total of 5 μL of BSA-GNP (citrate-GNS, PEG-GNR) or GNP sample in H_2O alone (PEG-GNS, PEG/PVA-GNS) was drop-casted on mesh copper grids at a final GNP concentration 20 $\mu\text{g}/\text{mL}$ and left to dry at room temperature. GNP size was subsequently calculated using ImageJ software at the following NP count: Citrate-GNS: $n=132$; PEG-GNS: $n=103$, PEG/PVA-GNS: $n=149$, PEG-GNR: $n=220$. Endotoxin levels of GNPs were determined by Pierce LAL Chromogenic Endotoxin Quantitation Kit (ThermoFisher, Switzerland), following the manufacturer's guidelines (Figure S9).

UV-Vis. UV-Vis spectra of GNPs was obtained using Jasco V-670 spectrophotometer. The colloidal stability was tested by incubation of GNPs in H_2O , 10mM PBS and culture medium (RPMI 1640 (Roswell

Results: Manuscript 1

Park Memorial Institute) with 10% human plasma, 1% PenStrep and 1% L-Glutamine) for 24 h at 37 °C, 5% CO₂. All GNPs were diluted to concentration 0.01 mg/ml in each solution.

Dynamic depolarized light scattering (DDLS). Citrate-GNS, PEG-GNS, PEG/PVA-GNS (all at 5 µg/mL) and PEG-GNR (20 µg/mL) were incubated in water or culture medium (RPMI with 10% human plasma, 1 % PenStrep and 1% L-Glutamine), at 37 °C for 24 h. Then, dynamic depolarized light scattering (DDLS) measurements were performed at constant temperature (21 °C) at a scattering angle of 30°, using a commercial goniometer instrument (3D LS Spectrometer, LS Instruments AG, Switzerland). To estimate the number-averaged hydrodynamic radii, the DDLS spectra were analyzed by the approach presented elsewhere.⁵⁹

ζ-potential. GNP charge was acquired with phase amplitude light scattering analyzer (PALS) (Brookhaven ZetaPALS). GNPs were measured at 0.05 mg/ml, at RT in H₂O (pH 7), PBS (pH 7) and culture media (pH 7), where PBS and media were pre-diluted in H₂O to 1:10. Measurements for each sample were obtained using the Smoluchowski model⁶⁰ with 10 cycles of electrophoretic mobility (EPM) and 10 repetitions to gain mean and standard deviation data. All incubations of GNPs in the cell-free biological media were solely performed for GNP characterization purposes.

Immune cell cultures. *Human B lymphocytes.* Buffy coats from healthy donors (BlutZentrum, Bern, Switzerland) were separated by gradient density (Lymphoprep™, Stemcell Technologies, Canada) followed by specific B lymphocyte magnetic bead isolation using anti-CD20 MicroBeads (Miltenyi Biotec, Germany). Fc receptor blocking reagent (Miltenyi Biotec) was added according to the manufacturer's instructions. A purity of > 96% CD20⁺ cells was obtained throughout the experiments (**Figure S5**). B lymphocytes were cultured in 6-well plates (0.25x10⁶ cells/ml) at 37 °C, 5% CO₂ in RPMI 1640, supplemented with 10% autologous human plasma from each donor, 1% PenStrep (ThermoFisher Scientific, USA, #15140122) and 1% L-Glutamine (ThermoFisher, Scientific, USA, #25030081). The seeding concentration was chosen based on the median B lymphocyte number typically found in healthy human peripheral blood.⁶¹

Monocyte sub-culture. Monocytes were isolated from buffy coats with anti-CD14 MicroBeads (Miltenyi Biotec) and cultured in 6-well plates (10⁶ cells/ml).⁶² Fc receptor blocking reagent (Miltenyi Biotec) was added in the purification protocol. In order to differentiate monocytes to macrophages (monocyte-derived macrophages, MDM) or dendritic cells (monocyte-derived dendritic cells, MDDC), 10 ng/ml macrophage colony-stimulating factor (M-CSF) or 10 ng/ml granulocyte-macrophage colony-stimulating factor (GM-CSF) and 10 ng/ml IL-4 were added into the culture, respectively, and incubated for 6 days at 37° C, 5%CO₂. All cell types were cultured at 37° C, 5% CO₂ in RPMI 1640, supplemented

Results: Manuscript 1

with 10% autologous human plasma from each donor, 1% PenStrep (ThermoFisher Scientific, USA, #15140122) and 1% L-Glutamine (ThermoFisher, Scientific, USA, #25030081).

Exposure to GNPs and stimulants. *B lymphocytes.* Cells were exposed to all GNS directly after purification for 24 h, at concentrations from 5-20 µg/ml and to PEG-GNR at 20 µg/ml.

MDMs/MDDCs. Cells were exposed to all GNS on day 6 of culture at 20 µg/ml for 24 h. R848 (Enzo, USA) at 2 µg/ml was used for B lymphocyte/MDM/MDDC and LPS control at 100 ng/ml (Sigma-Aldrich, Switzerland) was used for MDM/MDDC stimulation. The working concentrations of these immunostimulants was selected in order to induce robust activation in all donor samples.

GNP-cell association assessment. *Light microscopy.* Phase contrast images were captured at a magnification × 40, using an inverted light microscope (Motic AE2000, Germany) after 24 h NP exposure (**Figure S1**).

Enhanced dark-field optical microscopy with high-resolution hyperspectral imaging. Cells exposed to GNPs were fixed with 4% paraformaldehyde (PFA), permeabilized with 0.01% TritonX-100 (Sigma-Aldrich, Switzerland) in PBS and stained with Rhodamine-Phalloidin, diluted 1:40 in PBS and 4',6-diamidino-2-phenylindole (DAPI) using dilution 1:100 in PBS. Samples were imaged with high signal to noise ratio dark field hyperspectral imaging that uses oblique angle lighting (CytoViva, Auburn, Alabama, US). The system is coupled with an Olympus BX-51 microscope outfitted with a fluorescence light source (X-Cite series 120), halogen light source (Dolan-Jenner DC-950), UPL Fluorite 100 × objective, and SPECIM V10E imaging spectrograph with a PCO pixelfly detector (Kelhelm, Germany). All data acquisition was performed using the same exposure time and magnification (100 × oil immersion). Images from both dark field and fluorescent imaging were recorded using a 3D Exi blue camera (QImaging, Surrey, Canada) and ENVI 4.8 software. Images obtained from both sources were overlaid using Image J software. Hyperspectral images were recorded using the same system and software but in spectral mode, using above mentioned detector. Due to the strong scattering of light, gold nanoparticles appear as the brightest signal on the image. Linear enhancement was used to obtain the best contrast of the object against the image background. This type of enhancement shows the full intensity range, from lowest to highest, without clipping.

ICP-MS. Chemicals: Acids (HNO₃, HCl) were of PlasmaPure grade from SCP Science (Courtaboeuf, France). Ultrapure de-ionized water was provided by an Integral 3 Advantage A10 purification system (Merck-Millipore, Schaffhausen, Switzerland). The ICP-MS certified tuning solution consisted of 1 µg/L each of Li, Mg, Y, Ce, Tl and Co in a matrix of 2% HNO₃ was from SCP Science (cat n°701-021-194 5185-5959, batch n°S171122014). The gold certified standard solution (1000 ppm in 5% HCl) was purchased from Sigma-Aldrich (cat n°38168-100ML, batch n°BCBT4405).

Results: Manuscript 1

Sample preparation: B lymphocytes and MDMs were cultured and exposed to GNPs as described above. After 24 h, cells of 1-3 plates were pooled (cells in 18-54 ml), washed two times in 1x PBS (500 × g, 4 °C, 5 min) and counted (total cell number of the sample). After final centrifugation, supernatant was discarded and cell pellets were stored at -20 °C until further analysis. Cell pellets were re-suspended in 4.5 mL ultrapure Milli-Q water, with addition of 0.5 mL of concentrated aqua regia (HNO₃:HCl, 1:3), and digested by heating block for 1 hour at 80°C (EasyDigest, Analab, France). Then, digested cell pellets were diluted in 10% (v/v) aqueous *aqua regia* (10% AR) to be within the calibration range of the ICP-MS method. Final quantification of GNP-cell association was calculated as ng/10⁶ cells by dividing measured GNP mass per total cell number of each sample (cell count prior obtaining the cell pellet) and multiplication by 10⁶.

Instrumentation: The Agilent 7700x ICP-MS system (Agilent Technologies, Basel, Switzerland) was equipped with a Micromist nebulizer and a Scott type spray chamber. The ICP-MS parameters were tuned with a certified solution to obtain the best sensitivity, resolution and the lower RSD on ⁷Li, ⁸⁹Y and ²⁰⁵Tl, and also the lower oxide (156/140, CeO/Ce) and doubly charged (70/140, Ce²⁺/Ce) ratios. The ICP-MS parameters were optimized for the three collision cell modes (**Table S1**).

ICP-MS method: Gold (¹⁹⁷Au) was quantified (n=3) by ICP-MS with and without the use of a collision cell (CC), respectively termed [He] or [HEHe] and [No gas] mode. The two collision cell modes, [He] and [HEHe], with Helium gas at two flow rates: 4.3 mL/min and 10 mL/min, respectively, allow removing or reducing the potential spectral interferences. The ICP-MS calibration curve consisted of one blank (10% AR) and eight ¹⁹⁷Au concentration levels (0.1, 0.5, 1, 5, 10, 15, 20, 25 ppb in 10% AR). The linear regression correlation coefficients (R) were equal to 0.9997, 0.9995 and 0.9995 for ¹⁹⁷Au measured in [No Gas], [He] and [HEHe] modes, respectively (Figure S2), which was in agreement with the FDA guidelines (R ≥ 0.998).⁶³ Evaluation of the ICP-MS method accuracy and precision was also evaluated. The results fulfill the precision (RSD ≤ 15%) and accuracy (100% ± 15%) criteria.⁴³

Flow cytometry: Cell viability and immune cell status. Cells were stained for 15 min at room temperature with Zombie NIR™ Fixable Viability Kit (BioLegend, USA) and washed with FACS buffer (1% BSA, 0.5% sodium azide (Sigma-Aldrich, Switzerland) in PBS). Cells were then stained for 30 min with the following antibodies at 1:100 (unless stated otherwise). B cells: anti-human CD20-FITC (B cell-specific marker, BD Biosciences, USA), anti-human CD69-Pacific Blue™ (BioLegend, USA), CD86-PE-Cy5 (BioLegend, USA) and HLA-DR-PE-CF594 (at 1:300, BD Biosciences, USA); MDMs: CD14-FITC (monocyte/macrophage-specific marker, BioLegend, USA), CD69-PacificBlue (BioLegend, USA), CD86-PE-Cy5 (BioLegend, USA), HLA-DR-PE-CF594 (at 1:300, BD Biosciences, USA); MDDCs: CD1c-PacificBlue (dendritic cell-specific marker, BioLegend, USA), CD80-FITC, CD86-PE-Cy5 (BioLegend, USA), HLA-DR-

Results: Manuscript 1

PE-CF594 (at 1:300, BD Biosciences, USA). Cells were then washed and re-suspended in 0.5 ml FACS buffer for flow cytometer analysis (BD LSR Fortessa, Switzerland). Three independent experiments were performed for each cell type and each sample was set up to capture up to 30,000 events. Gating strategies for all cell types are shown and explained in the supplementary information (**Figure S5**). All flow cytometry data were analyzed with FlowJo software (Version 10, Tree Star, USA).

Pro-inflammatory response. After 24 h exposure of immune cells to GNPs, culture supernatants were collected and measured for concentrations of interleukin (IL)-6, IL-1 β and tumor necrosis factor(TNF)- α by ELISA. The assay was performed according to the manufacturer's instructions (Human IL-6 DuoSet ELISA, Human IL-1 β /IL-1F2 DuoSet ELISA and Human TNF- α DuoSet ELISA, all from R&D, USA). The experiment for each analyte was conducted three times in duplicates (n=3).

To ensure that GNPs did not interfere with the spectrophotometric analysis, an interference test were performed for IL-6 ELISA kit: GNPs (20 μ g/ml) alone were incubated in complete culture media for 24 h at 37 $^{\circ}$ C, 5% CO₂. Prior to the ELISA being conducted, GNP samples were incubated with a IL-6 standard (0-600 pg/ml) for 1 h at RT. Optical density for all the ELISA samples was measured at 450/570 nm, using a microplate reader (Benchmark Microplate reader, BioRad, Cressier, Switzerland). The test experiments were performed once in triplicate (**Figure S8**).

Data and Statistical Analysis. Results are presented as a mean of three separate experiments (three different donors (n=3)) \pm standard deviation (SD). Data were considered normally distributed and thus were evaluated using a non-parametric two-way analysis of variance (ANOVA) or one-way ANOVA. Subsequent analysis occurred in terms of a Tukey's multiple comparison post-hoc test (GraphPad Prism 7 software, USA). Data was considered significant when *p<0.05, **p<0.01 and ***p<0.001.

ASSOCIATED CONTENT

Supporting Information

The Supporting Information is available free of charge on the ACS Publications website at DOI: 10.1021/acsnano.9b01492.

SEM method (Abstract Graphic), light microscopy images of APCs, details about optimization of the ICP-MS method, additional DF-HSI image, GNP-cell association and FSC/SSC signal, cell purity and gating strategy, MDM and MDCC activation, MDM and MDCC pro-inflammatory response, GNP interference test (PDF).

AUTHOR INFORMATION

Corresponding Authors

*Martin J.D. Clift, e-mail: m.j.d.clift@swansea.ac.uk.

*Carole Bourquin, e-mail: carole.bourquin@unige.ch.

Present Addresses

†Empa, 9014 St. Gallen, Switzerland

§Nano4Environment Unit, Water Quality Group, INL - International Iberian Nanotechnology Laboratory, 4715-330 Braga, Portugal

Author Contributions

SH participated in the design of the study, performed UV-Vis and TEM measurements, all biological experimentation and analyzed the data. AM carried out DF-HSI measurements. DDLS was performed and analyzed by AM and LR-L. Synthesis of nanoparticles was conducted by LA-H. IM contributed as an advisor of the flow cytometry experiments. AP-F and BR-R participated in supervision of the experimental work and gave expert advice. CB and MJDC designed the project and supervised the experimental work. The manuscript was written by SH, CB and MJDC and commented by all authors.

*These authors contributed equally.

ACKNOWLEDGMENTS

The authors acknowledge the support by the Swiss National Science Foundation (SNSF) through the National Centre of Competence in Research “Bio-Inspired Nanomaterials” and projects no. 156871, 156372 and 182317, the Adolphe Merkle foundation (Fribourg, Switzerland), and the MZ 2.0 mass spectrometry core facility (University of Geneva) for the ICP-MS method development and sample measurements.

REFERENCES

- (1) Lebien, T. W.; Tedder, T. F. ASH 50th Anniversary Review B Lymphocytes : How They Develop and Function. *Am. Soc. Hematol.* 2008, 112, 1570–1580.
- (2) Pardi, N.; Hogan, M. J.; Naradikian, M. S.; Parkhouse, K.; Cain, D. W.; Jones, L.; Moody, M. A.; Verkerke, H. P.; Myles, A.; Willis, E.; LaBranche, C. C.; Montefiori, D. C.; Lobby, J. L.; Saunders, K. O.; Liao, H.-X.; Korber, B. T.; Sutherland, L. L.; Scarce, R. M.; Hraber, P. T.; et al. Nucleoside-Modified mRNA Vaccines Induce Potent T Follicular Helper and Germinal Center B Cell Responses. *J. Exp. Med.* 2018, 215, 1571–1588.
- (3) Fenton, O. S.; Kauffman, K. J.; Kaczmarek, J. C.; McClellan, R. L.; Jhunjhunwala, S.; Tibbitt, M. W.; Zeng, M. D.; Appel, E. A.; Dorkin, J. R.; Mir, F. F.; Yang, J. H.; Oberli, M. A.; Heartlein, M. W.; DeRosa, F.; Langer,

Results: Manuscript 1

- R.; Anderson, D. G. Synthesis and Biological Evaluation of Ionizable Lipid Materials for the In Vivo Delivery of Messenger RNA to B Lymphocytes. *Adv. Mater.* 2017, 29, 1–7.
- (4) Shen, X.; Pasha, M. A.; Hidde, K.; Khan, A.; Liang, M.; Guan, W.; Ding, Y.; Haczk, A.; Yang, Q. Group 2 Innate Lymphoid Cells Promote Airway Hyperresponsiveness through Production of VEGFA. *J. Allergy Clin. Immunol.* 2018, 141, 1929-1931.e4.
 - (5) Hua, Z.; Hou, B. TLR Signaling in B-Cell Development and Activation. *Cell. Mol. Immunol.* 2013, 10, 103–106.
 - (6) Boraschi, D.; Italiani, P.; Palomba, R.; Decuzzi, P.; Duschl, A.; Fadeel, B.; Moghimi, S. M. Nanoparticles and Innate Immunity: New Perspectives on Host Defence. *Semin. Immunol.* 2017, 34, 33–51.
 - (7) Kojima, S.; Negishi, Y.; Tsukimoto, M.; Takenouchi, T.; Kitani, H.; Takeda, K. Purinergic Signaling via P2X7 Receptor Mediates IL-1 β Production in Kupffer Cells Exposed to Silica Nanoparticle. *Toxicology* 2014, 321, 13–20.
 - (8) Turabekova, M.; Rasulev, B.; Theodore, M.; Jackman, J.; Leszczynska, D.; Leszczynski, J. Immunotoxicity of Nanoparticles: A Computational Study Suggests That CNTs and C60 Fullerenes Might Be Recognized as Pathogens by Toll-like Receptors. *Nanoscale* 2014, 6, 3488–3495.
 - (9) Xi, C.; Zhou, J.; Du, S.; Peng, S. Autophagy Upregulation Promotes Macrophages to Escape Mesoporous Silica Nanoparticle (MSN)-Induced NF- κ B-Dependent Inflammation. *Inflamm. Res* 2016, 65, 325–341.
 - (10) Debotton, N.; Dahan, A. Applications of Polymers as Pharmaceutical Excipients in Solid Oral Dosage Forms. *Med. Res. Rev.* 2017, 37, 52–97.
 - (11) European Food Safety Authority (EFSA). Scientific Opinion on the Safety of Polyvinyl Alcohol-Polyethylene Glycol-Graft-Co-Polymer as a Food Additive. *EFSA J.* 2013, 11, 3303.
 - (12) Lubich, C.; Allacher, P.; de la Rosa, M.; Bauer, A.; Prenninger, T.; Horling, F. M.; Siekmann, J.; Oldenburg, J.; Scheiflinger, F.; Reipert, B. M. The Mystery of Antibodies Against Polyethylene Glycol (PEG) - What Do We Know? *Pharm. Res.* 2016, 33, 2239–2249.
 - (13) Dykman, L.; Khlebtsov, N. Gold Nanoparticles in Biomedical Applications: Recent Advances and Perspectives. *Chem. Soc. Rev.* 2012, 41, 2256–2282.
 - (14) Climent, N.; García, I.; Marradi, M.; Chiodo, F.; Miralles, L.; José Maleno, M.; María Gatell, J.; García, F.; Penadés, S.; Plana, M. Loading Dendritic Cells with Gold Nanoparticles (GNPs) Bearing HIV- Peptides and Mannosides Enhance HIV-Specific T Cell Responses. *Nanomedicine* 2018, 14, 339–351.
 - (15) Assis, N. R. G.; Caires, A. J.; Figueiredo, B. C.; Morais, S. B.; Mambelli, F. S.; Marinho, F. V.; Ladeira, L. O.; Oliveira, S. C. The Use of Gold Nanorods as a New Vaccine Platform against Schistosomiasis. *J. Control. Release* 2018, 275, 40–52.
 - (16) Rodriguez-Lorenzo, L.; Fytianos, K.; Blank, F.; Von Garnier, C.; Rothen-Rutishauser, B.; Petri-Fink, A. Fluorescence-Encoded Gold Nanoparticles: Library Design and Modulation of Cellular Uptake into Dendritic Cells. *Small* 2014, 10, 1341–1350.
 - (17) Kinnear, C.; Rodriguez-Lorenzo, L.; Clift, M. J. D.; Goris, B.; Bals, S.; Rothen-Rutishauser, B.; Petri-Fink, A. Decoupling the Shape Parameter to Assess Gold Nanorod Uptake by Mammalian Cells. *Nanoscale* 2016, 8, 16416–16426.
 - (18) Ho, L. W. C.; Yung, W.-Y.; Sy, K. H. S.; Li, H. Y.; Choi, C. K. K.; Leung, K. C.-F.; Lee, T. W. Y.; Choi, C. H. J. Effect of Alkylation on the Cellular Uptake of Polyethylene Glycol-Coated Gold Nanoparticles. *ACS Nano* 2017, 11, 6085–6101.
 - (19) Ji, Z.; Jin, X.; George, S.; Xia, T.; Meng, H.; Wang, X.; Suarez, E.; Zhang, H.; Hoek, E. M. V.; Godwin, H.; Nel, A. E.; Zink, J. I. Dispersion and Stability Optimization of TiO₂ Nanoparticles in Cell Culture Media. *Environ. Sci. Technol.* 2010, 44, 7309–7314.
 - (20) Yang, S.-A.; Choi, S.; Jeon, S. M.; Yu, J. Silica Nanoparticle Stability in Biological Media Revisited. *Sci. Rep.* 2018, 8, 185.

Results: Manuscript 1

- (21) Jiang, W.; Hibbert, D. B.; Moran, G.; Herrmann, J.; Jämting, Å. K.; Coleman, V. A. Characterisation of Gold Agglomerates: Size Distribution, Shape and Optical Properties. *RSC Adv.* 2013, 3, 7367.
- (22) Dobrovolskaia, M. A.; Patri, A. K.; Zheng, J.; Clogston, J. D.; Ayub, N.; Aggarwal, P.; Neun, B. W.; Hall, J. B.; McNeil, S. E. Interaction of Colloidal Gold Nanoparticles with Human Blood: Effects on Particle Size and Analysis of Plasma Protein Binding Profiles. *Nanomedicine Nanotechnology, Biol. Med.* 2009, 5, 106–117.
- (23) Piella, J.; Bastús, N. G.; Puentes, V. Size-Dependent Protein–Nanoparticle Interactions in Citrate-Stabilized Gold Nanoparticles: The Emergence of the Protein Corona. *Bioconjug. Chem.* 2017, 28, 88–97.
- (24) Liu, Z.; Zhan, X.; Xu, X.; Wu, Y.; Gu, Z. Static Magnetic Field Dictates Protein Corona Formation on the Surface of Glutamine-Modified Superparamagnetic Iron Oxide Nanoparticles. *Part. Part. Syst. Charact.* 2018, 35, 1700418.
- (25) Manson, J.; Kumar, D.; Meenan, B. J.; Dixon, D. Polyethylene Glycol Functionalized Gold Nanoparticles: The Influence of Capping Density on Stability in Various Media. *Gold Bull.* 2011, 44, 99–105.
- (26) Rahme, K.; Chen, L.; Hobbs, R. G.; Morris, M. A.; O’Driscoll, C.; Holmes, J. D. PEGylated Gold Nanoparticles: Polymer Quantification as a Function of PEG Lengths and Nanoparticle Dimensions. *RSC Adv.* 2013, 3, 6085–6094.
- (27) Uz, M.; Bulmus, V.; Alsoy Altinkaya, S. Effect of PEG Grafting Density and Hydrodynamic Volume on Gold Nanoparticle–Cell Interactions: An Investigation on Cell Cycle, Apoptosis, and DNA Damage. *Langmuir* 2016, 32, 5997–6009.
- (28) Allen, J. M.; Xu, J.; Blahovec, M.; Canonico-May, S. A.; Santaloci, T. J.; Braselton, M. E.; Stone, J. W. Synthesis of Less Toxic Gold Nanorods by Using Dodecylethyltrimethylammonium Bromide as an Alternative Growth-Directing Surfactant. *J. Colloid Interface Sci.* 2017, 505, 1172–1176.
- (29) Kinnear, C.; Dietsch, H.; Clift, M. J. D.; Endes, C.; Rothen-Rutishauser, B.; Petri-Fink, A. Gold Nanorods: Controlling Their Surface Chemistry and Complete Detoxification by a Two-Step Place Exchange. *Angew. Chemie Int. Ed.* 2013, 52, 1934–1938.
- (30) He, C.; Hu, Y.; Yin, L.; Tang, C.; Yin, C. Effects of Particle Size and Surface Charge on Cellular Uptake and Biodistribution of Polymeric Nanoparticles. *Biomaterials* 2010, 31, 3657–3666.
- (31) Yue, Z.-G.; Wei, W.; Lv, P.-P.; Yue, H.; Wang, L.-Y.; Su, Z.-G.; Ma, G.-H. Surface Charge Affects Cellular Uptake and Intracellular Trafficking of Chitosan-Based Nanoparticles. *Biomacromolecules* 2011, 12, 2440–2446.
- (32) Blundell, E. L. C. J.; Healey, M. J.; Holton, E.; Sivakumaran, M.; Manstana, S.; Platt, M. Characterisation of the Protein Corona Using Tunable Resistive Pulse Sensing: Determining the Change and Distribution of a Particle’s Surface Charge. *Anal. Bioanal. Chem.* 2016, 408, 5757–5768.
- (33) Gräfe, C.; Weidner, A.; Lühe, M. V. D.; Bergemann, C.; Schacher, F. H.; Clement, J. H.; Dutz, S. Intentional Formation of a Protein Corona on Nanoparticles: Serum Concentration Affects Protein Corona Mass, Surface Charge, and Nanoparticle–Cell Interaction. *Int. J. Biochem. Cell Biol.* 2016, 75, 196–202.
- (34) Mottas, I.; Milosevic, A.; Petri-Fink, A.; Rothen-Rutishauser, B.; Bourquin, C. A Rapid Screening Method to Evaluate the Impact of Nanoparticles on Macrophages. *Nanoscale* 2017, 9, 2492–2504.
- (35) Villiers, C.; Freitas, H.; Couderc, R.; Villiers, M.-B.; Marche, P. Analysis of the Toxicity of Gold Nano Particles on the Immune System: Effect on Dendritic Cell Functions. *J. Nanopart. Res.* 2010, 12, 55–60.
- (36) Fytianos, K.; Rodriguez-Lorenzo, L.; Clift, M. J. D.; Blank, F.; Vanhecke, D.; von Garnier, C.; Petri-Fink, A.; Rothen-Rutishauser, B. Uptake Efficiency of Surface Modified Gold Nanoparticles Does Not Correlate with Functional Changes and Cytokine Secretion in Human Dendritic Cells In Vitro. *Nanomedicine* 2015, 11, 633–644.
- (37) Morbach, H.; Eichhorn, E. M.; Liese, J. G.; Girschick, H. J. Reference Values for B Cell Subpopulations from Infancy to Adulthood. *Clin. Exp. Immunol.* 2010, 162, 271–279.

Results: Manuscript 1

- (38) Bishop, G. A.; Ramirez, L. M.; Baccam, M.; Busch, L. K.; Pederson, L. K.; Tomai, M. A. The Immune Response Modifier Resiquimod Mimics CD40-Induced B Cell Activation. *Cell Immunol.* 2001, 208, 9–17.
- (39) Douagi, I.; Gujer, C.; Sundling, C.; Adams, W. C.; Smed-Sørensen, A.; Seder, R. A.; Karlsson Hedestam, G. B.; Loré, K. Human B Cell Responses to TLR Ligands Are Differentially Modulated by Myeloid and Plasmacytoid Dendritic Cells. *J Immunol.* 2009, 182, 1991–2001.
- (40) Souwer, Y.; Griekspoor, A.; Jorritsma, T.; de Wit, J.; Janssen, H.; Neefjes, J.; van Ham, S. M. B Cell Receptor-Mediated Internalization of Salmonella: A Novel Pathway for Autonomous B Cell Activation and Antibody Production. *J. Immunol.* 2009, 182, 7473–7481.
- (41) Gustafson, H. H.; Holt-Casper, D.; Grainger, D. W.; Ghandehari, H. Nanoparticle Uptake: The Phagocyte Problem. *Nano Today* 2015, 10, 487–510.
- (42) Zucker, R. M. D. of T. nanoparticles in cells by flow cytometry; Massaro, E. J.; Sanders, K. M.; Degn, L. L.; Boyes, W. K. Detection of TiO₂ Nanoparticles in Cells by Flow Cytometry. *Cytom. A.* 2010, 77A, 677–685.
- (43) Levine, K. E.; Tudan, C.; Grohse, P. M.; Weber, F. X.; Levine, M. A.; Kim, Y.-S. J. Aspects of Bioanalytical Method Validation for the Quantitative Determination of Trace Elements. *Bioanalysis* 2011, 3, 1699–1712.
- (44) Sharma, M.; Salisbury, R. L.; Maurer, E. I.; Hussain, S. M.; Sulentic, C. E. W. Gold Nanoparticles Induce Transcriptional Activity of NF- κ B in a B-Lymphocyte Cell Line. *Nanoscale* 2013, 5, 3747–3756.
- (45) Lee, C.-H.; Syu, S.-H.; Chen, Y.-S.; Hussain, S. M.; Aleksandrovich Onischuk, A.; Chen, W. L.; Steven Huang, G. Gold Nanoparticles Regulate the Blimp1/Pax5 Pathway and Enhance Antibody Secretion in B-Cells. *Nanotechnology* 2014, 25, 125103.
- (46) Dorner, M.; Brandt, S.; Tinguely, M.; Zucol, F.; Bourquin, J.-P.; Zauner, L.; Berger, C.; Bernasconi, M.; Speck, R. F.; Nadal, D. Plasma Cell Toll-like Receptor (TLR) Expression Differs from That of B Cells, and Plasma Cell TLR Triggering Enhances Immunoglobulin Production Introduction. *Immunology* 2009, 128, 573–579.
- (47) Nicolette, R.; dos Santos, D. F.; Faccioli, L. H. The Uptake of PLGA Micro or Nanoparticles by Macrophages Provokes Distinct In Vitro Inflammatory Response. *Int. Immunopharmacol.* 2011, 11, 1557–1563.
- (48) Silva, A. L.; Peres, C.; Conniot, J.; Matos, A. I.; Moura, L.; Carreira, B.; Sainz, V.; Scomparin, A.; Satchi-Fainaro, R.; Pr at, V.; Florindo, H. F. Nanoparticle Impact on Innate Immune Cell Pattern-Recognition Receptors and Inflammasomes Activation. *Semin. Immunol.* 2017, 34, 3–24.
- (49) Zhu, Q.; Zhang, M.; Shi, M.; Liu, Y.; Zhao, Q.; Wang, W.; Zhang, G.; Yang, L.; Zhi, J.; Zhang, L.; Hu, G.; Chen, P.; Yang, Y.; Dai, W.; Liu, T.; He, Y.; Feng, G.; Zhao, G. Human B Cells Have an Active Phagocytic Capability and Undergo Immune Activation upon Phagocytosis of Mycobacterium Tuberculosis. *Immunobiology* 2016, 221, 558–567.
- (50) Lichtenstein, D.; Meyer, T.; B hmert, L.; Juling, S.; Fahrenson, C.; Selve, S.; Th nemann, A.; Meijer, J.; Estrela-Lopis, I.; Braeuning, A.; Lampen, A. Dosimetric Quantification of Coating-Related Uptake of Silver Nanoparticles. *Langmuir* 2017, 33, 13087–13097.
- (51) Hong, S.; Zhang, Z.; Liu, H.; Tian, M.; Zhu, X.; Zhang, Z.; Wang, W.; Zhou, X.; Zhang, F.; Ge, Q.; Zhu, B.; Tang, H.; Hua, Z.; Hou, B. B Cells Are the Dominant Antigen-Presenting Cells That Activate Naive CD4⁺ T Cells upon Immunization with a Virus-Derived Nanoparticle Antigen. *Immunity* 2018, 49, 1–14.
- (52) Le G , X.; Palomares, F.; Torres, M. J.; Blanca, M.; Fernandez, T. D.; Mayorga, C. Nanoparticle Size Influences the Proliferative Responses of Lymphocyte Subpopulations. *RSC Adv.* 2015, 5, 85305–85309.
- (53) Saptarshi, S. R.; Duschl, A.; Lopata, A. L. Interaction of Nanoparticles with Proteins: Relation to Bio-Reactivity of the Nanoparticle. *J. Nanobiotechnology* 2013, 11, 26.

Results: Manuscript 1

- (54) Mortimer, G. M.; Butcher, N. J.; Musumeci, A. W.; Deng, Z. J.; Martin, D. J.; Minchin, R. F. Cryptic Epitopes of Albumin Determine Mononuclear Phagocyte System Clearance of Nanomaterials. *ACS Nano* 2014, 8, 3357–3366.
- (55) Food and Drug Administration (FDA). Drug Products, Including Biological Products, that Contain Nanomaterials - Guidance for Industry <https://www.fda.gov/downloads/Drugs/GuidanceComplianceRegulatoryInformation/Guidances/UCM588857.pdf> (accessed Sep 10, 2018).
- (56) Turkevich, J.; Stevenson, P. C.; Hillier, J. A Study of the Nucleation and Growth Processes in the Synthesis of Colloidal Gold. *Discuss. Faraday Soc.* 1951, 11, 55.
- (57) Zhu, J.; Yong, K.-T.; Roy, I.; Hu, R.; Ding, H.; Zhao, L.; Swihart, M. T.; He, G. S.; Cui, Y.; Prasad, P. N. Additive Controlled Synthesis of Gold Nanorods (GNRs) for Two-Photon Luminescence Imaging of Cancer Cells. *Nanotechnology* 2010, 21, 285106.
- (58) Michen, B.; Geers, C.; Vanhecke, D.; Endes, C.; Rothen-Rutishauser, B.; Balog, S.; Petri-Fink, A. Avoiding Drying-Artifacts in Transmission Electron Microscopy: Characterizing the Size and Colloidal State of Nanoparticles. *Sci. Rep.* 2015, 5, 9793.
- (59) Geers, C.; Rodriguez-Lorenzo, L.; Andreas Urban, D.; Kinnear, C.; Petri-Fink, A.; Balog, S. A New Angle on Dynamic Depolarized Light Scattering: Number-Averaged Size Distribution of Nanoparticles in Focus. *Nanoscale* 2016, 8, 15813–15821.
- (60) Beltran-Villegas, D. J.; Sehgal, R. M.; Maroudas, D.; Ford, D. M.; Bevan, M. A. A Smoluchowski Model of Crystallization Dynamics of Small Colloidal Clusters. *J. Chem. Phys.* 2011, 135, 154506.
- (61) Technologies Inc, S. Frequencies Cell Types Human Peripheral Blood https://www.stemcell.com/media/files/wallchart/WA10006-Frequencies_Cell_Types_Human_Peripheral_Blood.pdf (accessed Sep 10, 2018).
- (62) Steiner, S.; Mueller, L.; Popovicheva, O. B.; Raemy, D. O.; Czerwinski, J.; Comte, P.; Mayer, A.; Gehr, P.; Rothen-Rutishauser, B.; Clift, M. J. D. Cerium Dioxide Nanoparticles Can Interfere with the Associated Cellular Mechanistic Response to Diesel Exhaust Exposure. *Toxicol. Lett.* 2012, 214, 218–225.
- (63) Administration, U. S. F. a. d. Elemental Analysis Manual (EAM) for Food and Related Products <http://www.fda.gov/EAM> (accessed May 18, 2017).

1.1 Supporting information for manuscript 1

Polymer-Coated Gold Nanospheres Do Not Impair the Innate Immune Function of Human B Lymphocytes *in Vitro*

Sandra Hočevár^{1,2}, Ana Milošević¹, Laura Rodriguez-Lorenzo¹, Liliane Ackermann-Hirschi¹, Ines Mottas^{2,3}, Alke Petri-Fink¹, Barbara Rothen-Rutishauser¹, Carole Bourquin^{2,3,4*}, Martin J. D. Clift^{1,5*}

¹BioNanomaterials, Adolphe Merkle Institute, University of Fribourg, 1700 Fribourg, Switzerland.

²School of Pharmaceutical Sciences, University of Geneva, University of Lausanne, 1211 Geneva, Switzerland

³Chair of Pharmacology, Faculty of Science and Medicine, University of Fribourg, 1700 Fribourg, Switzerland

⁴Faculty of Medicine, University of Geneva, 1211 Geneva, Switzerland

⁵*In Vitro* Toxicology Group, Swansea University Medical School, Wales, SA2 8PP, UK

*These authors contributed equally.

Corresponding authors:

*Martin J.D. Clift, e-mail: m.j.d.clift@swansea.ac.uk.

*Carole Bourquin, e-mail: carole.bourquin@unige.ch.

Results: Supporting Information for Manuscript 1

Light microscopy images. In order to assess a potential increase in cell death upon 24 h GNP exposure (20 µg/ml), phase contrast images of the APC cultures were obtained. GNP formulations caused no significant impact upon APC density (Fig. S1). Interaction of citrate-GNS was observed with both MDMs and MDDCs (Fig. S1B and S1C), although not with B cells (Fig. S1A). For the polymer-coated GNP, images were unable to show interactions with the different cell types. Thus, in view of the lack of sensitivity of light microscopy, in order to correctly evaluate GNP-cell association, other methods were used (DF-HSI, ICP-MS, flow cytometry). Addition of R848 immunostimulant did not cause any qualitative increases in cell death or GNP-cell interaction. LPS was used as an additional positive control to highlight morphological changes of activated MDMs and MDDCs.

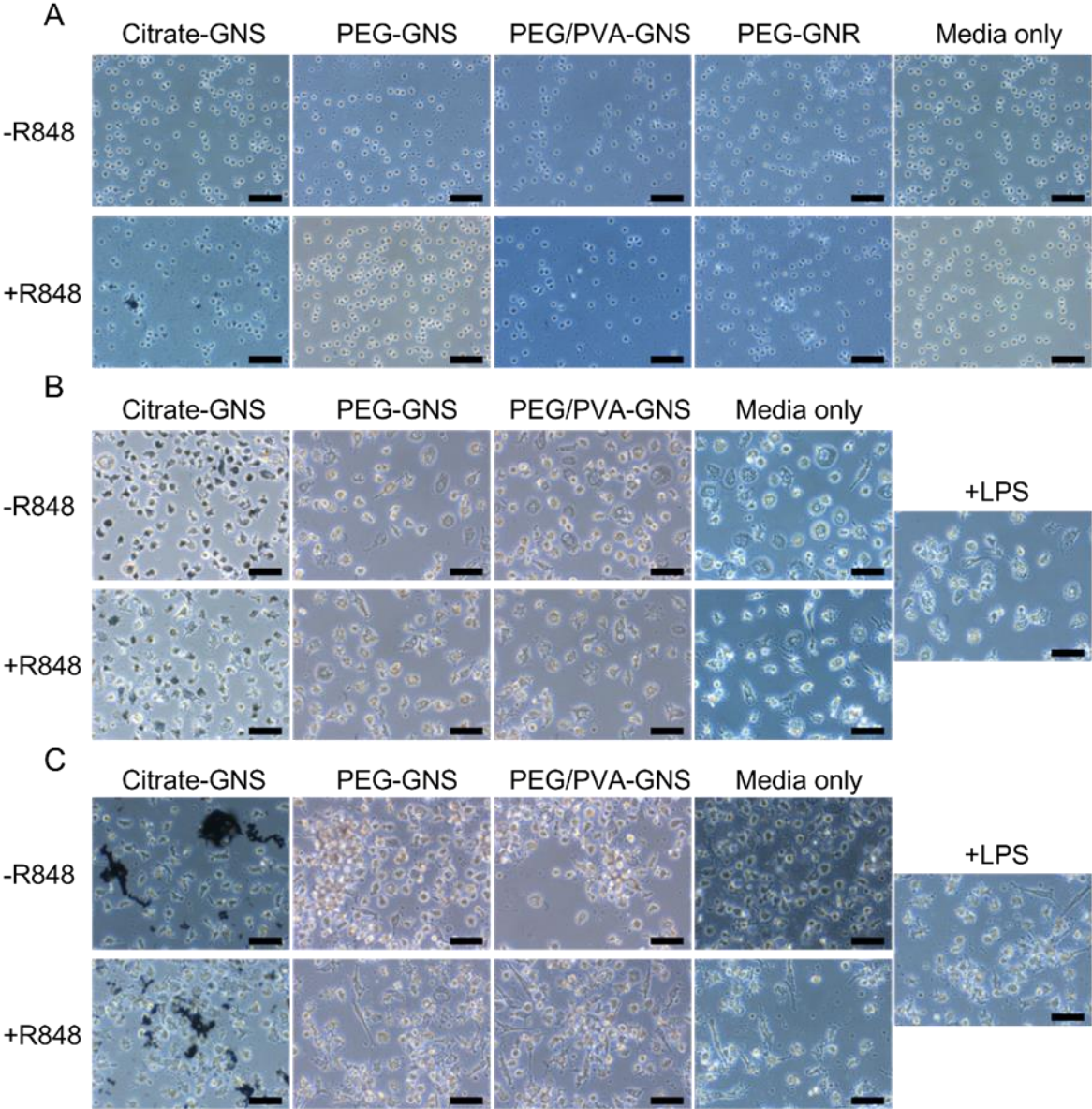


Figure S1. Light microscopy phase contrast images of antigen-presenting cells (APCs) exposed to gold nanoparticles (GNPs). B cells **(A)**, MDMs **(B)** and MDDCs **(C)** Cells were exposed for 24 h to GNS (20 $\mu\text{g/ml}$) with different surface functionalizations. B cells were as well exposed to PEG-GNR (20 $\mu\text{g/ml}$). All APCs were incubated with or without immunostimulant R848 (2 $\mu\text{g/ml}$). MDM and MDDCs were also incubated with LPS only (100 ng/ml). Scale bars: 50 μm .

Results: Supporting Information for Manuscript 1

Table S3: ICP-MS parameters optimized for the three collision cell models.

Collision cell modes:	[No gas]	[He]	[HEHe]
Plasma mode	Low matrix	Low matrix	Low matrix
Plasma RF Power(W)	1550	1550	1550
Collision gas (He) flow (mL/min)	0	4.3	10.0
Nebulizer gas (Ar) flow (L/min)	1.0	1.0	1.0
Auxiliary gas (Ar) flow (L/min)	0.9	0.9	0.9
Plasma gas (Ar) flow (L/min)	15.0	15.0	15.0
Extract 2 (V)	-165	-165	-165
Omega bias (V)	-90	-90	-90
Omega lens (V)	8.8	8.8	8.8
Deflect (V)	13.6	0.2	-73.2
OctP RF(V)	200	200	190
Energy discrimination (V)	5.0	3.0	7.0

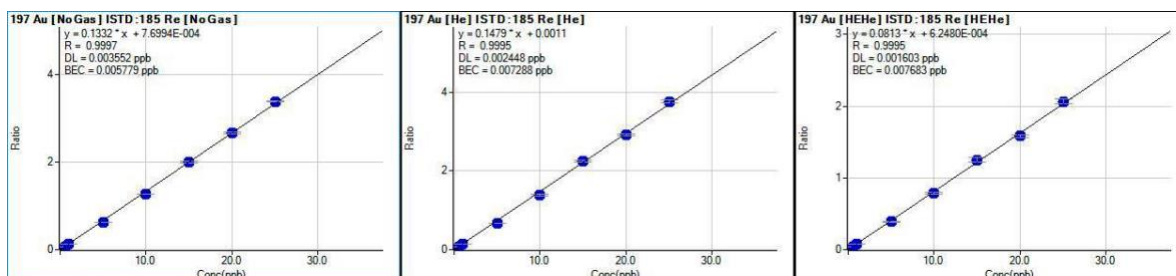


Figure S2. Calibration curves for ^{197}Au in the three collision cell modes.

Results: Supporting Information for Manuscript 1

PEG-GNR uptake by B lymphocytes. PEG-GNR were not detected in B lymphocytes by DF-HSI (Fig. S3). A low amount of PEG-GNR associating with B cells was further confirmed and quantified by highly sensitive ICP-MS (as described in the main text manuscript).

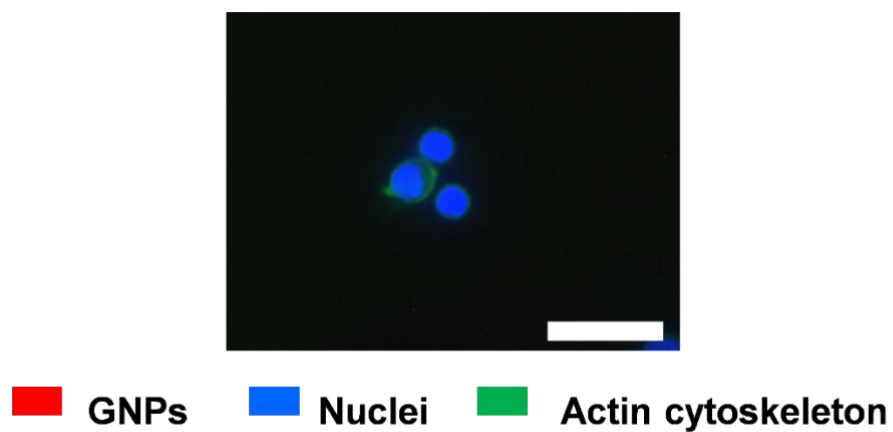


Figure S3. Dark field hyperspectral image of B lymphocytes exposed to PEG-GNR (20 $\mu\text{g/ml}$) for 24 h. Scale bar: 5 μm .

GNP-cell association *via* Flow Cytometry. GNPs that are internalized can be assessed by changes in the light scatter detected by flow cytometry. As indicated below, exposure to citrate GNS caused an increase in the side scatter (SSC) for B cells, but not exposure to polymer-protected GNS (Figure S4). In contrast, in MDMs and MDDCs exposed to polymer-protected GNS, an increase in SSC was observed.

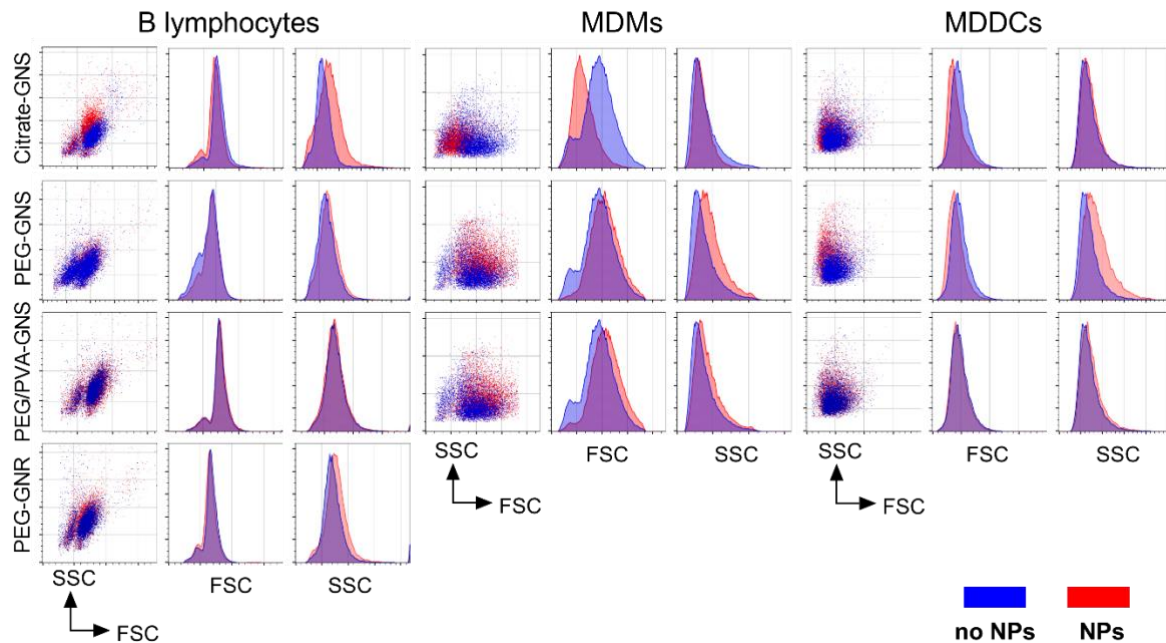


Figure S4. FSC/SSC flow cytometry dot plots and histograms of antigen-presenting cells exposed to GNPs. All APCs were exposed for 24 h to GNS (20 $\mu\text{g}/\text{ml}$) with different surface functionalizations. B cells were as well exposed to PEG-GNR (20 $\mu\text{g}/\text{ml}$).

Results: Supporting Information for Manuscript 1

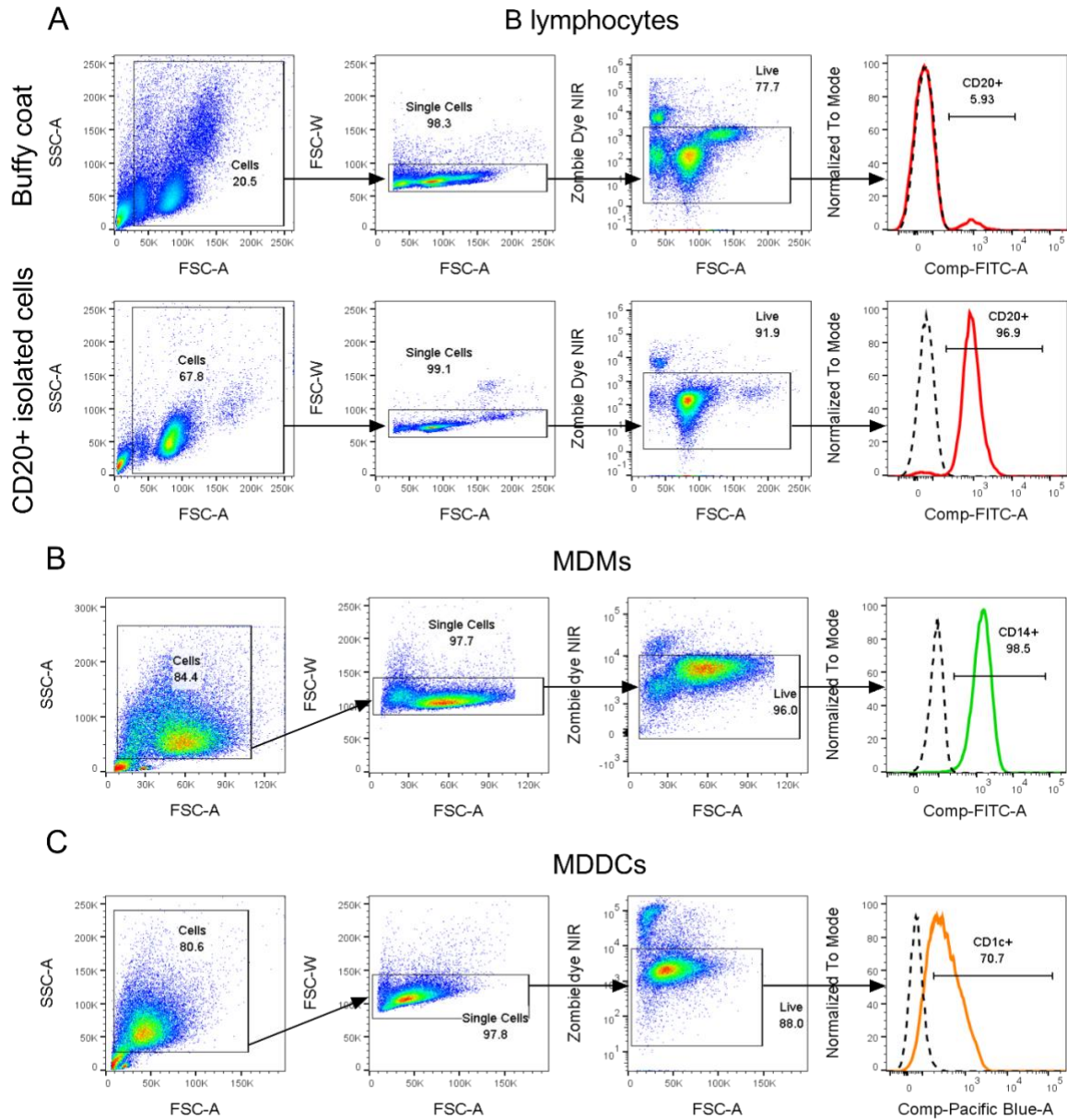


Figure S5. Gating strategy and B lymphocyte purity. All cells were first gated to exclude dead cells and cell debris followed by gating of single cells only. Next, live cells were determined by Zombie NIR viability dye. B cells were defined as percentage of CD20-FITC positive cells, before (buffy coat) and after purification. Approximately 96% B cell purity was achieved throughout the experiments **(A)**. MDMs were defined as CD14-FITC positive **(B)** and MDDCs as CD1c-Pacific Blue positive cells **(C)**.

Results: Supporting Information for Manuscript 1

MDM and MDDC activation. To compare how GNPs influence the activation potential of different APCs, MDMs and MDDCs were exposed to all the formulations of GNS at 20 $\mu\text{g}/\text{ml}$ for 24 h. In general, polymer-coated GNS did not impair the expression of activation markers in naïve as well as in R848-stimulated MDMs and MDDCs (Figure S6). It was observed that high MDM uptake of citrate-GNS interfered with Pacific Blue and PE-Texas Red channel, resulting in false decrease of MFI for CD69 and MHC II markers (Figure S6A). No such interference was detected for B cells and MDDCs. There was an upregulation of CD86 in MDDCs due to PEG-GNS without R848. However, an endotoxin test later confirmed contamination of that specific PEG-GNS batch, which resulted in a false positive increase of CD86 in MDDCs (Figure S6B and Figure S9). LPS served as a positive control for innate immune cell activation.

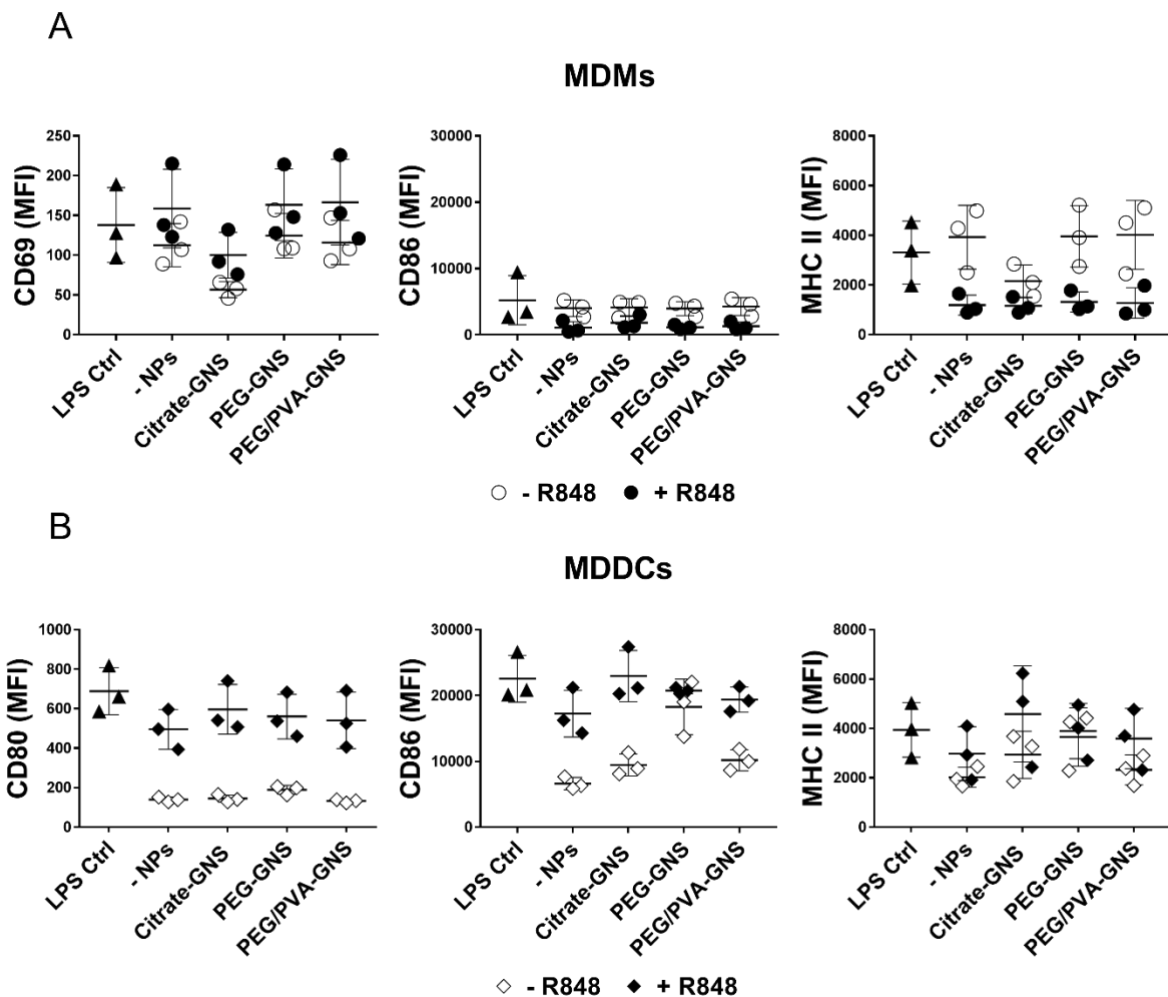


Figure S6. MDM and MDDC activation. Surface activation markers on MDMs (CD69, CD86 and MHC-II) (A) and MDDCs (CD80, CD86, MHC II) (B) measured by flow cytometry after 24 h exposure of cells to GNS (20 $\mu\text{g}/\text{ml}$) with different surface functionalization. Cells were incubated with or without the immunostimulant R848 (2 $\mu\text{g}/\text{ml}$) and with LPS only (100 ng/ml). Each point represents one donor (n=3). Error bars: mean \pm SD. Data were evaluated by two-way ANOVA, followed by Tukey's multiple comparison test.

MDM and MDDC pro-inflammatory response. MDMs and MDDCs were tested for the changes in their cytokine release, following 24h exposure with different surface functionalized GNS (20 $\mu\text{g}/\text{ml}$). TNF- α and IL-1 β release was not affected by GNS in MDM (Figure 7A) and TNF- α and IL-6 were not altered in MDDCs (Figure S7B), whether the cells were stimulated with R848 immunostimulant or not. LPS served as positive control for innate immune cell activation.

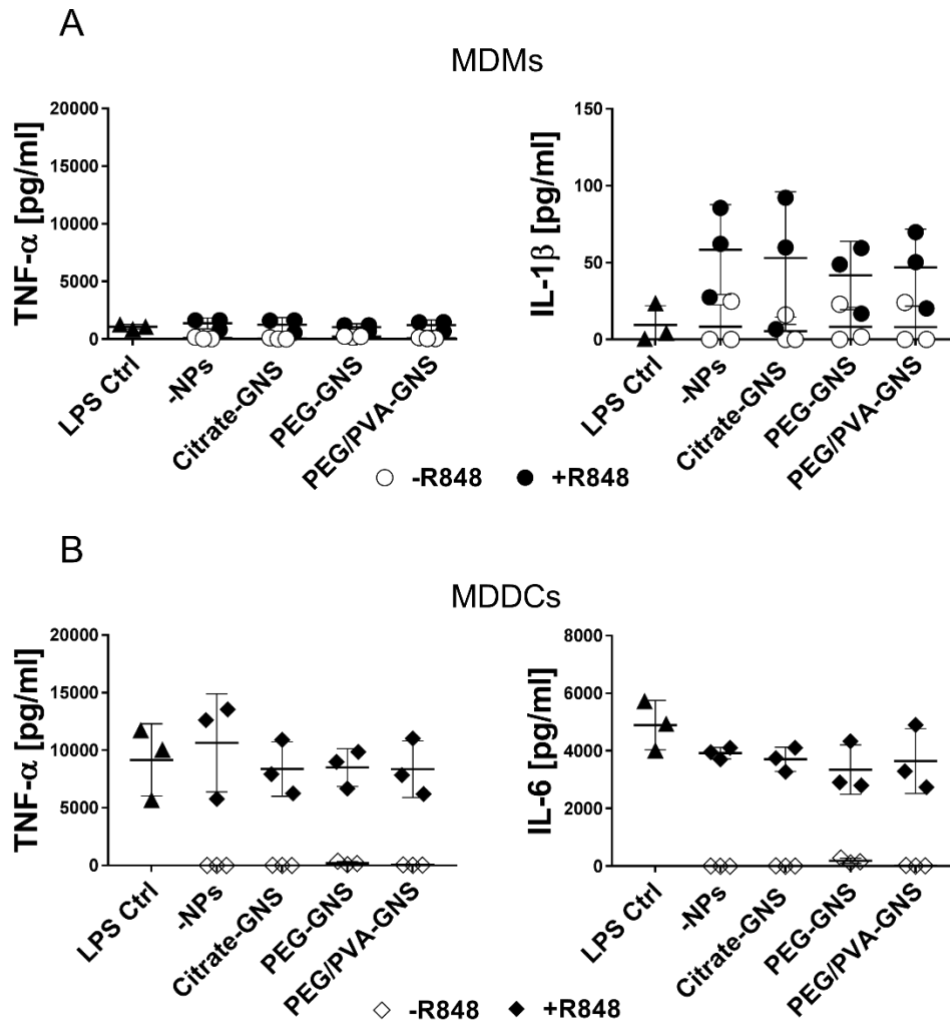


Figure S7. MDM and MDDC pro-inflammatory response. Pro-inflammatory cytokines released by MDMs (TNF- α , IL1- β) (A) and MDDCs (TNF- α , IL-6) (B) after 24 h exposure of B cells to GNS (20 $\mu\text{g}/\text{ml}$) with different surface functionalization. Cells were incubated with or without the immunostimulant R848 (2 $\mu\text{g}/\text{ml}$) and with LPS only (100 ng/ml). Each point represents one donor (n=3). Error bars: mean \pm SD. Data were evaluated by two-way ANOVA, followed by Tukey's multiple comparison test.

Results: Supporting Information for Manuscript 1

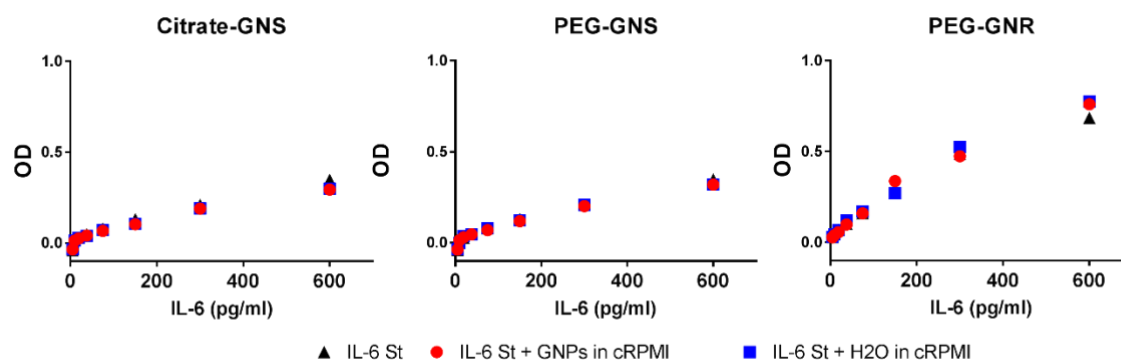


Figure S8. Gold nanoparticle interference test. Gold nanoparticle interference with ELISA by cytokine absorption to GNP surface. Citrate-GNS, PEG-GNS and PEG-GNR were incubated in complete culture media with human plasma for 24 h, 37 °C, 5% CO₂. H₂O was added to the media as a negative control. Samples were then incubated with IL-6 standards for 1 h at RT, followed by the normal ELISA protocol. The experiment was performed once. Each point on the graphs represents mean of triplicates. RPMI+HP: complete culture medium consisting of RPMI with 1% Pen/Strep, 1% L-Glutamine, 10% human plasma.

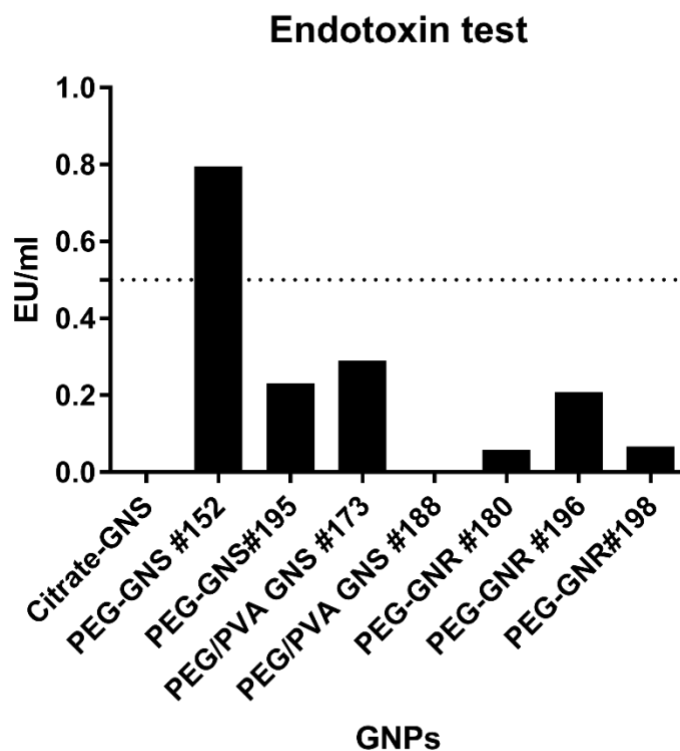


Figure S9: Endotoxin test of different batches of GNPs used in the study. All batches were below the FDA recommended level (> 0.5 EU/ml).¹ except batch #152, which was used for exposure of MDDCs.

(1) Food and Drug Administration (FDA). Guidance for Industry Pyrogen and Endotoxins Testing <https://www.fda.gov/downloads/Drugs/GuidanceComplianceRegulatoryInformation/Guidances/UCM310098.pdf> (accessed Mar 30, 2019).

2. Manuscript 2: Polymer-coated gold nanoparticles inhibit adaptive B cell function in mice

The following part of my thesis mainly focused on the biodistribution of GNPs and their impact on the development of innate and adaptive immune responses in mice. Formulations of polymer-coated GNPs were tested for their distribution in mice within different organs and cell types following s.c. and i.v. injections, potential impairment of B cell viability, activation and adaptive immune responses.

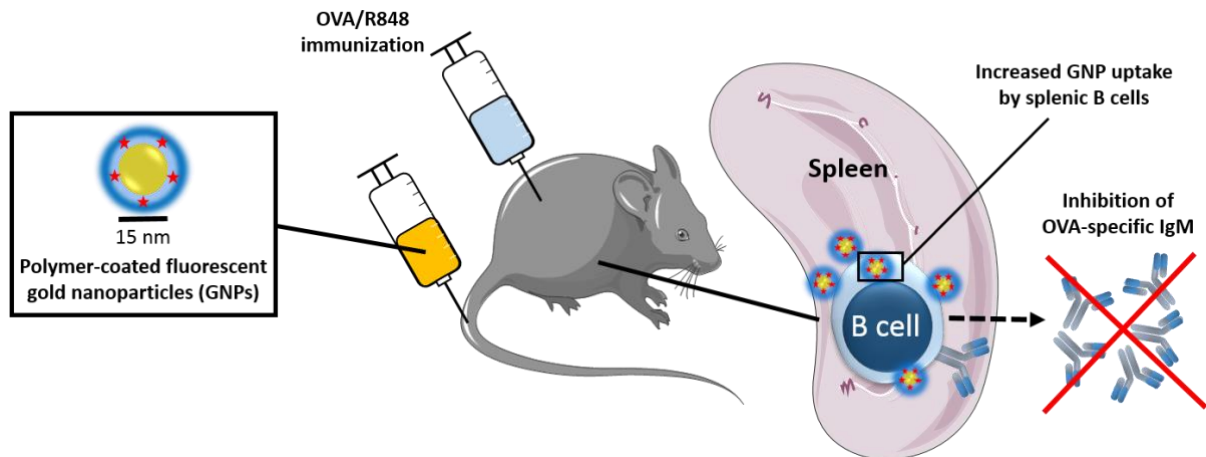


Figure 7: Graphical abstract of manuscript 2. 15 nm gold nanospheres were stabilized with double layer of protective polyethylene glycol (PEG). The primary PEG layer was conjugated with fluorochrome cyanine 5 (Cy5) in order to follow their biodistribution in mice. Mice were systemically injected with GNPs and with or without immunogenic stimulus (OVA antigen and R848 adjuvant). Association of GNPs with B cells in different organs (e.g., spleen) was investigated as well as GNP potential to interfere with B cell adaptive immune response.

The following manuscript is a preliminary draft prior to submission to a scientific journal and has not been yet reviewed by all the authors. For the purposes of the thesis, the manuscript involves an extended result section in order to include all the important findings of this PhD project and will be shortened and edited before submission, and after the revision by all the authors. Moreover, the current authors' list might not be the final one.

Polymer-coated gold nanoparticles inhibit adaptive B cell function in mice

Sandra Hočevár¹, Alke Petri-Fink³, Barbara Rothen-Rutishauser³, Martin James David Clift^{4}, Carole Bourquin^{1,2*}*

¹School of Pharmaceutical Sciences, University of Geneva, University of Lausanne, 1211 Geneva, Switzerland

²Faculty of Medicine, University of Geneva, Rue Michel-Servet 1, 1211 Geneva, Switzerland

³BioNanomaterials, Adolphe Merkle Institute, University of Fribourg, 1700 Fribourg, Switzerland.

⁴In Vitro Toxicology Group, Swansea University Medical School, Wales, SA2 8PP, UK

*These authors contributed equally.

Abstract

Engineered gold nanoparticles (GNPs) have become a useful tool in various therapeutic and diagnostic applications due to their unique optical properties as well as general biocompatibility. Nonetheless, doubts remain about whether GNPs are inert with regard to important physiological functions such as the immune system. Moreover, B cells are a crucial part of adaptive immunity and are also capable of a fast and unspecific response through the receptors of innate immunity. Due to their high numbers in lymphoid organs such as spleen and lymph nodes, B cells present a potential target for administered GNPs. Herein, we investigated the interactions of 15 nm polymer-coated GNPs with B cells and potential GNP impact on B cell function in mice. We have shown that 3 h after intravenous injection, GNPs initially interacted with marginal zone (MZ) B cells in the spleen. However, 14 days after injection, GNPs were highly detected in splenic follicular B cells, plasmablasts and germinal center (GC) B cells, where the GNP accumulation was significantly increased in antigen-immunized mice. Importantly, we showed that GNPs were generally biocompatible and did not impact the percentages of B cell populations and their subsets in different organs. Furthermore, after short-term systemic exposure, GNP did not activate B cell innate-like immune response nor did they impair B cell primary response in adjuvant-stimulated mice. Surprisingly, we observed a significant inhibition of antigen-specific IgM production 14 days after simultaneous injection of GNP and OVA antigen. Together, this data provides an important contribution to otherwise limited knowledge about GNP interference with B cell adaptive immune function.

INTRODUCTION

Gold nanoparticles (GNPs) have gained increasing attention over the past two decades in the field of nanomedicine due to their intriguing properties. First and foremost, GNPs are in general considered to be highly biocompatible and lacking immunogenicity, which are highly desirable features for the purpose of biomedical applications.¹ Furthermore, GNPs have unique optical properties as they are able to absorb incident light due to surface plasmon resonance.² This GNP ability has been used as an advantage in the development of numerous photo-based GNP applications, from biosensors and imaging agents to tools for photothermal therapies.³ Besides their intrinsic therapeutic and diagnostic competencies, GNPs are optimal carriers for drugs and therapeutics, and can serve as a convenient platform for vaccine delivery.⁴ Conjugation of GNPs with antigens of HIV, West Nile virus, foot-and-mouth disease virus, worm parasites, among others, has shown a significant improvement in the adaptive immune response, compared to immunization with soluble antigens.⁵⁻⁸ The mechanism behind it has been explained as the B cell preference to phagocytize particulate antigens via B cell receptors (BCR), which significantly enhances antigen presentation to T cells that leads to efficient activation of the cellular and humoral adaptive immune responses.^{9,10}

Nevertheless, as the numbers of various GNP biomedical applications increase, questions about their safe use in humans have been raised, especially due to GNP's prolonged accumulation in the system as an inorganic and poorly degradable material. Therefore, numerous nanotoxicology studies have been initiated to evaluate GNP potential toxicity and adverse impact on the immune system. It has been reported that GNPs were able to increase serum pro-inflammatory cytokines such as TNF- α and IL-8, caused an increase in T and B cell populations and shown to have an impact on antigen presentation in dendritic cells.¹¹⁻¹³ However, the presence and severity of these effects are strongly dependent on one or more of GNP physico-chemical properties such as size, surface charge, lack of protective coating, colloidal instability and high exposure concentrations.^{14,15}

To raise the level of biocompatibility and stability of the medically applicable GNPs, they are often protected with polymers such as FDA approved polyethylene glycol (PEG).¹⁶ Thus, the polymer coating of GNPs has been shown to reduce toxicity and improve their half-life in the system due to the inhibition of protein corona formation.¹⁷ Consequently, PEGylated GNPs are able to escape recognition and removal by the cells of the immune system. Nonetheless, it has been shown that PEGylated nanomedicines, including the ones already used in clinical practice (*e.g.*, PEGylated liposome-based drugs), are not entirely resistant to opsonization with plasma proteins, such as immunoglobulins and complement proteins, which can potentially lead to complement-mediated immune response.^{18,19}

Results: Manuscript 2

Whereas the vast majority of studies regarding GNP immunotoxicity focus on the innate immune system, there is insufficient knowledge about the GNP impact on the cells of adaptive immunity such as B cells. B cells play an important role in fighting against infections by generating an antigen-specific immune response. Mature B cells are residents of secondary lymphoid organs such as spleen and lymph nodes (LN), which in mice consist of about 20-50% and 30% of B cells, respectively.^{20,21} Importantly, systemically administered GNPs with a diameter of ~50 nm were detected throughout the body in the majority of the organs but had a stronger tendency to accumulate in the liver and spleen over time.²² Moreover, the subcutaneous injection of NPs smaller than 100 nm shown a passive draining and accumulation in the LN.²³ Thus, B cells in major lymphoid organs are a likely target following GNP administration.

Follicular B cells present in the spleen and LN are responsible for internalization, processing and presentation of antigen, which leads to the formation of germinal centers. Consequently, this further leads to the development of long-lived plasma cells that ensure a specific humoral immune response.²⁴ On the contrary, marginal zone (MZ) B cells are considered as innate-like B cell subset in the spleen and are localized at the border of B cell follicles and in direct proximity to the arterioles. Therefore, these cells are able to respond rapidly against blood-borne pathogens through the facilitation of T cell-independent low-affinity antibody production as well as proinflammatory reactions via Toll-like receptors (TLRs).²⁵ We reported before that polymer-coated gold nanorods have the ability to modulate innate immune function of primary human B cells *in vitro*, causing a decrease in IL-6 production in TLR7-stimulated B cells.²⁶ Moreover, the impact of GNPs on humoral immune function has also been reported, where studies showed that GNPs are able to induce antibody production *via* NF- κ B signaling pathway and blimp1/pax5 B cell lineage regulatory pathways in murine B cell lines.^{27,28} Nonetheless, to completely understand the extent of GNP-B cell interactions and GNP impact on B cell complex adaptive immune function, a fully functional immune system is needed.

Herein, we investigate how GNPs coated with a stable polymer interact with B cells in different organs and different immune cell subsets in mice. Importantly, we provide new information on how GNPs affect B cell function *in vivo* in the presence of antigen and adjuvant. Thus, this data provides a further understanding of potential unintentional GNP effects on B cell function in order to better evaluate GNP appropriateness for biomedical applications.

RESULTS

Polymer-coated GNPs are stable in different biological media

To investigate the interactions of GNPs with B cells and to follow their biodistribution in mice, fluorescently labeled 15 nm gold nanospheres coated with polyethylene glycol (PEG) were synthesized as previously reported by Rodriguez-Lorenzo *et al.*²⁹ This GNP formulation consisted of the two layers of PEG polymer. The first layer of PEG coating (NH₂-PEG) was conjugated with cyanine 5 (Cy5) fluorochrome, followed by the second layer of PEG in order to prevent Cy5 dissociation and to avoid the potential effect of Cy5 chemistry with the biological system (**Figure S1A**).²⁹ The average hydrodynamic diameter of GNPs was 54.7 nm, measured by dynamic light scattering (DLS), whereas the surface charge was measured at 13.4 mV. The double PEGylated Cy5-labeled GNPs were used throughout *in vivo* experiments in order to assure as high GNP biocompatibility as possible.

The stability of NPs can significantly decrease after contact with the biological media and can result in NP aggregation.³⁰ This can further lead to increased NP internalization by the cells and consequently increases the risk of NP toxicity.³¹ To evaluate the GNP stability, GNPs were incubated in different biological media (H₂O, PBS, complete culture medium with 10% FBS and 15% mouse serum) overnight at 37 °C. UV-Vis measurements showed that polymer-protected GNPs did not aggregate in biological media as all samples absorbed light at ~520 nm (**Figure S1B**), which is a typical absorption peak for stable 15 nm gold nanospheres.³² Thus, we could confirm high colloidal stability of polymer-protected GNPs in protein-rich environments such as culture medium and mouse serum.

GNPs accumulate in marginal zone B cells in spleen after short-term exposure

Prior to the investigation of the GNPs' ability to interfere with B cell function *in vivo*, we first looked into whether the GNPs physically interact with B cells in different organs. To determine GNP biodistribution, 400 µg of GNPs was intravenously injected via the tail vein. After 3 or 24 h mice were euthanized. Spleen, liver, and blood were collected and processed to obtain cell suspensions in order to determine GNP uptake by flow cytometry (**Figure 1A**). Next, we used the acidic wash method to evaluate GNP-cell association vs. uptake. Acidic wash is commonly used to measure phagocytized antibodies or immune complexes.³³ The method is based on the incubation of cells with an acidic buffer (~pH 4), which causes a dissolution of the surface-bound antibodies and allows the measurement of internalized antibodies only. We followed a similar approach, where the liver, splenic or blood cells were treated with an acidic buffer in order to remove surface-bound GNPs. Thus, the treatment of cells with acidic wash provided quantification of internalized GNPs, whereas no acidic wash incubation assured quantification of total GNP-cell association, all measured by flow cytometry as a percentage of GNP-Cy5 positive cells. We observed that GNPs accumulated in the liver and spleen after 3 h and

Results: Manuscript 2

24 h, but not significantly in the blood after 24 h. Specifically, the results suggested that among B cell subsets, marginal zone (MZ) B cells (CD19⁺/CD3⁻/CD21⁺/CD23⁻) internalized GNPs after 3 h (~4% of GNP positive cells) and 24 h (~2% of GNP positive cells), whereas GNPs most likely associated only with the surface of the follicular (FO) B cells (CD19⁺/CD3⁻/CD21⁺/CD23⁺) and were not internalized by these cells after 24 h (**Figure 1B**). This outcome is most likely the result of anatomical localization and the innate-like role of MZ B cells to remove blood-borne particulate matter. In comparison, GNPs did not associate with B cells present in the liver and blood (**Figure 1C** and **1D**). Additionally, we observed that macrophages (CD11b⁺/CD11c⁻) and dendritic cells (DCs) (CD11b⁺/CD11c⁺) in spleen and liver, and monocytes in the blood are the dominant immune cell types to take up GNPs up to 24 h after injection. On average, 30% and 15% of macrophages were GNP-positive after 3 and 24 h in the spleen, respectively (**Figure 1B**). Furthermore, approximately 40% at 3 h and 10% at 24 h of the macrophages in the liver, and 15% at 3 h and 2% at 24 h of the monocytes in the blood were GNP-positive (**Figure 1C** and **1D**). This is in accordance with the high phagocytic role of these cells in spleen and liver. In addition, it indicates that GNPs are extensively cleared from the blood after 24 h. On the contrary, T cells (CD19⁻/CD3⁺) did not significantly associate with GNPs in any of the organs tested at 3 and 24 h (**Figure 1**).

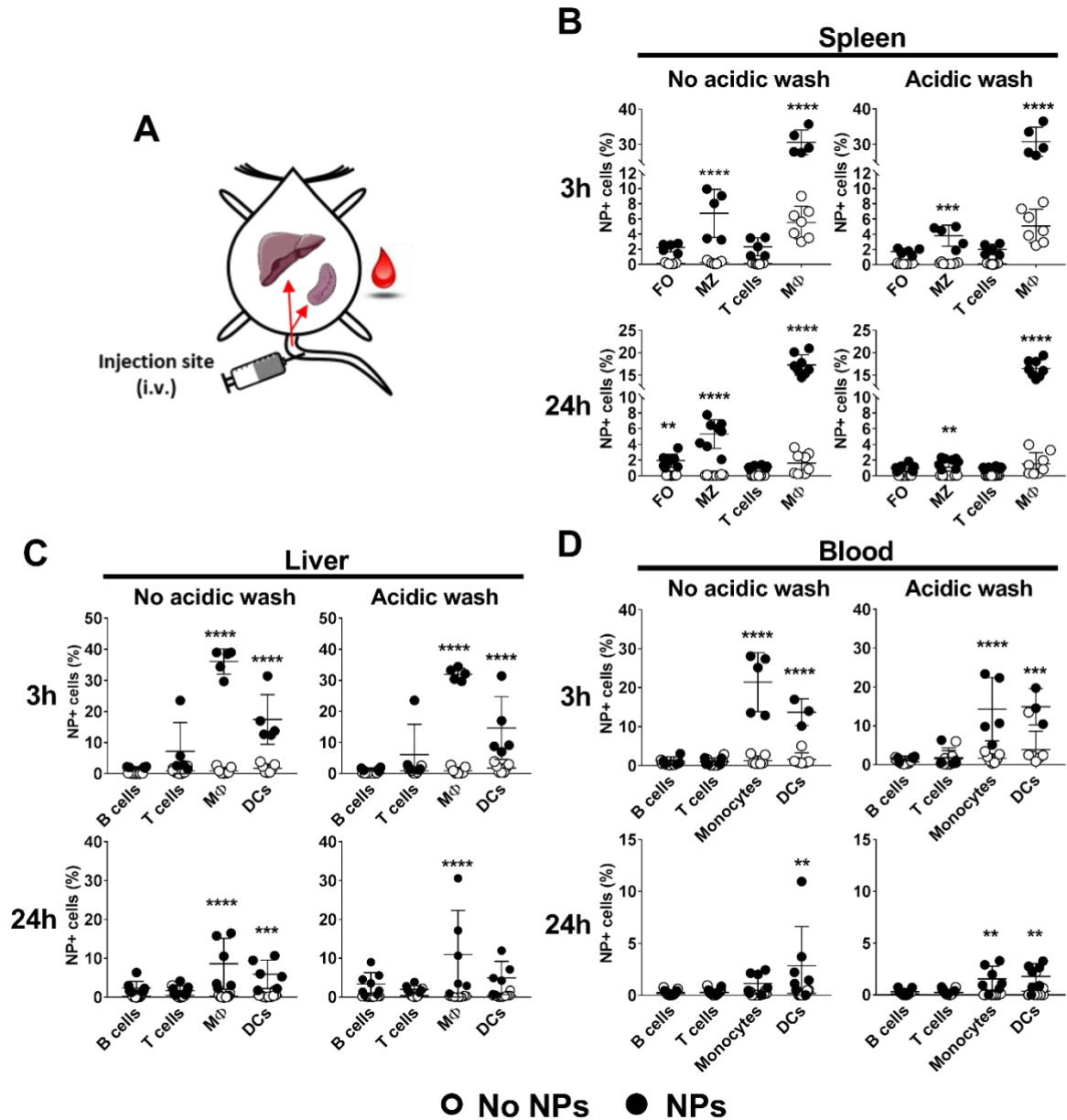


Figure 1: Biodistribution of GNPs after intravenous injection. **A)** Scheme of the GNP administration and targeted organs (spleen, liver and blood) in C57/BL6 mice. Total GNP-cell association (no acidic wash) and uptake of GNPs (acidic wash) were measured in different immune cell populations in the **B)** spleen, **C)** liver and **D)** blood 3h and 24 h after intravenous injection with 400 μ g GNPs in the tail vein. The acidic wash method was performed prior to cell staining and measurement of GNP-Cy5 positive cells by flow cytometry. Data for each time point show two separate experiments combined. Each dot represents cells from an individual mouse (n=5-8). Error bars: mean \pm SD of the pooled data; **p<0.01, ***p<0.001, p****<0.0001. Data were evaluated by two-way ANOVA, followed by Sidak's multiple comparison post-hoc test. B cells (CD19⁺/CD3⁻), MZ: marginal zone B cells (CD19⁺/CD21⁺/CD23⁻), FO: follicular B cells (CD19⁺/CD21⁺/CD23⁺), T cells (CD19⁻/CD3⁺), M ϕ /monocytes (CD11b⁺/CD11c⁻), DC: (CD11b⁺/CD11c⁺).

Results: Manuscript 2

In order to target B cells in the LN, GNPs were subcutaneously injected (300 µg) into the mouse flank. After 3 or 24 h, ipsilateral inguinal LN (ipsi. iLN or primary draining LN), ipsilateral axillary LN (ipsi. aLN or secondary draining LN), contralateral inguinal LN (contra. iLN or non-draining LN) and spleen were collected, processed and treated with acidic buffer prior to flow cytometry analysis (**Figure 2A**). The results suggested that GNPs were not significantly taken up by B cells in any of the LN up to 24 h after incubation. Instead, GNPs most likely associated with B cell surface (as seen without acidic wash), which was observed only at 3 h in both draining LN with 15% (ipsi. iLN) and 5% (ipsi. aLN) of GNP positive B cells, but not in non-draining LN (contra. iLN) (**Figure 2B** and **2C**). Again, macrophages, followed by DCs, were the leading cells to take up GNPs in draining LN (~40%) and non-draining LN (~30%) after 24 h (**Figure 2B** and **2C**). Additionally, it was observed that GNPs are detected in splenic macrophages and DCs only 24 h after subcutaneous injection, indicating that GNPs enter systemic circulation over time (**Figure 2D**). Taken together, we showed that the level of GNP biodistribution differed among different immune cell populations and their subsets in different organs, which was dependent on the time of exposure and route of administration.

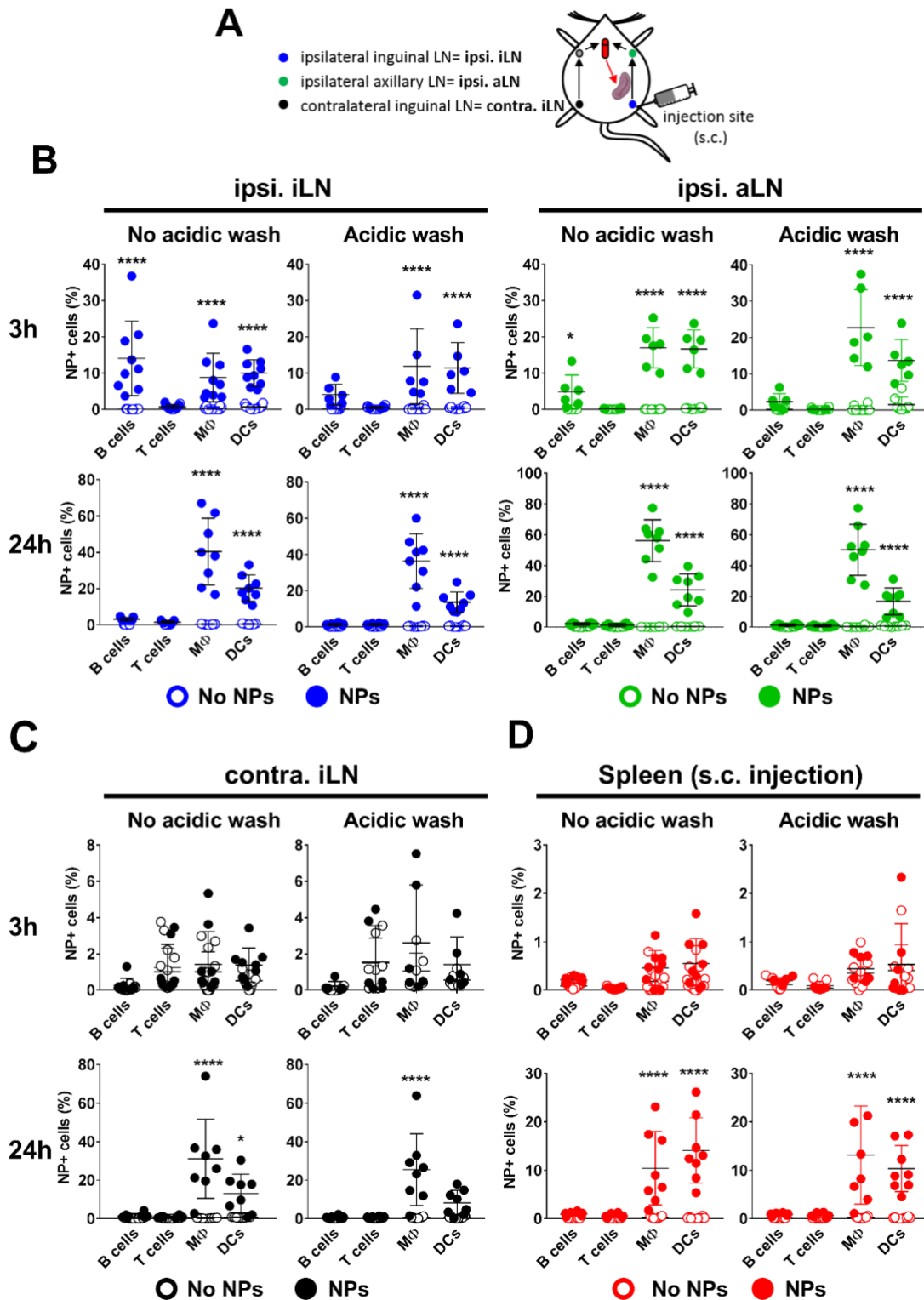


Figure 2: Biodistribution of GNPs after subcutaneous injection. A) Scheme of the GNP administration and targeted inguinal and axillary LN, based on their position in relation to the site of injection in C57/BL6 mice. Total GNP-cell association (no acidic wash) and uptake of GNPs (acidic wash) were measured in different immune cell populations in the **B)** ipsilateral inguinal LN (ipsi. iLN) or primary draining LN **C)** ipsilateral axillary LN (ipsi. aLN) or secondary draining LN and **D)** contralateral inguinal LN (contra. iLN) or non-draining LN 3h and 24 h after subcutaneous injection with 300 μ g GNPs in the flank. The acidic wash method was performed prior to cell staining and measurement of GNP-Cy5

Results: Manuscript 2

positive cells by flow cytometry. Data for each time point panel show two separate experiments combined. Each dot represents cells from an individual mouse (n=6-8). Error bars: mean \pm SD of the pooled data; *p<0.05, ****p<0.0001. Data were evaluated by two-way ANOVA, followed by Sidak's multiple comparison post-hoc test. B cells (CD19⁺/CD3⁻), T cells (CD19⁻/CD3⁺), M ϕ /monocytes (CD11b⁺/CD11c⁻), DC: (CD11b⁺/CD11c⁺).

Polymer-coated GNPs are highly immunocompatible

Next, we looked into the overall biocompatibility of intravenously injected GNPs. Cell viability was measured by flow cytometry, using an amine-reactive viability dye. The results showed no decrease in cell viability among splenocytes, blood and liver leukocytes up to 24 h after injection (**Figure 3A** and **Figure S2A**). Moreover, no significant changes in the percentage of different immune cell populations across the organs were observed. Importantly, the percentages of B cell populations and their subsets (MZ and FO B cells in spleen) remained unchanged in the spleen, liver and blood (**Figure 3B** and **Figure S2B**).

Some studies reported the GNP ability to activate the immune cell response, resulting in the expression of activation markers, production of proinflammatory cytokines and antibodies.^{27,34,35} To evaluate whether the GNPs could activate B cells and promote their immune response *in vivo*, we examined the expression of a common immune cell activation marker, CD86, and the production of IgM and IgG antibodies upon intravenous injection of GNPs. The results showed that GNPs did not cause any increase in CD86 expression in B cells or other immune cells (macrophages/monocytes, DCs) in any of the organs tested up to 24 h (**Figure 3C**). Moreover, it was observed that GNPs did not cause an increase in total serum IL-6 production (**Figure 3D**). Most importantly, GNPs did not affect the production of total IgM and IgG up to 24 h post-injection (**Figure 3E**).

Similar results were obtained in LN after subcutaneous injection of GNPs, showing no effect of GNPs on cell viability or change in the percentage of different LN immune cell populations up to 24 h. (**Figure S3**). Moreover, no significant increase in CD86 expression was observed in LN immune cells as well as no significant increase in serum IL-6, IgM and IgG concentrations up to 24 h post-injection (s.c.) was detected (**Figure S4**).

In order to investigate how LN and splenic immune cells are directly affected by GNPs at high concentrations, primary mouse splenocytes or LN cells were incubated with 20 μ g/ml of GNPs for 24 h at 37 °C, CO₂. We could confirm that despite these elevated GNP concentrations and high GNP-cell association *in vitro*, no death or increase in splenic or LN IL-6 release was detected (**Figure S5**). Together, these *in vivo* and *in vitro* results suggest high biocompatibility of GNPs, with no adverse effect cell viability or induction of B cell activation in adjuvant- and antigen-free conditions.

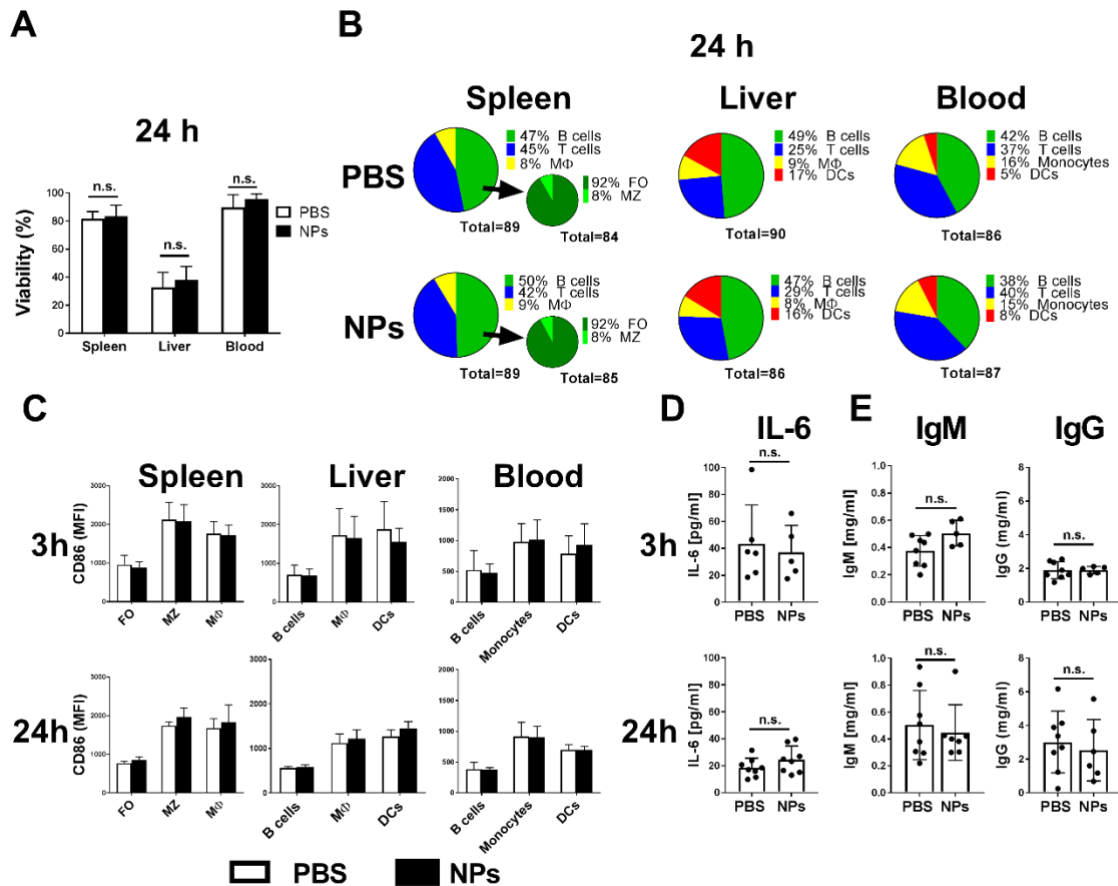


Figure 3: Cell viability in different organs and primary immune response after intravenous administration of GNPs. A) Total cell viability in spleen, liver and blood, 24 h post-intravenous injection with 400 μ g of GNPs in C57/BL6 mice, measured by flow cytometry using amine-reactive viability dye. **B)** Percentage of different immune cell populations in spleen, liver and blood, 24 h post-injection. **C)** Expression of surface immune activation marker CD86 in different immune cell populations of spleen, liver and blood after 3 and 24 h post-injection with GNPs measured by flow cytometry. **D)** Production of serum IL-6, 3 h and 24 h post-injection of GNPs measured by ELISA. **E)** Production of total serum IgM and IgG 3 and 24 h after injection with GNPs measured by ELISA. Data for each time point panel show two separate experiments combined. Each dot represents cells from an individual mouse ($n=5-8$). Error bars: mean \pm SD of the pooled data; n.s.: not significant = $p>0.05$. Data were evaluated by two-way ANOVA followed by Sidak's multiple comparison post-hoc test or by unpaired Student's t-test (ELISA data only). B cells (CD19⁺/CD3⁻), MZ: marginal zone B cells (CD19⁺/CD21⁺/CD23⁻), FO: follicular B cells (CD19⁺/CD21⁺/CD23⁺), T cells (CD19⁻/CD3⁺), Mφ/monocytes (CD11b⁺/CD11c⁻), DC: (CD11b⁺/CD11c⁺).

Adjuvant-activated isolated splenic B cells take up more GNPs, which causes attenuation of their primary immune response *in vitro*

After confirmation of the high biocompatibility of GNPs with B cells across different organs, we asked whether GNP are be internalized differently by activated B cells and if that would potentially affect B cell viability and innate-like B cell function. To investigate if activated B cells take up more GNPs, we first performed an *in vitro* experiment on a primary B cell population purified from mouse spleen. To achieve B cell activation, a TLR7-specific adjuvant R848 was used and served as a positive control for immune activation, cytokine and primary antibody production. B cells were co-incubated with R848 (2 µg/ml) and GNPs (20 µg/ml) for 1, 5 or 24 h at 37 °C, 5% CO₂. After GNP exposure and prior to flow cytometry acquisition, B cells were treated with an acidic wash in order to evaluate the GNP internalization. The results showed a high GNP-B cell association (without acidic wash) already after 1 and 5 h (~40-60%) and even higher after 24 h with ~80% of GNP-positive B cells. However, a significant uptake (after acidic wash) was detected only after 24 h (**Figure 4A**). Importantly, at the 24 h time point, GNP internalization in R848-activated B cells significantly increased to 70%, compared to 45% in R848-free B cells (**Figure 4A** and **4B**). Despite an increased uptake by activated B cells, the cell viability and expression of CD86 was not affected after 24 h (**Figure 4C** and **4D**). Interestingly, the concentration of IL-6 and IgM in supernatants of R848-activated B cells was significantly decreased upon 24 h GNP exposure (**Figure 4E** and **4F**). Thus, these results suggest that polymer-coated GNPs have the ability to inhibit primary B cell immune function *in vitro*. Moreover, after incubation of B cells at 4 °C for 1 and 5 h, we observed no GNP-B cell association or cell activation in R848 and R848-free conditions, suggesting that the process of GNP internalization in B cells is dependent on active metabolic processes that are greatly reduced at 4°C (**Figure S6**). Additionally, a different GNP formulation, without the second layer of PEG (homo) was tested on isolated splenic B cells in order to determine a possible effect of fluorochrome on B cell response. The results were highly comparable with the outcome of exposures with double PEGylated GNPs, suggesting that the fluorochrome incorporation is stable and does not contribute to the effect of GNP on B cells *in vitro* (**Figure S7**).

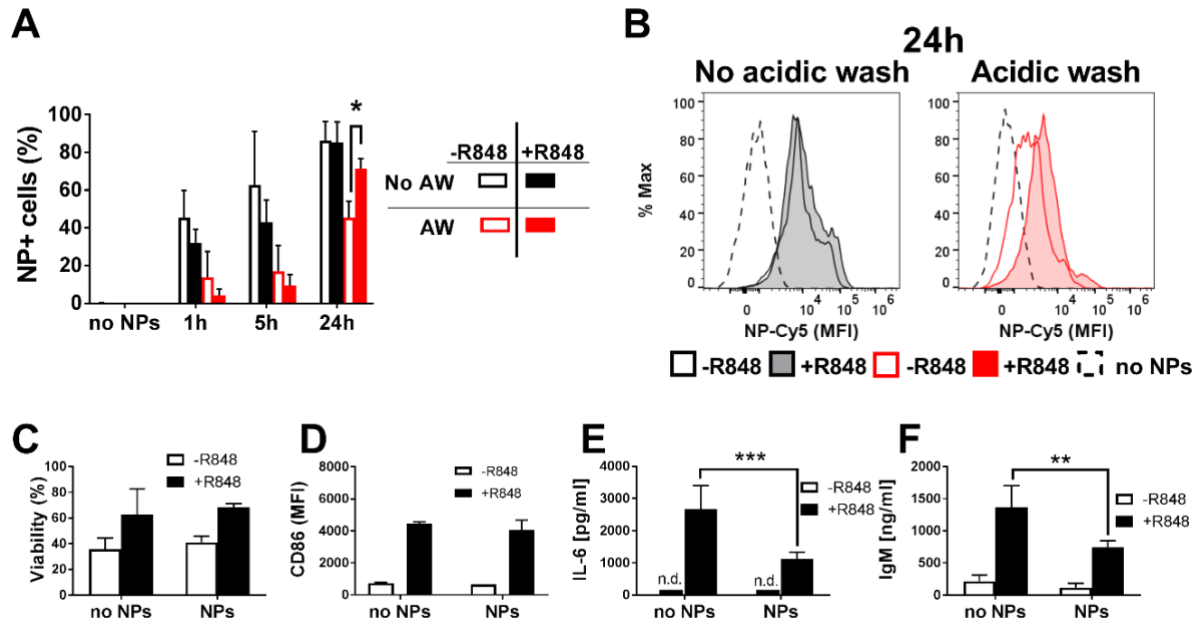


Figure 4: GNP effect on isolated splenic B cells *in vitro*. **A)** Total GNP-B cell association (no acidic wash) or GNP uptake (acidic wash) by isolated splenic B cells 1, 5 and 24 h after exposure to 20 $\mu\text{g}/\text{ml}$ GNPs in the presence or absence of R848 (2 $\mu\text{g}/\text{ml}$) adjuvant, measured by flow cytometry as a percentage of GNP-Cy5 positive cells. **B)** Histograms of median fluorescence intensity (MFI) of GNP-Cy5 associated with B cells (no acidic wash) or taken up by B cells (acidic wash), 24 h post-exposure in the presence or absence of R848 adjuvant. **C)** B cell viability after 24 h exposure with GNPs measured by flow cytometry using amine-reactive viability dye. **D)** Expression of surface activation marker CD86 on B cells, measured by flow cytometry 24 h after exposure. **E)** IL-6 production by B cells measured in the supernatant by ELISA 24 h after exposure with GNPs. **F)** Production of IgM measured in the supernatant by ELISA 24 h after exposure to GNPs. Data for each time point show three separate experiments combined ($n=3$). Error bars: mean \pm SD of the pooled data; * $p<0.05$, ** $p<0.01$ and *** $p<0.001$. Data were evaluated by two-way ANOVA followed by Tukey's multiple comparison post-hoc test. No AW: no acidic wash, AW: acidic wash.

Polymer-coated GNPs do not affect primary function in adjuvant-activated B cells *in vivo*

Based on our *in vitro* results on isolated B cells, we investigated if a similar increase in GNP uptake in activated B cells would also occur *in vivo* and if this would affect B cell primary immune response in the system. Again, we used R848 in order to induce innate-like immune activation in B cells *in vivo*. Interestingly, our results suggested that pre-administration of R848 (10 μg , s.c.), followed by intravenous injection with 400 μg GNPs, caused decrease of GNP-cell association and uptake in macrophages as well as B cells, 3 and 24 h after GNP injection (**Figure S8**). In order to test if this inhibition in uptake is somehow related to preactivation with the adjuvant, we next injected GNPs (400 μg , i.v.) and R848 (10 μg , s.c.) simultaneously for 3h (**Figure 5A**). Interestingly, in this experimental setup, no difference in GNP uptake by macrophages and B cells between R848-stimulated and R848-

free mice was observed at 3 h time point (**Figure 5B**). Importantly, GNPs did not cause a decrease in splenocyte viability or a change in B cell population percentage in adjuvant-stimulated mice (**Figure 5C**).

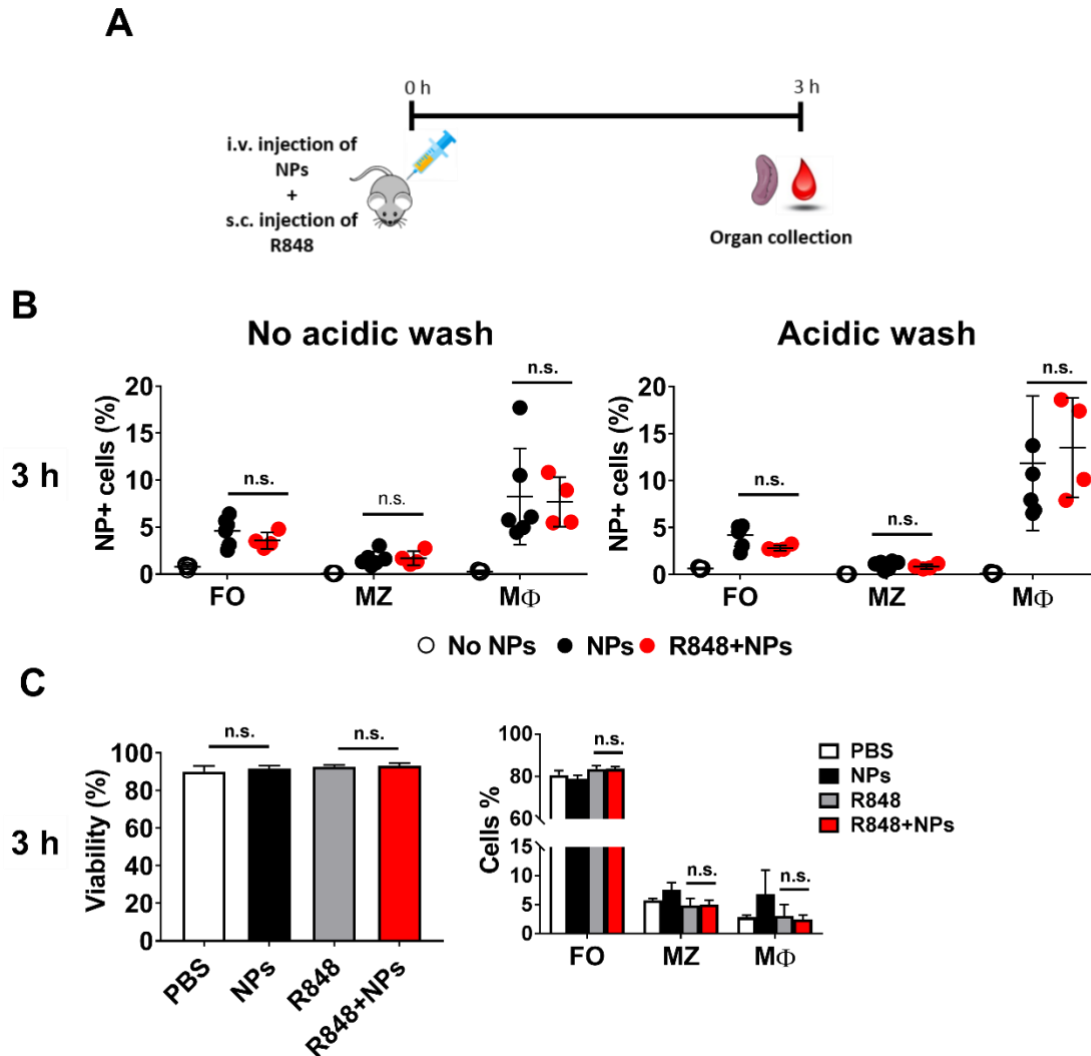


Figure 5: GNP uptake and cell viability after simultaneous injection of GNPs and adjuvant. A) Scheme of the experimental setup. C57/BL6 mice were intravenously injected with 400 μ g GNPs, immediately followed by subcutaneous injection with 10 μ g R848. After 3 h of incubation spleen and blood were collected. **B)** Total GNP-cell association (no acidic wash) and uptake of GNPs (acidic wash) measured in different immune cell populations. **C)** Total cell viability of splenocytes and the percentage of B cell subsets and macrophages measured by flow cytometry. Data show one biological experiment. Each dot represents an individual mouse (n=4-5). Error bars: mean \pm SD; n.s.: not significant= p>0.05. Data were evaluated by one-way ANOVA followed by Dunnett’s multi comparison post-hoc test or two-way ANOVA, followed by Tukey’s multiple comparison post-hoc test. MZ: marginal zone B cells (CD19⁺/CD21⁺/CD23⁻), FO: follicular B cells (CD19⁺/CD21⁺/CD23⁺), M ϕ (CD11b⁺/CD11c⁻).

Results: Manuscript 2

Further, we investigated whether the immune function in adjuvant-stimulated mice was affected by GNPs at the 3 h time point. The results showed that GNPs simultaneously administered with R848 did not interfere with the expression of B cell activation markers (CD86, MHC II, surface IgM) compared to R848 control mice (**Figure 6A**). In addition, no change in the concentration of total serum proinflammatory cytokines (IL-6 and TNF- α), as well as serum IgM and IgG was observed in mice 3 h after injected with R848 and GNPs (**Figure 6B**).

Next, we wanted to investigate the direct effect of GNPs on B cell primary immune responses *in vivo*. Therefore, 3 h after injections with GNPs, R848, or simultaneous injection of GNPs and R848, spleens were collected and purified populations of B cells were isolated, followed by B cell RNA isolation and gene expression measured by qRT-PCR with gene-specific primers. The results showed that GNPs did not significantly affect the expression of B cell *il-6*, *tnf-alpha*, *tlr7* and *il-1beta* in adjuvant-stimulated mice (**Figure 6C**). Overall, these results suggested that the B cell early innate-like immune response is not significantly affected by polymer-coated GNPs.

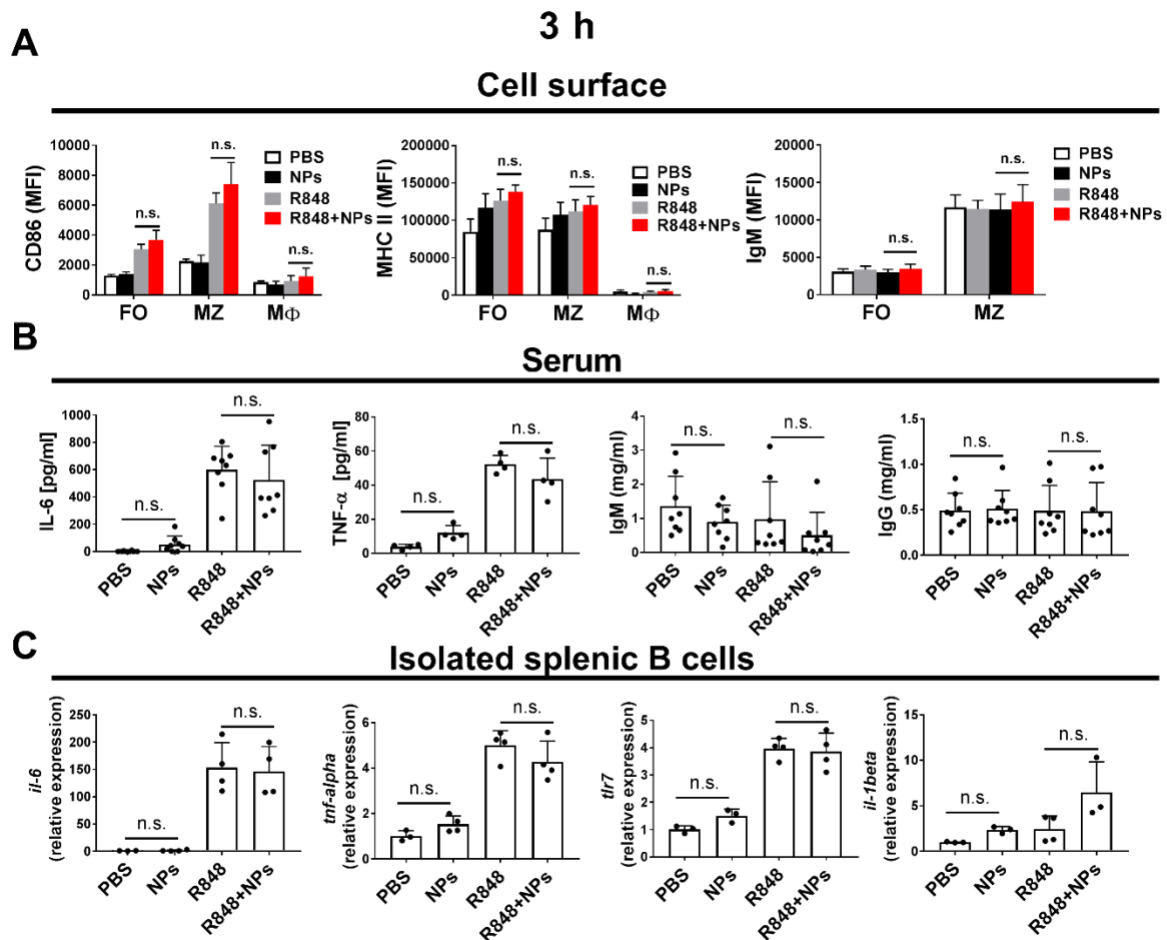


Figure 6: Effect of GNP on B cell activation and innate-like immune response *in vivo*. C57/BL6 mice were injected (i.v.) with 400 μ g GNPs, immediately followed by injection (s.c.) with 10 μ g R848, incubated for 3 h incubation. **A)** Expression of CD86, MHC II and IgM surface markers in splenic B cell subsets, measured by flow cytometry. **B)** Production of serum IL-6, IgM and IgG. **C)** Expression of *il-6*, *tnf-alpha*, *tlr7* and *il-1beta* genes in isolated B cell populations measured by qRT-PCR. Data are presented as a relative expression with respect to *nadph* housekeeping gene. Data for each panel show one biological experiment. Each dot represents cells from an individual mouse ($n=5-8$). Error bars: mean \pm SD; n.s: not significant = $p>0.05$. Data were evaluated by one way ANOVA or two-way ANOVA, both followed by Tukey's multiple comparisons post-hoc test.

Polymer-coated GNPs are significantly taken up by follicular B cells, germinal center B cells and plasmablasts in OVA-immunized mice

B cells play an important role in adaptive immunity and are the sole producers of antibodies upon stimulation with an antigen. Therefore, we were interested if B cells in mice stimulated with a known antigen are affected by the GNPs. First, we investigated if GNP uptake by different B cell subsets changes over time and how this might be reflected in antigen-primed B cells *in vivo*. Thus, mice were intravenously injected with GNPs and subcutaneously immunized with a mix of OVA protein and R848

Results: Manuscript 2

adjuvant to ensure a sufficient activation of antigen-specific B cells. After 7 or 14 days, mice were euthanized and spleen and blood were collected and processed for further analysis (**Figure 7A**). The flow cytometry results showed that on day 7 GNPs accumulated equally in FO and MZ B cells of OVA-immunized mice and mice without OVA. In detail, approximately 4% of FO and MZ B cells in both groups were GNP-positive (**Figure 7B**). Interestingly, on day 14, the association of FO B cells with GNPs in OVA-immunized mice was significantly higher (~5%) compared to the GNP group (~2%), suggesting that antigen-primed FO B cells are more susceptible to association with GNPs (**Figure 7C**). Of note, the signal from GNPs associated with macrophages was significantly decreased compared to the one we observed in short-term experiments, dropping from ~10-30% (3h) to close to 0% after 14 days (**Figure 1B** and **Figure 7C**). This phenomenon most likely occurred due to the clearance of GNPs out of the spleen *via* macrophage migration.

Next, B cells were further divided into the following subsets - transitional 1 (CD19⁺/IgM^{hi}/IgD^{low}), transitional 2 (CD19⁺/IgM^{hi}/IgD^{hi}), mature naive (CD19⁺/IgM^{low}/IgD^{int}) B cells, plasmablasts (CD19⁺/CD138⁺) and plasma cells (CD19⁻/CD138⁺). CD19⁺/IgM^{low}/IgD^{low} cells were further gated on germinal center (GC) B cells (GL7⁺/Fas⁺) and GC negative B cells (GL7⁻/Fas⁻) (**Figure S12**). Further flow cytometry analysis revealed that GNPs mainly accumulated in GC positive B cells on day 7, regardless of OVA-immunization or not (**Figure 7D**). Interestingly, on day 14 GNPs were significantly associated with plasmablasts of OVA-immunized mice (~10%), compared to GNP-plasmablasts association in mice without OVA immunization (~5%) (**Figure 7E**, upper panel). Moreover, a similar trend was observed in GC B cells, with 10% of GNP positive GC B cells in OVA-free vs. 30% in OVA-immunized mice (**Figure 7E**, lower panel). No significant GNP-cell association was detected in the rest of the B cell subsets (T1, T2, mature naive and plasma cells in both, GNP and OVA/R848+GNP group) (**Figure 7E**). These results indicate that B cells in antigen-primed mice are more susceptible to associate with GNPs, which is also subtype-dependent.

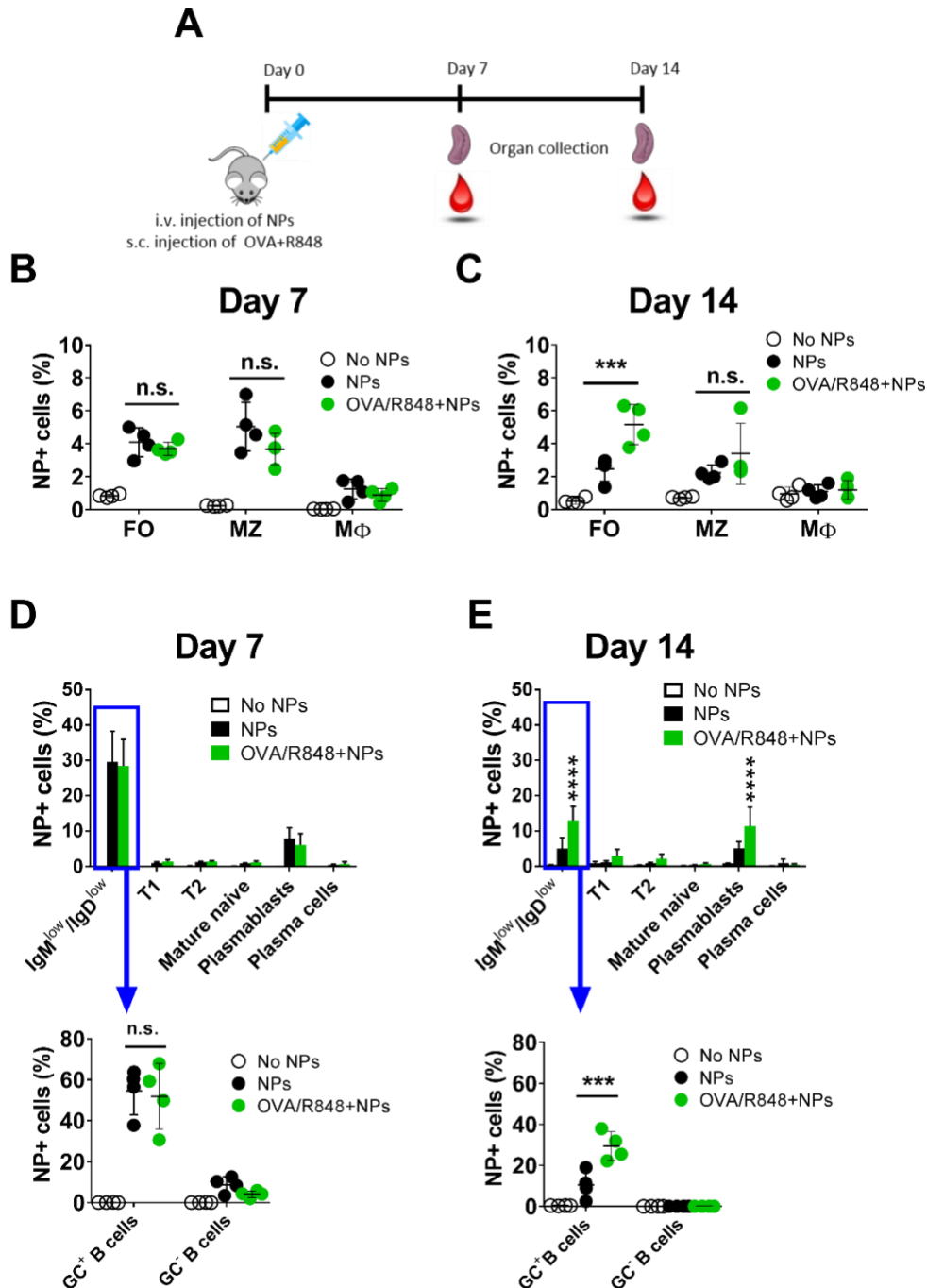


Figure 7: GNP association with different B cell subsets after simultaneous injection of GNPs and antigen. **A)** Scheme of the experimental setup. C57/BL6 mice were injected with 400 μ g GNPs, immediately followed by injection of a mixture of OVA antigen (100 μ g) and R848 (10 μ g). Total GNP-association measured in splenic marginal zone B cells, FO B cells and macrophages after **B)** 7 days or **C)** 14 days. **D)** GNP-cell association measures in different B cell subsets **D)** 7 days and **E)** 14 days after injections. Data for each time point show one biological experiment. Each dot represents an individual mouse (n=4). Error bars: mean \pm SD; ***p<0.001, ****p<0.0001, n.s.: not significant= p>0.05. Data were evaluated by two-way ANOVA, followed by Tukey's multiple comparison post-hoc test. MZ: marginal zone B cells (CD19⁺/CD21⁺/CD23⁻), FO: follicular B cells (CD19⁺/CD21⁺/CD23⁺), M Φ (CD11b⁺/CD11c⁻), T1: transitional 1 (CD19⁺/IgM^{hi}/IgD^{low}), T2: transitional 2 (CD19⁺/IgM^{hi}/IgD^{hi}), mature

Results: Manuscript 2

naive B cells (CD19⁺/IgM^{low}/IgD^{int}), plasmablasts (CD19⁺/CD138⁺), plasma cells (CD19⁻/CD138⁺), GC: germinal center B cells (CD19⁺/IgM^{low}/IgD^{low}/GL7⁺/Fas⁺), GC negative B cells (CD19⁺/IgM^{low}/IgD^{low}/GL7⁻/Fas⁻).

Polymer-coated GNPs do not impact the percentage of B cell subsets in immunized mice

Prolonged accumulation of inorganic GNPs in the system might have a delayed effect upon the immune cells, which can result in an increase of lymphocyte populations.¹ Therefore, we further analyzed if GNPs have an impact on the overall viability of splenocytes or if they influence the increase or decrease of different B cell subsets up to 14 days post-injection. Importantly, the results showed no adverse effect of GNPs on the viability of the splenocytes in antigen-free as well as in immunized mice up to 14 days (**Figure 8A** and **Figure S9A**). Similarly, GNPs did not cause significant change in the B cell repertoire, irrespective of immunization with OVA (**Figure 8B** and **8C**, **Figure S9B** and **S9C**). These results confirmed that polymer-coated GNPs remained biocompatible with B cells after longer accumulation in the non-immunized as well as immunized systems.

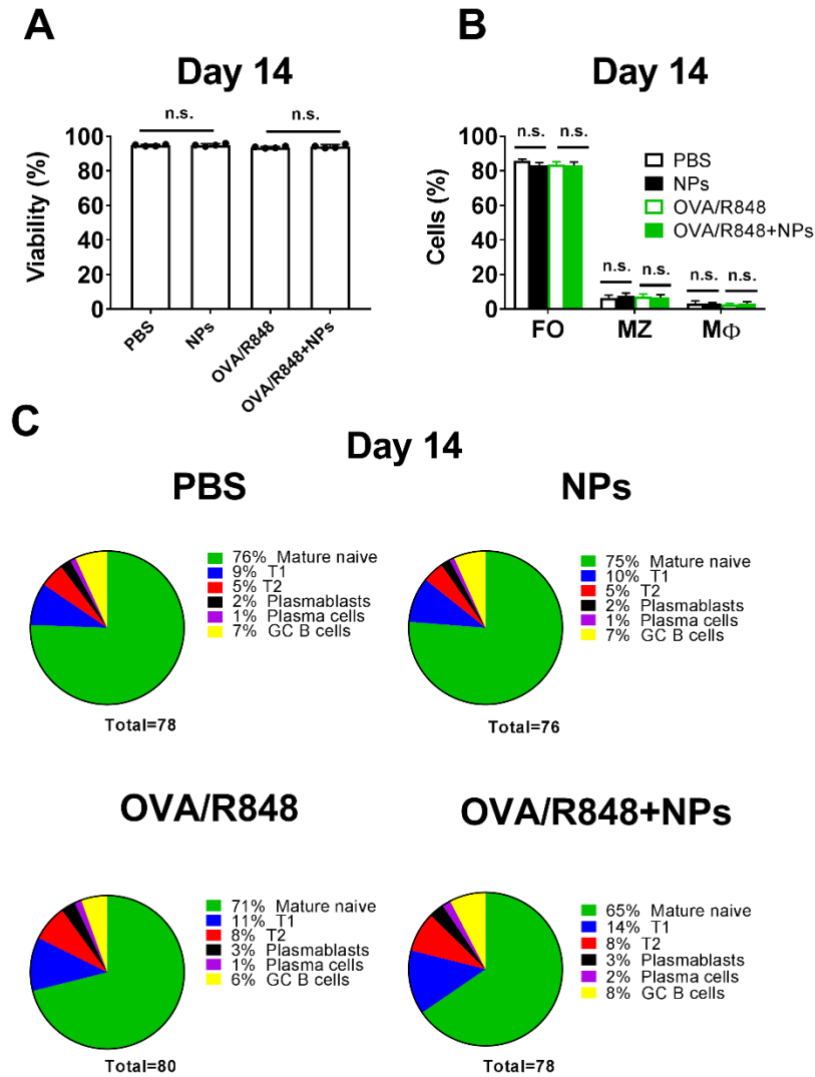


Figure 8: Viability of splenocytes after simultaneous injection of GNPs and antigen. **A)** Viability of splenocytes in C57/BL6 mice 14 days after injection with 400 μ g GNPs and OVA antigen (100 μ g)/R848 (10 μ g) measured by flow cytometry, using amine-reactive viability dye. **B)** Percentage of MZ B cells, FO B cells and macrophages in the spleen, 14 days post-injection with GNPs and OVA/R848. **C)** Percentage of different splenic B cell subsets upon injections with GNPs and OVA/R848. Data show one biological experiment. Each dot represents cells from an individual mouse (n=4). Error bars: mean \pm SD of the pooled data; n.s.: not significant. Data were evaluated by one-way ANOVA followed by Dunnett's multi comparison post-hoc test (viability) and two-way ANOVA, followed by Tukey's multiple comparisons post-hoc. MZ: marginal zone B cells (CD19⁺/CD21⁺/CD23⁻), FO: follicular B cells (CD19⁺/CD21⁺/CD23⁺), Mφ (CD11b⁺/CD11c⁻), T1: transitional 1 (CD19⁺/IgM^{hi}/IgD^{low}), T2: transitional 2 (CD19⁺/IgM^{hi}/IgD^{hi}), mature naive B cells (CD19⁺/IgM^{low}/IgD^{int}), plasmablasts (CD19⁺/CD138⁺), plasma cells (CD19⁺/CD138⁺), GC: germinal center B cells (CD19⁺/IgM^{low}/IgD^{low}/GL7⁺/Fas⁺).

Polymer-coated GNPs cause attenuation of B cell adaptive immune response

Based on the results regarding an increased B cell association with GNPs in OVA-immunized mice, we further investigated if this reflects upon B cell expression of surface markers and most importantly upon B cell adaptive immune response. The results showed no change in MZ and FO B cell expression of surface markers (CD86, MHC II and IgM) in non-immunized or immunized mice 14 days after GNP injection (**Figure 9A** and **9B**). Surprisingly, the production of OVA-specific IgM antibodies measured in the serum was suppressed at day 7 (**Figure 9C**) and significantly inhibited by day 14 in mice exposed to GNPs (**Figure 9D**). These results suggested that GNPs have the ability to interfere with B cell antigen-specific immune response, resulting in its suppression.

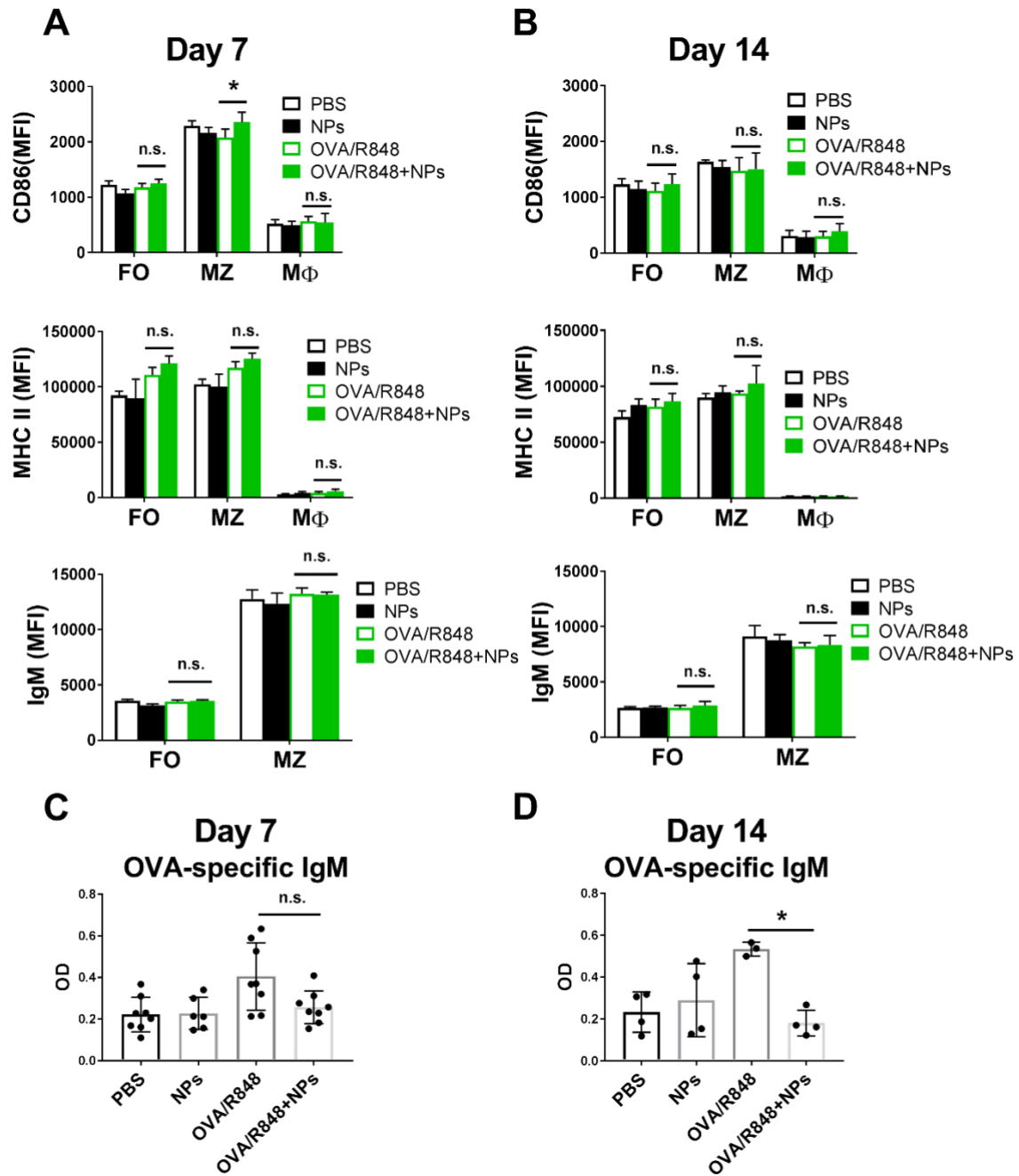


Figure 9: Effect of GNP on B cell activation and adaptive immune response *in vivo*. **A)** Expression of surface activation markers on MZ, FO B cells and macrophages **A)** 7 days and **B)** 14 days after injection of C57/BL6 mice with 400 μ g GNPs and OVA antigen (100 μ g)/R848 (10 μ g). **C)** Production of OVA-specific IgM **C)** 7 days and **D)** 14 days after injection with GNP and OVA/R848. Data show two separate experiments combined (7 days) or one biological experiment (14 days). Each dot represents cells from an individual mouse (n=4-8). Error bars: mean \pm SD of the pooled data; *p<0.05, n.s.: not significant=p>0.05. Data were evaluated by one-way ANOVA, followed by Dunnett's multi comparison post-hoc test or two-way ANOVA, followed by Tukey's multiple comparisons post-hoc test. MZ: marginal zone B cells (CD19⁺/CD21⁺/CD23⁻), FO: follicular B cells (CD19⁺/CD21⁺/CD23⁺), M ϕ (CD11b⁺/CD11c⁻).

DISCUSSION

Understanding the interactions between GNPs and B cells and the impact of GNPs on B cell function is crucial for the future design of medically applicable GNPs. This is especially important in GNP-based vaccine applications, where B cells are often directly targeted. Our findings reported here provide new insights about the general biocompatibility of polymer-coated GNPs and their ability to interact with B cells and their primary and adaptive immune response *in vivo*.

Our initial results suggested that in the first 24 h GNPs primarily associate with and are taken up by MZ B cells, whereas FO B cells do not significantly interact with GNPs in the first 3 h after systemic administration. In fact, GNPs reached FO B cells after 24 h but were not significantly internalized at that time. A similar observation was reported before, where 50 nm PEGylated GNPs were predominantly visualized in the marginal zone and red pulp after 1 h, followed by border distribution after 24 h, detected deeper in the follicles.³⁶ The early association of GNPs with MZ B cells may be explained by the possible opsonization of GNP with serum proteins such as complement proteins and the ability of B cells to phagocytose opsonized particular matter *via* complement receptors (*eg.*, C1R), which are highly expressed on MZ B cells.³⁷ However, we observed that cell biodistribution in the spleen can differ due to batch-to-batch differences of the polymer. Therefore, the importance of the physico-chemical characteristics of the GNPs and their stability in the biological system needs to be stressed. Additionally, we could not observe any strong association of GNPs with B cells in the liver and blood. On the contrary, Tsoi *et al.* reported high uptake of PEGylated quantum dots (d_h : ~15 nm) by hepatic B cells 4 and 12 h after systemic administration.³⁸ Again, this may suggest the variations in the endocytic ability of B cells based on the characteristics of the nanomaterial. Furthermore, we could detect no internalization of GNPs by LN B cells up to 24 h after subcutaneous injection. In comparison, it was reported that 1000 nm polystyrene particles were not detected close to B cell follicles, whereas a strong accumulation of 20 nm NPs inside B cell follicles was visualized 48 h post-injection.³⁹ Therefore, the route of administration, time of incubation, level of protein opsonization and size of the NPs are important factors in the NP biodistribution and their association with B cells in different organs.

Dutt *et al.* reported that higher uptake of single-walled carbon nanotubes in LPS-activated B cells caused an increase in B cell toxicity *in vivo*.⁴⁰ In contrast, we observed no change in GNP uptake in adjuvant-activated B cells in mice. Moreover, no decrease in cell viability or modulation of B cell early immune response, such as expression of cytokines IL-6 and TNF- α or production of primary IgM was observed. In fact, no adverse impact on the cells in the spleen was observed 14 days post-injection. Together, these data suggest high biocompatibility of polymer-coated GNPs with B cells *in vivo*, which

Results: Manuscript 2

is in agreement with the literature that generally reports low or no cytotoxicity and immunogenicity of GNPs in comparison to other engineered metal NPs.²²

B cells play a crucial function in the recognition of antigens, which leads to their activation and formation of germinal centers, eventually leading to their differentiation into antibody-producing plasma cells. It has been shown that BCR-dependent phagocytosis of antigen-conjugated 1 μm beads by FO B cells led to efficient formation of B cell germinal centers, where beads were detected close to the GC B cells 5 h post-injection.¹⁰ Importantly, it has been reported that B cells effectively phagocytized particulate antigens, which resulted in improved adaptive immune response, whereas B cells were insufficient in doing so when introduced to a soluble antigen.^{9,10} Here, we reported that despite separated administration of GNPs and antigen, this resulted in increased detection of GNPs in FO B cells, GC B cells as well as plasmablasts, but not in plasma cells 14 days post-injections. Hereof, the question remains regarding the mechanism of the increased uptake of antigen-unconjugated, polymer-coated GNPs in the immunized mice. Possibly, GNPs were opsonized by OVA in the system, forming a “particulate antigens”. The latter may have provided better availability of OVA to BCRs, which led to higher uptake of GNPs by B cells. On the other hand, it is possible that GNPs, which bound to the B cell surface unspecifically, were simply “piggyback” phagocytized along with the antigen. However, further studies are needed to investigate and understand this important aspect.

Most importantly, we obtained new information on how polymer-coated GNPs impact B cell humoral response. Here, we reported that GNPs significantly inhibited antigen-specific IgM production, seemingly due to increased uptake in B cell subsets crucial in differentiation towards antibody-producing cells, such as FO B cells, GC B cells and plasmablasts. On the contrary, some studies reported that GNPs have the ability to induce antibody production in immortalized B cell lines.^{27,28} In contrast, Hirohata *et al.* reported strong immunosuppression in antigen-specific IgM production in human B cells *in vitro* after exposure with gold compounds used for the treatment of rheumatoid arthritis.⁴¹ Moreover, a clinical study reported significant suppression in immunoglobulins, especially IgM, in rheumatoid arthritis patients treated with gold salts.⁴² Therefore, this data suggests that gold as a material has a unique ability to suppress B cell humoral response. Indeed, immunosuppression of the innate immune response by GNPs was reported before in macrophages, DCs and B cells as attenuation of production of proinflammatory cytokines such as TNF- α , IL-6, IL-12 and IL-1 β and is considered to be the result of GNPs ability to interfere with the NF κ -B signaling pathway.^{26,43–45} However, it is not yet clear how exactly GNPs are able to suppress B cell adaptive function, which should be answered with further studies.

CONCLUSION

In conclusion, we showed that polymer-protected GNPs are highly biocompatible with B cells and do not impair B cell populations and their subsets. Moreover, we showed that GNPs are not inflammatory towards B cells and do not have an adverse effect on their early innate-like immune function. However, we demonstrated that GNPs accumulate in the splenic B cell follicle over time and have the ability to inhibit B cell adaptive immune response. This information gives important insights for the future GNP-based medical applications to understand the potential consequences of GNPs directed to target B cells as well as to better predict GNP off-target effects on the B cell function.

METHODS

GNP synthesis and characterization

15 nm citrate-stabilized gold nanospheres were synthesized as reported by Trkevich et al.⁴⁶ Thiolated PEG polymers (NH₂-PEG-SH) conjugated with Cy5 fluorochrome were synthesized, followed by polymer coating of GNPs to obtain homo-functionalized fluorescently labeled GNPs as previously reported by Rodriguez-Lorenzo *et al.*²⁹ To obtain hetero GNP formulation, homo-functionalized GNPs were coated with the second PEG coating (methoxy PEG).²⁹

GNP stability was evaluated by the optical characterization with Cary 60 UV-vis spectrophotometer (Agilent Technologies). Prior to measurements of GNP spectra, 20 µg/ml of GNPs were incubated in water, PBS, complete culture medium (RPMI 1640 with L-Glutamine culture medium (Gibco) supplemented with 10% fetal calf serum (FCS, Biowest), 1% Penicillin/Streptomycin, 1% Sodium Pyruvate, 1% Non-Essential Amino Acid (NEAA), 0.1% β-mercaptoethanol (all from Gibco) and 15% mouse serum (obtained from mouse blood) and incubated at 37 °C overnight. The size and ζ-potential of GNPs were measured with Zetasizer 7.11 (Malvern) using dynamic light scattering (DLS) and electrophoretic light scattering, respectively. For this purpose, GNPs were diluted in water to 0.05 mg/ml.

Mice

7-12 weeks old female C57BL/6J mice were used throughout the experiments. Mice were maintained under specific pathogen-free conditions in the animal facility at the Centre Médical Universitaire, University of Geneva. All animal experiments were conducted according to Swiss regulations. Animals were purchased from Charles River Laboratories, Saint Germain Nuelles, France.

Organ processing

Spleens harvested from mice were cut and smashed through 40 µm strainer and washed with PBS. After centrifugation (5 min, 400 × g, 4° C) supernatant was discarded and red blood cells were removed by adding 1 ml of lysing buffer BD Pharm Lyse (BD Biosciences) for 1 min at RT. Lymph nodes were cut and incubated at 37° C on a shaker (150 rpm) for 20-30 min in complete culture medium with 2mM CaCl₂ (Acros Organics), 3 mg/ml collagenase and 200 U/ml DNase I (both from Worthington). After incubation, digested lymph nodes were filtered through 40 µm strainer and washed with PBS. Liver tissue (~750-1200 mg) was dissociated with Liver Dissociation Kit (Miltenyi), following the manufacturer's protocol and further processed with gentleMACS Dissociator with Heaters run with the 37C_m_LIDK_1 program (Miltenyi). After obtaining a cell suspension from liver tissue, red blood lysis was performed (1 min, RT). ~100 µl of the collected blood sample was added into PBS with 2% EDTA, followed by red blood lysis (5 min, RT) and several washes with PBS, prior to flow cytometry measurements. The rest of the blood was used to collect serum by centrifugation with microcentrifuge (30 min, 21130 × g at RT) and stored at -20 °C for further ELISA assay.

Primary cell cultures

Obtained heterogeneous cell suspensions from spleen or LN were plated at 2×10^5 cells/well in a U-bottom 96-well plate (Corning) in RPMI 1640 with L-Glutamine culture medium (Gibco) supplemented with 10% fetal calf serum (FCS, Biowest), 1% Penicillin/Streptomycin, 1% Sodium Pyruvate, 1% Non-Essential Amino Acid (NEAA), 0.1% β-mercaptoethanol (all from Gibco). The pure B cell populations were isolated from splenocytes with mouse B cell Isolation Kit (negative selection, Miltenyi Biotech), following the manufacturer's protocol. > 96% purity was reached throughout the experiments and is presented in Figure S10B. Isolated splenic B cells were plated at 2×10^5 cells/well in a U-bottom 96-well plate in a complete culture medium (as described above).

GNP exposures *in vitro*

Heterogeneous cell suspensions from spleen or LN were exposed to GNPs (20 µg/ml) for 24 h at 37 °C, 5% CO₂. R848-ALX (Enzo) immunostimulant (2 µg/ml) was used as a positive control for activation. After GNP exposure, supernatants were collected and stored at -20° C for ELISA analysis. Isolated splenic B cells were exposed to different formulations (homo and hetero) of GNPs for 1 h, 5 h and 24 h at 37 °C and for 1 h and 5 h at 4 °C at GNP concentration of 20 µg/ml. R848 immunostimulant (2 µg/ml) was used as a positive control for activation of innate-like B cell immune response.

Acidic wash method (GNP uptake)

After GNP exposures, cells were incubated with an acidic wash buffer (100 nM NaCl, 50 nM Glycin in H₂O; pH 3) for 1 min on ice to remove the cell surface-associated GNPs. Next, cells were washed 2 x with PBS. Cells were then stained as normal with a viability dye and antibodies prior to flow cytometry measurements.

GNP biodistribution

Mice were injected intravenously with 400 µg GNPs in the tail vein or with 300 µg GNPs subcutaneously in the flank. 3 h or 24 h after injections mice were euthanized by CO₂ inhalation and different organs (spleen, liver, LN) and blood were collected and processed as described above. Acidic wash was then performed on cell suspensions of the spleen, LN, liver and blood, followed by staining for flow cytometry measurements.

Effect of GNPs in adjuvant- and antigen-stimulated mice

Pre-activation with adjuvant:

10 µg of R848 (Invivogen) in PBS was subcutaneously injected into mouse flank. After 3 h incubation, 400 µg GNPs in PBS was intravenously administrated in the tail vein. After an additional 3 or 24 h of incubation, mice were euthanized by CO₂ inhalation. Spleen and blood were collected and processed for further flow cytometry and ELISA analysis.

Simultaneous administration of adjuvant and GNPs:

Mice were intravenously injected with 400 µg GNPs in PBS. Immediately after, 10 µg R848 in PBS was subcutaneously injected into mouse flank. After 3 h of incubation, mice were euthanized by CO₂ inhalation and spleen and blood were collected and processed for further flow cytometry and ELISA analysis, respectively.

Simultaneous administration of antigen/adjuvant and GNPs :

Mice were intravenously injected with 400 µg GNPs in PBS. Immediately after, a mixture of 100 µg ovalbumin (OVA, Invivogen) and 10 µg R848 in PBS was subcutaneously injected into mouse flank. On day 7 or day 14 mice were euthanized by CO₂ inhalation and spleen and blood were collected and processed for further flow cytometry and ELISA analysis, respectively.

Flow cytometry

NovoCyte 3000 (ACEA Biosciences) was used for all flow cytometry measurements. Prior to flow cytometry measurements, compensation for the corresponding staining was performed by

Results: Manuscript 2

compensation beads UltraComp eBeads (Invitrogen). FlowJo (version 10) was used for post-measurement analysis. Cells were first stained with Zombie viability dye (Biolegend) in 1:1000 dilution with PBS and incubated for 15 min at RT. Next, cells were washed with FACS buffer (0.5 % BSA and 0.5 mM EDTA in PBS). Cells were then stained with the corresponding antibody mix diluted (all from Biolegend and all diluted at 1:200 in FACS buffer unless stated otherwise). FcBlock TruStain fcX-CD16/32 (1:100, Biolegend) was added into the mix. Gating strategies for *in vitro* and *in vivo* experiments are presented in Figures S10, S11 and S12. List of antibodies used in the study:

Leukocytes: CD45-PE-Cy7; B cells: CD19-BV510 (6D5), CD19-BV605 (6D5), CD19-BV650 (6D5), CD19-BV510 (6D5), B220-PerCP (RA3-6B2), CD23-PE (B3B4), CD21/35-PE-Cy7 (7E9), IgM-BV605 (RMM-1), IgM-BV605 (RMM-1), IgD-A488 (11-26c2a), CD138-PE-Cy7 (281-2), GL7-PE (GL7), CD95 (Fas)-PE-CF594 (Jo2) from BD; T cells: CD3-FITC (17A2), CD3-Pacific Blue (17A2); Macrophages and dendritic cells: CD11b-BV785 (M1/70), CD11b-BV785 (M1/70), CD11b-BV570 (M1/70), CD11c-PE (N418); Immune activation: MHC II-FITC (from MACS), CD86-BV510 (GL-1), CD86-BV605 (GL-1), CD86-BV785 (GL-1)

Quantitative real-time PCR (qRT-PCR)

Mice were simultaneously injected with 400 µg GNP (i.v.) and 10 µg R848 (s.c.). After 3h of incubation, mice were euthanized by CO₂ inhalation and pure splenic B cell population was isolated with mouse B cell Isolation Kit (negative selection, Miltenyi Biotech), following the manufacturer's protocol.

Next, RNA was isolated from pure B cells by trizol-based RNA extraction. Briefly, B cell pellets were collected and lysed with 1 ml of trizol (Life Technologies). Cell lysates were then centrifuged in a microcentrifuge (14000 rpm, 10 min, 4 °C) and the supernatant was collected. 200 µl of biphenol:chloroform:isoamyl alcohol = 25:24:1 (Biosolve) was added and vortexed. Samples were incubated for 3 min at room temperature and centrifuged (12000 rpm, 15 min, 4 °C). Next, the RNA phase was carefully collected and 500 µl of isopropanol was added. Samples were vortexed and incubated for 10 min at RT. After, samples were centrifuged (12000 rpm, 10 min, 4 °C) and the pellet was re-suspended in 1 ml of 75% ethanol. Samples were vortexed and centrifuged for (5 min at 7500 x g, 4 °C). Supernatants were discarded, pellets were dried and re-suspended in 20 µl of nuclease-free water (Invitrogen). RNA concentration was measured by NanoDrop ONE^C (Thermo Scientific). 1 µg of RNA was used for cDNA synthesized by High-Capacity cDNA Reverse Transcription Kit (Applied Biosystems), following manufacturer's instruction. RNA expression was quantified by QuantStudio 5 qRT-PCR machine (Applied Biosystems) using PowerUPTM SYBERTM Green Master Mix (Applied Biosystems). The following primers were used: housekeeping gene *gapdh*: CAAAGTGGAGATTGTTGCCA (forward), GCCTTGACTGTGCCGTTGAA (reverse); *tlr7*: TGATCCTGGCCTATCTCTGAC (forward), CGTGTCCACATCGAAAACA (reverse); *il-6*: AGTCCGGAGAGGAGACTTCA (forward), ATT TCCACG ATT TCC

Results: Manuscript 2

CAGAG (reverse); *tnf-alpha*: AAATGGCCTCCCTCAT (forward), CCTCCACTTGGTGGTTTG (reverse); *il-1beta*: GAAGAAGAGCCCATCCTCTG (forward), TCATCTCGGAGCCTGTAGTG (reverse).

ELISA assays

Mouse IL-6 ELISA MAX Standard Set and ELISA MAX Deluxe Set TNF- α (Biolegend) were used to measure the concentration of cytokines in supernatants or serum, following manufacturer's instructions.

Total IgG and IgM in supernatants and mouse serum were measured by ELISA, following the in-house developed ELISA protocol. Goat-Anti-Mouse IgG and Goat-Anti-Mouse IgM were used as coating antibodies (SouthernBiotech). Unconjugated mouse IgG and mouse IgM isotype control were used for standards (ThermoFisher). For the detection of IgM and IgG in the samples, Goat-Anti-Mouse Ig-HPR (Southern Biotech) was used. The antibody, standard and sample dilutions used are presented in (Table 1). 96 half-well plates (Corning) were coated with coating antibodies in coating buffer (70 mM NaHCO₃, 30 mM Na₂CO₃ in ddH₂O, pH 9.6) and left overnight at 4° C. Next, the plates were washed with 0.05% Tween-20 in PBS and blocked with blocking buffer (2% BSA in PBS) for 2h at RT. After washing, samples (diluted in ELISA Assay Diluent from Biolegend) and corresponding standards were added and incubated for 2h at RT. Plates were washed and detection antibodies were added for 30 min at RT. After washing, TMB Substrate Reagent Set (BD Biosciences) was added. After approximately 6 min stop solution (1M H₂SO₄) was added. Absorbance was measured at 450 nm and 570 nm by plate reader CLARIOstar (BMG Labtech).

For the measurement of OVA-specific IgM antibodies, ELISA was performed, following in-house developed OVA-specific IgM ELISA protocol. 96 half-well plate was coated with 0.5 μ g of OVA/well in coating buffer overnight at 4 °C. Next, plates were washed (0.05% Tween-20 in PBS) and blocked (2% BSA in PBS) for 2 h at RT. After washing, serum samples were added and incubated for 2 h at RT. After incubation, plates were washed and detection Goat-Anti-Mouse IgM-HPR antibodies (Southern Biotech) were added. After 1 h of incubation at RT, plates were washed and substrate (TMB) was added. After sufficient development of the color (~4 min) stop solution (1M H₂SO₄) was added. Absorbance was measured at 450 nm and 570 nm by plate reader CLARIOstar (BMG Labtech).

Results: Manuscript 2

Table 1: List of dilutions and concentrations of antibodies, samples or antigens used in the in-house ELISA protocols for total IgM, IgG and OVA-specific IgM.

	IgM		IgG		OVA-specific IgM
<i>Type of sample</i>	<i>Supernatant</i>	<i>Serum</i>	<i>Supernatant</i>	<i>Serum</i>	<i>Serum</i>
<i>Coating Ab/Ag</i>	1:1000	1:1000	1:1000	1:1000	OVA:10 µg/ml
<i>Samples dilutions</i>	1:4	1:10 ⁴	1:4	1:10 ⁶	1:100
<i>Standards</i>	Max at 1000 ng/ml; 1:2 serial dilutions	Max at 200 ng/ml; 1:3 serial dilutions	Max at 200 ng/ml; 1:2 serial dilutions	Max at 200 ng/ml; 1:3 serial dilutions	/
<i>Detection Ab</i>	1:8000	1:8000	1:8000	1:8000	1:500

Data and Statistical Analysis

Data were evaluated for significance using unpaired two-tailed Student's t-test for comparison between two groups. For comparison between multiple groups one-way ANOVA, followed by Dunnett's multi comparison test or two-way ANOVA followed by Tukey's or Sidak's multi comparison test was used (GraphPad Prism 7 software). Data was considered significant when * $p < 0.05$, ** $p < 0.01$ and *** $p < 0.001$, **** $p < 0.0001$.

References

- (1) Dobrovolskaia, M. A.; McNeil, S. E.; Neil, S. E. M. Immunological Properties of Engineered Nanomaterials. *Nat. Nanotechnol.* 2007, 2, 469–478.
- (2) Amendola, V.; Pilot, R.; Frasconi, M.; Maragò, O. M.; Iatì, M. A. Surface Plasmon Resonance in Gold Nanoparticles: A Review. *J. Phys. Condens. Matter* 2017, 29, 203002.
- (3) L.A, D.; Khlebtsov, N. G. Gold Nanoparticles in Biology and Medicine: Recent Advances and Prospects. *Acta Naturae* 2011, 3, 34–55.
- (4) Farooq, M. U.; Novosad, V.; Rozhkova, E. A.; Wali, H.; Ali, A.; Fateh, A. A.; Neogi, P. B.; Neogi, A.; Wang, Z. Gold Nanoparticles-Enabled Efficient Dual Delivery of Anticancer Therapeutics to HeLa Cells. *Sci. Rep.* 2018, 8, 2907.
- (5) Climent, N.; García, I.; Marradi, M.; Chiodo, F.; Miralles, L.; José Maleno, M.; María Gatell, J.; García, F.; Penadés, S.; Plana, M. Loading Dendritic Cells with Gold Nanoparticles (GNPs) Bearing HIV- Peptides and Mannosides Enhance HIV-Specific T Cell Responses. *Nanomedicine* 2018, 14, 339–351.
- (6) Niikura, K.; Matsunaga, T.; Suzuki, T.; Kobayashi, S.; Yamaguchi, H. Gold Nanoparticles as a Vaccine Platform : Influence of Size and Shape on Immunological Responses in Vitro and in Vivo. 2013, 3926–3938.
- (7) Assis, N. R. G.; Caires, A. J.; Figueiredo, B. C.; Morais, S. B.; Mambelli, F. S.; Marinho, F. V.; Ladeira, L. O.; Oliveira, S. C. The Use of Gold Nanorods as a New Vaccine Platform against Schistosomiasis. *J. Control. Release* 2018, 275, 40–52.

Results: Manuscript 2

- (8) Chen, Y.-S.; Hung, Y.-C.; Lin, W.-H.; Huang, G. S. Assessment of Gold Nanoparticles as a Size-Dependent Vaccine Carrier for Enhancing the Antibody Response against Synthetic Foot-and-Mouth Disease Virus Peptide. *Nanotechnology* 2010, 21, 195101.
- (9) Hong, S.; Zhang, Z.; Liu, H.; Tian, M.; Zhu, X.; Zhang, Z.; Wang, W.; Zhou, X.; Zhang, F.; Ge, Q.; Zhu, B.; Tang, H.; Hua, Z.; Hou, B. B Cells Are the Dominant Antigen-Presenting Cells That Activate Naive CD4+ T Cells upon Immunization with a Virus-Derived Nanoparticle Antigen. *Immunity* 2018, 49, 1–14.
- (10) Martínez-Riaño, A.; Bovolenta, E. R.; Mendoza, P.; Oeste, C. L.; Martín-Bermejo, M. J.; Bovolenta, P.; Turner, M.; Martínez-Martín, N.; Alarcón, B. Antigen Phagocytosis by B Cells Is Required for a Potent Humoral Response. *EMBO Rep.* 2018, 19, e46016.
- (11) Małaczewska, J. Effect of Oral Administration of Commercial Gold Nanocolloid on Peripheral Blood Leukocytes in Mice. *Pol. J. Vet. Sci.* 2015, 18, 273–282.
- (12) Bahamonde, J.; Brenseke, B.; Chan, M. Y.; Kent, R. D.; Vikesland, P. J.; Prater, M. R. Gold Nanoparticle Toxicity in Mice and Rats: Species Differences. *Toxicol. Pathol.* 2018, 46, 431–443.
- (13) Bartneck, M.; Keul, H. A.; Wambach, M.; Bornemann, J.; Gbureck, U.; Chatain, N.; Neuss, S.; Tacke, F.; Groll, J.; Zwadlo-Klarwasser, G. Effects of Nanoparticle Surface-Coupled Peptides, Functional Endgroups, and Charge on Intracellular Distribution and Functionality of Human Primary Reticuloendothelial Cells. *Nanomedicine Nanotechnology, Biol. Med.* 2012, 8, 1282–1292.
- (14) Zhang, X.-D.; Wu, D.; Shen, X.; Liu, P.-X.; Yang, N.; Zhao, B.; Zhang, H.; Sun, Y.-M.; Zhang, L.-A.; Fan, F.-Y. Size-Dependent in Vivo Toxicity of PEG-Coated Gold Nanoparticles. *Int. J. Nanomedicine* 2011, 6, 2071–2081.
- (15) Liu, X.; Huang, N.; Li, H.; Jin, Q.; Ji, J. Surface and Size Effects on Cell Interaction of Gold Nanoparticles with Both Phagocytic and Nonphagocytic Cells. *Langmuir* 2013, 29, 9138–9148.
- (16) Manson, J.; Kumar, D.; Meenan, B. J.; Dixon, D. Polyethylene Glycol Functionalized Gold Nanoparticles: The Influence of Capping Density on Stability in Various Media. *Gold Bull.* 2011, 44, 99–105.
- (17) Uz, M.; Bulmus, V.; Alsoy Altinkaya, S. Effect of PEG Grafting Density and Hydrodynamic Volume on Gold Nanoparticle–Cell Interactions: An Investigation on Cell Cycle, Apoptosis, and DNA Damage. *Langmuir* 2016, 32, 5997–6009.
- (18) Vu, V. P.; Gifford, G. B.; Chen, F.; Benasutti, H.; Wang, G.; Groman, E. V.; Scheinman, R.; Saba, L.; Moghimi, S. M.; Simberg, D. Immunoglobulin Deposition on Biomolecule Corona Determines Complement Opsonization Efficiency of Preclinical and Clinical Nanoparticles. *Nat. Nanotechnol.* 2019, 14, 260–268.
- (19) Shimizu, T.; Mima, Y.; Hashimoto, Y.; Ukawa, M.; Ando, H.; Kiwada, H.; Ishida, T. Anti-PEG IgM and Complement System Are Required for the Association of Second Doses of PEGylated Liposomes with Splenic Marginal Zone B Cells. *Immunobiology* 2015, 220, 1151–1160.
- (20) Hensel, J. A.; Khattar, V.; Ashton, R.; Ponnazhagan, S. Characterization of Immune Cell Subtypes in Three Commonly Used Mouse Strains Reveals Gender and Strain-Specific Variations. *Lab. Invest.* 2019, 99, 93–106.
- (21) Turner, V. M.; Mabbott, N. A. Structural and Functional Changes to Lymph Nodes in Ageing Mice. *Immunology* 2017, 151, 239–247.
- (22) Khlebtsov, N.; Dykman, L. Biodistribution and Toxicity of Engineered Gold Nanoparticles: A Review of in Vitro and in Vivo Studies. *Chem. Soc. Rev.* 2011, 40, 1647–1671.
- (23) Moyer, T. J.; Zmolek, A. C.; Irvine, D. J. Beyond Antigens and Adjuvants: Formulating Future Vaccines. *J. Clin. Invest.* 2016, 126, 799–808.
- (24) Lebien, T. W.; Tedder, T. F. ASH 50th Anniversary Review B Lymphocytes : How They Develop and Function. *Am. Soc. Hematol.* 2008, 112, 1570–1580.

Results: Manuscript 2

- (25) Zouali, M.; Richard, Y. Marginal Zone B-Cells, a Gatekeeper of Innate Immunity. *Front. Immunol.* 2011, 2, 63.
- (26) Hočevar, S.; Milošević, A.; Rodriguez-Lorenzo, L.; Ackermann-Hirschi, L.; Mottas, I.; Petri-Fink, A.; Rothen-Rutishauser, B.; Bourquin, C.; Clift, M. J. D. Polymer-Coated Gold Nanospheres Do Not Impair the Innate Immune Function of Human B Lymphocytes in Vitro. *ACS Nano* 2019, 13, 6790–6800.
- (27) Lee, C.-H.; Syu, S.-H.; Chen, Y.-S.; Hussain, S. M.; Aleksandrovich Onischuk, A.; Chen, W. L.; Steven Huang, G. Gold Nanoparticles Regulate the Blimp1/Pax5 Pathway and Enhance Antibody Secretion in B-Cells. *Nanotechnology* 2014, 25, 125103.
- (28) Sharma, M.; Salisbury, R. L.; Maurer, E. I.; Hussain, S. M.; Sulentic, C. E. W. Gold Nanoparticles Induce Transcriptional Activity of NF- κ B in a B-Lymphocyte Cell Line. *Nanoscale* 2013, 5, 3747–3756.
- (29) Rodriguez-Lorenzo, L.; Fytianos, K.; Blank, F.; Von Garnier, C.; Rothen-Rutishauser, B.; Petri-Fink, A. Fluorescence-Encoded Gold Nanoparticles: Library Design and Modulation of Cellular Uptake into Dendritic Cells. *Small* 2014, 10, 1341–1350.
- (30) Moore, T. L.; Rodriguez-Lorenzo, L.; Hirsch, V.; Balog, S.; Urban, D.; Jud, C.; Rothen-Rutishauser, B.; Lattuada, M.; Petri-Fink, A. Nanoparticle Colloidal Stability in Cell Culture Media and Impact on Cellular Interactions. *Chem. Soc. Rev.* 2015, 44, 6287–6305.
- (31) Hirsch, V.; Kinnear, C.; Moniatte, M.; Rothen-Rutishauser, B.; Clift, M. J. D.; Fink, A. Surface Charge of Polymer Coated SPIONs Influences the Serum Protein Adsorption, Colloidal Stability and Subsequent Cell Interaction in Vitro. *Nanoscale* 2013, 5, 3723–3732.
- (32) Haiss, W.; Thanh, N. T. K.; Aveyard, J.; Fernig, D. D. G. Determination of Size and Concentration of Gold Nanoparticles from UV-Vis Spectra. *Anal. Chem.* 2007, 79, 4215–4221.
- (33) Mellman, I.; Plutner, H.; Ukkonen, P. Internalization and Rapid Recycling of Macrophage Fc Receptors Tagged with Monovalent Antireceptor Antibody: Possible Role of a Prelysosomal Compartment. *J. Cell Biol.* 1984, 98, 1163–1169.
- (34) Cho, W.-S.; Cho, M.; Jeong, J.; Choi, M.; Cho, H.-Y.; Han, B. S.; Kim, S. H.; Kim, H. O.; Lim, Y. T.; Chung, B. H.; Jeong, J. Acute Toxicity and Pharmacokinetics of 13nm-Sized PEG-Coated Gold Nanoparticles. *Toxicol. Appl. Pharmacol.* 2009, 236, 16–24.
- (35) Ye, F.; Vallhov, H.; Qin, J.; Daskalaki, E.; Sugunan, A.; Toprak, M. S.; Fornara, A.; Gabrielsson, S.; Scheynius, A.; Muhammed, M. Synthesis of High Aspect Ratio Gold Nanorods and Their Effects on Human Antigen Presenting Dendritic Cells. *Int. J. Nanotechnol.* 2011, 8, 631.
- (36) Almeida, J. P. M.; Lin, A. Y.; Langsner, R. J.; Eckels, P.; Foster, A. E.; Drezek, R. A. In Vivo Immune Cell Distribution of Gold Nanoparticles in Naïve and Tumor Bearing Mice. *Small* 2014, 10, 812–819.
- (37) Zhu, Q.; Zhang, M.; Shi, M.; Liu, Y.; Zhao, Q.; Wang, W.; Zhang, G.; Yang, L.; Zhi, J.; Zhang, L.; Hu, G.; Chen, P.; Yang, Y.; Dai, W.; Liu, T.; He, Y.; Feng, G.; Zhao, G. Human B Cells Have an Active Phagocytic Capability and Undergo Immune Activation upon Phagocytosis of Mycobacterium Tuberculosis. *Immunobiology* 2016, 221, 558–567.
- (38) Tsoi, K. M.; MacParland, S. A.; Ma, X.-Z.; Spetzler, V. N.; Echeverri, J.; Ouyang, B.; Fadel, S. M.; Sykes, E. A.; Goldaracena, N.; Kathis, J. M.; Conneely, J. B.; Alman, B. A.; Selzner, M.; Ostrowski, M. A.; Adeyi, O. A.; Zilman, A.; McGilvray, I. D.; Chan, W. C. W. Mechanism of Hard-Nanomaterial Clearance by the Liver. *Nat. Mater.* 2016, 15, 1212–1221.
- (39) Manolova, V.; Flace, A.; Bauer, M.; Schwarz, K.; Saudan, P.; Bachmann, M. F. Nanoparticles Target Distinct Dendritic Cell Populations According to Their Size. *Eur. J. Immunol.* 2008, 38, 1404–1413.
- (40) Dutt, T. S.; Mia, M. B.; Saxena, R. K. Elevated Internalization and Cytotoxicity of Polydispersed Single-Walled Carbon Nanotubes in Activated B Cells Can Be Basis for Preferential Depletion of Activated B Cells in Vivo. *Nanotoxicology* 2019, 13, 849–860.

Results: Manuscript 2

- (41) Hirohata, S.; Nakanishi, K.; Yanagida, T.; Kawai, M.; Kikuchi, H.; Isshi, K. Synergistic Inhibition of Human B Cell Activation by Gold Sodium Thiomalate and Auranofin. *Clin. Immunol.* 1999, 91, 226–233.
- (42) Lorber, A.; Simon, T.; Leeb, J.; Peter, A.; Wilcox, S. Chrysotherapy. Suppression of Immunoglobulin Synthesis. *Arthritis Rheum.* 1978, 21, 785–791.
- (43) Tsai, C.-Y.; Lu, S.-L.; Hu, C.-W.; Yeh, C.-S.; Lee, G.-B.; Lei, H.-Y. Size-Dependent Attenuation of TLR9 Signaling by Gold Nanoparticles in Macrophages. *J. Immunol.* 2011, 188, 68–76.
- (44) Villiers, C.; Freitas, H.; Couderc, R.; Villiers, M.-B.; Marche, P. Analysis of the Toxicity of Gold Nano Particles on the Immune System: Effect on Dendritic Cell Functions. *J. Nanopart. Res.* 2010, 12, 55–60.
- (45) Sumbayev, V. V.; Yasinska, I. M.; Garcia, C. P.; Gilliland, D.; Lall, G. S.; Gibbs, B. F.; Bonsall, D. R.; Varani, L.; Rossi, F.; Calzolari, L. Gold Nanoparticles Downregulate Interleukin-1 β -Induced Pro-Inflammatory Responses. *Small* 2013, 9, 472–477.
- (46) Turkevich, J.; Stevenson, P. C.; Hillier, J. A Study of the Nucleation and Growth Processes in the Synthesis of Colloidal Gold. *Discuss. Faraday Soc.* 1951, 11, 55.

2.1 Supporting information for manuscript 2

Polymer-coated gold nanoparticles inhibit adaptive B cell function in mice

Sandra Hočevár¹, Alke Petri-Fink³, Barbara Rothen-Rutishauser³, Martin James David Clift^{4}, Carole Bourquin^{1,2*}*

¹School of Pharmaceutical Sciences, University of Geneva, University of Lausanne, 1211 Geneva, Switzerland

²Faculty of Medicine, University of Geneva, Rue Michel-Servet 1, 1211 Geneva, Switzerland

³BioNanomaterials, Adolphe Merkle Institute, University of Fribourg, 1700 Fribourg, Switzerland.

⁴In Vitro Toxicology Group, Swansea University Medical School, Wales, SA2 8PP, UK

*These authors contributed equally.

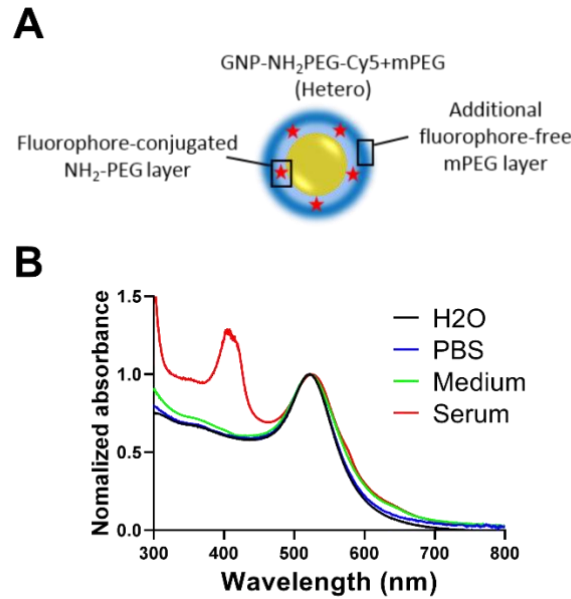


Figure S1: Polymer-coated gold nanoparticles and their stability in different biological media. A) Schematic presentation of fluorescently-labeled (Cy5) gold nanoparticles coated with a double layer of PEG (NH₂-PEG-mPEG). **B)** UV-Vis spectra of GNPs after incubation in water, PBS, complete RPMI medium with 10% FBS and in 15% mouse serum. The additional peak at ~400 nm for the spectrum of GNP incubated in the serum occurred due to the interference of hemoglobin residue present in the serum obtained from mouse blood. mPEG: methoxy PEG.

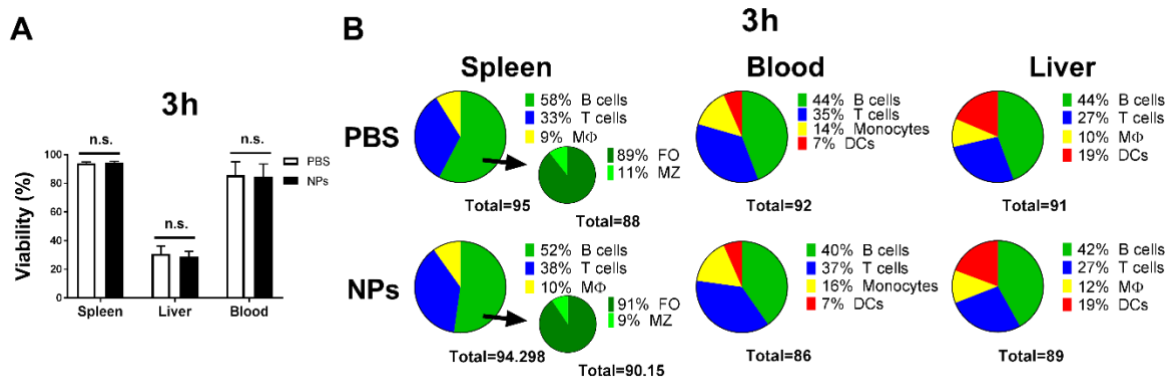


Figure S2: Cell viability in different organs 3h after intravenous administration of GNPs. A) Total cell viability in spleen, liver and blood 3h post-intravenous injection with 400 μg GNPs in C57/BL6 mice, measured by flow cytometry using amine-reactive viability dye. **B)** Percentage of different leukocyte populations in spleen, liver and blood, 3 h post-injection with GNPs. Data show two separate experiments combined, with 5-8 mice per group. Error bars: mean ± SD of the pooled data; n.s.: not significant = $p > 0.05$. Data were evaluated by two-way ANOVA, followed by Sidak's multiple comparison post-hoc test. B cells (CD19⁺/CD3⁻), MZ: marginal zone B cells (CD19⁺/CD21⁺/CD23⁻), FO: follicular B cells (CD19⁺/CD21⁺/CD23⁺), T cells (CD19⁻/CD3⁺), Mφ/monocytes (CD11b⁺/CD11c⁻), DC: (CD11b⁺/CD11c⁺).

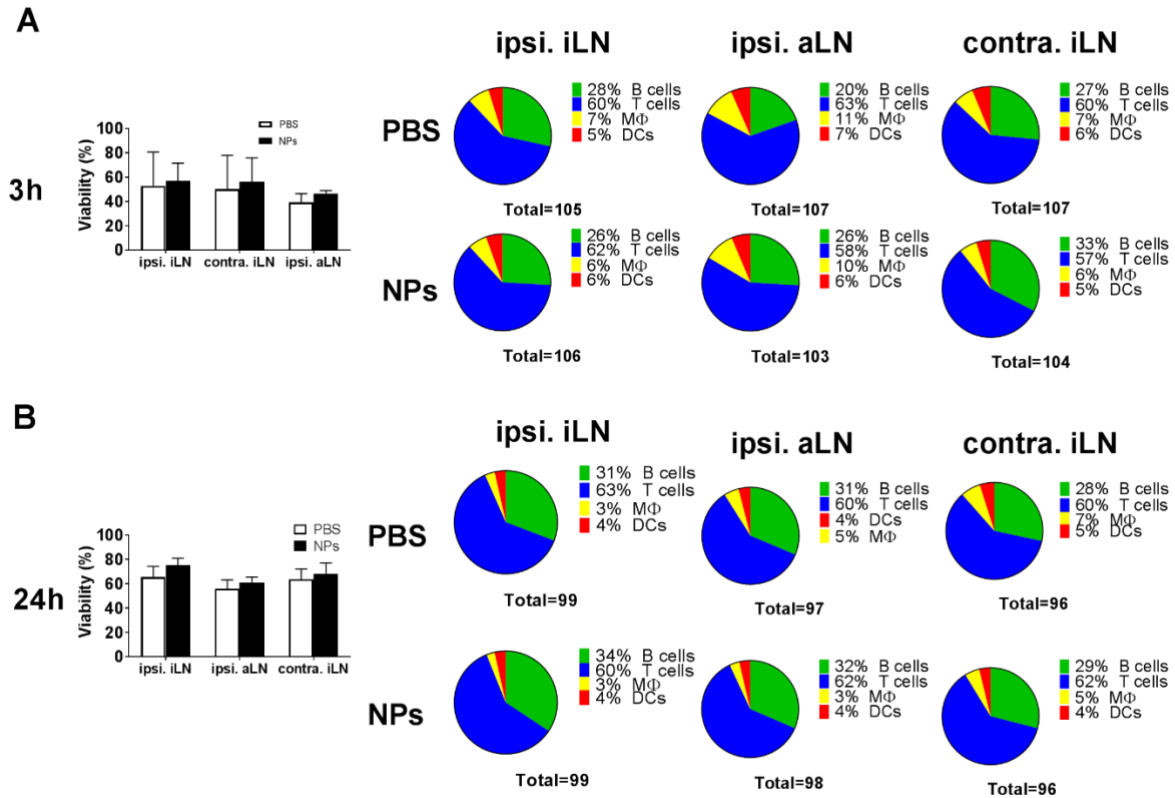


Figure S3: Cell viability in different LN after subcutaneous administration of GNPs. A) Total cell viability in different LN and percentage of different immune cell populations in ipsilateral inguinal LN (ipsi. iLN) or primary draining LN, ipsilateral axillary LN (ipsi. aLN) or secondary draining LN and contralateral inguinal LN (contra. iLN) or non-draining LN **A)** 3h and **B)** 24 h after subcutaneous injection of 300 µg GNPs in the mouse flank. Data show two separate experiments combined, with 5-8 mice per group. Error bars: mean ± SD of the pooled data. Data were evaluated by two-way ANOVA followed by Sidak's multiple comparison post-hoc test. B cells (CD19⁺/CD3⁻), T cells (CD19⁻/CD3⁺), Mφ(CD11b⁺/CD11c⁻), DC: (CD11b⁺/CD11c⁺).

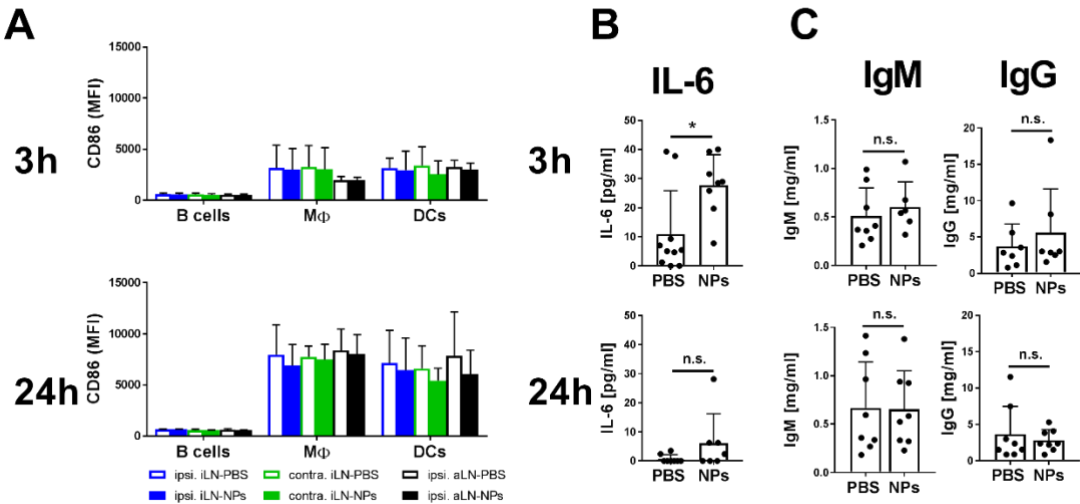


Figure S4: Primary immune response after subcutaneous administration of GNPs. A) Expression of surface immune activation marker CD86 in different immune cell populations in different LN 3 and 24 h post-subcutaneous injection with 300 µg GNPs in C57/BL6 mice. **B)** Production of serum IL-6 3 h and 24 h post-injection with GNPs measured by ELISA. **C)** Production of total serum IgM and IgG 3 and 24 h after injection with GNPs measured by ELISA. Data for each time point panel show two separate experiments combined. Each dot represents cells from an individual mouse (n=5-8). Error bars: mean ± SD of the pooled data; n.s: not significant = p>0.05. Data were evaluated by two-way ANOVA followed by Sidak’s multiple comparison post-hoc test or by unpaired Student’s t-test. B cells (CD19⁺/CD3⁻), T cells (CD19⁻/CD3⁺), Mφ(CD11b⁺/CD11c⁻), DC: (CD11b⁺/CD11c⁺).

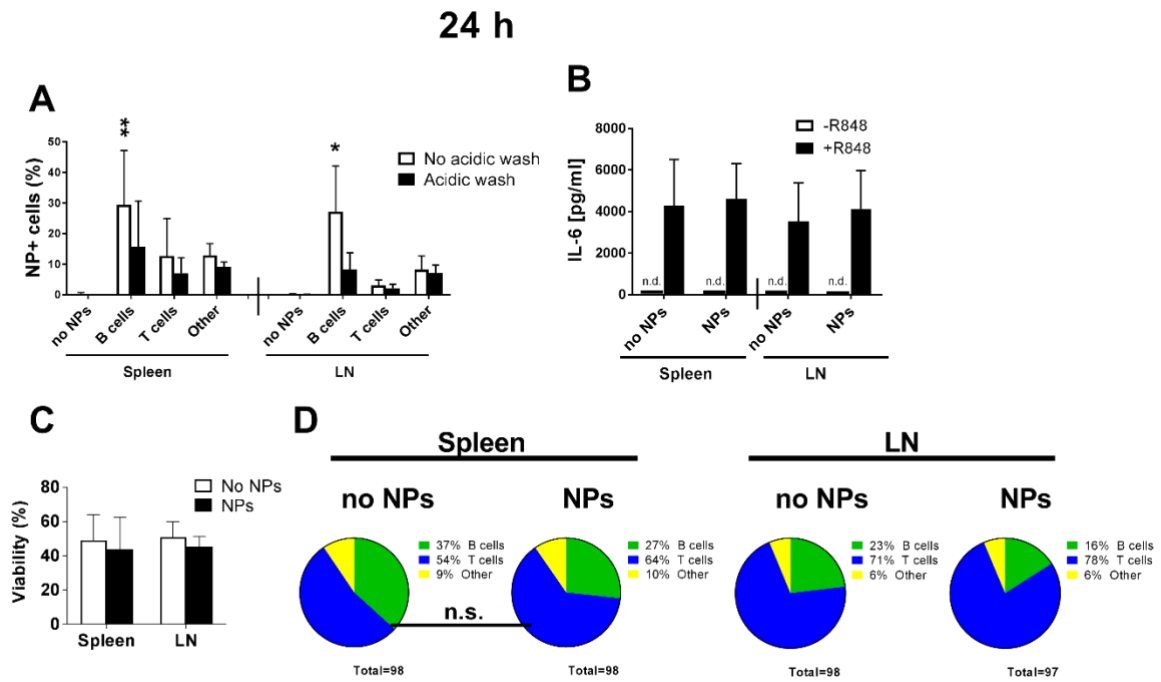


Figure S5: Effect of GNPs on splenocytes and LN cells *in vitro*. **A)** Total GNP-B cell association (no acidic wash) or GNP uptake (acidic wash) by different immune cells of spleen and LN 24 h after exposure to 20 $\mu\text{g}/\text{ml}$ GNPs in the presence or absence of R848 (2 $\mu\text{g}/\text{ml}$) adjuvant, measured by flow cytometry as a percentage of GNP-Cy5 positive cells. **B)** IL-6 production by splenocytes measured in the supernatant by ELISA. **C)** Cell viability in spleen and LN after exposure to GNPs measured by flow cytometry using amine-reactive viability dye. **D)** Percentage of immune cells in spleen and LN. Data show three separate experiments combined ($n=3$). Error bars: mean \pm SD of the pooled data; * $p<0.05$, ** $p<0.01$, n.s.: not significant = $p>0.05$. Data were evaluated by two-way ANOVA followed by Tukey's multiple comparison post-hoc test. B cells ($\text{CD}19^+/\text{CD}3^-$), T cells ($\text{CD}19^-/\text{CD}3^+$), other ($\text{CD}19^-/\text{CD}3^-$).

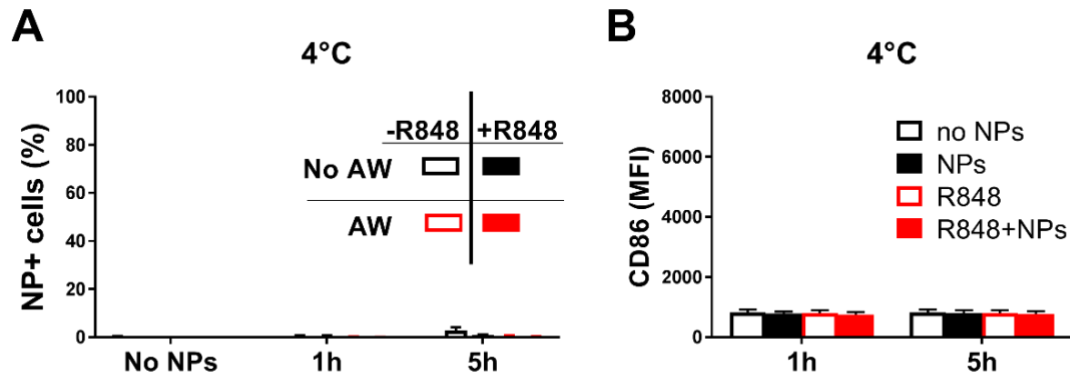


Figure S6: Evaluation of GNP effect on isolated splenic B cells *In vitro* at 4 °C. A) Total GNP-B cell association (no acidic wash) or GNP uptake (acidic wash) by isolated splenic B cells after 1 and 5 h after exposure with 20 $\mu\text{g}/\text{ml}$ GNPs in the presence or absence of R848 (2 $\mu\text{g}/\text{ml}$) adjuvant, incubated at 4 °C and measured by flow cytometry as a percentage of GNP-Cy5 positive cells. **B)** Expression of surface activation marker CD86 on B cells. Data for each time point show three separate experiments combined (n=3). Error bars: mean \pm SD of the pooled data. Data were evaluated by two-way ANOVA followed by Tukey's multiple comparison post-hoc test. No AW: no acidic wash, AW: acidic wash.

Results: Supporting Information for Manuscript 2

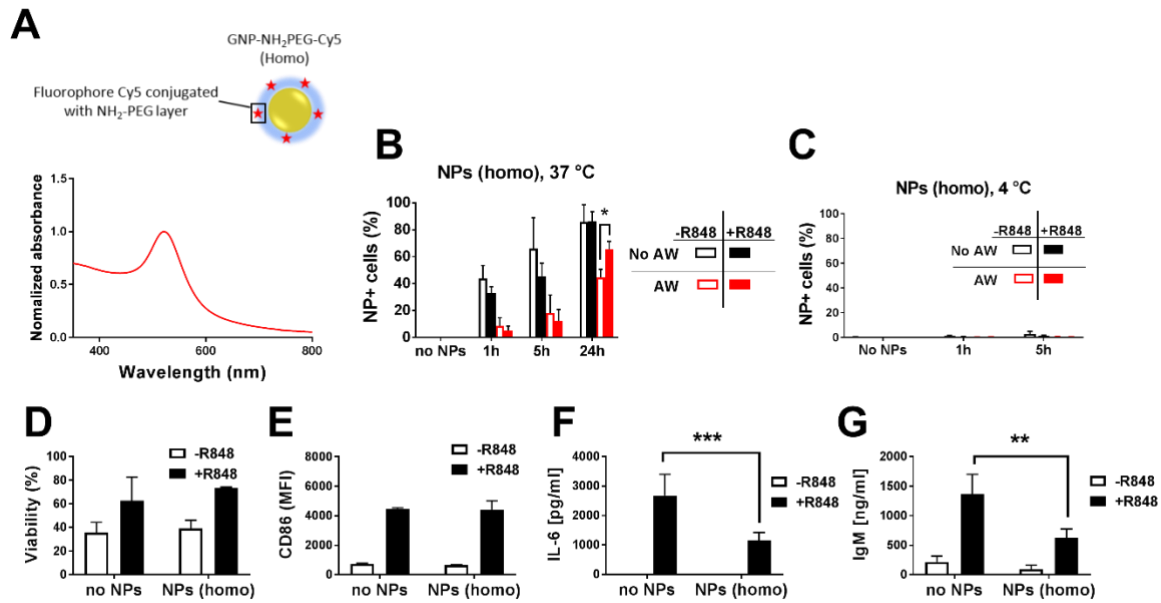


Figure S7: Homo formulation of GNPs and its effect on isolated splenic B cells *in vitro*. **A)** Schematic presentation of fluorescently-labeled (Cy5) gold nanoparticles coated with a single PEG layer (NH₂-PEG) and UV-Vis spectra of homo GNPs in water. **B)** Total GNP-B cell association (no acidic wash) or GNP uptake (acidic wash) by isolated splenic B cells after 1, 5 and 24 h after exposure with 20 µg/ml GNPs in the presence or absence of R848 (2 µg/ml) adjuvant, measured by flow cytometry as a percentage of GNP-Cy5 positive cells. **C)** Total GNP-B cell association (no acidic wash) or GNP uptake (acidic wash) by isolated splenic B cells after 1 and 5 h after exposure with 20 µg/ml GNPs in the presence or absence of R848 (2 µg/ml) adjuvant, incubated at 4 °C and measured by flow cytometry as a percentage of GNP-Cy5 positive cells. **D)** B cell viability after 24 h exposure with GNPs measured by flow cytometry using amine-reactive viability dye. **E)** Expression of surface activation marker CD86 on B cells, measured by flow cytometry 24 h after exposure. **F)** IL-6 production by B cells measured in the supernatant by ELISA 24 h after exposure. **G)** Production of IgM measured in the supernatant by ELISA 24 h after exposure with GNPs. Data for each time point show three separate experiments combined (n=3). Error bars: mean ± SD of the pooled data; **p*<0.05, ***p*<0.01 and ****p*<0.001. Data were evaluated by two-way ANOVA followed by Tukey's multiple comparison post-hoc test. No AW: no acidic wash, AW: acidic wash

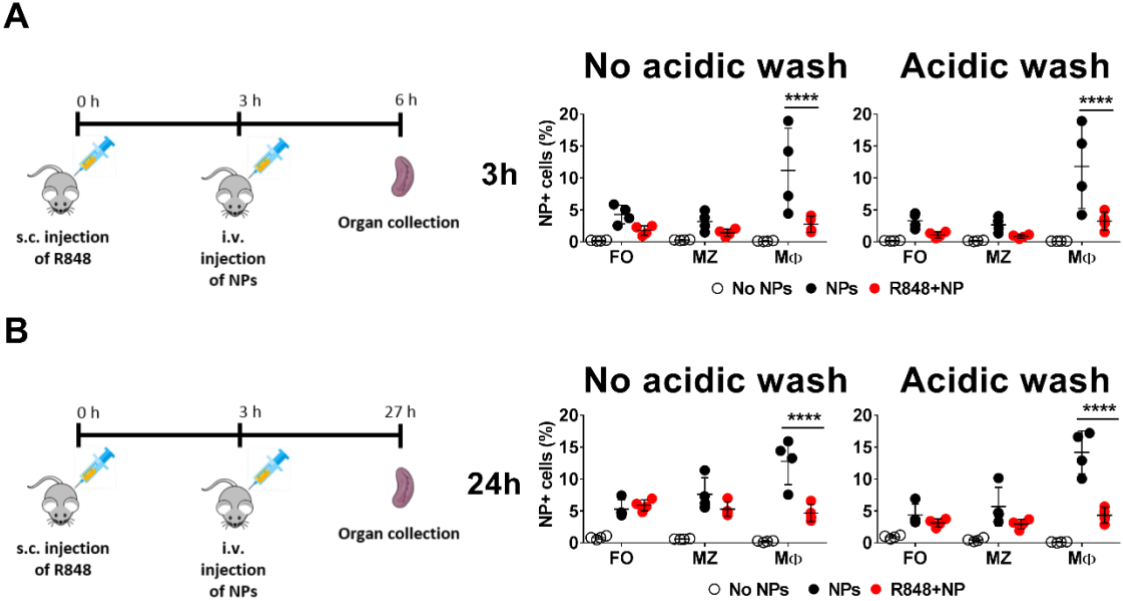


Figure S8: GNP uptake after preactivation with adjuvant. Total GNP-cell association (no acidic wash) and uptake of GNPs (acidic wash) measured in different immune cell populations. C57/BL6 mice were subcutaneous injection with 10 µg R848, followed by 3 h incubation. Mice were then intravenously injected with 400 µg GNPs and incubated for additional **A)** 3 h or **B)** 24 h. Data show one biological experiment. Each dot represents an individual mouse (n=4). Error bars: mean ± SD; ****p<0.0001. Data were evaluated by two-way ANOVA, followed by Tukey’s multiple comparisons post-hoc test. MZ: marginal zone B cells (CD19⁺/CD21⁺/CD23⁻), FO: follicular B cells (CD19⁺/CD21⁺/CD23⁺), Mφ (CD11b⁺/CD11c).

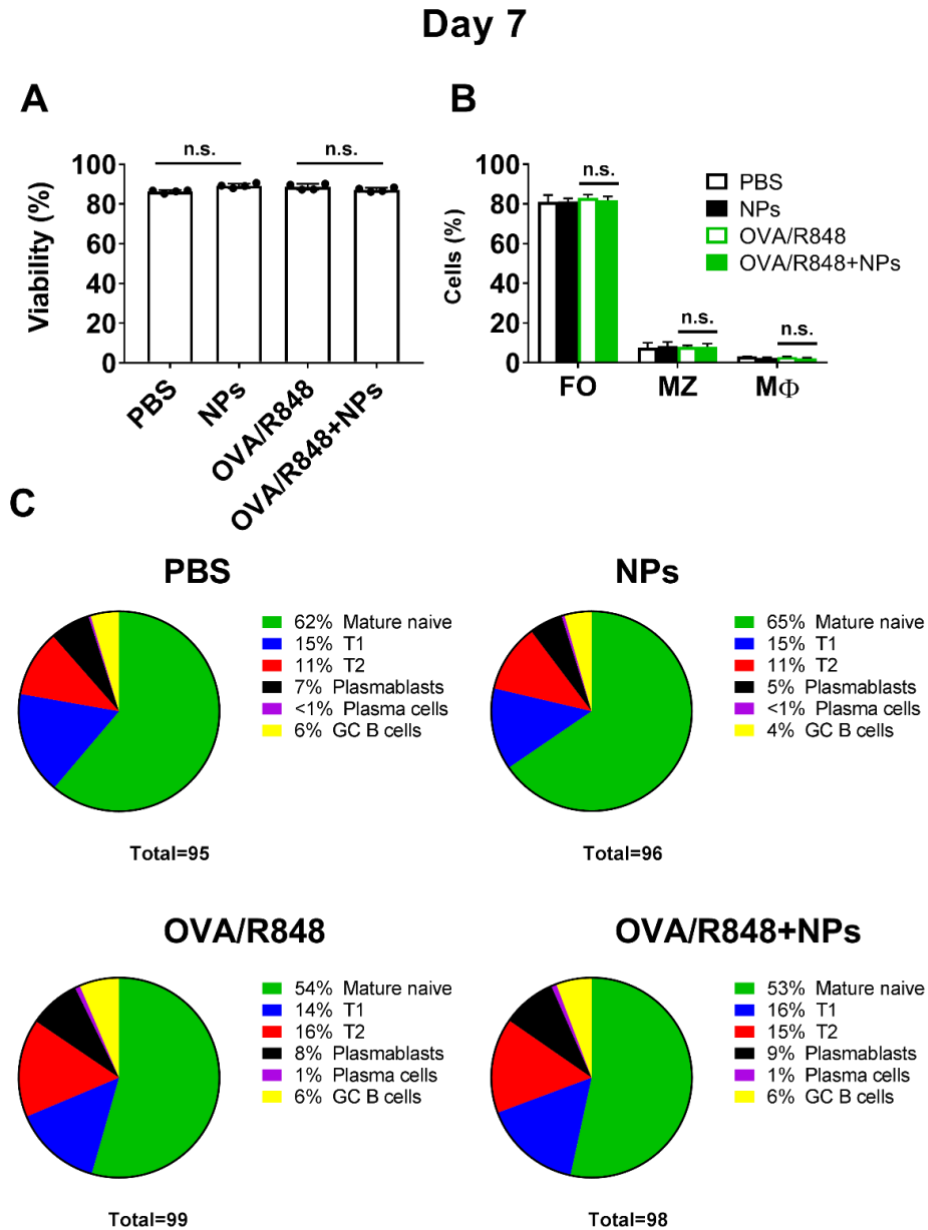


Figure S9: Viability of splenocytes after simultaneous injection of GNPs and antigen. **A)** Viability of splenocytes in C57/BL6 mice 7 days after injection with 400 μ g GNPs and OVA antigen (100 μ g)/R848 (10 μ g) measured by flow cytometry, using amine-reactive viability dye. **B)** Percentage of MZ B cells, FO B cells and macrophages in the spleen, 7 days post-injection with GNPs and OVA/R848. **C)** Percentage of different splenic B cell subsets upon injections with GNPs and OVA/R848. Data show one biological experiment. Each dot represents cells from an individual mouse (n=4). Error bars: mean \pm SD; n.s.: not significant = $p > 0.05$. Data were evaluated by one-way ANOVA followed by Dunnett's multi comparison post-hoc test (viability) and two-way ANOVA, followed by Tukey's multiple comparisons post-hoc. MZ: marginal zone B cells ($CD19^+/CD21^+/CD23^-$), FO: follicular B cells ($CD19^+/CD21^+/CD23^+$), M Φ ($CD11b^+/CD11c^+$), T1: transitional 1 ($CD19^+/IgM^{hi}/IgD^{low}$), T2: transitional 2 ($CD19^+/IgM^{hi}/IgD^{hi}$), mature naive B cells ($CD19^+/IgM^{low}/IgD^{int}$), plasmablasts ($CD19^+/CD138^+$), plasma cells ($CD19^-/CD138^+$), GC B cells: germinal center B cells ($CD19^+/IgM^{low}/IgD^{low}/GL7^+/Fas^+$).

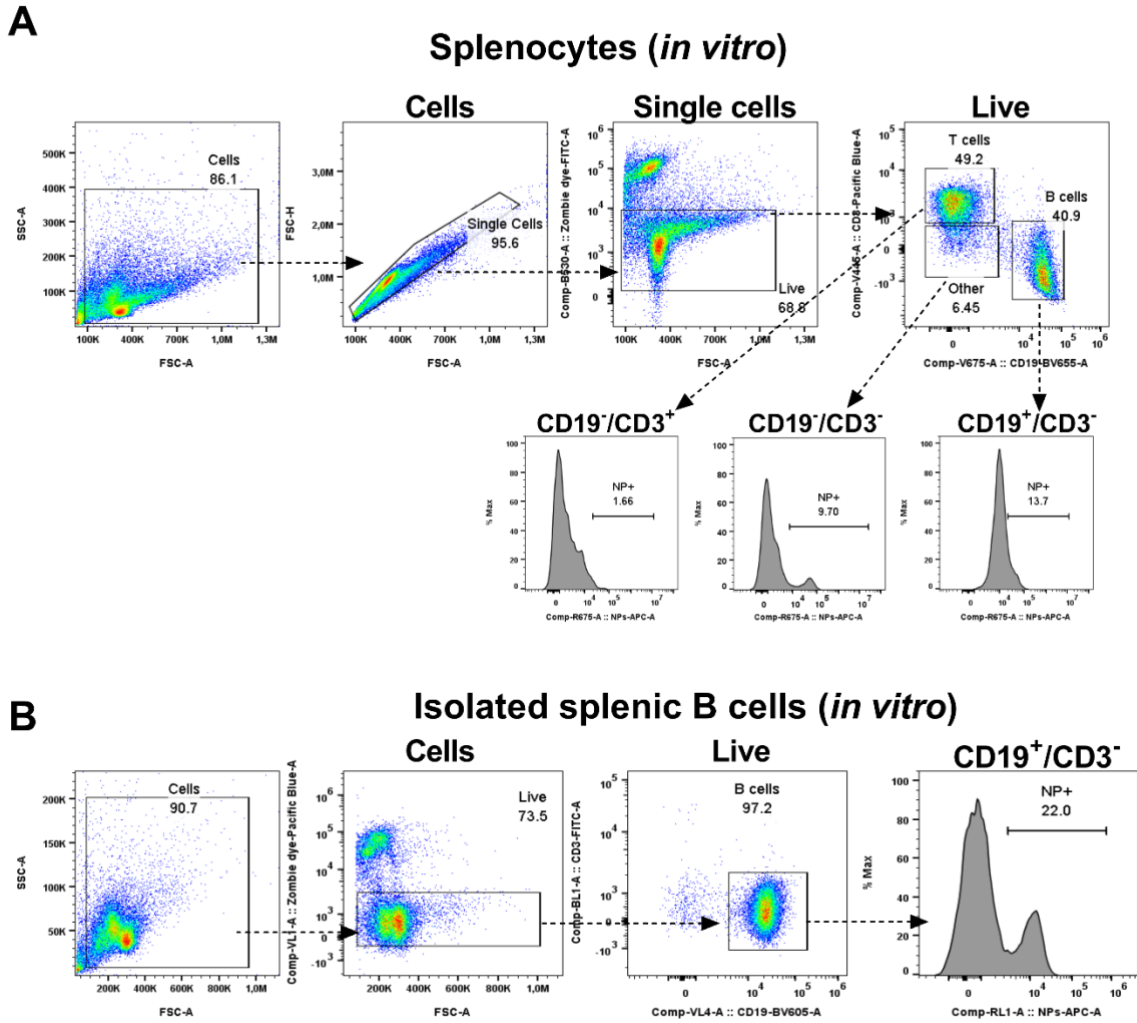


Figure S10: Gating strategy for *in vitro* experiments. A) Gating strategy for splenocytes after *in vitro* exposure to GNPs. All cells were first gated to exclude dead cells and cell debris, followed by gating of single cells only. Next, live cells were determined by amine-reactive viability dye. Different cell populations were defined as followed: B cells (CD19⁺/CD3⁻), T cells (CD19⁻/CD3⁺), other (CD19⁻/CD3⁻). Finally, GNP-Cy5 positive cells were gated (NP+). **B)** Gating strategy for isolated splenic B cells after *in vitro* exposure with GNPs and B cell purity. All cells were first gated to exclude dead cells and cellular debris followed by gating of live cells (amine-reactive viability dye). B cells were defined as CD19⁺/CD3⁻ with >96% purity. Finally, GNP-Cy5 positive B cells were defined (NP+).

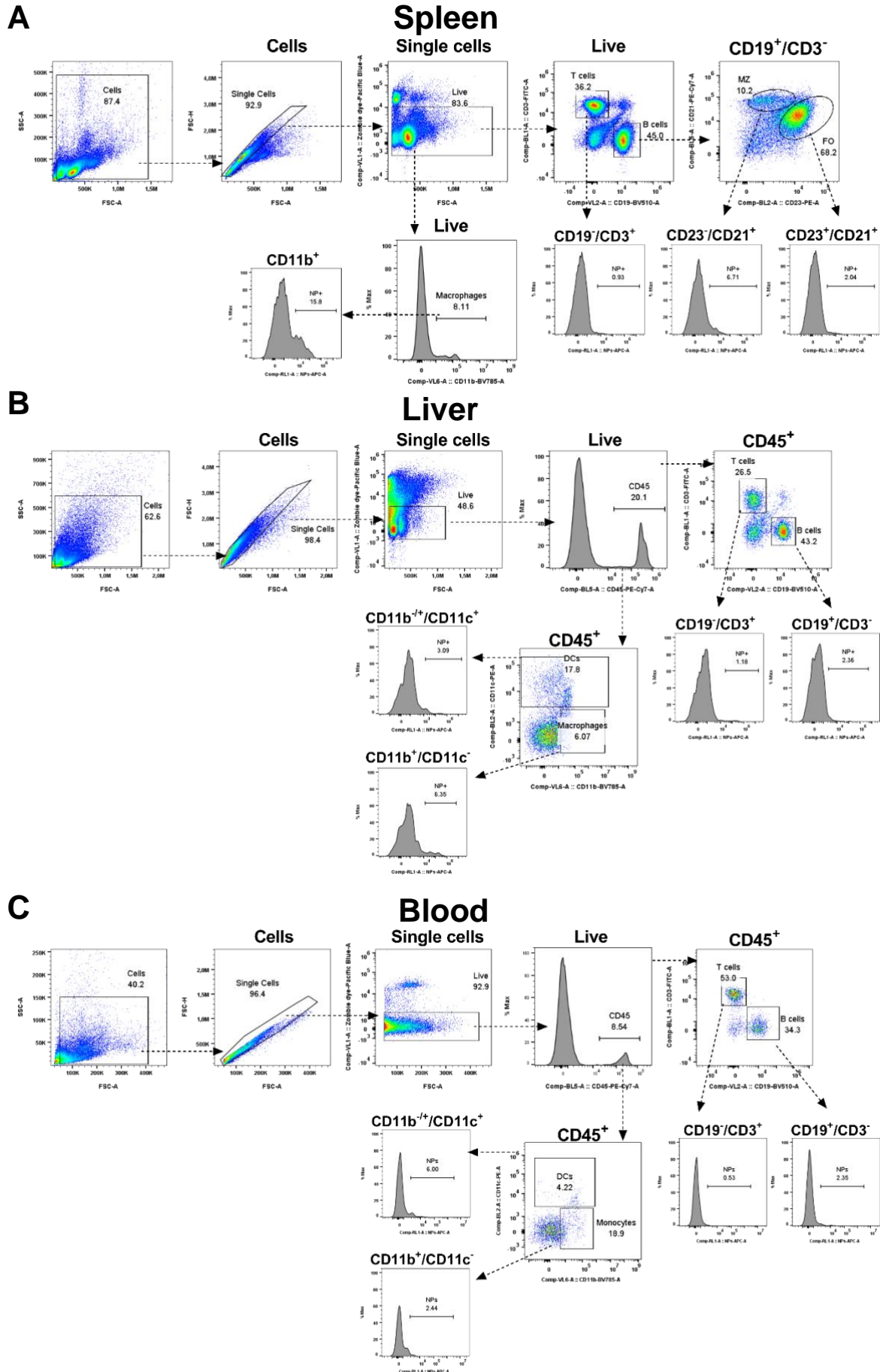


Figure S11: Gating strategy for different organs in *in vivo* experiments. **A)** Gating strategy for splenocytes after *in vivo* exposure to GNPs. All cells were first gated to exclude dead cells and cellular debris, followed by gating of single cells only. Next, live cells were determined by amine-reactive viability dye. Different cell populations were defined as followed: B cells (CD19⁺/CD3⁻), T cells (CD19⁻/CD3⁺), other (CD19⁻/CD3⁻). B cells were further gated for marginal zone B cells (MZ: CD23⁻/CD21⁺) and follicular B cells (FO: CD23⁺/CD21⁺). Finally, defined cell populations were gated on GNP-Cy5 positive cells (NP+). **B)** Gating strategy for liver cells after *in vivo* exposure to GNPs. All cells were first gated to exclude dead cells and cellular debris followed by gating of single cells only. Next, leukocytes (CD45⁺) were gated, followed by the exclusion of dead cells with amine-reactive viability dye. Different cell populations were defined as followed: B cells (CD19⁺/CD3⁻), T cells (CD19⁻/CD3⁺), Mφ(CD11b⁺/CD11c⁻), DC (CD11b^{+/-}/CD11c⁺). Finally, defined cell populations were gated on GNP-Cy5 positive cells (NP+). **C)** Gating strategy for blood leukocytes after *in vivo* exposure to GNPs. All cells were first gated to exclude dead cells and cell debris followed by gating of single cells only. Next, leukocytes (CD45⁺) were gated, followed by the exclusion of dead cells with amine-reactive viability dye. Different cell populations were defined as followed: B cells (CD19⁺/CD3⁻), T cells (CD19⁻/CD3⁺), Mφ(CD11b⁺/CD11c⁻), DC (CD11b^{+/-}/CD11c⁺). Finally, defined cell populations were gated on GNP-Cy5 positive cells (NP+).

Results: Supporting Information for Manuscript 2

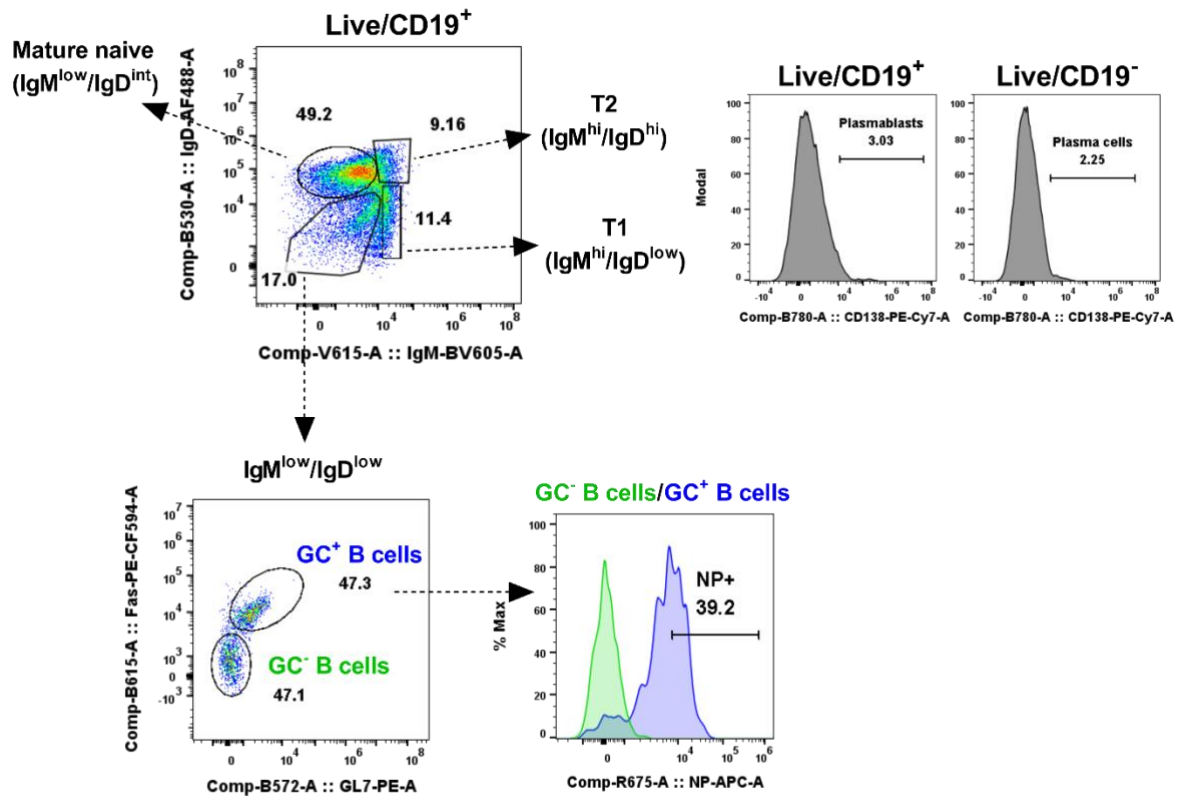


Figure S12: Gating strategy to determine B cell germinal centers in the spleen after *in vivo* exposure to GNPs. After the exclusion of cell debris, doublets and dead cells, CD19⁺ B cells were defined (see Figure S10A). CD19⁺ B cells were further gated for T1: transitional 1 (CD19⁺/IgM^{hi}/IgD^{low}), T2: transitional 2 (CD19⁺/IgM^{hi}/IgD^{hi}), mature naive B cells (CD19⁺/IgM^{low}/IgD^{int}), plasmablasts (CD19⁺/CD138⁺), plasma cells (CD19⁻/CD138⁺), germinal center positive (GC⁺) B cells (CD19⁺/IgM^{low}/IgD^{low}/GL7⁺/Fas⁺) and germinal center negative (GC⁻) B cells (CD19⁺/IgM^{low}/IgD^{low}/GL7⁻/Fas⁻). Defined cell populations were further gated on GNP-Cy5 positive cells. Only an example for GC⁺ GNP-Cy5⁺ and GC⁻ GNP-Cy5⁺ positive B cells is shown.

GENERAL DISCUSSION

The understanding of the interactions between immune cells and NPs is crucial for the development of safe NPs that can be applied in medicine. Nevertheless, alterations in immune responses caused by NPs are challenging to study from two different perspectives. On one hand, the immune system is a very complex network of different cells and immune modulators, whereas NPs possess a variety of different and complex physico-chemical properties. Additionally, complex interactions between NPs and the biological environment can further influence the course of cellular processes, such as NP uptake, immune response and apoptosis.¹⁸⁰ Complexity on both sides can be broken down by focusing studies on a specific immune cell type, using well-optimized and well-characterized NPs.

GNPs are especially interesting as a theranostic tool, with applications in diagnostics, drug delivery, photothermal therapy and vaccine-based applications.¹⁵⁸ Yet, as every new drug or therapeutic, they need to be carefully evaluated for their toxicological potential on the immune system. B cells, on the other hand, are valuable players in the specific as well as innate-like immune responses but are poorly investigated with regard to GNP potential interference on their function and viability. In order to fill the knowledge gap, this project specifically focused on determining the interactions of physico-chemically different GNPs with B cells and provided some important information for future research in the field.

1. GNP cytotoxicity and immune cells

In general, GNPs were shown to be highly biocompatible by numerous toxicological studies involving various cell lines as well as in vivo models.¹⁷⁹ In the past ten years, scientists have been increasingly investigating GNP cytotoxic potential toward immune cells. The majority of these studies mainly consider highly phagocytic immune cells such as macrophages and dendritic cells as the main concern towards GNP immunotoxicity. Despite GNP high uptake by phagocytes, they show limited adverse effects for these cells.⁸¹ For instance, Oh and Park showed no reduction in macrophage viability after 72h exposure to GNPs at a concentration as high as 100 μM (approx. 20 $\mu\text{g}/\text{mL}$). Instead, they were able to show a decrease in nitric oxide production caused by GNPs.¹⁸¹ Indeed, several other studies reported a decline in ROS and nitric oxide production, suggesting a strong antioxidant property of GNPs.^{182,113,183} The NF- κB pathway is one of the key pathways responsible for the regulation of oxidative stress and pro-inflammatory cytokine production and GNPs have the ability to bind and block NF- κB and its components (*e.g.*, I κB kinase).¹⁸⁴ In contrast to these studies, Yen and *et al.* demonstrated size and concentration-dependent adverse effects of GNP on macrophages.¹¹⁷ They showed GNP increased cytotoxicity, decrease cell proliferation, change in macrophage morphology and increased expression

General Discussion

of pro-inflammatory genes, which was more potent with smaller GNPs (2 and 5 nm) and at higher concentration (10 µg/ml). However, it needs to be stressed that GNPs in this study were synthesized with no surface stabilization, compared to the otherwise commonly use synthesis of citrate-coated GNPs.¹⁶⁰ Thus, these examples show that the differences in GNP preparation, size, surface chemistry, concentration and exposure time play a critical role in these contradictory results regarding GNP biocompatibility.

Nevertheless, all these reports provide a great amount of information about the impact and mechanisms of the uptake of various physiological and chemically different GNPs on innate immune cells. However, there is still very little focus on the lymphocytes with regard to GNP cytotoxicity and function. To this day, there are only few studies that investigated unconjugated GNPs and their direct effect on B cells *in vitro*.^{137,138,185} Importantly, these studies reported no decrease in B cell viability. Sharma *et al.* tested 10 nm citrate-functionalized GNPs on a murine lymphoma B cell line for up to 48 h. The authors reported no change in B cell viability, morphology or proliferation despite detected uptake and a concentration 2.5 fold higher than what was used in our studies.¹³⁷ Similarly, Lee *et al.*, exposed mouse hybridoma B cells (splenic cells fused with myeloma cells) to citrate-functionalized GNPs in a range from 2 to 50 nm and reported no decrease in viability after 24 h at 1 µg/ml.¹³⁸ These comparable results suggest that GNPs do not cause cell death in B cells *in vitro* in short term exposure (up to 48h), even without a protective polymer and at high exposure concentrations (up to 50 µg/ml). With regard to cell viability, B cells seemingly have low susceptibility to GNPs. However, the two studies discussed here showed GNP ability to induce B cell function, which is discussed below.

Similarly, little is known about the impact on B cells after systemic administration of GNPs. Almeida *et al.* injected 50 nm PEGylated GNPs intravenously (approx. 200 µg/mouse) and looked at the change in splenocyte populations.¹⁸⁶ There was no significant change in the percentage of B cells found 24h after administration of GNPs. In agreement with these results, we could also confirm no changes in percentage of B cell populations in the spleen, lymph nodes, blood and liver 24h after injection of 15 nm double PEGylated GNPs, at concentration approximately two times higher (400 µg/mouse) than the one used in Almeida *et al.* study. Moreover, even 14 days after GNP injection, there was no sign of change in different splenic B cell subsets. Taken together, B cells tolerate exposure to GNPs *in vivo* after short- to medium-term incubation (up to 14 days).

1.1 Considerations for future immunotoxicological studies of GNP

The vast majority of immunotoxicological studies of GNPs, including ours, are focused on the acute effect of GNPs on the immune system, with shorter incubation time points. As a result, there is a lack of long term *in vivo* studies on GNP interactions with the immune system. This is probably due to the

General Discussion

long duration and high costs of these types of studies. Nevertheless, potential chronic immunological effects of GNPs need to be investigated, including the impact of one-time as well as after repeated GNP administrations. This is crucial to further understand the appropriateness of GNP-based nanomedicines and what are their potential side effects on the immune system over time. So far, long term studies showed the overall low GNP toxicity and no significant impact on the immune system.¹⁸⁷ For example, there was no inflammation detected 28 (at 0.7 mg/kg) and 90 (1250 ug/kg) days after single dose of GNPs in mice.^{188,189} In comparison, Bahamonde *et al.* showed an elevation of IL-8 on day 7 after high single-dose injection (1000 mg/kg). However, IL-8 level was then normalized on day 14 and remain unchangeable until day 28 endpoint.¹⁹⁰ In contrast, one study measured an increase in the percentage of blood B and T cells upon oral administration of GNPs.¹⁹¹ Importantly, these increase in mouse lymphocytes occurred only after day 28 and not at earlier time point. This could mean that GNPs might have a delayed adverse effect on the immune cells, possibly due to a decrease in their stability over time in the complex biological environment. Indeed, more of these long term effect studies are needed, with more specific immune cell targets. This would help to determine the origin of the possible long-term immunological responses towards GNPs, which can remain in the system for months, mainly accumulated in spleen and liver.¹⁸⁷

2. Biodistribution of GNPs

Numerous studies on biodistribution suggest that GNPs can generally be detected through the body in all the main organs.¹⁷⁹ However, the level of biodistribution strongly depends on the GNP size. For example, smaller GNPs (15 nm), had higher biodistribution across the body and were longer detected in blood, whereas larger GNPs (200 nm) had a higher tendency to be quickly removed from the blood and captured mainly in spleen and liver after 24 h.⁶⁷

Nonetheless, less is reported about more specific distribution across resident immune cells of different organs. So far, it has been commonly reported that tissue-resident macrophages are the main immune cells involved in the removal of GNPs, such as Kupffer cells in the liver.¹⁹² Similarly, we could confirm that monocytes/macrophages are indeed the leading immune cell type that takes up GNPs (~50 nm, hydrodynamic diameter) in blood, spleen, liver and lymph nodes up to 24 h post-injection. We could also observe that GNPs were initially accumulating in marginal zone B cells in the spleen (3 h and 24 h), whereas after longer exposure time GNPs were more intensely associating with the follicular B cells (14 days). A similar study also showed that the marginal zone B cells were strongly associated with 50 nm PEG-GNPs in the first 24 h post-injection.¹⁸⁶ Marginal zone B cells have a natural tendency to quickly associate with the blood-borne pathogens and particular matter in the spleen.¹⁹³ Thus, their primary role and anatomical localization may explain their involvement in the early GNP uptake in mice.

General Discussion

Upon the encounter with the antigen at the edge of the B cell follicle, B cells migrate to the center of the follicle and form germinal centers. There they undergo proliferation, differentiation and somatic hypermutations of the variable region of immunoglobulin genes in order to develop a strong antigen-specific immune response.¹⁰³ We could observe that GNPs prefer to associate with germinal zone B cells within the B cell follicle at the later time point (7 and 14 days). One possible explanation for a high GNP association with these B cell subsets is that their high metabolic activity upon encounter with an antigen increases GNP internalization compared to low GNP uptake in dormant naïve B cells. In sum, it is important that the exact mechanisms of GNP trafficking are further identified in order to understand the significance of the GNPs' impact on different B cell subsets at different times after exposure.

3. Effect of physico-chemical properties of GNPs on B cells

Numerous studies have shown how different GNP characteristics, such as size, shape, surface coating, a surface charge are important in how a cell or organism interacts with and responds to GNP.¹⁹⁴ Similarly, the outcomes in the GNP-B cell interactions were strongly dependent on the GNP properties. Throughout the project, we used several different GNPs, with distinct physico-chemical properties and are summarized in Table 4. GNPs differed in shape, hydrodynamic diameter, surface coating, surface charge, and presence or absence of fluorochrome. We investigated how B cells respond to these specific GNP characteristics. The specifics about GNP-related changes in B cell immune function are discussed further on.

General Discussion

Table 4: Overview of the GNPs and their physico-chemical characteristics used throughout the project.*

GNP name	Shape	Size: gold core (nm)	Size: d_h (nm)	Coating	ζ -potential	Fluorochrome
Citrate-GNS	Sphere	~15	16.8	Citrate	-34.7	/
PEG-GNS	Sphere	~15	26.8	mPEG	-5.8	/
PEG/PVA-GNS	Sphere	~15	23.7	mPEG and PVA	-6.5	/
PEG-GNR	Rod	57/15; AR: 3.8	34.8	mPEG	-13.6	/
Homo-PEG	Sphere	~15	n/a	NH ₂ -PEG	19.5	Cy5
Hetero-PEG	Sphere	~15	54.7	NH ₂ -PEG (inner layer)+mPEG (outer layer)	13.6	Cy5

*All the presented sizes and ζ -potentials were measured in H₂O by dynamic depolarized light scattering and phase-amplitude light-scattering analyzer, respectively; AR: aspect ratio, mPEG: methoxy PEG

Lack of coating on GNPs in the biological media causes aggregation and formation of protein corona and leads to increased GNP uptake.¹¹⁸ We observed citrate-coated GNS increased deposition in cell culture and increased association with the B cells, which caused interference with the pro-inflammatory response of activated B cells.

GNS with a hydrodynamic diameter (d_h) around 25 nm, protective polymers (mPEG and mPEG/PVA) and slightly negative charge showed the lowest internalization and no interference with B cell function in mouse and human *in vitro*, compared to other GNPs. In contrast, larger PEGylated spheres ($d_h \approx 55$ nm), positively charged (Hetero-PEG) were significantly taken up *in vitro* by splenic B cells and *in vivo* by macrophages, marginal zone and germinal center B cells. The increased uptake of positively charged NPs is commonly observed and explained as a result of electrostatic interactions with the negatively-charged cell membrane. However, other factors should be considered such as the effect of protein absorption, which was shown to be significantly increased for positively-charged NPs, compared to negatively-charged NPs.¹⁹⁵

Interestingly, compared to PEG-GNS and PEG/PVA-GNS, only rod-shaped GNPs (PEG-GNR) significantly affected the innate immune response in activated human B cells, despite their low association with the cells. It has been shown that ligand-coated PEG-GNR (aspect ratio from 2 to 7) are taken up *via* receptor-mediated endocytosis and predominantly accumulated in the late endosomes and were not detected in lysosomes, endoplasmic reticulum or cytosol 24 h after incubation.¹⁹⁶ However, trafficking of ligand-free PEG-GNR and mechanism of their interference with cell processes are still poorly understood. It is possible that small amounts of PEG-GNR were indeed internalized by B cells *via* endocytosis by unspecific-binding to the cell membrane. Certainly, it is difficult to explain how exactly small amounts of GNRs interfered with B cell function from inside the cell and how is this related to the GNP shape. Possibly, shape-specific NP-membrane interactions or distinct mechanisms of

General Discussion

internalization and sites of intracellular accumulation could be involved and should be further investigated.

To summarize, the physical and chemical properties of GNPs affected B cells as followed:

- GNPs with a different shape (rod vs. sphere), yet similar surface charge, did not differ in association with B cells and did not compromise their viability. However, shape played a role in modulation of B cell innate immune response, suggesting that B cells might be more susceptible to the rod-shaped GNPs compared to GNS
- Polymer coatings ensured GNP stability and reduced their association with B cells
- The positive surface charge of sphere-shaped GNPs contributed to increased internalization in B cells *in vitro*

4. GNP effect on B cells and their function

There are many reports involving GNPs as a vaccine carrier, showing that GNPs are able to enhance antigen immunogenicity and improve antibody titer.^{170,47} GNPs serve as a great antigen platform that enables a more efficient BCR cross-linking and elicit a stronger immune response.¹⁵⁰ Despite these promising results of antigen-conjugated GNPs, there is very little information about unconjugated GNPs and their off-target effect on B cells. This is especially important as B cells are crucial in the development of adaptive immunity as well as their contribution to innate responses and antigen presentation.⁵⁹

4.1 Effect on the B cell innate-like immune response

In general, the literature indicates that unconjugated, well-optimized and surface-stabilized GNPs do not stimulate cytokine response in macrophages and dendritic cells.^{197–199} In fact, several studies have shown a suppressive role of GNPs in TLR-associated immune response in phagocytic cells.^{200–202} Tsai *et al.* investigated how GNPs interfere with TLR9-mediated stimulation in macrophages. They showed that 4 nm PEGylated GNP manipulated NF- κ B phosphorylation and affected TLR9 translocation from the ER to endosomes. Consequentially, this resulted in decreased release of pro-inflammatory cytokines (TNF- α).¹¹⁵

Although B cells are generally classified as part of the adaptive immune system, they also express several TLRs, which are involved in cytokine and innate-like IgM release upon stimulation with pathogen-associated molecular patterns (*e.g.*, LPS) or synthetic adjuvants (*e.g.*, R848).^{96,203,204} Our results showed GNP type-dependent (negatively-charged PEG-GNR and positively-charged PEG-GNS) attenuation of TLR-induced cytokine secretion in pure B cell population. Moreover, we observed a decline in TLR7-induced IgM production after incubation with GNPs *in vitro* by PEGylated spheres.

General Discussion

Cytokine and immunoglobulin light and heavy chain genes rely on transcriptional activation by NF- κ B and it is possible that this pathway is also attenuated by GNPs in B cells.^{205,206} However, we could not confirm the GNP interference of B cell innate function *in vivo* as GNPs did not cause a significant decrease in expression of NF- κ B-associated genes (*e.g.*, il-6, tnf-alpha). The reason for the lack of detection of the GNP suppressive effect on B cell innate function in mice may be due to the lower amount of GNP internalized by B cells compared to *in vitro*.

Thus, the potential immunosuppressive effect of GNPs in pathological conditions where B cell suppression is desirable (*e.g.*, autoimmune diseases) should be further investigated. For instance, the production of autoantibodies in lupus is connected to overexpression of TLR7 and in B cells.²⁰⁷ Importantly, GNPs are already studied as a potential TLR inhibitor in innate immune cells.²⁰⁸ Taken together, B cells might present an additional target of interest in studies aiming to silence pathological TLR-signaling pathways by GNPs.

4.2 Effect on the B cell adaptive immune response

There are limited reports about GNP (not conjugated with antigens) interference with the adaptive immune response. Two studies showed the ability of GNPs to stimulate the production of antibodies such as IgG and IgA in B cell lines in a size- and concentration-dependent manner, where GNPs between 2 and 12 nm and at lower concentration (0.5 μ g/ml and 1 μ g/ml) had the most potent effect.^{138,137} On the contrary, we showed that GNPs did not increase basal IgM or IgG production *in vitro* and *in vivo* at 20 μ g/ml and 20 mg/kg, respectively. The reasons for these opposing results could be several, including the use of immortalized B cells vs. primary B cells and the effect of GNP characteristics such as size and lack of polymer coating.²⁰⁹

Moreover, we detected a clear decline in antigen-specific IgM due to GNPs, which was most likely related to increased uptake in highly metabolically active germinal center B cells. In agreement with our results, a similar decrease in IgM was also observed in a report from 1999 in primary human B cells after incubation with gold compounds (used in the treatment of rheumatoid arthritis) and the presence of antigen. These results indicated that inhibition of antibody production by gold might be affected directly *via* BCR signaling. Taken together, GNPs have the potential to interfere with B cell effector function. Further insights in the mechanism of interference of B cell adaptive immune response by GNPs are needed as this might present a crucial point for the development of new GNP applications.

Be that as it may, numerous studies have shown that antigen-conjugated GNPs are an effective tool for increased immunization with high antibody titers compared to soluble antigens and due to a proposed GNP adjuvant property. However, this adjuvant effect may be a consequence of the property

General Discussion

of NPs as an efficient antigen delivery system rather than GNPs themselves, as the GNPs alone are not considered immunogenic material. Nonetheless, based on our results of the GNP effect on antigen-primed B cells, GNPs should be further considered whether they are the most optimal NP type to be used as a vaccine platform as they might interfere with further antigen-specific B cell effector function.

Of note, there is sufficient evidence to show that repeated administration of PEGylated drugs or NPs causes the production of PEG specific antibodies, which leads to accelerated clearance of the PEGylated medicine from the system.¹³⁵ In our study, we used PEGylated GNPs only as single-dose injections. However, for future PEGylated NP applications for which repeated administrations are intended, the half-life and the therapeutic effect of the nanomedicine should be evaluated with regard to anti-PEG antibody production. This can be potentially avoided by changing the protective coating with a zwitterionic based shield (*e.g.*, (poly)carboxybetaine), which is highly hydrophilic and is less prone to unspecific binding to proteins compared to PEG.²¹⁰ These types of zwitterionic coatings already showed the absence of anti-coating IgM production and significantly improved GNP half-life.²¹¹

5. B cell experimental models and their relevance

5.1 Human *in vitro* model

Human primary B cells are difficult to maintain in the cell culture and do not survive long without additional complex stimulation or immortalization.²¹² Therefore, they are not often chosen as a cell culture model. Nevertheless, primary human *in vitro* B cell culture indeed has a great advantage over the mouse model as it can provide a better understanding of how a substance such as NPs would affect B cells in humans. This PhD project was initiated with the establishment of primary cell cultures of purified human blood B cells. Importantly, we were able to obtain stable human B cells (up to 24 h), cultured in 10% of allogenic human plasma instead of using the standard 10% FBS. This is not only important to bring B cells closer to their natural environment, but also to include the possible influence of GNP-plasma protein interactions on B cell function and gain a more realistic perspective on how GNPs would behave in human blood.¹⁸⁰ Additionally, the use of primary human cell culture provides donor-to-donor variation and ensures more realistic results. This type of *in vitro* system is a great tool that helps to understand how GNPs affect exclusively human B cells in their natural state.

5.2 Mouse *in vitro* model

Prior to moving on to mouse *in vivo* experimentation, it was essential to first test the GNP impact on mouse primary B cells *in vitro*. This step was important to determine the possible GNP toxicity on mouse B cells, choose appropriate targets of interest in mouse and GNP exposure time points, and to gain a first impression about the strength of GNP-B cell association and uptake. *In vitro* testing allowed

General Discussion

optimization of the screening methods, with a minimal number of animals needed. It was a useful preparation stage before the continuation *in vivo*, where more complex outcomes are expected. Additionally, we could draw a cross-species comparison of the GNP effect on mouse vs. human B cells, which is discussed below.

5.3 Mouse *in vivo* model

In vivo models are important to understand the overall GNP biodistribution and toxicological potential on the immune system.¹⁷⁹ In the scope of the project, the *in vivo* part was particularly informative about the time-dependent GNP biodistribution in different organs as well as to determine B cell-specific and B cell subset-specific GNP uptake, which was also dependent on the route of administration (*e.g.*, subcutaneously, intravenously). This type of information is useful when B cell targeting is desired and can help to evaluate the therapeutic potential of GNP-based nanomedicines for the treatment of B cell-related pathologies or the strength of B cell prophylactic response in a nanovaccine.

Moreover, B cell adaptive immune response is a complex process that strongly depends on the immunogenicity of the antigen, communication between different immune cells, time frame as well as the spatial distribution of different cell types in lymphoid organs. Taken together, two-dimensional cultures are not sufficient to determine the ultimate GNP effect on B cells and their adaptive immune function.

5.4 Room for improvement

One of the common reasons for the early termination of clinical trials is immune hypersensitivity or immunotoxicity of the developed drug.²¹³ NP-based medicines lack specific regulations for their safety assessments by regulatory agencies. Therefore, they are less predictable and present a higher risk of low success in clinical trials. Novel *in vitro* technologies are being developed in order to better predict drug toxicity already *in vitro* to avoid the later failure in the clinical studies. For example, Purwada *et al.* established first *ex-vivo* primary B cell follicle organoids connected to the scaffold of stromal cells that formed into a stiff organ-like structure, encapsulated in a body temperature stable silica NP hydrogel.²¹⁴ This model is intended for studying B cell proliferation, germinal center formation and isotype switching in relation to B cell pathogenesis or biotherapeutics and vaccine efficacy. Thus, it would be also an optimal three-dimensional platform for studying the safety of the NP or nanomedicines with regard to B cell response.

Primary and secondary lymphoid organs-on-chip are increasingly being developed, including lymph node, spleen and bone marrow.²¹⁵ Such models include a fluidic system with inlets and outlets to

General Discussion

establish lymphatic or blood microcirculation and several chambers containing immune cell cultures and co-cultures.²¹⁶ This type of technology is already being applied for screening of NP toxicity with the purpose to ensure higher throughput in translation to clinical studies.²¹⁷

Despite the great potential of these *ex-vivo* systems, they still have some limitations such as the scale of the organoid, cell numbers and the lack of connections with the other organs and parts of the immune system.²¹⁵ On their own, they may still not be sufficient to evaluate NP immunotoxicity for clinical translation. Thus, the use of animals with a humanized immune system is an advanced alternative for *in vivo* studies of the immune system.²¹⁸ These models are based on adoptive transfer of human immune cells (*e.g.*, PBMCs or hematopoietic stem cells) into mice. The advantage over wild type animal models is, to some extent, to exclude mouse-specific immune responses and to offer more human-like responses. Such humanized mouse models are already used for testing the potential immunotoxicity and immunomodulatory effect of NPs on the innate immune system, which could further promote better clinical translation of NPs.²¹⁹

6. Cross-species comparison of B cell-GNP interactions

Clearly, GNPs have been intensively studied for their toxicological effect on numerous cell targets and animal models.¹⁷⁹ All this information is indeed beneficial in order to help with the overall evaluation of GNP safety. However, among hundreds of studies using different exposure times, GNP concentrations, GNP properties and cell targets, it is often difficult to directly compare and draw a final conclusion, if one or more GNP-related variables are present (*e.g.*, the same GNP surface chemistry but different size/concentration/cell target).

In the scope of this PhD project, I supervised a master student (Millie Porzi) and assigned her a side project. The aim was to investigate the impact of the same panel of GNPs that was used on human B cells (Manuscript 1) on primary mouse splenic B cells. Importantly, exposure times, NP concentration, methods and immune activation and pro-inflammatory targets were equivalent. The main results of this master project are summarized in Appendix 1. These results, together with results on human B cells *in vitro*, enable a direct and critical cross-species comparison of GNP effect on B cells due to detailed knowledge about the biological conditions and the use of identical GNPs on both models.

Table 5 presents an overview of the main outcomes of the GNP impact on human and mouse B cells *in vitro*. Both cultures were exposed to the same panel of different GNPs (citrate-GNS, PEG-GNS, PEG/PVA-GNS, PEG-GNR) at the same high concentration and the same exposure time (20 µg/ml, 24h). The most important and mutual conclusion is that GNPs were not cytotoxic to the B cells and did not cause immune activation in unstimulated B cells. Interestingly, polymer-free citrate-GNS caused the opposite effect regarding cytokine production in stimulated cells. Whereas human B cells responded

General Discussion

to citrate-GNS with diminished cytokine release, mouse B cells exposed to these types of GNPs responded with an increasing trend of pro-inflammatory secretion. In comparison, Devanamanda *et al.* tested GNP effect on proliferating mouse and human primary lymphocytes *in vitro* and found that GNPs caused concentration-dependent suppression in proliferation in both species.¹⁸⁵ However, they did not investigate how this interferes with their immune response. Yet, they similarly showed no GNP cytotoxic effect on unstimulated and stimulated human and mouse cells.

The opposite outcomes in cytokine production in activated B cells observed in our studies may stem from differences in species-specific tolerability to internalized GNP concentrations. This is based on the observation of different responses to different GNPs within the species. For example, the increased uptake of positively charged but stable PEGylated spheres (Homo-PEG and Hetero-PEG) in mouse B cells *in vitro* caused a decrease in cytokine production, compared to its increase after exposure to aggregated citrate-GNS. To elaborate, even though the cells were exposed to the same external GNP concentration (20 µg/ml), the internalized concentration between the two GNP formulations most likely differed. Consequently, this may have resulted in dissimilar immune modulations. Thus, certain concentrations of the internalized GNPs might be tipping-points between immuno-suppression and immuno-activation and might also be species dependent. Nonetheless, additional information about the uptake and cell response for each species are still needed in order to draw a more definite conclusion.

Table 5: Overview of the GNP impact on the mouse and human primary B cells in vitro.

	Citrate-GNS	PEG-GNS	PEG/PVA-GNS	PEG-GNR	Citrate-GNS	PEG-GNS	PEG/PVA-GNS	PEG-GNR	Homo-PEG	Hetero-PEG
Viability	No effect	No effect	No effect	No effect	No effect	No effect	No effect	No effect	No effect	No effect
NP-cell association	High	Low	Low	Low	n.d.	n.d.	n.d.	n.d.	High	High
Immune activation	No	No	No	No	No	No	No	No	No	No
Pro-inflammatory response	Decrease of IL-6 in TLR7-activated cells	No	No	Decrease of IL-6 in TLR7-activated cells	Trend in increase of IL-6 in TLR7-activated cells	No	No	No	Decrease of IL-6 in TLR7-activated cells	Decrease of IL-6 in TLR7-activated cells
Antibody production	n.d.	n.d.	n.d.	n.d.	Decrease of IgM in TLR7-activated cells	No	No	No	Decrease of IgM in TLR7-activated cells	Decrease of IgM in TLR7-activated cells

Results are summarized based on the same GNP exposure concentration and incubation time (20 µg/ml, 24h) for mouse and human B cells; n.d.= not done

General Discussion

6.1 Dose prediction for translation to clinical trials

An important aspect that should be also considered is the appropriateness of the dose administered in pre-clinical studies with regard to future translation to the clinic. Indeed, high dose studies are important for the comprehensive evaluation of NP safety. However, as we could observe some differences in response between mouse and human cells, more attention should be directed in the evaluation of which doses are tolerable in animals and what estimated doses would be tolerable in humans. With the help of FDA guidelines, human equivalent dose (HED) can be calculated from the animal doses (AD) with dose by the factor method, which is commonly used among pre-clinical researchers to estimate doses across species.²²⁰ Scaling of a dose is based on the differences in metabolic rates and physiological processes, which is conditioned by weight and body surface.²²¹ A simple factor method for dose conversion is based on the correction factors (K_m = body weight [kg]/body surface [m^2]; K_m (mouse) ≈ 3 , K_m (human) ≈ 37) that include the above mentioned cross-species differences and is calculated as followed:

$$\text{HED [mg/kg]} = \text{AD [mg/kg]} \times \left(\frac{K_m \text{ (mouse)}}{K_m \text{ (human)}} \right)$$

In mice experiments, we used a concentration of approximately 20 mg/kg (injected intravenously), which equals a HED of 1.6 mg/kg. As a reference for human dose: in the phase I clinical trial (NCT00356980) 30 nm PEGylated GNPs were used as a delivery system for TNF- α in order to reduce its high systemic toxicity in cancer patients.¹⁶⁶ The lowest and highest GNP concentrations administered intravenously were 0.03 and 0.4 mg/kg, respectively. The results showed no adverse effect of the nanomedicine, even at the highest dose injected (at least two injections per patient). To compare, our estimated GNP human dose is approximately 4-fold higher than the highest dose administered in cancer patients in the clinical trial. Taken together, based on our *in vivo* results on GNP ability to alter B cell immune response, lower doses in mice should be also tested in order to determine the maximal dose at which no B cell immune-modulation is observed. Followed by the conversion to HED, this could then further help to determine the appropriates of GNP dose once they are ready for translation to clinical studies.

7. Conclusions

To this day, this PhD project presents one of the very limited studies exclusively focused on GNP interactions with B cells *in vitro* and *in vivo*. Most importantly, we were able to evaluate the direct impact of GNPs on B cell function. GNP properties such as shape and surface charge, protein corona formation as well as B cell origin and activation status were confirmed to be important factors in GNP-B cell distinct interactions. To summarize, we demonstrated the following:

General Discussion

- GNPs, independently of their physico-chemical properties, did not compromise B cell viability (*in vitro*) or influence percentage of any of the B cell subsets (*in vivo*)
- Biodistribution of GNPs across B cell subsets differs based on their primary function and anatomical localization (*e.g.*, higher uptake in marginal B cell zone (short exposure time) and in follicular/germinal center B cells (longer exposure time))
- GNPs did not significantly influence the expression of B cell surface immune activation markers (CD69, CD86, MHC II)
- GNP shape (rod) played a role in attenuation of B cell cytokine production (IL-6)
- Antigen-specific and short-lived antibody responses were attenuated by GNPs
- Antigen activated B cells are considerably more susceptible to GNP internalization and immune-modulation than unstimulated cells

Taken together, these results provide important new information about immune cell type-specific interactions and the impact of GNP on immune response, which will hopefully contribute to the development of novel and safer biomedical applications.

8. Outlook

The general outcome of the results suggested that GNPs have a suppressive impact on the functionally active B cells. Moreover, it seems that naive and dormant B cells are not significantly affected by GNPs. Therefore, GNP-based applications might be useful in studies where B cells need to be silenced (*e.g.*, autoimmune diseases). Nevertheless, further studies are needed to first better understand the mechanisms which are involved in B cell immune-modulation and GNP internalization. Furthermore, information about the upper dose limit, long-term effects and possible impairment of B cell ability of antigen presentation as well as the impact on memory B cells should be investigated, as this could compromise adaptive immunity over time. Importantly, it should be always carefully considered the effect of specific GNP characteristics and their stability in the biological system. GNP-based applications have already reached the clinic and with further studies, they will hopefully achieve even broader theranostic impact.

REFERENCES

- (1) Laura Soriano, M.; Zougagh, M.; Valcárcel, M.; Ríos, Á. Analytical Nanoscience and Nanotechnology: Where We Are and Where We Are Heading. *Talanta* **2018**, *177*, 104–121.
- (2) ISO/TS 80004-1:2015. Nanotechnologies -Vocabulary - Part 1: Core terms <https://www.iso.org/obp/ui/#iso:std:iso:ts:80004:-1:ed-2:v1:en> (accessed Mar 10, 2019).
- (3) Feynman, R. There's Plenty of Room at the Bottom. *Engineering and Science*. 1960, pp 22–36.
- (4) Krukemeyer, M. G.; Krenn, V.; Wagner, W.; Resch R. History and Possible Uses of Nanomedicine Based on Nanoparticles and Nanotechnological Progress. *J Nanomed Nanotechnol* **2015**, *6*, 336.
- (5) Pelaz, B.; Alexiou, C.; Alvarez-Puebla, R. A.; Alves, F.; Andrews, A. M.; Ashraf, S.; Balogh, L. P.; Ballerini, L.; Bestetti, A.; Brendel, C.; Bosi, S.; Carril, M.; Chan, W. C. W.; Chen, C.; Chen, X.; Chen, X.; Cheng, Z.; Cui, D.; Du, J.; et al. Diverse Applications of Nanomedicine. *ACS Nano* **2017**, *11*, 2313–2381.
- (6) Chaudhry, Q.; Castle, L. Food Applications of Nanotechnologies: An Overview of Opportunities and Challenges for Developing Countries. *Trends Food Sci. Technol.* **2011**, *22*, 595–603.
- (7) Léonard, F.; Talin, A. A. Electrical Contacts to One- and Two-Dimensional Nanomaterials. *Nat. Nanotechnol.* **2011**, *6*, 773–783.
- (8) Yousefi, N.; Lu, X.; Elimelech, M.; Tufenkji, N. Environmental Performance of Graphene-Based 3D Macrostructures. *Nat. Nanotechnol.* **2019**, *14*, 107–119.
- (9) Yetisen, A. K.; Qu, H.; Manbachi, A.; Butt, H.; Dokmeci, M. R.; Hinstroza, J. P.; Skorobogatiy, M.; Khademhosseini, A.; Yun, S. H. Nanotechnology in Textiles. *ACS Nano* **2016**, *10*, 3042–3068.
- (10) Chamsa-ard, W.; Brundavanam, S.; Fung, C. C.; Fawcett, D.; Poinern, G. Nanofluid Types, Their Synthesis, Properties and Incorporation in Direct Solar Thermal Collectors: A Review. *Nanomaterials* **2017**, *7*, 131.
- (11) ISO/TS 80004-2:2015. Nanotechnologies - Vocabulary - Part 2: Nano-objects <https://www.iso.org/obp/ui/#iso:std:iso:ts:80004:-2:ed-1:v1:en> (accessed Mar 5, 2019).
- (12) Dulińska-Litewka, J.; Łazarczyk, A.; Hałubiec, P.; Szafranski, O.; Karnas, K.; Krawiec, A. Superparamagnetic Iron Oxide Nanoparticles-Current and Prospective Medical Applications. *Materials (Basel)*. **2019**, *12*, 617.
- (13) Jeevanandam, J.; Barhoum, A.; Chan, Y. S.; Dufresne, A.; Danquah, M. K. Review on Nanoparticles and Nanostructured Materials: History, Sources, Toxicity and Regulations. *Beilstein J. Nanotechnol.* **2018**, *9*, 1050–1074.
- (14) Lim, E.-K.; Kim, T.; Paik, S.; Haam, S.; Huh, Y.-M.; Lee, K. Nanomaterials for Theranostics: Recent Advances and Future Challenges. *Chem. Rev.* **2015**, *115*, 327–394.
- (15) Choi, Y. H.; Han, H.-K. Nanomedicines: Current Status and Future Perspectives in Aspect of Drug Delivery and Pharmacokinetics. *J. Pharm. Investig.* **2018**, *48*, 43–60.
- (16) Bobo, D.; Robinson, K. J.; Islam, J.; Thurecht, K. J.; Corrie, S. R. Nanoparticle-Based Medicines: A Review of FDA-Approved Materials and Clinical Trials to Date. *Pharm. Res.* **2016**, *33*, 2373–2387.
- (17) Soares, S.; Sousa, J.; Pais, A.; Vitorino, C. Nanomedicine: Principles, Properties, and Regulatory Issues. *Front. Chem.* **2018**, *6*, 360.
- (18) Farjadian, F.; Ghasemi, A.; Gohari, O.; Roointan, A.; Karimi, M.; Hamblin, M. R. Nanopharmaceuticals and Nanomedicines Currently on the Market: Challenges and Opportunities. *Nanomedicine* **2019**, *14*, 93–126.
- (19) Anselmo, A. C.; Mitragotri, S. Nanoparticles in the Clinic: An Update. *Bioeng. Transl. Med.* **2019**, *4*.
- (20) ClinicalTrials.gov <https://clinicaltrials.gov/ct2/home> (accessed Oct 19, 2019).

References

- (21) Magforce - The Nanomedicine Company <https://www.magforce.com/en/home/> (accessed Oct 19, 2019).
- (22) Maier-Hauff, K.; Ulrich, F.; Nestler, D.; Niehoff, H.; Wust, P.; Thiesen, B.; Orawa, H.; Budach, V.; Jordan, A. Efficacy and Safety of Intratumoral Thermotherapy Using Magnetic Iron-Oxide Nanoparticles Combined with External Beam Radiotherapy on Patients with Recurrent Glioblastoma Multiforme. *J. Neurooncol.* **2011**, *103*, 317–324.
- (23) Kharlamov, A. N.; Tyurnina, A. E.; Veselova, V. S.; Kovtun, O. P.; Shur, V. Y.; Gabinsky, J. L. Silica-Gold Nanoparticles for Atheroprotective Management of Plaques: Results of the NANOM-FIM Trial. *Nanoscale* **2015**, *7*, 8003–8015.
- (24) Anchordoquy, T. J.; Barenholz, Y.; Boraschi, D.; Chorny, M.; Decuzzi, P.; Dobrovolskaia, M. A.; Farhangrazi, Z. S.; Farrell, D.; Gabizon, A.; Ghandehari, H.; Godin, B.; La-Beck, N. M.; Ljubimova, J.; Moghimi, S. M.; Pagliaro, L.; Park, J. H.; Peer, D.; Ruoslahti, E.; Serkova, N. J.; et al. Mechanisms and Barriers in Cancer Nanomedicine: Addressing Challenges, Looking for Solutions. *ACS Nano* **2017**, *11*, 12–18.
- (25) Ioannidis, J. P. A.; Kim, B. Y. S.; Trounson, A. How to Design Preclinical Studies in Nanomedicine and Cell Therapy to Maximize the Prospects of Clinical Translation. *Nat. Biomed. Eng.* **2018**, *2*, 797–809.
- (26) Ventola, C. L. The Nanomedicine Revolution: Part 1: Emerging Concepts. *P T* **2012**, *37*, 512–525.
- (27) Bosetti, R. Cost–Effectiveness of Nanomedicine: The Path to a Future Successful and Dominant Market? *Nanomedicine* **2015**, *10*, 1851–1853.
- (28) Etheridge, M. L.; Campbell, S. A.; Erdman, A. G.; Haynes, C. L.; Wolf, S. M.; McCullough, J. The Big Picture on Nanomedicine: The State of Investigational and Approved Nanomedicine Products. *Nanomedicine* **2013**, *9*, 1–14.
- (29) European Medicines Agency. Multidisciplinary: nanomedicines <https://www.ema.europa.eu/en/human-regulatory/research-development/scientific-guidelines/multidisciplinary/multidisciplinary-nanomedicines> (accessed Oct 20, 2019).
- (30) Bremer-Hoffmann, S.; Halamoda-Kenzaoui, B.; Borgos, S. E. Identification of Regulatory Needs for Nanomedicines. *J. Interdiscip. Nanomedicine* **2018**, *3*, 4–15.
- (31) Astier, A.; Barton Pai, A.; Bissig, M.; Crommelin, D. J. A.; Flühmann, B.; Hecq, J.-D.; Knoeff, J.; Lipp, H.-P.; Morell-Baladrón, A.; Mühlebach, S. How to Select a Nanosimilar. *Ann. N. Y. Acad. Sci.* **2017**, *1407*, 50–62.
- (32) Nel, A. E.; Mädler, L.; Velegol, D.; Xia, T.; Hoek, E. M. V.; Somasundaran, P.; Klaessig, F.; Castranova, V.; Thompson, M. Understanding Biophysicochemical Interactions at the Nano-Bio Interface. *Nat. Mater.* **2009**, *8*, 543–557.
- (33) Zhang, X.; Pandiakumar, A. K.; Hamers, R. J.; Murphy, C. J. Quantification of Lipid Corona Formation on Colloidal Nanoparticles from Lipid Vesicles. *Anal. Chem.* **2018**, *90*, 14387–14394.
- (34) Winzen, S.; Schoettler, S.; Baier, G.; Rosenauer, C.; Mailaender, V.; Landfester, K.; Mohr, K. Complementary Analysis of the Hard and Soft Protein Corona: Sample Preparation Critically Effects Corona Composition. *Nanoscale* **2015**, *7*, 2992–3001.
- (35) Vroman, L.; Adams, A. L. Findings with the Recording Ellipsometer Suggesting Rapid Exchange of Specific Plasma Proteins at Liquid/Solid Interfaces. *Surf. Sci.* **1969**, *16*, 438–446.
- (36) Xia, T.; Kovoichich, M.; Liong, M.; Mädler, L.; Gilbert, B.; Shi, H.; Yeh, J. I.; Zink, J. I.; Nel, A. E. Comparison of the Mechanism of Toxicity of Zinc Oxide and Cerium Oxide Nanoparticles Based on Dissolution and Oxidative Stress Properties. *ACS Nano* **2008**, *2*, 2121–2134.
- (37) Tenzer, S.; Docter, D.; Kuharev, J.; Musyanovych, A.; Fetz, V.; Hecht, R.; Schlenk, F.; Fischer, D.; Kiouptsi, K.; Reinhardt, C.; Landfester, K.; Schild, H.; Maskos, M.; Knauer, S. K.; Stauber, R. H. Rapid Formation of Plasma Protein Corona Critically Affects Nanoparticle Pathophysiology. *Nat. Nanotechnol.* **2013**, *8*, 772–781.
- (38) Lundqvist, M.; Stigler, J.; Elia, G.; Lynch, I.; Cedervall, T.; Dawson, K. A. Nanoparticle Size and Surface Properties Determine the Protein Corona with Possible Implications for Biological Impacts. *Proc. Natl.*

References

- Acad. Sci. U. S. A.* **2008**, *105*, 14265–14270.
- (39) Deng, Z. J.; Mortimer, G.; Schiller, T.; Musumeci, A.; Martin, D.; Minchin, R. F. Differential Plasma Protein Binding to Metal Oxide Nanoparticles. *Nanotechnology* **2009**, *20*, 455101.
- (40) Walkey, C. D.; Olsen, J. B.; Guo, H.; Emili, A.; Chan, W. C. W. Nanoparticle Size and Surface Chemistry Determine Serum Protein Adsorption and Macrophage Uptake. *J. Am. Chem. Soc.* **2012**, *134*, 2139–2147.
- (41) Cedervall, T.; Lynch, I.; Lindman, S.; Berggård, T.; Thulin, E.; Nilsson, H.; Dawson, K. A.; Linse, S. Understanding the Nanoparticle-Protein Corona Using Methods to Quantify Exchange Rates and Affinities of Proteins for Nanoparticles. *Proc. Natl. Acad. Sci. U. S. A.* **2007**, *104*, 2050–2055.
- (42) Lundqvist, M.; Augustsson, C.; Lilja, M.; Lundkvist, K.; Dahlbäck, B.; Linse, S.; Cedervall, T. The Nanoparticle Protein Corona Formed in Human Blood or Human Blood Fractions. *PLoS One* **2017**, *12*, e0175871.
- (43) Aggarwal, P.; Hall, J. B.; McLeland, C. B.; Dobrovolskaia, M. A.; McNeil, S. E. Nanoparticle Interaction with Plasma Proteins as It Relates to Particle Biodistribution, Biocompatibility and Therapeutic Efficacy. *Adv. Drug Deliv. Rev.* **2009**, *61*, 428–437.
- (44) Sanfins, E.; Augustsson, C.; Dahlbäck, B.; Linse, S.; Cedervall, T. Size-Dependent Effects of Nanoparticles on Enzymes in the Blood Coagulation Cascade. *Nano Lett.* **2014**, *14*, 4736–4744.
- (45) Chithrani, B. D.; Ghazani, A. A.; Chan, W. C. W. Determining the Size and Shape Dependence of Gold Nanoparticle Uptake into Mammalian Cells. *Nano Lett.* **2006**, *6*, 662–668.
- (46) Xie, X.; Liao, J.; Shao, X.; Li, Q.; Lin, Y. The Effect of Shape on Cellular Uptake of Gold Nanoparticles in the Forms of Stars, Rods, and Triangles. *Sci. Rep.* **2017**, *7*, 3827.
- (47) Niikura, K.; Matsunaga, T.; Suzuki, T.; Kobayashi, S.; Yamaguchi, H. Gold Nanoparticles as a Vaccine Platform : Influence of Size and Shape on Immunological Responses *in Vitro* and *in Vivo*. **2013**, 3926–3938.
- (48) Hühn, D.; Kantner, K.; Geidel, C.; Brandholt, S.; De Cock, I.; Soenen, S. J. H.; Riveragil, P.; Montenegro, J. M.; Braeckmans, K.; Müllen, K.; Nienhaus, G. U.; Klapper, M.; Parak, W. J. Polymer-Coated Nanoparticles Interacting with Proteins and Cells: Focusing on the Sign of the Net Charge. *ACS Nano* **2013**, *7*, 3253–3263.
- (49) Yue, Z.-G.; Wei, W.; Lv, P.-P.; Yue, H.; Wang, L.-Y.; Su, Z.-G.; Ma, G.-H. Surface Charge Affects Cellular Uptake and Intracellular Trafficking of Chitosan-Based Nanoparticles. *Biomacromolecules* **2011**, *12*, 2440–2446.
- (50) Alvarez, B.; Carballal, S.; Turell, L.; Radi, R. Formation and Reactions of Sulfenic Acid in Human Serum Albumin. *Methods Enzymol.* **2010**, *473*, 117–136.
- (51) Hirsch, V.; Kinnear, C.; Moniatte, M.; Rothen-Rutishauser, B.; Clift, M. J. D.; Fink, A. Surface Charge of Polymer Coated SPIONs Influences the Serum Protein Adsorption, Colloidal Stability and Subsequent Cell Interaction *in Vitro*. *Nanoscale* **2013**, *5*, 3723–3732.
- (52) Cho, E. C.; Zhang, Q.; Xia, Y. The Effect of Sedimentation and Diffusion on Cellular Uptake of Gold Nanoparticles. *Nat. Nanotechnol.* **2011**, *6*, 385.
- (53) Fleischer, C. C.; Payne, C. K. Nanoparticle–Cell Interactions: Molecular Structure of the Protein Corona and Cellular Outcomes. *Acc. Chem. Res.* **2014**, *47*, 2651–2659.
- (54) Gessner, A.; Waicz, R.; Lieske, A.; Paulke, B. R.; Mäder, K.; Müller, R. H. Nanoparticles with Decreasing Surface Hydrophobicities: Influence on Plasma Protein Adsorption. *Int. J. Pharm.* **2000**, *196*, 245–249.
- (55) Sahoo, S. K.; Panyam, J.; Prabha, S.; Labhsetwar, V. Residual Polyvinyl Alcohol Associated with Poly (D,L-Lactide-Co-Glycolide) Nanoparticles Affects Their Physical Properties and Cellular Uptake. *J. Control. Release* **2002**, *82*, 105–114.
- (56) Owens, D. E.; Peppas, N. A. Opsonization, Biodistribution, and Pharmacokinetics of Polymeric

References

- Nanoparticles. *Int. J. Pharm.* **2006**, *307*, 93–102.
- (57) Seong, S.-Y.; Matzinger, P. Hydrophobicity: An Ancient Damage-Associated Molecular Pattern That Initiates Innate Immune Responses. *Nat. Rev. Immunol.* **2004**, *4*, 469–478.
- (58) Moyano, D. F.; Goldsmith, M.; Solfiell, D. J.; Landesman-Milo, D.; Miranda, O. R.; Peer, D.; Rotello, V. M. Nanoparticle Hydrophobicity Dictates Immune Response. *J. Am. Chem. Soc.* **2012**, *134*, 3965–3967.
- (59) Abbas, A. K.; Lichtman, A. H.; Phillai, S. *Cellular and Molecular Immunology*, 9th ed.; Elsevier, 2017.
- (60) Vu, V. P.; Gifford, G. B.; Chen, F.; Benasutti, H.; Wang, G.; Groman, E. V.; Scheinman, R.; Saba, L.; Moghimi, S. M.; Simberg, D. Immunoglobulin Deposition on Biomolecule Corona Determines Complement Opsonization Efficiency of Preclinical and Clinical Nanoparticles. *Nat. Nanotechnol.* **2019**, *14*, 260–268.
- (61) Maiorano, G.; Sabella, S.; Sorce, B.; Brunetti, V.; Malvindi, M. A.; Cingolani, R.; Pompa, P. P. Effects of Cell Culture Media on the Dynamic Formation of Protein–Nanoparticle Complexes and Influence on the Cellular Response. *ACS Nano* **2010**, *4*, 7481–7491.
- (62) Sen, T.; Haldar, K. K.; Patra, A. Au Nanoparticle-Based Surface Energy Transfer Probe for Conformational Changes of BSA Protein. *J. Phys. Chem. C* **2008**, *112*, 17945–17951.
- (63) Mahmoudi, M.; Abdelmonem, A. M.; Behzadi, S.; Clement, J. H.; Dutz, S.; Ejtehadi, M. R.; Hartmann, R.; Kantner, K.; Linne, U.; Maffre, P.; Metzler, S.; Moghadam, M. K.; Pfeiffer, C.; Rezaei, M.; Ruiz-Lozano, P.; Serpooshan, V.; Shokrgozar, M. A.; Nienhaus, G. U.; Parak, W. J. Temperature: The “Ignored” Factor at the NanoBio Interface. *ACS Nano* **2013**, *7*, 6555–6562.
- (64) Foroozandeh, P.; Aziz, A. A. Merging Worlds of Nanomaterials and Biological Environment: Factors Governing Protein Corona Formation on Nanoparticles and Its Biological Consequences. *Nanoscale Res. Lett.* **2015**, *10*, 221.
- (65) Nguyen, V. H.; Lee, B. J. Protein Corona: A New Approach for Nanomedicine Design. *International Journal of Nanomedicine*. Dove Press 2017, pp 3137–3151.
- (66) De Jong, W. H.; Hagens, W. I.; Krystek, P.; Burger, M. C.; Sips, A. J. A. M.; Geertsma, R. E. Particle Size-Dependent Organ Distribution of Gold Nanoparticles after Intravenous Administration. *Biomaterials* **2008**, *29*, 1912–1919.
- (67) Sonavane, G.; Tomoda, K.; Makino, K. Biodistribution of Colloidal Gold Nanoparticles after Intravenous Administration: Effect of Particle Size. *Colloids Surfaces B Biointerfaces* **2008**, *66*, 274–280.
- (68) Kaga, S.; Truong, N. P.; Esser, L.; Senyschyn, D.; Sanyal, A.; Sanyal, R.; Quinn, J. F.; Davis, T. P.; Kaminskas, L. M.; Whittaker, M. R. Influence of Size and Shape on the Biodistribution of Nanoparticles Prepared by Polymerization-Induced Self-Assembly. *Biomacromolecules* **2017**, *18*, 3963–3970.
- (69) Moyer, T. J.; Zmolek, A. C.; Irvine, D. J. Beyond Antigens and Adjuvants: Formulating Future Vaccines. *J. Clin. Invest.* **2016**, *126*, 799–808.
- (70) Teleanu, D. M.; Chircov, C.; Grumezescu, A. M.; Volceanov, A.; Teleanu, R. I. Impact of Nanoparticles on Brain Health: An Up to Date Overview. *J. Clin. Med.* **2018**, *7*.
- (71) Ceña, V.; Játiva, P. Nanoparticle Crossing of Blood–Brain Barrier: A Road to New Therapeutic Approaches to Central Nervous System Diseases. *Nanomedicine* **2018**, *13*, 1513–1516.
- (72) Soo Choi, H.; Liu, W.; Misra, P.; Tanaka, E.; Zimmer, J. P.; Itty Ipe, B.; Bawendi, M. G.; Frangioni, J. V. Renal Clearance of Quantum Dots. *Nat. Biotechnol.* **2007**, *25*, 1165–1170.
- (73) Tsoi, K. M.; MacParland, S. A.; Ma, X.-Z.; Spetzler, V. N.; Echeverri, J.; Ouyang, B.; Fadel, S. M.; Sykes, E. A.; Goldaracena, N.; Kathis, J. M.; Conneely, J. B.; Alman, B. A.; Selzner, M.; Ostrowski, M. A.; Adeyi, O. A.; Zilman, A.; McGilvray, I. D.; Chan, W. C. W. Mechanism of Hard-Nanomaterial Clearance by the Liver. *Nat. Mater.* **2016**, *15*, 1212–1221.
- (74) Cheng, S.-H.; Li, F.-C.; Souris, J. S.; Yang, C.-S.; Tseng, F.-G.; Lee, H.-S.; Chen, C.-T.; Dong, C.-Y.; Lo, L.-W. Visualizing Dynamics of Sub-Hepatic Distribution of Nanoparticles Using Intravital Multiphoton

References

- Fluorescence Microscopy. *ACS Nano* **2012**, *6*, 4122–4131.
- (75) Li, Y.; Monteiro-Riviere, N. A. Mechanisms of Cell Uptake, Inflammatory Potential and Protein Corona Effects with Gold Nanoparticles. *Nanomedicine* **2016**, *11*, 3185–3203.
- (76) Zhang, S.; Gao, H.; Bao, G. Physical Principles of Nanoparticle Cellular Endocytosis. *ACS Nano* **2015**, *9*, 8655–8671.
- (77) Behzadi, S.; Serpooshan, V.; Tao, W.; Hamaly, M. A.; Alkawareek, M. Y.; Dreaden, E. C.; Brown, D.; Alkilany, A. M.; Farokhzad, O. C.; Mahmoudi, M. Cellular Uptake of Nanoparticles: Journey inside the Cell. *Chem. Soc. Rev.* **2017**, *46*, 4218–4244.
- (78) Sosale, N. G.; Spinler, K. R.; Alvey, C.; Discher, D. E. Macrophage Engulfment of a Cell or Nanoparticle Is Regulated by Unavoidable Opsonization, a Species-Specific “Marker of Self” CD47, and Target Physical Properties. *Curr. Opin. Immunol.* **2015**, *35*, 107–112.
- (79) Champion, J. A.; Walker, A.; Mitragotri, S. Role of Particle Size in Phagocytosis of Polymeric Microspheres. *Pharm. Res.* **2008**, *25*, 1815–1821.
- (80) Oh, N.; Park, J.-H. Endocytosis and Exocytosis of Nanoparticles in Mammalian Cells. *Int. J. Nanomedicine* **2014**, 51–63.
- (81) Dykman, L. A.; Khlebtsov, N. G. Immunological Properties of Gold Nanoparticles. *Chem. Sci.* **2017**, *8*, 1719–1735.
- (82) França, A.; Aggarwal, P.; Barsov, E. V.; Kozlov, S. V.; Dobrovolskaia, M. A.; González-Fernández, Á. Macrophage Scavenger Receptor A Mediates the Uptake of Gold Colloids by Macrophages in Vitro. *Nanomedicine (Lond)*. **2011**, *6*, 1175–1188.
- (83) Tsuji, T.; Yoshitomi, H.; Usukura, J. Endocytic Mechanism of Transferrin-Conjugated Nanoparticles and the Effects of Their Size and Ligand Number on the Efficiency of Drug Delivery. *Microscopy* **2013**, *62*, 341–352.
- (84) Hong, S.; Zhang, Z.; Liu, H.; Tian, M.; Zhu, X.; Zhang, Z.; Wang, W.; Zhou, X.; Zhang, F.; Ge, Q.; Zhu, B.; Tang, H.; Hua, Z.; Hou, B. B Cells Are the Dominant Antigen-Presenting Cells That Activate Naive CD4+ T Cells upon Immunization with a Virus-Derived Nanoparticle Antigen. *Immunity* **2018**, *49*, 1–14.
- (85) Martínez-Riaño, A.; Bovolenta, E. R.; Mendoza, P.; Oeste, C. L.; Martín-Bermejo, M. J.; Bovolenta, P.; Turner, M.; Martínez-Martín, N.; Alarcón, B. Antigen Phagocytosis by B Cells Is Required for a Potent Humoral Response. *EMBO Rep.* **2018**, *19*, e46016.
- (86) Stone, V.; Miller, M. R.; Clift, M. J. D.; Elder, A.; Mills, N. L.; Møller, P.; Schins, R. P. F.; Vogel, U.; Kreyling, W. G.; Alstrup Jensen, K.; Kuhlbusch, T. A. J.; Schwarze, P. E.; Hoet, P.; Pietroiusti, A.; De Vizcaya-Ruiz, A.; Baeza-Squiban, A.; Teixeira, J. P.; Tran, C. L.; Cassee, F. R. Nanomaterials Versus Ambient Ultrafine Particles: An Opportunity to Exchange Toxicology Knowledge. *Environ. Health Perspect.* **2017**, *125*, 106002.
- (87) Drinker, C. K.; Thomson, R. M.; Finn, J. L. Metal Fume Fever: IV. Threshold Doses of Zinc Oxide, Preventive Measures, and the Chronic Effects of Repeated Exposures. *J. Ind. Hyg.* **1927**, *9*, 331–345.
- (88) Oberdörster, G.; Stone, V.; Donaldson, K. Toxicology of Nanoparticles: A Historical Perspective. *Nanotoxicology* **2007**, *1*, 2–25.
- (89) Ferin, J.; Oberdörster, G.; Penney, D. P.; Soderholm, S. C.; Gelein, R.; Piper, H. C. Increased Pulmonary Toxicity of Ultrafine Particles? I. Particle Clearance, Translocation, Morphology. *J. Aerosol Sci.* **1990**, *21*, 381–384.
- (90) Oberdörster, G.; Ferin, J.; Gelein, R.; Soderholm, S. C.; Finkelstein, J. Role of the Alveolar Macrophage in Lung Injury: Studies with Ultrafine Particles. *Environ. Health Perspect.* **1992**, *97*, 193–199.
- (91) Donaldson, K.; Stone, V.; Tran, C. L.; Kreyling, W.; Borm, P. J. A. Nanotoxicology. *Occup. Environ. Med.* **2004**, *61*, 727–728.

References

- (92) Lynch, I.; Dawson, K. A. Protein-Nanoparticle Interactions. *Nano Today* **2008**, *3*, 40–47.
- (93) Manke, A.; Wang, L.; Rojanasakul, Y. Mechanisms of Nanoparticle-Induced Oxidative Stress and Toxicity. *Biomed Res. Int.* **2013**, *2013*, 942916.
- (94) Unfried, K.; Albrecht, C.; Klotz, L.; Von Mikecz, A.; Grether-Beck, S.; Schins, R. P. F. F. Cellular Responses to Nanoparticles: Target Structures and Mechanisms. *Nanotoxicology* **2007**, *1*, 52–71.
- (95) Sydlik, U.; Bierhals, K.; Soufi, M.; Abel, J.; Schins, R. P. F.; Unfried, K. Ultrafine Carbon Particles Induce Apoptosis and Proliferation in Rat Lung Epithelial Cells via Specific Signaling Pathways Both Using EGF-R. *Am. J. Physiol. Cell. Mol. Physiol.* **2006**, *291*, L725–L733.
- (96) Chen, L.; Liu, J.; Zhang, Y.; Zhang, G.; Kang, Y.; Chen, A.; Feng, X.; Shao, L. The Toxicity of Silica Nanoparticles to the Immune System. *Nanomedicine* **2018**, *13*, 1939–1962.
- (97) Brzicova, T.; Javorkova, E.; Vrbova, K.; Zajicova, A.; Holan, V.; Pinkas, D.; Philimonenko, V.; Sikorova, J.; Klema, J.; Topinka, J.; Rossner, P.; Jr. Molecular Responses in THP-1 Macrophage-Like Cells Exposed to Diverse Nanoparticles. *Nanomater. (Basel, Switzerland)* **2019**, *9*.
- (98) Hussain, S.; Vanoirbeek, J. A. J.; Hoet, P. H. M. Interactions of Nanomaterials with the Immune System. *Wiley Interdiscip. Rev. Nanomedicine Nanobiotechnology* **2012**, *4*, 169–183.
- (99) Park, E. J.; Cho, W. S.; Jeong, J.; Yi, J.; Choi, K.; Park, K. Pro-Inflammatory and Potential Allergic Responses Resulting from B Cell Activation in Mice Treated with Multi-Walled Carbon Nanotubes by Intratracheal Instillation. *Toxicology* **2009**, *259*, 113–121.
- (100) Mortimer, G. M.; Butcher, N. J.; Musumeci, A. W.; Deng, Z. J.; Martin, D. J.; Minchin, R. F. Cryptic Epitopes of Albumin Determine Mononuclear Phagocyte System Clearance of Nanomaterials. *ACS Nano* **2014**, *8*, 3357–3366.
- (101) Lavin, Y.; Mortha, A.; Rahman, A.; Merad, M. Regulation of Macrophage Development and Function in Peripheral Tissues. *Nat. Rev. Immunol.* **2015**, *15*, 731–744.
- (102) Embgenbroich, M.; Burgdorf, S. Current Concepts of Antigen Cross-Presentation. *Frontiers in Immunology*. Frontiers Media SA 2018, p 1643.
- (103) Lebien, T. W.; Tedder, T. F. ASH 50th Anniversary Review B Lymphocytes : How They Develop and Function. *Am. Soc. Hematol.* **2008**, *112*, 1570–1580.
- (104) Passey, S.; Pellegrin, S.; Mellor, H.; Passey, S.; Pellegrin, S.; Mellor, H. Scanning Electron Microscopy of Cell Surface Morphology. *Curr Protoc Cell Biol.* **2007**, *37*, 4.17.1-4.17.13.
- (105) Allman, D.; Pillai, S. Peripheral B Cell Subsets. *Curr. Opin. Immunol.* **2008**, *20*, 149–157.
- (106) Kurosaki, T.; Kometani, K.; Ise, W. Memory B Cells. In *Nature Reviews Immunology*; Nature Publishing Group, 2015; Vol. 15, pp 149–159.
- (107) Cerutti, A.; Cols, M.; Puga, I. Marginal Zone B Cells: Virtues of Innate-like Antibody-Producing Lymphocytes. *Nat. Rev. Immunol.* **2013**, *13*, 118–132.
- (108) Rodríguez-pinto, D. B Cells as Antigen Presenting Cells. *Cell Immunol.* **2006**, *238*, 67–75.
- (109) Yildirimer, L.; Thanh, N. T. K.; Loizidou, M.; Seifalian, A. M. Toxicological Considerations of Clinically Applicable Nanoparticles. *Nano Today* **2011**, *6*, 585–607.
- (110) Engin, A. B.; Hayes, A. W. The Impact of Immunotoxicity in Evaluation of the Nanomaterials Safety. *Toxicol. Res. Appl.* **2018**, *2*, 1–9.
- (111) Yazdi, A. S.; Guarda, G.; Riteau, N.; Drexler, S. K.; Tardivel, A.; Couillin, I.; Tschopp, J. Nanoparticles Activate the NLR Pyrin Domain Containing 3 (Nlrp3) Inflammasome and Cause Pulmonary Inflammation through Release of IL-1 α and IL-1 β . *Proc. Natl. Acad. Sci. U. S. A.* **2010**, *107*, 19449–19454.
- (112) Mukherjee, S. P.; Bondarenko, O.; Kohonen, P.; Andón, F. T.; Brzicová, T.; Gessner, I.; Mathur, S.; Bottini, M.; Calligari, P.; Stella, L.; Kisin, E.; Shvedova, A.; Autio, R.; Salminen-Mankonen, H.; Lahesmaa, R.; Fadeel,

References

- B. Macrophage Sensing of Single-Walled Carbon Nanotubes via Toll-like Receptors. *Sci. Rep.* **2018**, *8*, 1115.
- (113) Ma, J. S.; Kim, W. J.; Kim, J. J.; Kim, T. J.; Ye, S. K.; Song, M. D.; Kang, H.; Kim, D. W.; Moon, W. K.; Lee, K. H. Gold Nanoparticles Attenuate LPS-Induced NO Production through the Inhibition of NF- κ B and IFN- β /STAT1 Pathways in RAW264.7 Cells. *Nitric Oxide* **2010**, *23*, 214–219.
- (114) Chen, Y.-W.; Hwang, K. C.; Yen, C.-C.; Lai, Y.-L. Fullerene Derivatives Protect against Oxidative Stress in RAW 264.7 Cells and Ischemia-Reperfused Lungs. *Am. J. Physiol. Integr. Comp. Physiol.* **2004**, *287*, R21–R26.
- (115) Tsai, C.-Y.; Lu, S.-L.; Hu, C.-W.; Yeh, C.-S.; Lee, G.-B.; Lei, H.-Y. Size-Dependent Attenuation of TLR9 Signaling by Gold Nanoparticles in Macrophages. *J. Immunol.* **2011**, *188*, 68–76.
- (116) Ye, F.; Vallhov, H.; Qin, J.; Daskalaki, E.; Sugunan, A.; Toprak, M. S.; Fornara, A.; Gabrielsson, S.; Scheynius, A.; Muhammed, M. Synthesis of High Aspect Ratio Gold Nanorods and Their Effects on Human Antigen Presenting Dendritic Cells. *Int. J. Nanotechnol.* **2011**, *8*, 631.
- (117) Yen, H.-J.; Hsu, S.; Tsai, C.-L. Cytotoxicity and Immunological Response of Gold and Silver Nanoparticles of Different Sizes. *Small* **2009**, *5*, 1553–1561.
- (118) Fytianos, K.; Rodriguez-Lorenzo, L.; Clift, M. J. D.; Blank, F.; Vanhecke, D.; von Garnier, C.; Petri-Fink, A.; Rothen-Rutishauser, B. Uptake Efficiency of Surface Modified Gold Nanoparticles Does Not Correlate with Functional Changes and Cytokine Secretion in Human Dendritic Cells *In Vitro*. *Nanomedicine* **2015**, *11*, 633–644.
- (119) Cho, W.-S.; Cho, M.; Jeong, J.; Choi, M.; Cho, H.-Y.; Han, B. S.; Kim, S. H.; Kim, H. O.; Lim, Y. T.; Chung, B. H.; Jeong, J. Acute Toxicity and Pharmacokinetics of 13nm-Sized PEG-Coated Gold Nanoparticles. *Toxicol. Appl. Pharmacol.* **2009**, *236*, 16–24.
- (120) Zhu, M.-T.; Feng, W.-Y.; Wang, B.; Wang, T.-C.; Gu, Y.-Q.; Wang, M.; Wang, Y.; Ouyang, H.; Zhao, Y.-L.; Chai, Z.-F. Comparative Study of Pulmonary Responses to Nano- and Submicron-Sized Ferric Oxide in Rats. *Toxicology* **2008**, *247*, 102–111.
- (121) Yang, E.-J.; Kim, S.; Kim, J. S.; Choi, I.-H. Inflammasome Formation and IL-1 β Release by Human Blood Monocytes in Response to Silver Nanoparticles. *Biomaterials* **2012**, *33*, 6858–6867.
- (122) Galbiati, V.; Cornaghi, L.; Gianazza, E.; Potenza, M. A.; Donetti, E.; Marinovich, M.; Corsini, E. In Vitro Assessment of Silver Nanoparticles Immunotoxicity. *Food Chem. Toxicol.* **2018**, *112*, 363–374.
- (123) Kim, C. S.; Nguyen, H. D.; Ignacio, R. M.; Kim, J. H.; Cho, H. C.; Maeng, E. H.; Kim, Y. R.; Kim, M. K.; Park, B. K.; Kim, S. K. Immunotoxicity of Zinc Oxide Nanoparticles with Different Size and Electrostatic Charge. *Int. J. Nanomedicine* **2014**, *9*, 195–205.
- (124) Dhupal, M.; Oh, J.-M.; Tripathy, D. R.; Kim, S.-K.; Koh, S. B.; Park, K.-S. Immunotoxicity of Titanium Dioxide Nanoparticles via Simultaneous Induction of Apoptosis and Multiple Toll-like Receptors Signaling through ROS-Dependent SAPK/JNK and P38 MAPK Activation. *Int. J. Nanomedicine* **2018**, *13*, 6735–6750.
- (125) Sohaebuddin, S. K.; Thevenot, P. T.; Baker, D.; Eaton, J. W.; Tang, L. Nanomaterial Cytotoxicity Is Composition, Size, and Cell Type Dependent. *Part. Fibre Toxicol.* **2010**, *7*, 22.
- (126) Chou, C.-C.; Chen, W.; Hung, Y.; Mou, C.-Y. Molecular Elucidation of Biological Response to Mesoporous Silica Nanoparticles in Vitro and in Vivo. *ACS Appl. Mater. Interfaces* **2017**, *9*, 22235–22251.
- (127) Leclerc, L.; Rima, W.; Boudard, D.; Pourchez, J.; Forest, V.; Bin, V.; Mowat, P.; Perriat, P.; Tillement, O.; Grosseau, P.; Bernache-Assollant, D.; Cottier, M. Size of Submicrometric and Nanometric Particles Affect Cellular Uptake and Biological Activity of Macrophages in Vitro. *Inhal. Toxicol.* **2012**, *24*, 580–588.
- (128) Liu, Y.; Chen, X.; Wang, L.; Yang, T.; Yuan, Q.; Ma, G. Surface Charge of PLA Microparticles in Regulation of Antigen Loading, Macrophage Phagocytosis and Activation, and Immune Effects in Vitro. *Particuology* **2014**, *17*, 74–80.
- (129) Barillet, S.; Fattal, E.; Mura, S.; Tsapis, N.; Pallardy, M.; Hillaireau, H.; Kerdine-Römer, S. Immunotoxicity

References

- of Poly (Lactic-Co-Glycolic Acid) Nanoparticles: Influence of Surface Properties on Dendritic Cell Activation. *Nanotoxicology* **2019**, *13*, 606–622.
- (130) Smith, D. M.; Simon, J. K.; Baker, J. R. Applications of Nanotechnology for Immunology. *Nat. Rev. Immunol.* **2013**, *13*, 592–605.
- (131) Luo, Y.-H.; Chang, L. W.; Lin, P. Metal-Based Nanoparticles and the Immune System: Activation, Inflammation, and Potential Applications. *Biomed Res. Int.* **2015**, *2015*, 1–12.
- (132) Hendrickson, O.; Fedyunina, N.; Zherdev, A.; Solopova, O.; Sveshnikov, P.; Dzantiev, B. Production of Monoclonal Antibodies against Fullerene C 60 and Development of a Fullerene Enzyme Immunoassay. *Analyst* **2012**, *137*, 98–105.
- (133) Lee, S. C.; Parthasarathy, R.; Duffin, T. D.; Botwin, K.; Zobel, J.; Beck, T.; Lange, G.; Kunneman, D.; Janssen, R.; Rowold, E.; Voliva, C. F. Recognition Properties of Antibodies to PAMAM Dendrimers and Their Use in Immune Detection of Dendrimers. *Biomed. Microdevices* **2001**, *3*, 53–59.
- (134) Zhao, L.; Seth, A.; Wibowo, N.; Zhao, C. X.; Mitter, N.; Yu, C.; Middelberg, A. P. J. Nanoparticle Vaccines. *Vaccine* **2014**, *32*, 327–337.
- (135) Garay, R. P.; El-Gewely, R.; Armstrong, J. K.; Garratty, G.; Richette, P. Antibodies against Polyethylene Glycol in Healthy Subjects and in Patients Treated with PEG-Conjugated Agents. *Expert Opin. Drug Deliv.* **2012**, *9*, 1319–1323.
- (136) Shimizu, T.; Mima, Y.; Hashimoto, Y.; Ukawa, M.; Ando, H.; Kiwada, H.; Ishida, T. Anti-PEG IgM and Complement System Are Required for the Association of Second Doses of PEGylated Liposomes with Splenic Marginal Zone B Cells. *Immunobiology* **2015**, *220*, 1151–1160.
- (137) Sharma, M.; Salisbury, R. L.; Maurer, E. I.; Hussain, S. M.; Sulentic, C. E. W. Gold Nanoparticles Induce Transcriptional Activity of NF- κ B in a B-Lymphocyte Cell Line. *Nanoscale* **2013**, *5*, 3747–3756.
- (138) Lee, C.-H.; Syu, S.-H.; Chen, Y.-S.; Hussain, S. M.; Aleksandrovich Onischuk, A.; Chen, W. L.; Steven Huang, G. Gold Nanoparticles Regulate the Blimp1/Pax5 Pathway and Enhance Antibody Secretion in B-Cells. *Nanotechnology* **2014**, *25*, 125103.
- (139) Dutt, T. S.; Mia, M. B.; Saxena, R. K. Elevated Internalization and Cytotoxicity of Polydispersed Single-Walled Carbon Nanotubes in Activated B Cells Can Be Basis for Preferential Depletion of Activated B Cells in Vivo. *Nanotoxicology* **2019**, *13*, 849–860.
- (140) Kasturi, S. P.; Kozlowski, P. A.; Nakaya, H. I.; Burger, M. C.; Russo, P.; Pham, M.; Kovalenkov, Y.; Silveira, E. L. V.; Havenar-Daughton, C.; Burton, S. L.; Kilgore, K. M.; Johnson, M. J.; Nabi, R.; Legere, T.; Sher, Z. J.; Chen, X.; Amara, R. R.; Hunter, E.; Bosinger, S. E.; et al. Adjuvanting a Simian Immunodeficiency Virus Vaccine with Toll-Like Receptor Ligands Encapsulated in Nanoparticles Induces Persistent Antibody Responses and Enhanced Protection in TRIM5 α Restrictive Macaques. *J. Virol.* **2017**, *91*, 1844–1860.
- (141) Chakravarty, P.; Qian, W.; El-Sayed, M. A.; Prausnitz, M. R. Delivery of Molecules into Cells Using Carbon Nanoparticles Activated by Femtosecond Laser Pulses. *Nat. Nanotechnol.* **2010**, *5*, 607–611.
- (142) Birrenbach, S. Polymerized Micelles and Their Use as Adjuvants in Immunology. *J. Pharm. Sci.* **1976**, *65*, 1763–1966.
- (143) Noad, R.; Roy, P. Virus-like Particles as Immunogens. *Trends Microbiol.* **2003**, *11*, 438–444.
- (144) Iyer, S. S.; Gangadhara, S.; Victor, B.; Shen, X.; Chen, X.; Nabi, R.; Kasturi, S. P.; Sabula, M. J.; Labranche, C. C.; Reddy, P. B. J.; Tomaras, G. D.; Montefiori, D. C.; Moss, B.; Spearman, P.; Pulendran, B.; Kozlowski, P. A.; Amara, R. R. Virus-Like Particles Displaying Trimeric Simian Immunodeficiency Virus (SIV) Envelope Gp160 Enhance the Breadth of DNA/Modified Vaccinia Virus Ankara SIV Vaccine-Induced Antibody Responses in Rhesus Macaques. *J. Virol.* **2016**, *90*, 8842–8854.
- (145) Marcandalli, J.; Fiala, B.; Ols, S.; Perotti, M.; de van der Schueren, W.; Snijder, J.; Hodge, E.; Benhaim, M.; Ravichandran, R.; Carter, L.; Sheffler, W.; Brunner, L.; Lawrenz, M.; Dubois, P.; Lanzavecchia, A.; Sallusto, F.; Lee, K. K.; Veessler, D.; Correnti, C. E.; et al. Induction of Potent Neutralizing Antibody Responses by a

References

- Designed Protein Nanoparticle Vaccine for Respiratory Syncytial Virus. *Cell* **2019**, *176*, 1420-1431.e17.
- (146) Gause, K. T.; Wheatley, A. K.; Cui, J.; Yan, Y.; Kent, S. J.; Caruso, F. Immunological Principles Guiding the Rational Design of Particles for Vaccine Delivery. *ACS Nano* **2017**, *11*, 54–68.
- (147) Huang, W.-C.; Deng, B.; Lin, C.; Carter, K. A.; Geng, J.; Razi, A.; He, X.; Chitgupi, U.; Federizon, J.; Sun, B.; Long, C. A.; Ortega, J.; Dutta, S.; King, C. R.; Miura, K.; Lee, S.-M.; Lovell, J. F. A Malaria Vaccine Adjuvant Based on Recombinant Antigen Binding to Liposomes. *Nat. Nanotechnol.* **2018**, *13*, 1174–1181.
- (148) Shae, D.; Becker, K. W.; Christov, P.; Yun, D. S.; Lytton-Jean, A. K. R.; Sevimli, S.; Ascano, M.; Kelley, M.; Johnson, D. B.; Balko, J. M.; Wilson, J. T. Endosomolytic Polymersomes Increase the Activity of Cyclic Dinucleotide STING Agonists to Enhance Cancer Immunotherapy. *Nat. Nanotechnol.* **2019**, *14*, 269–278.
- (149) Smith, J. D.; Morton, L. D.; Ulery, B. D. Nanoparticles as Synthetic Vaccines. *Curr. Opin. Biotechnol.* **2015**, *34*, 217–224.
- (150) Zilker, C.; Kozlova, D.; Sokolova, V.; Yan, H.; Epple, M.; Überla, K.; Temchura, V. Nanoparticle-Based B-Cell Targeting Vaccines: Tailoring of Humoral Immune Responses by Functionalization with Different TLR-Ligands. *Nanomedicine* **2017**, *13*, 173–182.
- (151) Pardi, N.; Hogan, M. J.; Naradikian, M. S.; Parkhouse, K.; Cain, D. W.; Jones, L.; Moody, M. A.; Verkerke, H. P.; Myles, A.; Willis, E.; LaBranche, C. C.; Montefiori, D. C.; Lobby, J. L.; Saunders, K. O.; Liao, H.-X.; Korber, B. T.; Sutherland, L. L.; Scearce, R. M.; Hraber, P. T.; et al. Nucleoside-Modified mRNA Vaccines Induce Potent T Follicular Helper and Germinal Center B Cell Responses. *J. Exp. Med.* **2018**, *215*, 1571–1588.
- (152) Rappuoli, R.; Serruto, D. Self-Assembling Nanoparticles Usher in a New Era of Vaccine Design. *Cell.* **2019**, *176*, 1245–1247.
- (153) Belogurov, A. A.; Stepanov, A. V.; Smirnov, I. V.; Melamed, D.; Bacon, A.; Mamedov, A. E.; Boitsov, V. M.; Sashchenko, L. P.; Ponomarenko, N. A.; Sharanova, S. N.; Boyko, A. N.; Dubina, M. V.; Friboulet, A.; Genkin, D. D.; Gabibov, A. G. Liposome-Encapsulated Peptides Protect against Experimental Allergic Encephalitis. *FASEB J.* **2013**, *27*, 222–231.
- (154) Pozsgay, J.; Babos, F.; Uray, K.; Magyar, A.; Gyulai, G.; Kiss, É.; Nagy, G.; Rojkovich, B.; Hudecz, F.; Sármay, G. In Vitro Eradication of Citrullinated Protein Specific B-Lymphocytes of Rheumatoid Arthritis Patients by Targeted Bifunctional Nanoparticles. *Arthritis Res. Ther.* **2016**, *18*, 15.
- (155) Smith, M. R. Rituximab (Monoclonal Anti-CD20 Antibody): Mechanisms of Action and Resistance. *Oncogene* **2003**, *22*, 7359–7368.
- (156) Zhou, S.; Wu, D.; Yin, X.; Jin, X.; Zhang, X.; Zheng, S.; Wang, C.; Liu, Y. Intracellular PH-Responsive and Rituximab-Conjugated Mesoporous Silica Nanoparticles for Targeted Drug Delivery to Lymphoma B Cells. *J. Exp. Clin. Cancer Res.* **2017**, *36*, 1–14.
- (157) Capolla, S.; Garrovo, C.; Zorzet, S.; Lorenzon, A.; Rampazzo, E.; Spretz, R.; Pozzato, G.; Núñez, L.; Tripodo, C.; Macor, P.; Biffi, S. Targeted Tumor Imaging of Anti-CD20-Polymeric Nanoparticles Developed for the Diagnosis of B-Cell Malignancies. *Int. J. Nanomedicine* **2015**, *10*, 4099–4109.
- (158) Dykman, L.; Khlebtsov, N. Gold Nanoparticles in Biomedical Applications: Recent Advances and Perspectives. *Chem. Soc. Rev.* **2012**, *41*, 2256–2282.
- (159) Turkevich, J.; Stevenson, P. C.; Hillier, J. A Study of the Nucleation and Growth Processes in the Synthesis of Colloidal Gold. *Discuss. Faraday Soc.* **1951**, *11*, 55.
- (160) Frens, G. Controlled Nucleation for the Regulation of the Particle Size in Monodisperse Gold Suspensions. *Nat. Phys. Sci.* **1973**, *241*, 20–22.
- (161) Hočevár, S.; Milošević, A.; Rodríguez-Lorenzo, L.; Ackermann-Hirschi, L.; Mottas, I.; Petri-Fink, A.; Rothen-Rutishauser, B.; Bourquin, C.; Clift, M. J. D. Polymer-Coated Gold Nanospheres Do Not Impair the Innate Immune Function of Human B Lymphocytes in Vitro. *ACS Nano* **2019**, *13*, 6790–6800.
- (162) Huang, X.; El-Sayed, M. A. Plasmonic Photo-Thermal Therapy (PPTT). *Alexandria J. Med.* **2011**, *47*, 1–9.

References

- (163) Sina, A. A. I.; Carrascosa, L. G.; Liang, Z.; Grewal, Y. S.; Wardiana, A.; Shiddiky, M. J. A.; Gardiner, R. A.; Samaratunga, H.; Gandhi, M. K.; Scott, R. J.; Korbie, D.; Trau, M. Epigenetically Reprogrammed Methylation Landscape Drives the DNA Self-Assembly and Serves as a Universal Cancer Biomarker. *Nat. Commun.* **2018**, *9*, 4915.
- (164) Peng, C.; Qin, J.; Zhou, B.; Chen, Q.; Shen, M.; Zhu, M.; Lu, X.; Shi, X. Targeted Tumor CT Imaging Using Folic Acid-Modified PEGylated Dendrimer-Entrapped Gold Nanoparticles. *Polym. Chem.* **2013**, *4*, 4412–4424.
- (165) Saha, S.; Xiong, X.; Chakraborty, P. K.; Shameer, K.; Arvizo, R. R.; Kudgus, R. A.; Dwivedi, S. K. D.; Hossen, M. N.; Gillies, E. M.; Robertson, J. D.; Dudley, J. T.; Urrutia, R. A.; Postier, R. G.; Bhattacharya, R.; Mukherjee, P. Gold Nanoparticle Reprograms Pancreatic Tumor Microenvironment and Inhibits Tumor Growth. *ACS Nano* **2016**, *10*, 10636–10651.
- (166) Libutti, S. K.; Paciotti, G. F.; Byrnes, A. A.; Richard Alexander Jr, H.; Gannon, W. E.; Walker, M.; Seidel, G. D.; Yuldasheva, N.; Tamarkin, L. Phase I and Pharmacokinetic Studies of CYT-6091, a Novel PEGylated Colloidal Gold-RhTNF Nanomedicine Translational Relevance. *Clin Cancer Res. Clin Cancer Res. December* **2010**, *15*, 6139–6149.
- (167) Jensen, S. A.; Day, E. S.; Ko, C. H.; Hurley, L. A.; Luciano, J. P.; Kouri, F. M.; Merkel, T. J.; Luthi, A. J.; Patel, P. C.; Cutler, J. I.; Daniel, W. L.; Scott, A. W.; Rotz, M. W.; Meade, T. J.; Giljohann, D. A.; Mirkin, C. A.; Stegh, A. H. Spherical Nucleic Acid Nanoparticle Conjugates as an RNAi-Based Therapy for Glioblastoma. *Sci. Transl. Med.* **2013**, *5*, 209ra152.
- (168) Robinson, W. H. Sequencing the Functional Antibody Repertoire—Diagnostic and Therapeutic Discovery. *Nat. Rev. Rheumatol.* **2015**, *11*, 171–182.
- (169) Mottas, I.; Bekdemir, A.; Cereghetti, A.; Spagnuolo, L.; Yang, Y.-S. S.; Müller, M.; Irvine, D. J.; Stellacci, F.; Bourquin, C. Amphiphilic Nanoparticle Delivery Enhances the Anticancer Efficacy of a TLR7 Ligand via Local Immune Activation. *Biomaterials* **2018**, *190*, 111–120.
- (170) Dykman, L. A.; Staroverov, S. A.; Fomin, A. S.; Khanadeev, V. A.; Khlebtsov, B. N.; Bogatyrev, V. A. Gold Nanoparticles as an Adjuvant: Influence of Size, Shape, and Technique of Combination with CpG on Antibody Production. *Int. Immunopharmacol.* **2018**, *54*, 163–168.
- (171) Assis, N. R. G.; Caires, A. J.; Figueiredo, B. C.; Morais, S. B.; Mambelli, F. S.; Marinho, F. V.; Ladeira, L. O.; Oliveira, S. C. The Use of Gold Nanorods as a New Vaccine Platform against Schistosomiasis. *J. Control. Release* **2018**, *275*, 40–52.
- (172) Xu, L.; Liu, Y.; Chen, Z.; Li, W.; Liu, Y.; Wang, L.; Liu, Y.; Wu, X.; Ji, Y.; Zhao, Y.; Ma, L.; Shao, Y.; Chen, C. Surface-Engineered Gold Nanorods: Promising DNA Vaccine Adjuvant for HIV-1 Treatment. *Nano Lett.* **2012**, *12*, 2003–2012.
- (173) Gold for Rheumatoid Arthritis. *Br. Med. J.* **1971**, *1*, 471–472.
- (174) Kirdaite, G.; Leonaviciene, L.; Bradunaite, R.; Vasiliauskas, A.; Rudys, R.; Ramanaviciene, A.; Mackiewicz, Z. Antioxidant Effects of Gold Nanoparticles on Early Stage of Collagen-Induced Arthritis in Rats. *Res. Vet. Sci.* **2019**, *124*, 32–37.
- (175) Abraham, G. E.; Himmel, P. B. Management of Rheumatoid Arthritis: Rationale for the Use of Colloidal Metallic Gold. *J. Nutr. Environ. Med.* **1997**, *7*, 295–305.
- (176) Colloidal Gold - MesoGold™ <https://www.purestcolloids.com/mesogold.php> (accessed Jun 16, 2019).
- (177) Clene Nanomedicine <http://www.clene.com/targets.html> (accessed Jun 16, 2019).
- (178) Alkilany, A. M.; Murphy, C. J. Toxicity and Cellular Uptake of Gold Nanoparticles: What We Have Learned so Far? *J. Nanoparticle Res.* **2010**, *12*, 2313–2333.
- (179) Khlebtsov, N.; Dykman, L. Biodistribution and Toxicity of Engineered Gold Nanoparticles: A Review of in Vitro and in Vivo Studies. *Chem. Soc. Rev.* **2011**, *40*, 1647–1671.
- (180) Moore, T. L.; Rodriguez-Lorenzo, L.; Hirsch, V.; Balog, S.; Urban, D.; Jud, C.; Rothen-Rutishauser, B.;

References

- Lattuada, M.; Petri-Fink, A. Nanoparticle Colloidal Stability in Cell Culture Media and Impact on Cellular Interactions. *Chem. Soc. Rev.* **2015**, *44*, 6287–6305.
- (181) Oh, N.; Park, J.-H. Surface Chemistry of Gold Nanoparticles Mediates Their Exocytosis in Macrophages. *ACS Nano* **2014**, *8*, 6232–6241.
- (182) Yang, J. P.; Merin, J. P.; Nakano, T.; Kato, T.; Kitade, Y.; Okamoto, T. Inhibition of the DNA-Binding Activity of NF-Kappa B by Gold Compounds in Vitro. *FEBS Lett.* **1995**, *361*, 89–96.
- (183) Sul, O.-J.; Kim, J.-C.; Kyung, T.-W.; Kim, H.-J.; Kim, Y.-Y.; Kim, S.-H.; Kim, J.-S.; Choi, H.-S. Gold Nanoparticles Inhibited the Receptor Activator of Nuclear Factor-B Ligand (RANKL)-Induced Osteoclast Formation by Acting as an Antioxidant. *Biosci Biotechnol Biochem* **2010**, *74*, 2209–2213.
- (184) Jeon, K.-I.; Jeong, J.-Y.; Jue, D.-M. Thiol-Reactive Metal Compounds Inhibit NF-KB Activation by Blocking Ikb Kinase. *J Immunol Ref.* **2000**, *164*, 5981–5989.
- (185) Devanabanda, M.; Latheef, S. A.; Madduri, R. Immunotoxic Effects of Gold and Silver Nanoparticles: Inhibition of Mitogen-Induced Proliferative Responses and Viability of Human and Murine Lymphocytes in Vitro. *J. Immunotoxicol.* **2016**, *13*, 897–902.
- (186) Almeida, J. P. M.; Lin, A. Y.; Langsner, R. J.; Eckels, P.; Foster, A. E.; Drezek, R. A. In Vivo Immune Cell Distribution of Gold Nanoparticles in Naïve and Tumor Bearing Mice. *Small* **2014**, *10*, 812–819.
- (187) Goel, R.; Shah, N.; Visaria, R.; Paciotti, G. F.; Bischof, J. C. Biodistribution of TNF-Alpha-Coated Gold Nanoparticles in an in Vivo Model System. *Nanomedicine (Lond).* **2009**, *4*, 401–410.
- (188) Naz, F.; Koul, V.; Srivastava, A.; Gupta, Y. K.; Dinda, A. K. Biokinetics of Ultrafine Gold Nanoparticles (AuNPs) Relating to Redistribution and Urinary Excretion: A Long-Term in Vivo Study. *J. Drug Target.* **2016**, *24*, 720–729.
- (189) Fraga, S.; Brandão, A.; Soares, M. E.; Morais, T.; Duarte, J. A.; Pereira, L.; Soares, L.; Neves, C.; Pereira, E.; Bastos, M. de L.; Carmo, H. Short- and Long-Term Distribution and Toxicity of Gold Nanoparticles in the Rat after a Single-Dose Intravenous Administration. *Nanomedicine Nanotechnology, Biol. Med.* **2014**, *10*, 1757–1766.
- (190) Bahamonde, J.; Brenseke, B.; Chan, M. Y.; Kent, R. D.; Vikesland, P. J.; Prater, M. R. Gold Nanoparticle Toxicity in Mice and Rats: Species Differences. *Toxicol. Pathol.* **2018**, *46*, 431–443.
- (191) Małaczewska, J. Effect of Oral Administration of Commercial Gold Nanocolloid on Peripheral Blood Leukocytes in Mice. *Pol. J. Vet. Sci.* **2015**, *18*, 273–282.
- (192) Sadauskas, E.; Wallin, H.; Stoltenberg, M.; Vogel, U.; Doering, P.; Larsen, A.; Danscher, G. Kupffer Cells Are Central in the Removal of Nanoparticles from the Organism. *Part. Fibre Toxicol.* **2007**, *4*, 10.
- (193) Pillai, S.; Cariappa, A. The Follicular versus Marginal Zone B Lymphocyte Cell Fate Decision. *Nat. Rev. Immunol.* **2009**, *9*, 767–777.
- (194) Walkey, C. D.; Olsen, J. B.; Song, F.; Liu, R.; Guo, H.; Olsen, D. W. H.; Cohen, Y.; Emili, A.; Chan, W. C. W. Protein Corona Fingerprinting Predicts the Cellular Interaction of Gold and Silver Nanoparticles. *ACS Nano* **2014**, *8*, 2439–2455.
- (195) Patil, S.; Sandberg, A.; Heckert, E.; Self, W.; Seal, S. Protein Adsorption and Cellular Uptake of Cerium Oxide Nanoparticles as a Function of Zeta Potential. *Biomaterials* **2007**, *28*, 4600–4607.
- (196) Yang, H.; Chen, Z.; Zhang, L.; Yung, W.-Y.; Leung, K. C.-F.; Chan, H. Y. E.; Choi, C. H. J. Mechanism for the Cellular Uptake of Targeted Gold Nanorods of Defined Aspect Ratios. *Small* **2016**, *12*, 5178–5189.
- (197) Shukla, R.; Bansal, V.; Chaudhary, M.; Basu, A.; Bhonde, R. R.; Sastry, M. Biocompatibility of Gold Nanoparticles and Their Endocytotic Fate Inside the Cellular Compartment: A Microscopic Overview. *Langmuir* **2005**, *21*, 10644–10654.
- (198) Bastús, N. G.; Sánchez-Tilló, E.; Pujals, S.; Farrera, C.; López, C.; Giral, E.; Celada, A.; Lloberas, J.; Puntès, V. Homogeneous Conjugation of Peptides onto Gold Nanoparticles Enhances Macrophage Response. *ACS*

References

- Nano* **2009**, *3*, 1335–1344.
- (199) Bastús, N. G.; Sánchez-Tilló, E.; Pujals, S.; Farrera, C.; Kogan, M. J.; Giralte, E.; Celada, A.; Lloberas, J.; Puentes, V. Peptides Conjugated to Gold Nanoparticles Induce Macrophage Activation. *Mol. Immunol.* **2009**, *46*, 743–748.
- (200) Pereira, D. V.; Petronilho, F.; Pereira, H. R. S. B.; Vuolo, F.; Mina, F.; Possato, J. C.; Vitto, M. F.; de Souza, D. R.; da Silva, L.; da Silva Paula, M. M.; de Souza, C. T.; Dal-Pizzol, F. Effects of Gold Nanoparticles on Endotoxin-Induced Uveitis in Rats. *Investig. Ophthalmology Vis. Sci.* **2012**, *53*, 8036.
- (201) Yang, H.; Kozicky, L.; Saferali, A.; Fung, S.-Y.; Afacan, N.; Cai, B.; Falsafi, R.; Gill, E.; Liu, M.; Kollmann, T. R.; Hancock, R. E. W.; Sly, L. M.; Turvey, S. E. Endosomal pH Modulation by Peptide-Gold Nanoparticle Hybrids Enables Potent Anti-Inflammatory Activity in Phagocytic Immune Cells. *Biomaterials* **2016**, *111*, 90–102.
- (202) Foit, L.; Thaxton, C. S. Synthetic High-Density Lipoprotein-like Nanoparticles Potently Inhibit Cell Signaling and Production of Inflammatory Mediators Induced by Lipopolysaccharide Binding Toll-like Receptor 4. *Biomaterials* **2016**, *100*, 67–75.
- (203) Genestier, L.; Taillardet, M.; Mondiere, P.; Gheit, H.; Bella, C.; Defrance, T. TLR Agonists Selectively Promote Terminal Plasma Cell Differentiation of B Cell Subsets Specialized in Thymus-Independent Responses. *J. Immunol.* **2007**, *178*, 7779–7786.
- (204) Bishop, G. A.; Ramirez, L. M.; Baccam, M.; Busch, L. K.; Pederson, L. K.; Tomai, M. A. The Immune Response Modifier Resiquimod Mimics CD40-Induced B Cell Activation. *Cell Immunol.* **2001**, *208*, 9–17.
- (205) Salisbury, R. L.; Sulentic, C. E. W. The AhR and NF- κ B/Rel Proteins Mediate the Inhibitory Effect of 2,3,7,8-Tetrachlorodibenzo-p-Dioxin on the 3' Immunoglobulin Heavy Chain Regulatory Region. *Toxicol. Sci.* **2015**, *148*, 443.
- (206) Sen, R.; Baltimore, D. Multiple Nuclear Factors Interact with the Immunoglobulin Enhancer Sequences. *Cell* **1986**, *46*, 705–716.
- (207) Nickerson, K. M.; Christensen, S. R.; Shupe, J.; Kashgarian, M.; Kim, D.; Elkon, K.; Shlomchik, M. J. TLR9 Regulates TLR7- and MyD88-Dependent Autoantibody Production and Disease in a Murine Model of Lupus. *J. Immunol.* **2010**, *184*, 1840–1848.
- (208) Gao, W.; Xiong, Y.; Li, Q.; Yang, H. Inhibition of Toll-Like Receptor Signaling as a Promising Therapy for Inflammatory Diseases: A Journey from Molecular to Nano Therapeutics. *Front. Physiol.* **2017**, *8*, 508.
- (209) Hirohata, S.; Nakanishi, K.; Yanagida, T.; Kawai, M.; Kikuchi, H.; Isshi, K. Synergistic Inhibition of Human B Cell Activation by Gold Sodium Thiomalate and Auranofin. *Clin. Immunol.* **1999**, *91*, 226–233.
- (210) Yang, W.; Liu, S.; Bai, T.; Keefe, A. J.; Zhang, L.; Ella-Menye, J.-R.; Li, Y.; Jiang, S. Poly(Carboxybetaine) Nanomaterials Enable Long Circulation and Prevent Polymer-Specific Antibody Production. *Nano Today* **2014**, *9*, 10–16.
- (211) Zhao, J.; Qin, Z.; Wu, J.; Li, L.; Jin, Q.; Ji, J. Zwitterionic Stealth Peptide-Protected Gold Nanoparticles Enable Long Circulation without the Accelerated Blood Clearance Phenomenon. *Biomater. Sci.* **2018**, *6*, 200–206.
- (212) Wiesner, M.; Zentz, C.; Mayr, C.; Wimmer, R.; Hammerschmidt, W.; Zeidler, R.; Moosmann, A. Conditional Immortalization of Human B Cells by CD40 Ligation. *PLoS One* **2008**, *3*, e1464.
- (213) Guengerich, F. P. Mechanisms of Drug Toxicity and Relevance to Pharmaceutical Development. *Drug Metab. Pharmacokinet.* **2011**, *26*, 3–14.
- (214) Purwada, A.; Jaiswal, M. K.; Ahn, H.; Nojima, T.; Kitamura, D.; Gaharwar, A. K.; Cerchietti, L.; Singh, A. Ex Vivo Engineered Immune Organoids for Controlled Germinal Center Reactions. *Biomaterials* **2015**, *63*, 24–34.
- (215) Shanti, A.; Teo, J.; Stefanini, C. In Vitro Immune Organs-on-Chip for Drug Development: A Review. *Pharmaceutics* **2018**, *10*, 278.

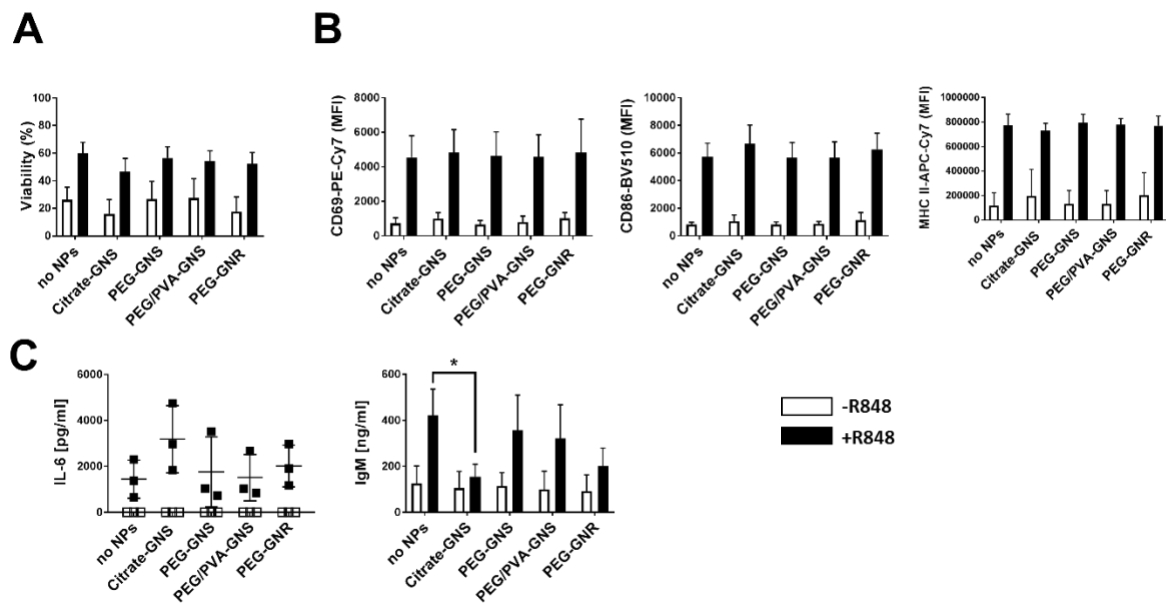
References

- (216) Mitra, B.; Jindal, R.; Lee, S.; Xu Dong, D.; Li, L.; Sharma, N.; Maguire, T.; Schloss, R.; Yarmush, M. L. Microdevice Integrating Innate and Adaptive Immune Responses Associated with Antigen Presentation by Dendritic Cells. *RSC Adv.* **2013**, *3*, 16002–16010.
- (217) McCormick, S.; Kriel, F.; Ivask, A.; Tong, Z.; Lombi, E.; Voelcker, N.; Priest, C. The Use of Microfluidics in Cytotoxicity and Nanotoxicity Experiments. *Micromachines* **2017**, *8*, 124.
- (218) Allen, T. M.; Brehm, M. A.; Bridges, S.; Ferguson, S.; Kumar, P.; Mirochnitchenko, O.; Palucka, K.; Pelanda, R.; Sanders-Bear, B.; Shultz, L. D.; Su, L.; PrabhuDas, M. Humanized Immune System Mouse Models: Progress, Challenges and Opportunities. *Nat. Immunol.* **2019**, *20*, 770–774.
- (219) Robbins, G. R.; Roberts, R. A.; Guo, H.; Reuter, K.; Shen, T.; Sempowski, G. D.; McKinnon, K. P.; Su, L.; DeSimone, J. M.; Ting, J. P.-Y. Analysis of Human Innate Immune Responses to PRINT Fabricated Nanoparticles with Cross Validation Using a Humanized Mouse Model. *Nanomedicine* **2015**, *11*, 589–599.
- (220) FDA. Estimating the Maximum Safe Starting Dose in Initial Clinical Trials for Therapeutics in Adult Healthy Volunteers <https://www.fda.gov/regulatory-information/search-fda-guidance-documents/estimating-maximum-safe-starting-dose-initial-clinical-trials-therapeutics-adult-healthy-volunteers> (accessed Oct 13, 2019).
- (221) Nair, A. B.; Jacob, S. A Simple Practice Guide for Dose Conversion between Animals and Human. *J. basic Clin. Pharm.* **2016**, *7*, 27–31.

APPENDICES

1. Appendix 1: Overview of the results obtained by a master student

Millie Porzi was a master student who carried out a series of *in vitro* experiments under my supervision and successfully completed and defended her master thesis. The project focused on the investigation of the impact of the set of physico-chemical different GNPs on primary mouse B cells *in vitro*. A detailed description of the results and discussion of this part of the project is presented in her master thesis titled: Interactions of gold nanoparticles with mouse B cells *in vitro*, University of Geneva, 2017.



Appendix 1: Isolated mouse splenic B cells *in vitro*, exposed to 20 $\mu\text{g/ml}$ GNPs (Citrate-GNS, PEG-GNS, PEG/PVA, PEG-GNR) for 24 h, with or without TLR7 stimulant (R848, 2 $\mu\text{g/ml}$). B cell viability **A**) and expression of immune activation markers (CD69, CD86, MHC II) **B**). Secretion of IL-6 and total IgM **C**). Cell viability was determined by staining with Zombie viability dye (Biolegend) and measured by flow cytometry. Surface activation markers were measured by flow cytometry. IL-6 was measured by ELISA kit (Biolegend) and IgM by ELISA, following in-house protocol (described in the method part of the manuscript 2 of the current thesis). All the graphs are presented as a mean of at least three separate biological experiments. Error bars: mean \pm SD; * $p < 0.05$. Data were evaluated by two-way ANOVA, followed by Tukey's multiple comparisons posthoc test.

CURRICULUM VITAE



Name: **Sandra Hočevar**
Address: Rue Vignier 8, 1205 Geneva, Switzerland
Date of birth: 07.12.1988
Tel.: +41(0)78 628 60 96
E-mail: sandra.hocevar@gmail.com

Education

- 01.05.2015-ongoing **PhD candidate in Pharmaceutical Sciences**, University of Geneva and Adolphe Merkle Institute/University of Fribourg, Switzerland
Topic: *Interactions of gold nanoparticles with B lymphocytes in vitro and in vivo*
Supervisors: Prof. Dr. Carole Bourquin, MD and Prof. Dr. Martin Clift
- 17.06.2014 **MSc in Molecular biology**, University of Ljubljana, Slovenia and University of Portsmouth, UK
Topic: *Isolation and characterization of pure glial cell populations from adult mouse central nervous system white matter*
Supervisors: Prof. Dr. Robert Zorec and Prof. Dr. Arthur Butt
- 10.09.2010 **BSc in Biotechnology**, University of Ljubljana, Slovenia
Topic: *Use of stem cells for treatment of leukemia*
Supervisor: Dr. Miomir Knezevic

Continuous education

- 11-12.2017 **Immunity module**, University of Geneva
- 03.04. and 19.05.2017 **Drug discovery: an industrial perspective** (workshop), University of Geneva
- 09-12.2015 **Cutting edge microscopy** course, University of Bern

Work experiences and skills

- 01.05.2015-ongoing Graduate researcher, **BioNanomaterials** group (Adolphe Merkle Institute, Fribourg, Switzerland) and **Immunopharmacology of Cancer** group (Centre médical universitaire Medical, Geneva, Switzerland)
- 05-12.2014 Student job in quality control laboratory, JUB d.o.o., Dol pri Ljubljani, Slovenia
- 11.2012-03.2013 Undergraduate researcher, **Neurophysiology** group, Portsmouth, UK
- 06-09.2011 Intern, Department of **Genetic Toxicology and Cancer Biology**, National Institute of Biology, Ljubljana, Slovenia

Advance knowledge in **immunotoxicology**, primary **cell culturing** (mouse and human), mouse **ex vivo/in vivo** experimentation, **flow cytometry** and **microscopy** (LSM, TEM), ELISA. Background in **cancer immunotherapy**.

Curriculum Vitae

Other responsibilities:

- Member of **Swiss Society of Pharmacology and Toxicology**, Switzerland
- Member of National Center of Competence in Research (**NCCR**) for **Bio-Inspired Materials**, Switzerland
- **Animal license writing**, University of Geneva
- Teaching assistant of **Biopharmacy**, University of Geneva
- **Supervision** of master students and interns, University of Geneva
- Responsible for FACS facility at Adolphe Merkle Institute, Fribourg, Switzerland

Language skills

Slovenian (mother tongue), English (C1), German (A1)

Presentations

- Spring meeting of the Swiss Society of **Pharmacology and Toxicology**, Bern, Switzerland, April 19th, 2018 and 11th April 2019 (poster presentation)
- ProDoc **Cell Migration** retreat in Bellinzona, Switzerland, 22nd-24th September 2017 (oral presentation)
- European Foundation for **Clinical Nanomedicine** (CLINAM), Basel, Switzerland, 7th-10th May 2017 (poster presentation)
- ProDoc Cell Migration workshop in Bern (Gurten), Switzerland, 17th -18th November 2015 (oral presentation)

Certificates and awards

- **Best poster award: NanoTox 2018** – 9th International Conference on Nanotoxicology, September 18th-21st, 2018
- **Certificate of LTK Module 1: Introductory of Course in Laboratory Animal Science** (Mice/Rats); FELASA Category B Course 027/08, University of Zürich, Switzerland, June 1st-5th, 2015

Publications

Hočevar S., Milošević A., Rodriguez-Lorenzo L., Ackermann-Hirschi L., Mottas I., Petri-Fink A., Rothen-Rutishauser B., Bourquin C., Clift M.J.D. **Polymer-coated gold nanospheres do not impair the innate immune response of human B lymphocytes *in vitro***. *ACS Nano*, 2019, 13, 6: 6790-6800. doi: 10.1021/acsnano.9b01492

Thauvin C., Widmer J., Mottas I., Hočevar S., Allémann E., Bourquin C., Delie F. **Development of resiquimod-loaded modified PLA-based nanoparticles for cancer immunotherapy: A kinetic study**. *Eur. J. Pharm. Biopharm.* 2019, 139, 253-261. doi:10.1016/j.ejpb.2019.04.007

Clift M. J. D., Fytianos K., Vanhecke D., Hočevar S., Petri-Fink A., Rothen-Rutishauser. 2017. **A novel technique to determine the cell type specific response within an *in vitro* co-culture model via multi-colour flow cytometry**. *Sci. Rep.* 2017, 7, 1: 434. doi: 10.1038/s41598-017-00369-4.

ACKNOWLEDGMENTS

My very special thanks go to Prof. Martin Clift who trusted me with this PhD project and supervised, supported and advised me throughout my thesis. I would like to gratefully thank Prof. Carole Bourquin for her supervision, scientific contribution and guidance through all the important steps of my thesis. A special thanks go to Prof. Barbara Rothen-Rutishauser and Prof. Alke Petri-Fink for their scientific contribution to the project as well as to all the friends and colleagues from BioNanomaterials group for help and support. I would especially thank Ana and Laura for their scientific contribution and discussion. Furthermore, I would express my gratitude to all my friends and colleagues from the Immunopharmacology of Cancer group for enormous moral support. I would especially like to thank Betül, Julia and Montsé for their unselfish help with the sometimes overwhelming experimental workload. Also, I would like to thank Aristeia, Aurélien and Eloïse for the French translation of the thesis summary.

Additionally, I would like to thank my aunt and grandfather for encouragement from back home. Furthermore, I would like to thank my good friends Mojca and Vesna for all the support over the years. Finally, I would like to mention my mother and grandmother, who unfortunately left too soon and could not be part of my PhD journey. Nevertheless, they were my constant subconscious support, which helped me greatly to push through to the finish line.